Approches intégrés des mécanismes moléculaires de la tolérance au cuivre chez les algues brunes

Andrés Ritter Traub

Avertissement

THESE DE DOCTORAT DE
L'UNIVERSITE PIERRE ET MARIE CURIE

Spécialité
Biologie

Ecole doctorale
La logique du vivant (ED223)

Présentée par

M. Andrés Ritter Traub

Pour obtenir le double grade de
DOCTEUR de l'UNIVERSITÉ PIERRE ET MARIE CURIE
Et
DOCTOR en Ciencias Biológicas Mención Ecología
de la Pontificia Universidad Católica de Chile

Approches intégrées des mécanismes moléculaires de la tolérance au cuivre chez les algues brunes

soutenue le 16, janvier 2009

devant le jury composé de :

M. Cyrille Forestier	Ingénieur de Recherche-HDR CEA	(Rapporteur)
M. Didier Marion	Directeur de Recherche INRA	(Rapporteur)
M. Christophe Destombe	Prof. Université Pierre et Marie Curie	(Président)
M. Frithjof C. Küpper	P.I. Lect. Scottish Association for Marine Science	(Examinateur)
M. Sylvain Faugeron	Prof. Pontifica Universidad Católica de Chile	(Examinateur)
M. Philippe Potin	Directeur de Recherche C.N.R.S	(Directeur)
M. Juan A. Correa	Prof. Pontificia Universidad Católica de Chile	(Co-Directeur)
M. Thierry Tonon	M.d.C. Université Pierre et Marie Curie	(Examinateur)

Université Pierre & Marie Curie - Paris 6
Bureau d'accueil, inscription des doctorants et base de données
Esc G, 2ème étage
15 rue de l'école de médecine
75270-PARIS CEDEX 06

Tél. Secrétariat : 01 42 34 68 35
Fax : 01 42 34 68 40
Tél. pour les étudiants de A à EL : 01 42 34 69 54
Tél. pour les étudiants de EM à ME : 01 42 34 68 41
Tél. pour les étudiants de MF à Z : 01 42 34 68 51
E-mail : scolarite.doctorat@upmc.fr

A mis Padres
A Blanche
A mi abuela Lina

Acknowledgments

I thank Catherine Boyen for allowing me to carry my research in her laboratory, and for her kind support as well.

I express all my gratitude to the members of my PhD committee (jury et comités de these) for their contribution to the evaluation of my work during all of these years.

I thank the French embassy and the CONICYT for providing me a fellowship for my third year.

This research adventure started over six years ago when Bernard Kloareg introduced me to Philippe. I still remember all the fusing ideas coming out of Philippe's mind, who was programming a research project for the next 10 years within only a 5-minutes-discussion… At the end of this meeting I didn't understood much about the funny topics described by Philippe, but at least I understood that I could work with seaweeds in collaboration with a Chilean lab. Six years latter, I still have troubles sometimes understanding your crazy ideas Philippe, but at least the ones that I understood have helped me to enlarge my scientific culture and to influence my research towards a wide view of biological processes. In addition to scientific issues, I also discovered in you a friend with whom I could discuss multiple subjects such as politics, fishing or nature. I thank you Philippe for supporting and believing me for all these years. It has really been a pleasure to have you as a supervisor.

A couple of months following my first meeting with Philippe, I arrived as a tourist from France to live my first experience in Juan's lab in Santiago. This was in the middle of summer vacations, so no one was working at this time of the year. After a couple of hours waiting for someone to show up, as I was about to leave the lab, I ran into a "chief-looking-person". This is how I met Juan. Then we both realised that there had been a misunderstanding about the date of my arrival (the first but not the last). Since then I have been his "atypical" Chilean-French or French-Chilean (who knows?) student responsible for more than one of his white hairs… Thank you Juan for your support, understanding and patience. I must underline that I started my PhD without any fellowship, which made of myself a heavy financial burden for both labs. Therefore I must thank Juan and Philippe for all the efforts they deployed to solve this issue and guarantee the best conditions to carry my research work.

The third masterpiece of my PhD is Thierry. I met him during my Master. I noticed right away his funny southern French accent, but also the characteristics of a serious and capable researcher eager to friendly help and advice my work. Thierry had been the "stabilizer" element of my thesis, putting down onto the ground the "megalomaniac" plans we built up with Philippe. On top of that, Thierry had the heavy task to supervise me and my pal PO. I can imagine how many aspirins we made him swallow… I thank you Thierry for your guidance, efforts and patience. With you I have learned how to work in a lab. I also thank you for your friendship and loyalty.

Philippe, Juan and Thierry have helped me in a very complementary manner. I was very lucky to have them and I thank you all for being there in good and less good moments.

I must specially thank Sophie Goulitquer, Jean Pierre Salaün, Fanny Gaillard, Sarah Romac, Aaron Man, Jessica Beltrand, Santiago Andrade and Loretto Contreras,

who have closely collaborated with me. Our interaction was determining for the good development of my project, providing me interesting and very complementary skills.

A great thanks to the students who provided me with precious work during this project: Martin Ubertini, Francis Lemadec, Carolina Henriquez. Working with you has been a pleasure, and I thank you for your enthusiasm, humour and initiatives. In addition to your generous help, you offered me your friendship, which I really appreciated.

J'ai aussi une pensée particulière pour mes collègues de bureau, PO et Maud. Vous avez été de bien fidèles compagnons de parcours, et je vous en remercie. J'ai tellement de bons souvenirs et anecdotes dans notre bazar de bureau qu'une thèse ne suffirait pas pour les raconter… Merci mon grand PO pour ces bonnes discussions autour de notre bon vieux billard (quand est-ce qu'on met la pâtée à Robert ?), à propos de la pêche « sportive » ou de la chasse (sans palmes). Je n'aurais pas pu avoir de meilleur pote pendant ces années, merci d'avoir été là, tes blagues vont me manquer au labo.

Un grand merci à l'UMR7139 pour toute votre aide, votre généreuse disponibilité et votre bonne ambiance et dynamisme qui ont fortement enrichi mon travail. Un grand merci pour tous les bons moments passés avec vous, votre amitié et générosité.

Enfin un grand merci à tout le personnel de la Station Biologique de Roscoff, grâce à qui j'ai pu réaliser ma thèse dans des conditions idéales. J'ai une pensée particulière pour le personnel du Gulf Stream, merci pour tous ces moments autours de vos bons petits plats qui ont su agrémenter mon travail au quotidien.

Agradezco igualmente la ayuda de todo el departamento de ecología de la PUC, por haberme acogido y ayudado a lo largo de estos tres años.

Je voudrais également remercier ma Blanche pour son grand soutien pendant chaque minute de ces trois années. Si je suis arrivé jusqu'ici c'est en grande partie grâce à toi. Merci d'avoir cru en moi plus que je n'ose croire en moi-même et pour avoir toujours été là dans les bons et les mauvais moments. Merci d'avoir supporté mes horaires « flexibles » du boulot (même si tu n'en comprenais pas toujours la raison…) et mes humeurs changeantes pendant la rédaction. Je profite au passage pour remercier ma chatoune « ploma », qui a été une compagne fidèle (même aux heures avancées de la nuit) pendant la rédaction de ce manuscrit.

Comment pourrais-je oublier ma famille d'adoption, les Magariños-Rey. Merci à vous de m'avoir encouragé à suivre ma voie. Merci de votre soutien et de l'intérêt que vous avez porté à ma thèse. Je souligne que c'est grâce à vous que j'ai découvert la Bretagne et ses algues. Sans vos « stages de découverte et cuisine des algues » (que je recommande vivement aux lecteurs de cette thèse), je n'aurais sûrement pas fait une thèse de phycologie.

En último lugar agradezco especialmente mis padres y familia. Gracias por haber aceptado mis desiciones, auque no siempre hayan estado de acuerdo con ellas. Su apoyo incondicional, me ha dado la confianza necesaria para poder desarrollarme plenamente. Gracias por haber creido en la importancia de mi trabajo. Sin su ejemplo ni apoyo, nunca hubiese podido llegar a ser él que soy. Aunque no este presente con ustedes los llevo siempre en mis pensamientos.

LIST OF ABREVIATIONS

12-OPDA	12-oxo-phytodienoic acid
12*R*,13S-diHEPE	12*R*,13*S*-dihydroxi-5(*Z*),8(*Z*),10(*E*),14(*Z*),17(*Z*)-eicosapentaenoic acid
12*R*,13*S*-diHETE	12*R*,13*S*-dihydroxi-5(*Z*),8(*Z*),10(*E*),14(*Z*)-eicosatetraenoic acid
12*S*-HEPE	12*S*-hydroxieicosapentaenoic acid
12*S*-HETE	12*S*-hydroxieicosatetraenoic acid
13*S*-HODE	13*S*-hydroxioctadecadienoic acid
13*S*-HOTrE	13*S*-hydroxioctadecatrienoic acid
17H-18-oxo-ETE	18-hydroxi-17-oxo-eicosatetraenoic acid
2-DE	Two-dimensional gel electrophoresis
4-HDDE	4-Hydroxy-dodecadienal
4-HHE	4-hydroxy-(*E*)-2-hexenal
4-HNE	4-hydroxy-(*E*)-2-nonenal
9*S*-HETE	9*S*-hydroxieicosatetraenoic acid
ACN	acetonitrile
afc%	Percentage of autofluorescent cells
AOC	Allene Oxyde Synthase
AOS	Allene Oxyde Cyclase
AsA	Ascorbic Acid
ATX	Antioxidant
CALR	Calreticulin
CAT	Catalase
CAX	Calcium exchangers
CCH	Copper chaperone
CCS	Copper chaperone for Superoxide dismutase
CDF	Cation diffusion facilitator
Chl	Chlorophyll
COX	Cytochrome C
ECH	enoyl-CoA hydratase
EST	Expressed sequence Tag
FA	Fatty acid
Fcp	Fucoxanthine chlorophyll a-c binding protein
FFA	Free Fatty Acid
Fv/Fm	Photosynthetic yield
GAPD	glyceraldehyde-3-phosphate deshydrogenase
GC	Gas Chromatography
GOGAT	glutamate synthase
GPX	Glutathione Peroxidase
GR	Glutathione Reductase
GS	glutamine synthetase
GSH	Reduced Glutathione
GST	Glutathione-S-Transferase

HMA	Heavy Metal Associated
HPL	Hydroperoxide lyase
HSP	Heat Shock Protein
IEF	Isoelectric focusing
IPG	Immobilized pH Gradient
LC	Liquid Chromatography
LC50	Median (50%) lethal concentration
LHC	Ligth Harvesting Complex
LOX	Lipoxygenase
LOX	lipoxygenase
LT	Leukotriene
MALDI	Matrix Assisted Laser Desorption Ionisation
ManA	Mannose-6-phosphate isomerase
MC	Metacaspase
MDA	Malonaldehyde
MDAR	Monodeshydroascorbade reductase
MeJA	Methyljasmonate
MS	Mass spectrometry
MSR	Methionine sulfoxide reductase
MT	Metallothionein
NA	Nicotianamine
OEC	Oxygen Evolving Complex
PAM	Pulse AmplitudeModulated Fluorimetry
PC	Phytochelatin
PCS	Phytochelatin synthase
PG	Prostaglandin
PKK	phosphoribulokinase
PMF	Protein mass fingerprint
PRX	Peroxiredoxin
PVP	polyvinylpyrrolidone
RC	Reaction Center
ROS	Reactive Oxygen Species
SAM	S-adenosylmethionine synthetase
SHMT	serine hydroxymethyl transferase
SMALDO	fructose 1,6-bisphosphate aldolase
SOD	Superoxide Dismutase
TCA	Trichloroacetic acid
TCA	Trichloroacetic acid
TFA	Trifluoroacetic acid
TKT	transketolase
TOF	Time of flight
TRX	Thioredoxine
vBPO	vanadium dependent Bromoperoxidase

TABLE OF CONTENTS

Résumé

Les algues brunes (Phaeophyceae) sont des organismes photosynthétiques macroscopiques fixés qui représentent une biomasse considérable dans les écosystèmes rocheux des côtes tempérés et froides de tous les océans en zone intertidale et subtidale. Par conséquent elles doivent faire face à des agressions constantes d'origine naturelle ou anthropique. Le déversement des métaux lourds comme le cuivre provenant des activités minières, portuaires et agricoles constitue une importante source de pollution dans l'environnement marin. De part son potentiel redox, le cuivre est un micronutriment essentiel pour diverses metalloprotéines, mais par opposition à fortes doses, ces qualités se transforment en défauts, pouvant causer de sérieux dommages cellulaires. Parmi ces dommages comptent l'inactivation d'enzymes, la dépolarisation des membranes et la production de formes activées de l'oxygène. Le Chili produit plus de 30% du cuivre mondial; en conséquence des grands volumes de déchets rejetés en mer depuis les années 1930 ont fortement affecté la biodiversité des écosystèmes côtiers. Dans ces zones, un faible nombre d'espèces arrive à s'établir, parmi lesquelles l'algue brune *Ectocarpus sp*. Bien que les mécanismes moléculaires de la tolérance aux métaux lourds soient bien décrits dans la littérature chez d'autres organismes, très peu d'exemples concernent les algues brunes. Dans ce contexte, l'objectif de mon travail visait à apporter des réponses concernant le maintien d'une biodiversité algale très réduite dans les zones impactées par les rejets des mines de cuivre sur les côtes du nord du Chili par de nouvelles approches intégratives pour comprendre l'adaptation dans des environnements pollués. Plus particulièrement, il s'agissait de déterminer les mécanismes biochimiques et moléculaires de la tolérance au cuivre chez les algues brunes. Pour cela, nous avons choisi comme modèles d'étude *Laminaria digitata* et *Ectocarpus siliculosus.*

Laminaria digitata est une espèce d'une grande importance écologique des côtes nord atlantiques. De part la composition de sa paroi, cette algue peut accumuler des quantités importantes de métaux lourds, cependant peu d'études la décrivent comme tolérante. En réponse à des stress biotiques cette algue produit des oxylipines dérivées à la fois des eicosanoides et des octadécanoides qui sont probablement impliquées dans des mécanismes de défense. L'existence de ce métabolisme rend ce modèle intéressant à considérer pour l'étude du stress chez les algues brunes.

D'autre part ce projet s'est centré sur le modèle *Ectocarpus siliculosus.* Cette petite algue brune filamenteuse a un grand intérêt à la fois pour des raisons techniques et biologiques. Cette espèce est développée au laboratoire comme modèle de génétique, génomique et protéomique pour les algues brunes. Son génome a été entièrement séquencé et est en cours d'annotation actuellement. D'autre part, de nombreux travaux antérieurs décrivent cette espèce comme metallotolérante. De plus *Ectocarpus* est une des rares espèces d'algues brunes à pouvoir se développer dans les zones impactées par les rejets des mines de cuivre sur les côtes du nord du Chili.

Ce projet de doctorat en co-tutelle s'est développé dans le cadre du Laboratoire International Associé LIA <DIAMS> (Dispersal and Adaptation in Marine Species ; responsables Myriam Valero et Juan Correa). L'objectif général du LIA créé en Juin 2004 entre les équipes françaises de la Station Biologique de Roscoff (SBR) et les équipes chiliennes de la Pontificia Universidad Catolica de Chile (PUCCh) est d'étudier, en relation avec les changements climatiques et l'activité humaine, les processus qui sont responsables des changements dans la biodiversité marine côtière au sein des communautés et des populations. Cette collaboration est fondée sur la complémentarité des approches menées à la SBR et à la PUCCh (génétique des populations, biologie évolutive, biochimie, génétique,

génomique fonctionnelle, écologie moléculaire, -incluant l'écologie larvaire-, écologie chimique des populations et des communautés, biologie de la conservation ; gestion des ressources côtières, impacts humains et écologie des zones côtières).

Etude de l'implication des oxylipines dans la réponse des *L. digitata* aux métaux lourds.

Les oxylipines sont des composés produits au cours du métabolisme des acides gras polyinsaturés par réaction avec des espèces activées de l'oxygène. Chez de nombreux organismes, ces molécules sont toxiques lorsqu'elles sont synthétisées en trop grande quantité. Cependant, elles peuvent aussi intervenir dans les mécanismes de signalisation lorsqu'elles sont présentes en très faible concentration et dans des conditions physiologiques bien spécifiques. La biosynthèse des oxylipines est précédée par l'activation d'une lipase qui libère des acides gras libres, qui deviennent substrats pour un certain nombre d'enzymes, dont des lipoxygénases (LOX); des cyclooxygénases (COX) et des cytochromes P450 (CYP450). Chez les plantes vasculaires ces métabolites régulent les mécanismes de defense suite à des stress biotiques et abiotiques et chez les animaux ils contrôlent la réponse inflammatoire. Tenant compte de ce dernier point, un de nos objectifs a consisté à étudier la possible implication des oxylipines dans les réponses aux métaux lourds chez les algues brunes.

Au cours de mes travaux, j'ai notamment développé une approche de profilage métabolique des acides gras oxydés en étroite collaboration avec Sophie Goulitquer (U.BO., Brest). Ces résultats m'ont permis d'appréhender la nature des lipoperoxydes produits suite au stress par le cuivre, mais aussi de leur attribuer des fonctions potentielles notamment dans la signalisation cellulaire qui contrôle les mécanismes de tolérance au cuivre. Chez les plantes supérieures, la signalisation par les composés organiques volatiles (COV) induit la mise en place des mécanismes de défense. Les aldéhydes sont impliqués dans cette signalisation. Ils sont formés par l'action de l'enzyme hydroperoxyde lyase (HPL) sur des hydroperoxydes

d'acides gras polyinsaturés et sont libérés après un stress biotique ou abiotique. Nous nous sommes intéressés à la signature métabolique, relative aux aldéhydes, lors de la réponse de *L. digitata* au stress par le cuivre dans un laps de temps réduit (1 heure). Ainsi nous avons démontré pour la première fois chez ces algues qu'un stress par le cuivre engendre l'émission d'une grande diversité d'aldehydes parmi lesquels comptent des composés comparables à ceux trouvés chez les plantes vasculaires en C_6 et en C_9. D'autre part nous avons démontré qu'une exposition longue de 24h induit la libération des acides gras polyinsaturés en C_{18} et C_{20} qui servent de substrat pour la production des oxylipines à longue chaine. Parmi les oxylipines synthétisés, nous avons détecté pour la première fois des structures cycliques complexes telles que le précurseur des jasmonates, le 12-OPDA, ou les dérivés eicosanoides de type prostaglandines. Enfin, nous avons mis en évidence la production d'un nouveau composé apparemment spécifique des algues brunes, l'acide 18-Hydroxy,17oxo-eicosatetraénoique (18-H,17-OETE). La synthèse de ces composés s'est accompagnée par l'induction des gènes codant pour des protéines impliquées dans des mécanismes de détoxication tels qu'une Glutathion-S-transferase (GST) ou la Heat Shock Protein 70 (HSP70) entre autres. Ceci suggère fortement l'implication des oxylipines dans le déclenchement des mécanismes de protection cellulaire.

Etude protéomique différentielle chez *Ectocarpus siliculosus*

La tolérance au cuivre a été étudiée chez la souche d'*E. siliculosus* Es524 provenant d'une zone impactée par des rejets de cuivre au nord du Chili, en la comparant avec la souche Es32 provenant d'un site non pollué au sud du Perou. Pour ceci, j'ai mené des tests de survie à différentes concentrations, accompagnés par des analyses physiologiques tels que l'étude des paramètres photosynthétiques et l'observation par microscopie à epifluorescence de la dégradation des chloroplastes par perte d'autofluorescence. Les résultats indiquent que la

souche Es524 est remarquablement plus tolérante que la souche Es32. Alors que les concentrations naturelles de cuivre dans l'eau de mer s'établissent à des concentrations de l'ordre du 1 µg/L, Es524 ne montre pas de variations majeures dans son métabolisme jusqu'à des concentrations de 250 µg/L (Lc_{50}). Au contraire, Es32 est bien plus sensible, montrant des effets délétères pour des concentrations supérieures à 50 µg/L (Lc_{50}). Ces premiers résultats prouvent que la tolérance des souches est corrélée avec l'historique de pollution par le cuivre des sites d'échantillonnage, ce qui pourrait constituer un signe d'adaptation locale. Dans un deuxième temps je me suis intéressé d'une part aux mécanismes communs de réponse au cuivre chez ses deux souches, et également, aux traits qui pourraient expliquer la tolérance accrue de Es524. Pour ceci, j'ai mené une approche protéomique globale par électrophorèse bidimensionnelle (2-DE). Cependant, avant de pouvoir mener cette analyse, il a été nécessaire de mettre au point une méthode d'extraction du protéome soluble, fiable et compatible avec la technique 2-DE. J'ai évalué les qualités des nombreux protocoles décrits chez d'autres organismes, cependant aucun n'a donné des résultats satisfaisants. Nous avons donc adapté à notre modèle biologique une méthode basée sur l'extraction par le phénol. Ce protocole abouti à des gels d'une grande résolution (800 – 1000 spots) en éliminant les contaminants pour une faible biomasse de départ. D'ailleurs des tests sur d'autres espèces d'algue brune donnent des résultats comparables à ceux obtenus chez *E. siliculosus*, ce qui nous fait penser que ce protocole peut aussi bénéficier à d'autres espèces d'algues. Suite à cette mise au point technique, j'ai mené une étude protéomique différentielle des réponses au stress causé par le cuivre chez Es32 et Es524. Les résultats montrent premièrement des mécanismes communs de réponse au cuivre chez les deux souches. Ainsi l'accumulation suite au stress des enzymes intervenant dans des voies métaboliques tels que la β-oxydation ou la voie des pentose phosphates, nous font penser que la régulation des processus énergétiques est importante chez les deux souches. De même ces deux souches régulent de façon positive des mécanismes de

renouvellement et recyclage protéique, faisant intervenir des protéines tels que des HSP. Ces résultats confirment ceux obtenus au préalable pour le gène de HSP70 chez *L. digitata.* De façon intéressante chez les deux souches, plusieurs enzymes appartenant à la synthèse du métabolisme du glutathion (GSH) sont induites. Le GSH participe d'une façon déterminante chez d'autres modèles pour la détoxication des ROS et aussi des métaux. D'une part c'est un antioxidant notoire, participant aux cycles comme celui du glutathion-ascorbate, et d'autre part il sert de substrat pour la synthèse des phytochelatines qui est un des principaux moyens de chélation des métaux lourd chez les plantes vasculaires. Le GSH sert aussi de substrat aux enzymes de détoxication GSTs, qui sont induites lors d'un stress par le cuivre chez *L. digitata*. Enfin la synthèse ou la modification de composés phénoliques pourrait aussi jouer un rôle important dans la détoxication des deux souches.

Dans un deuxième temps j'ai comparé les profils d'expression 2-DE entre des individus stressés de Es524 et Es32 afin de chercher des protéines qui pourraient être responsables de la différence de tolérance observée. Parmi les protéines accumulées uniquement chez Es524, plusieurs enzymes qui confèrent une résistance aux stress abiotiques ont été identifiées comme par exemple deux hélicases à ARN de la famille des DEAD box et une bromopéroxydase à vanadium (vBPO). Cette dernière protéine a été proposée comme une enzyme clé du métabolisme halogéné des algues brunes qui a d'ailleurs été récemment reconnu comme étant un mécanisme antioxidant unique à ces organismes. Un autre aspect qui a différentié Es524 par rapport à Es32 est l'accumulation marquée des protéines structurelles photosynthétiques telles que la composante du complexe de production d'oxygène OEC33 ou la protéine du complexe collecteur de lumière Fucoxanthine cholophyll a-c binding protein. La photosynthèse étant une des principales cibles de toxicité chez les organismes photosynthétiques, ces résultats suggèrent que l'expression de ces protéines pourrait être en relation avec la tolérance de Es524.

En conclusion, mon étude contribue à apporter des réponses sur les bases biochimiques et moléculaires menant à la tolérance des algues brunes des zones polluées par le cuivre. De plus, il est fort probable que les mécanismes spécifiques de réponse au stress chez les individus tolérants soient la résultante d'une forte pression de sélection opérant dans ces sites.

Annotation du génome d'*E. siliculosus* : étude *in silico* des l'homéostasie et la tolérance au cuivre chez *Ectocarpus*

Le séquençage du génome d'*Ectocarpus* a été finalisé en 2007. Ce projet a été méné au Centre National de Séquençage-Génoscope d'Evry par un consortium des laboratoires coordonné par Mark Cock de l'UMR7139 à la Station Biologique de Roscoff. L'annotation automatisée du génome a identifie un total de 17920 gènes lesquels ont ensuite été annotés pour une grande partie manuellement par les membres du consortium. Dans ce cadre, j'ai pu contribuer à l'annotation du génome en m'intéressant aux gènes impliqués dans l'homéostasie et la tolérance au cuivre, identifiés par homologie aux autres modèles biologiques. Les résultats indiquent qu'une grande partie des processus de transport du cuivre sont conservés tels que des CTR, P-ATPases ou des chaperones du cuivre. Au contraire des facteurs de transcriptions connus pour agir comme senseurs du taux de cuivre cellulaire n'ont pas été identifiés. D'autre part, j'ai pu identifier des gènes codant pour des protéines de impliquée dans la chélation intracellulaire du cuivre telle que des metallothionéines (MT) et une phytochelatine synthase (PCS). Malgré la présence de ces systèmes conservés chez d'autres organismes, il est fort probable que les algues brunes utilisent aussi des mécanismes propres d'absorption ou de chélation. Un exemple pourrait être l'utilisation de leur paroi chargée come un système d'échange ionique, cependant il est nécessaire de mener des études approfondies avant de confirmer cette théorie.

Ce travail a contribué à augmenter sensiblement la compréhension des réponses de défense des algues brunes à des concentrations excessives de cuivre. Cependant, la poursuite d'approches globales, notamment de transcriptomique, en utilisant une puce à ADN représentant la quasi-totalité du génome mise au point au laboratoire par S. Dittami et T. Tonon, n'a pu être réalisée dans le temps imparti pour ce travail. L'intégration des données d'expression de gènes, des données de protéomique déjà obtenues ou nouvelles et la poursuite des approches métaboliques initiées permettra d'élargir le spectre de protéines et de voies métaboliques impliquées dans la détoxication et la régulation des réponses des algues brunes au stress cuivrique. Les prolongements de mon travail, qui a fortement suggéré l'existence d'une adaptation locale au cuivre chez *E. siliculosus* doivent aussi se placer dans un contexte de génomique des populations en exploitant les marqueurs moléculaires neutres développés pour la carte génétique d'*E. siliculosus* dans l'UMR 7139. Ceci pourrait permettre d'utiliser des approches de cartographie d'associations sur des souches isolées du milieu naturel de degré de tolérance contrasté, voire de développer des lignées pour des études de type QTLs (Quantitative Traits Loci). Ces études de génétique quantitative sont susceptibles de révéler des gènes de tolérance fortement sélectionnés dans ces régions du génome impliquée dans la tolérance. D'autres, des approches fonctionnelles nouvelles sans a priori telle que la génétique formelle ou des approches à priori sur des gènes candidats pourront être menées au sein de l'UMR 7139 par mutagénèse UV de gamètes d'*Ectocarpus.* La mise au point de cribles robustes de sélection de mutants sensibles ou résistants au cuivre pourra être menée, de même qu'une approche de type TILLING sur des gènes comme le gène de la vBPO.

Les éléments de réponse à toutes les questions restées ouvertes à l'issue de ce travail affineront la connaissance sur les mécanismes de tolérance aux métaux conservés avec les autres eucaryotes ou spécifiques aux algues brunes qui leur permettent de survivre dans des environnements pollués.

1 INTRODUCTION

1.1. GENERAL INTRODUCTION

1.1.1. Ecological and physiological features of brown algae (Phaeophyceae)

Research into the biology of the brown algae has been stimulated by their global economic and ecological importance. Brown seaweeds (Phaeophyceae) represent an important resource, with a wide range of uses in the food, cosmetic, and fertilizer industries, and are attracting increasing attention as a source of active biomolecules [1]. The class of Phaeophyceae is an important assemblage of organisms that are classified in about 265 genera with more than 1500 species [2]. They occur primarily in the marine environment where they appear mainly as an intertidal component. Brown algae belong to the heterokont lineage which bear one of the evolutionary distinct branches of the tree of life (Fig. 1A) [3]. Heterokont stands for the presence of a flagellate cell (at one point of their life cycle) with two different flagella. One of these flagella is a long mastigonemate flagellum, directing forward during swimming, and the other flagella is a shorter smooth flagellum which lacks the stiff hairs, situated backwards [2,4].

Brown algae are also of interest from a developmental point of view, because they represent one of the only five eukaryotic lineages that have independently evolved complex multicellularity (the four others being animals, fungi, green plants, and red algae). In addition, the alternation between gametophyte and sporophytes (Fig. 2D; 5), which involves sequential development of two independent complex multicellular organisms, represents a novel situation compared with to life cycles of model organisms from other groups, such as green plants and animals, in which the gametophyte generation is usually highly reduced or absent [5]. The marine environment affects several aspects of photosynthesis in brown algae. When immersed, they do not receive the full light spectrum, and they have adapted to these

conditions by the build-up of light harvesting complexes that can absorb wider light spectra than land plants [6]. Chlorophyll c and the caroteonoid fucoxhantin are the main light-harvesting pigments of Phaeophyceae, which give them their characteristic brown color. Plastids of green and red algae originate from the primary endosymbiosis of a cyanobacterium in a eukaryotic host cell, while brown algae derive from a secondary endosymbiosis of a unicellular red alga in a eukaryotic host cell [7]. As a consequence, the plastid of the green plants and red algae is surrounded by two membranes, whereas it is surrounded by four membranes in the brown algae (Fig. 4.).

The brown algal cell wall also represents an original feature of this class. It does not only provide rigidity, it is also essential for processes such as cell growth, development, reproduction, host – pathogen interactions, ionic exchange and environmental adaptation [6,8-11]. The cell wall is composed of a polysaccharide fibrillar skeleton and an amorphous embedding matrix. The fibrillar skeleton is composed of neutral polysaccharides such as cellulose, whereas the matrix contains the unique anionic polysaccharides alginates and in smaller amounts the sulphated polysaccharide fucoidan [9]. In contrast to Chlorophyta, Phaeophyceae utilize soluble carbon storage polysaccharides such as laminarin and mannitol, the latter compound also being employed by these organisms as an osmolyte [12]. Around the nucleus, lie numerous stongly refractile vesicles (physodes), whose contents are formed within the chloroplast (Fig. 4). These vesicles contain secondary metabolites known as “phaeophycean tannin” or phlorotannin. These are polymers of phoroglucinol only known in brown algae. The exact role of these compounds is not fully determined, however it is likely that they play important roles in biotic stress responses against grazers and in abiotic stress through UV protection, scavenging of reactive oxygen species (ROS) and heavy metal chelation [13-16]. Iodide metabolism constitutes also an original feature in brown algae with important implications for the coastal marine environment [17]. Brown algal kelps are the

most effective known living iodine accumulators with tissue concentrations often exceeding 50 mM, which constitutes over 30,000 times the iodine concentration in seawater [18]. In the past years, major advances have been done in the understanding of the function of iodide in brown algae. Iodide acts as ROS scavengers in brown algae by its massive efflux upon stress, which constitutes a unique process [19]. In *Laminaria digitata*, iodide is highly concentrated in the apoplasmic subcellular region, which provides an abundant and accessible source of labile iodine species that can be easily remobilized for potential chemical defense and antioxidative activities [20].

In addition to its evolutionary distance from other well-studied biological models, few genomic and genetic data are available within the Phaeophyceae. For this reason, in 2004, a consortium of laboratories led by the Station Biologique in Roscoff and Genoscope has initiated a project to sequence the genome of *Ectocarpus siliculosus*, which is a key step for the emergence of this species as a model for the brown algae. Therefore, during my PhD. thesis I have focused my work on both species, *L. digitata* and *E. siliculosus*.

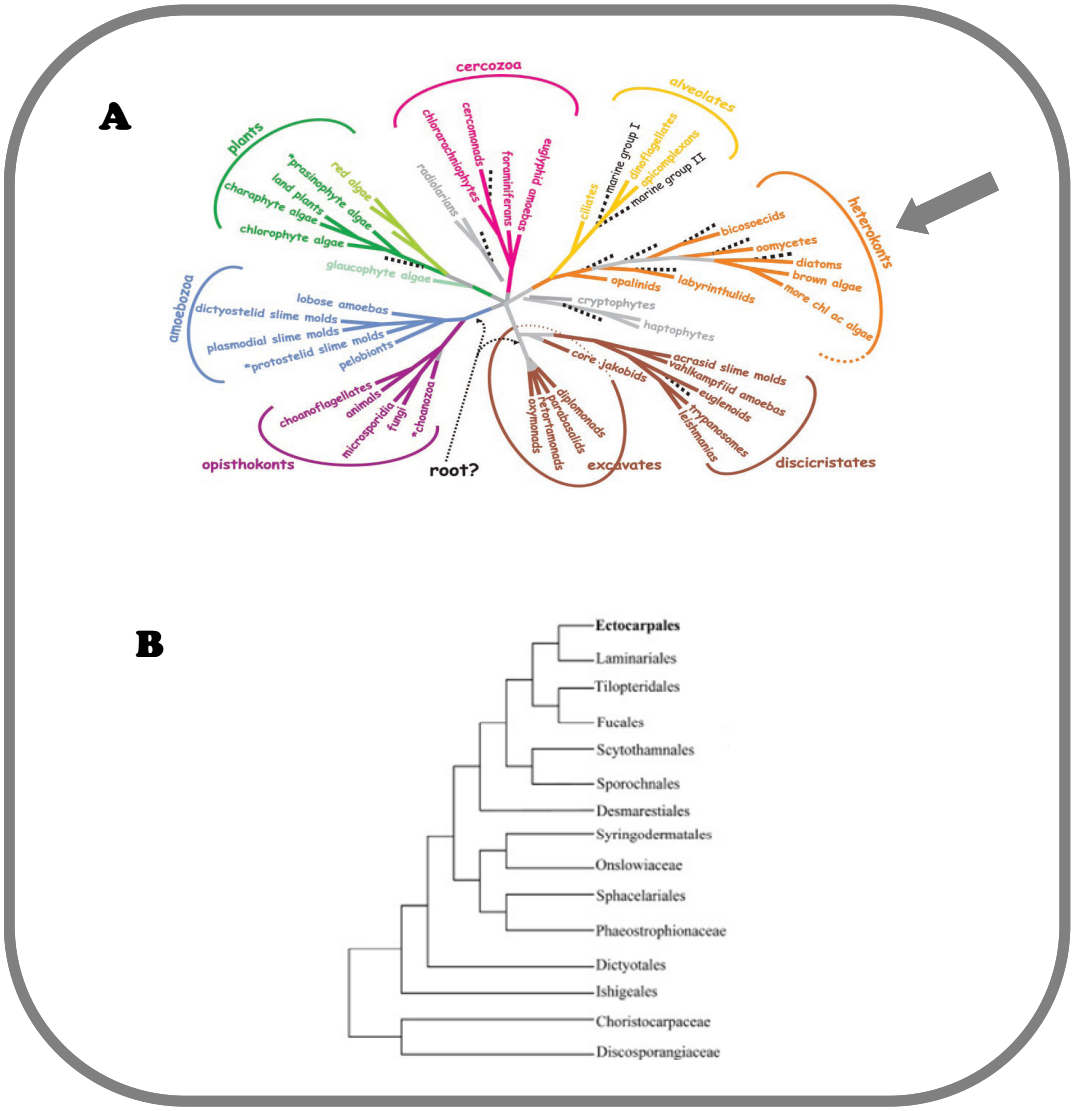

Figure 1. Phylogeny of brown algae and Ectocarpales. (A) Position of brown algae within the eukaryotes (adapted from Baldauf, 2003 [3]). Brown algae belong to the heterokont phylum, which is phylogenetically distant from land plants and the green and red algae. Brown algae are arrowed. (B) Position of the Ectocarpales (in bold) within the brown algae (adapted from Charrier et al. 2008).

1.1.1.1. *Laminaria digitata*

Laminaria is a reduced genus of 63 species commonly called kelps which includes the largest known seaweeds. This order was recently reviewed by Bartsch et al. [21]. The ecological significance of kelp is great in most temperate rocky coasts of the world. Due to the large size of many species, kelp communities make up three dimensional landscapes, much like an underwater forest (Fig. 2A-C). The kelp forest bears a unique and complex

ecosystem with a high diversity of organisms, and its productivity is comparable to a temperate terrestrial forest [22]. In addition, brown seaweeds represent a considerable biomass which is used for the commercial extraction of alginates, a cell-wall polysaccharide present in all brown algae but particularly abundant in kelps. The industrial applications of alginates are numerous, ranging from their use as thickeners in the food industry to medical applications such as wound dressing and medical capsule materials.

Laminaria digitata (Hudson) J.V. Lamouroux is an intertidal kelp distributed along the north western Atlantic coasts. More specifically, this species is found in the lower intertidal zone; being therefore rarely exposed to emersion. This means that its physical and chemical environment is relatively stable. For this reason, *L. digitata* is relatively sensitive to the exposure to abiotic stresses compared to algae of the upper intertidal zone [23]. Concidering its ecological importance, this species represents an important biological model for research [21]. *Laminaria* has a heteromorphic and diplohaplontic life cycle with an alternation between a highly differentiated diploid sporophyte and a microscopic, haploid filamentous gametophyte (Fig. 2D). Sporophytes bear up to 2 meter long macrothalli which present a complex parenchymatous structure and exhibit intercalary growth, through the activity of a meristoderm (Fig. 2C). The whole life cycle of *L. digitata* can theoretically be carried out in laboratory conditions (Fig. 2F); however, due to the large size of the sporophytes, its cycle is usually only partially completed in culture by isolating spores from fertile wild sporophytes, to give gametophytes and then juvenile sporophytes which are used for experimentation. (Fig 2E). Over the last years, new methods in physiology and ecology have drastically changed the old perception of kelps [21]. From a genomic point of view, cDNA libraries had been constructed from sporophytes, gametophytes (Fig. 2D), protoplasts, and elicited sporophytes of *L. digitata*, representing 4,000 (about 1,800 putative proteins) expressed sequence tags (EST) altogether. Several of those identified proteins are of interest for our understanding of

the molecular physiology of kelps, such as the ones involved in carbon-concentrating mechanisms, cell wall biosynthesis and stress responses [24,25].

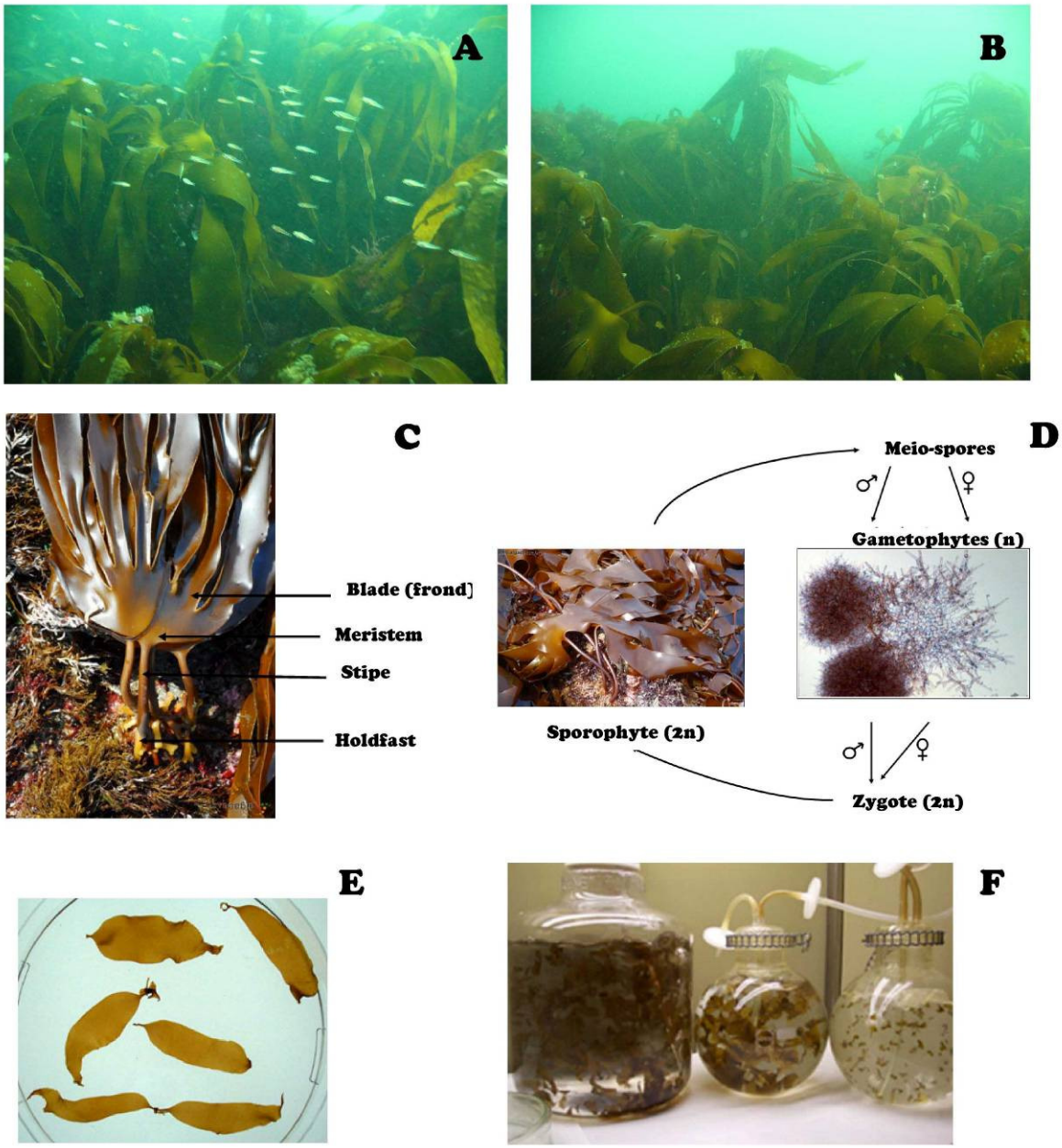

Figure 2. Presentation of *Laminaria digitata.* (A-B) Underwater *Laminaria sp*. forest (pictures A. Ritter). (C) Morphological description. (D) Life cycle. Diploid macroscopic sporophytes produce meiospores in sporangia (sori). Meiospores grow into male or female microscopic gametophytes producing gametes. Gametophytes produce gametes. Fusion of gametes produces a zygote that grows into a diploid sporophyte, completing the sexual cycle. (E) *L. digitata* juveniles (picture D. Scornet). (F) *L. digitata* sporophyte cultures (picture P.O. de Franco)

1.1.1.2. *Ectocarpus siliculosus*

Ectocarpus is a genus of filamentous uniseriate marine brown algae that contains 98 species. This latter number may be largely overestimated because of the difficulties to differentiate some of the species within this genus. Two species are currently recognized, *E. fasciculatus* (Harvey) and *E. siliculosus* (Dillwyn) Lyngbye. They are short-lived annual organisms, which can develop on many inert substrates, or as epiphytes on big seaweeds (Fig. 3 A-B). In the intertidal zone, *Ectocarpus* members occur from the top of the intertidal zone, for instance in rocky pools, to the sublittoral zone. *E. siliculosus* (Fig 3E-F) is a cosmopolitan alga, present on all coasts of temperate climate zones. This species has the remarkable ability to develop in hostile environments, and has been described as growing at extremely low salinities (even in freshwater) or in copper-enriched environments [26-28]. Although the Ectocarpales have long been considered as the most primitive members of Phaeophyceae, mainly because of their morphology, molecular systematics has shown that this order belongs to a group of brown algae that has evolved quite recently (Fig. 1B). In addition, they are closely related to kelps, which have a large size and complex morphology. *E. siliculosus* has been intensively studied since the 19th century, with emphasis on its reproduction and life history (Fig. 4A-E). The basic plan of the life cycle is diplohaplontic and isomorphic. The diploid sporophytes produce haploid meiospores in unilocular meiosporangia which become gametophytes and asexual diploid mitospores in plurilocular sporangia, which then produce diploid sporophytes. The haploid gametophytes produce haploid gametes in plurilocular gametangia. Unfused gametes may grow parthenogenetically and form haploid parthenosporophytes. (Fig. 5) [2,5]. Other major aspects that have been studied include sexual pheromone signaling, viral infections, cell ultrastructure, photosynthesis, carbon uptake, gamete recognition and resistance to anti-fouling agents such as copper [5]. Altogether, several features of *E. siliculosus* make it relevant for its emergence as a model organism.

These include its small size, the fact that the entire life cycle is well known and can be completed in the laboratory (Fig. 3C-D), its high fertility and rapid growth (the life cycle can be completed within 2 months) [29]. The genus *Ectocarpus* is the only brown alga for which detailed genetic studies have been described, its genome (214 Mbp) has been sequenced and is currently being annotated (Cock et al 2009). In addition, an international consortium has been created to establish this species as a genomic and genetic model in Phaeophyceae [5,29].

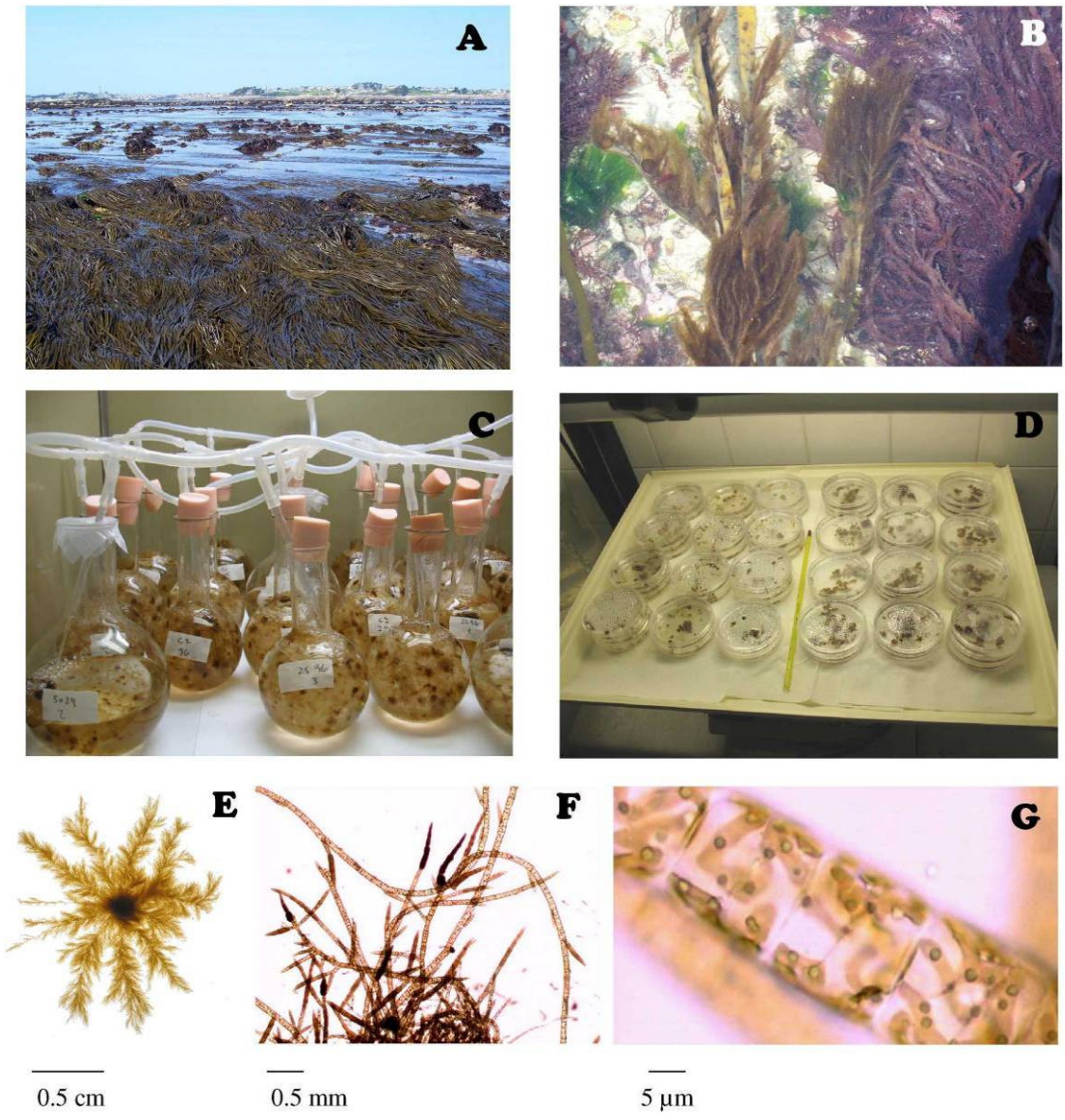

Figure 3. Macroscopic and microscopic images of *E. siliculosus*. (A-B) *Ectocarpus* in the field (pictures A.R.). (C-D) Cultures of *E. siliculosus* (pictures A.R.). (E-F) Microscopic view of *E. siliculosus* (pictures D. Scornet and J. Beltrand).

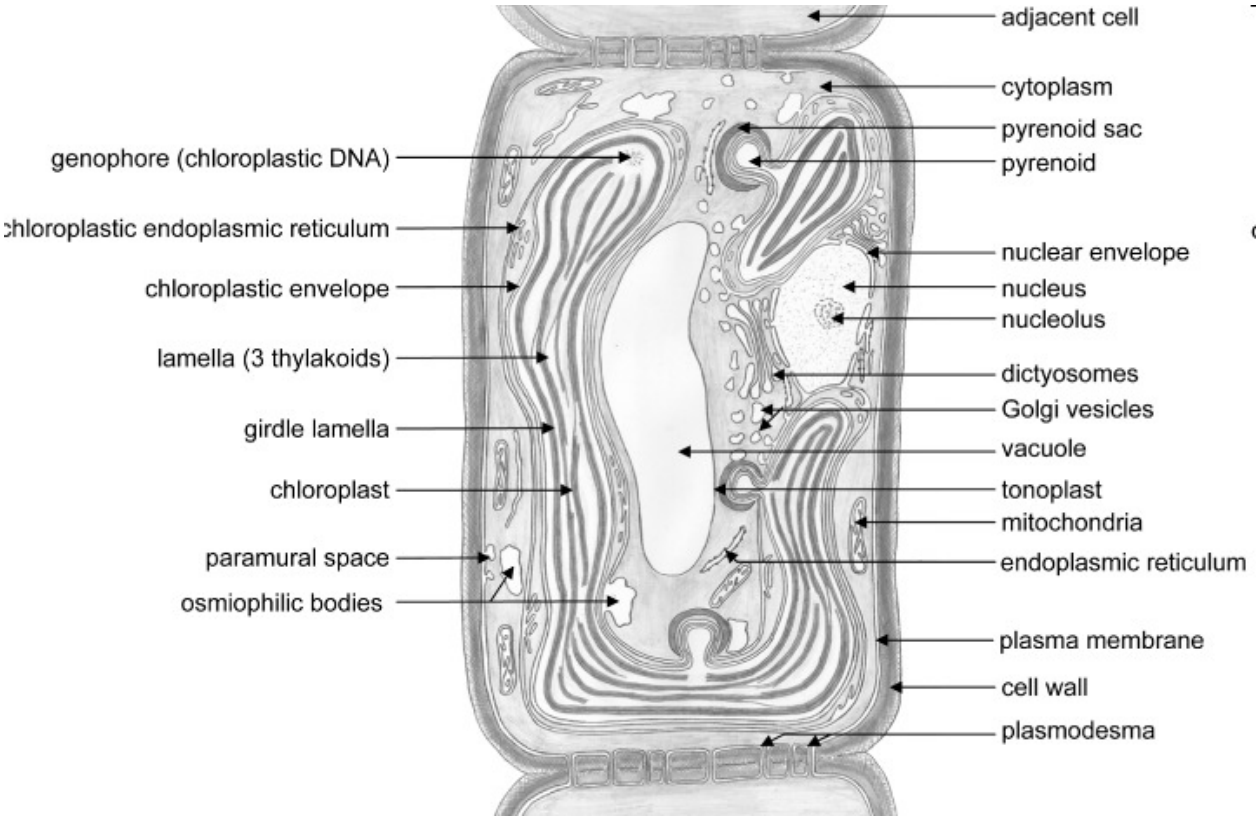

Figure 4. General ultrastructure of a vegetative cell of *Ectocarpus siliculosus*. The general ultrastructure of a vegetative cell is similar in both prostrate and erect filaments (Adapted from Charrier *et al* 2008 [5]). The different compartments of the cell are illustrated (see text for details). Lines represent membranes and define subcellular compartments, except for thylakoids, drawn as a thick black line. Depending on their type and age, the vegetative cell size varies from 10 to 35 µm in length, and 5 to 15 µm in width (under laboratory culture conditions).

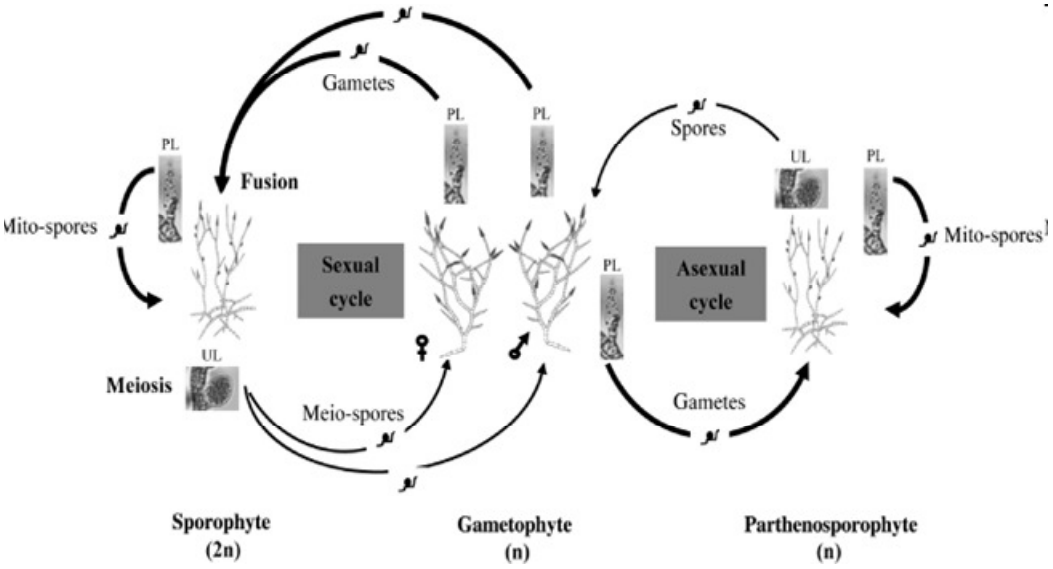

Figure 5. Life cycle of *Ectocarpus siliculosus*. Adapted from Charrier *et al*. 2008 [5].

1.1.2. General aspects of abiotic stress in seaweeds

Marine macroalgae are multicellular benthic photosynthetic eukaryotes. They dominate coastal intertidal and subtidal areas of temperate, cold and tropical regions. Coastal regions and especially the intertidal zone, represent a steep gradient of environmental variations over a small spatial scale, from marine to fully terrestrial conditions (Fig. 6). Under emersion marine organisms are exposed to different stressors, such as variable temperature, UV radiation, salinity changes, and they are affected by reduced amount of nutrients [22,23]. In addition to natural oscillations, seaweeds may also be exposed to several sources of stress resulting from industrial, urban and agricultural activities [30,31]. As a result, seaweeds growing along the intertidal zone must be adapted to their environment and tolerate constant fluctuating abiotic conditions. Most of the stress conditions trigger the production of ROS [11,32-36], by different processes. Under abiotic stress, ROS synthesis results from altered photosynthesis and inefficient reparation processes. During biotic stress, a so-called "oxidative burst" is observed and corresponds to a rapid, transient, and intense ROS production by enzymatic processes.

All organisms, even within the same species, are not responding in the same way to changes in environmental conditions. If tolerance is expressed as a differential response to a stressor, then selection may occur to produce genetically adapted individuals [37]. In macroalgae, previous studies report some inter-population differences inherited against environmental stress, such as tolerance to excess copper [38,39]. At the biochemical level, seaweeds alter their metabolism in various ways to acclimate/adapt to environmental stresses [22,23], however, the molecular basis of this phenomenon is poorly understood. In contrast, the molecular events linking the perception of a stress signal to the metabolic responses leading to tolerance have been intensively investigated recently in land plants, underlining the involvement of ROS metabolism [40,41]. In the past years, the importance of ROS as

signaling molecules has been highlighted [42]. ROS produced under abiotic or biotic stress can trigger a variety of cellular responses [43]. One of them is the activation of fatty acids by the synthesis of oxygenated polyunsaturated fatty acid derivatives known as oxylipins, which are know to play a pivotal role during abiotic and biotic stress in plants and metazoans. In plants, their implication during wounding stress and pathogen and herbivore attacks has been recognized in the past and is still an active field of research [44,45]. In macroalgae, oxylipins have been shown to trigger defensive mechanisms upon biotic aggression [46,47]. Today, new analytical tools developed within the "omics" era open a large panel of possibilities towards the understanding of the molecular bases leading to the tolerance of seaweeds against stressful environments.

Figure 6. Influence of the tidal cycle in Roscoff coastal area. The pictures were taken at high and low tide the same day. Only 6 hours separate the first and the second picture (pictures P.O. de Franco).

1.1.3. Ecological effects of copper excess in seaweeds: example of mine wasted areas in northern Chile

Metals occur naturally, and several of them are essential components of global ecosystems. In seawater, most metals are bound to organic matter, which decrease their low bioavailability. The term "heavy metal" designates those metals having densities greater than 5 g/cm^3 (in their elemental stage). However, from a biological point of view, this term is utilized for those metals and metalloids that cause toxic effects on living organisms [48]. Metals such as copper (Cu) and zinc (Zn) are essential micronutrients, whereas others such as lead (Pb) and mercury (Hg) are not known to have useful biochemical function. Environmental pollution by metals extended as mining and industrial activities increased in the late 19th and early 20th centuries. The current worldwide mine production of Cu, Cd, Pb, and Hg is considerable. These pollutants, ultimately derived from a growing number of diverse anthropogenic sources (industrial effluents and wastes, urban runoff, sewage, boating activities, agricultural fungicide runoff, domestic garbage dumps, mining operations), have progressively affected different ecosystems [15,30]. Copper, in its ionic state (Cu^{2+}), is the second most toxic metal for living organisms [6]. In seawater, copper concentration vary widely, fluctuating between 0.5 and 3 µg/L; the most meaningful concentration is the bioavailable fraction which ranges at 10^{-7}-10^{-8} µg/L [49].

Copper mining activities are still one of the most significant worldwide sources of this metal, which is released into the environment due to the large volumes of wastes produced. Copper mine wastes had severe negative effects on the coasts of England [50], Australia [51] and Chile [30]. Historically, copper mines of Andes Mountains have been a major economic input into Chilean budget. In 2007 the mineral production was 1,665 Mt, representing over US$ 17,000 millions gains (http://www.codelco.cl/la_corporacion/cifras.asp). On the other side, copper mine tailings discharged have severely affected coastal ecosystems. One of these

areas is the Chañaral bay, which received tailings from the mine El Salvador from 1938 to 1975. During this period, more than 150 $x10^6$ t of untreated tailings dumped caused severe beach degradation and total loss in the biodiversity (Fig. 7A-B) [52,53]. From 1976 to 1989 the dumping site was moved to Caleta Palito (26°16'S, 70°41'W), located 10 km northward, which has received $130x10^6$ t of tailings during the thirteen years. From 1990 to 2005, after the building of a sedimentation dam inside the land (at 80 Km of the coast), wastewaters have been channeled from the dam to Caleta Palito at a flow rate of 200-250 L/s, thereby maintaining severe degradation into biota (Fig. 7C-E) [28,30]. Persistently high copper concentrations prevent the growth of most algae, allowing only some opportunistic species to develop, such as the green alga *Ulva sp* or the brown algae *Scytosiphon lomentaria* or *E. siliculosus* [28,30]. Studies on some of these species have identified their special capability to tolerate metal stress, and the inheritance of this character has been discussed [35,54,55]. In 2005 a study indicated that no significant reduction of total dissolved copper had occurred in the surroundings of the Chañaral bay since 1994 [28]. In relation to this results, high amonts of dissolved copper were still observed at the sites of La Lancha and Palito (Fig. 5A) [28]. Despite sutained high copper concentrations, an increase in the species richness has been observed, accounting for the occurrence of a recovery process. These results were explained by a top-down effect caused by the absence of carnivores and the development of copper avoidance strategies. Furthermore, no population genetics studies have been carried out at this site in order to assess adaptative traits linked to this environment. Heavy metal tolerance was firmly established in the literature as one of the best examples of adaptation [56-59], and *Ectocarpus* could provide an excellent model system of the genetic bases of an adaptative trait in seaweeds.

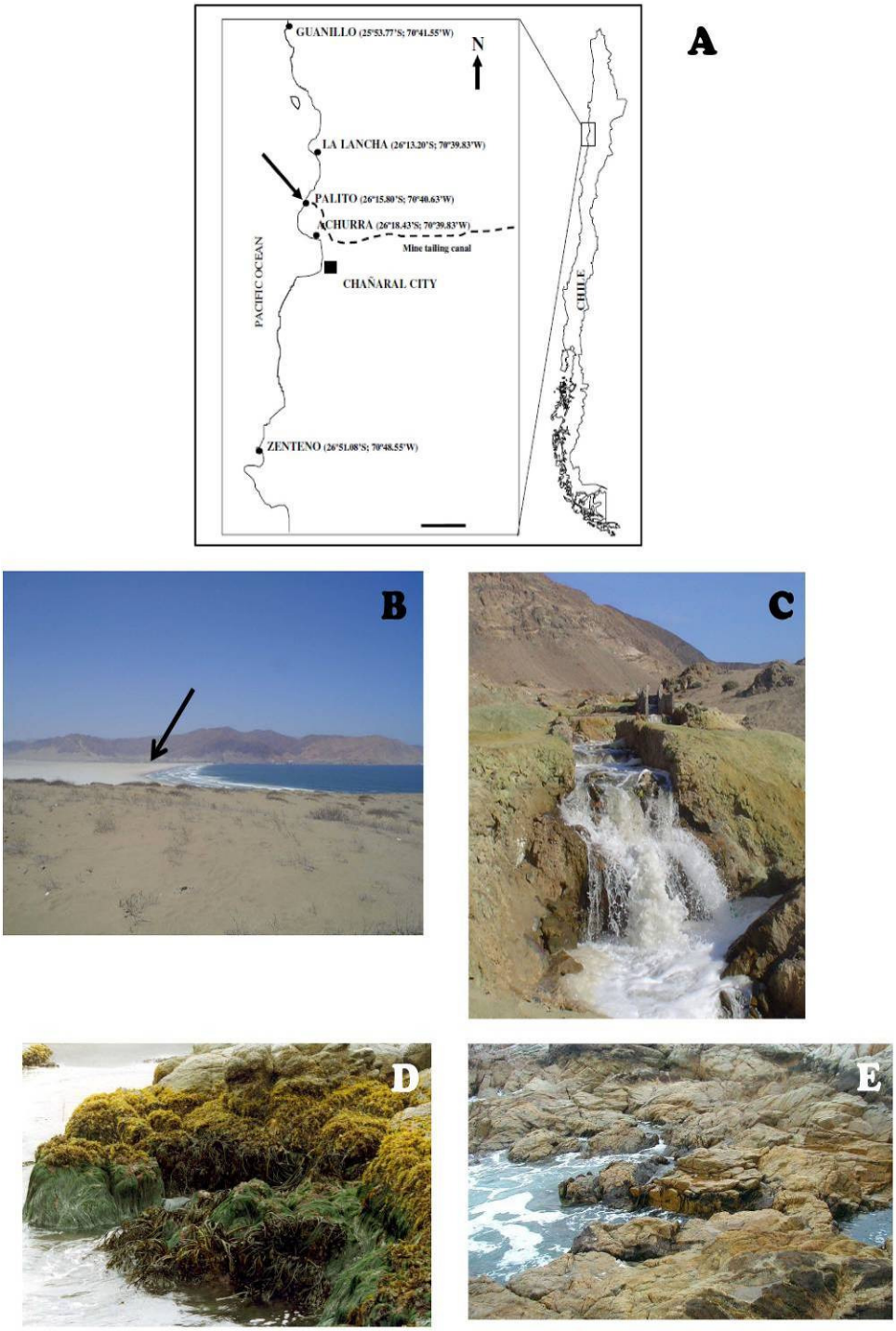

Figure 7. (A) Chañaral area and "study sites". The discharge point of the copper mine tailing is indicated with an arrow (Adapted from Medina *et al* 2005 [28]). (B) Image of the Chañaral bay, the artificial tailings created beach is indicated with an arrow (picture J. Correa). (C) River channeling copper-enriched water from the mine (picture J. Correa). (D) Representative picture of northern Chile intertidal coast (picture L. Contreras); (E) Caleta Palito (Chañaral zone) intertidal rocky shore (picture L. Contreras).

1.2. TOXIC EFFECTS OF COPPER IN LAND PLANTS AND MACROALGAE

Because of its redox properties, copper is essential for biology; however, for this same reason it also represents a serious threat for cellular processes at high concentrations [60]. Copper homeostasis should therefore be tightly controlled to avoid excess or limitations, and in this way ensure effective delivery into the active centres of many proteins and enzymes (Box 1) [61,62]. High concentration of copper causes protein inactivation, oxidative stress propagation and cell charge modification. All of these effects can lead to severe cell damage and death. In this chapter, we will focus on the observed physiological effects of copper with special focus on land plants and macroalgae.

1.2.1. Inhibition of growth and spore germination

Growth decrease and mortality represent the first parameters accounting for the toxicity of a product. Copper excess as well as other heavy metals largely inhibit elongation growth of land plants and algae [63,64]. Although several explanations have been proposed, the exact biochemical process inhibiting growth is not yet well understood. Some authors consider that copper inhibition of the cell cycle is the basis for the growth inhibition [65,66]. During the past years, ROS have been found responsible for modulating cell cycle and developmental processes [67,68]. Therefore, the copper-induced ROS production may explain the modulation of growth upon stress. In marine diatoms, it has been proposed that the high reactivity of Cu with most amino acids could cause cross linking with hydroxyproline-rich protein cell wall components, thereby inhibiting normal proliferation [69]. It has also been hypothesized that Cu-induced growth inhibition in land plants could result from the involvement of systemic responses triggered by oxylipins [70]. Finally, the ion uptake competition caused by excess of copper could also cause reduced elongation via modification

of ionic processes (such as calcium signaling) [64]. Further research needs to be carried out to determine particular growth inhibition processes.

The toxicity threshold of copper is highly variable in plants and macroalgae. In addition, the toxicity threshold varies within the tissues and life stages. In non-metallophyte plants, inhibitory effects arise at concentrations higher than 20 ppm, whereas in sedges the toxicity threshold is 575 ppm [71]. In extreme cases, such as the metallophyte copper flower (*Haumaniastrum katangense*), optimal growth is observed when copper concentrations reach 1000 ppm, although these authors do not specify the bioavailable copper concentration [72]. As in land plants, copper toxicity affects growth and causes mortality of seaweeds. Metal sensitivity varies among species, however the toxic concentration affecting growth for a wide range of seaweeds ranges around 12-75 µg/L [49]. In some cases, populations naturally exposed to high concentrations of copper present differences in their growth rate within the same species, accounting for local adaptation. The green alga *E. compressa* harvested from copper-enriched areas showed faster growth than non-tolerant isolates for concentrations up to 600 µg/L of copper [55]. Similar patterns of response to copper enrichment have been reported for copper-tolerant populations of *E. siliculosus* from England [27]. Macroalgae can have complex life histories, and different stages have been found to have different tolerance to copper. In the kelp *Lessonia nigrescens*, a high sensitivity to copper was demonstrated for early developmental gametophytic and sporophytic stages, which is not the case for adult sporophytes [30,73]. Furthermore, these authors have suggested that the absence of *L. nigrescens* from copper-polluted areas resulted from the high sensitivity of its early life cycle stages.

1.2.2. Inhibition of photosynthesis

Copper is a potent inhibitor of photosynthesis, both in algae and higher plants. The photosynthetic apparatus, both its primary photochemical side and its biochemical carbon-

fixing part, is the most important site of inhibition [61,70,74]. In all studies investigating this, a much stronger inhibition is observed in photosystem II (PSII) compared to photosystem I [75,76]. Drastically different types of damages seem to occur, depending on the irradiance conditions. The so-called shade reaction occurs in the chlorophyll (Chl) molecules of the Light Harvesting Complex (LHC) II in Chlorophyta and in the homologous Chl *a/c* complex in brown algae [61,77]. Substitution of Mg^{2+} in Chl by Cu^{2+} results in an impairment of the correct function of the LHC antenna. At high irradiance, the so-called "sun reactions" cause direct damage to PSII reaction center [61]. The PS contains several metalloenzyme components, thus copper toxicity targets are likely to be diverse. Several studies have concluded that the target of copper is close to the primary photochemical event in PSII either at the donor or at the acceptor sides [74,78,79]. Moreover, in vivo studies have concluded that Cu inhibits charge separation in PSII by the insertion of Cu^{2+} into the phaeophytin of the PSII reaction center (RC) which would cause a blockage in the electron transfer from chlorophyll to phaeophytin [77,80]. This Cu-induced blocking of electron flux leads to the production of ROS [70]. Copper-induced inhibition of photosynthesis can be observed by fluorescence measurements [81]. This method is currently used today for measuring copper stress in field and laboratory experiments [38,82,83].

1.2.3. Copper-induced oxidative stress

The term "reactive oxygen species" is employed for those forms of oxygen, sometimes combined with hydrogen, which are more reactive than the relatively stable molecule O_2. Formation of ROS is a normal process in brown algae and land plants. The fundamental electron chain reactions, photosynthesis and respiration, are the two main processes by which ROS are produced. In fact, these oxygen species represent intermediates emerging during the successive reduction of O_2 to H_2O. ROS formation starts by the excitation of O_2 leading to singlet oxygen or by transfer of one, two or three electrons to O_2, which then results in the

formation of superoxide radicals ($\cdot O_2^-$), hydrogen peroxide (H_2O_2) or hydroxyl radicals (·OH), respectively (Fig. 8A) [84]. Under normal growth conditions, the production of ROS in cell is low, thereby scavenged by cellular antioxidant systems [85]. Under uncontrolled stress conditions, ROS production can overcome antioxidant systems, shifting balance towards ROS accumulation [42]. As previously exposed, copper inhibition of photosystems results in the blockage of electron transport which causes active generation of singlet oxygen and superoxide radicals [70,86]. Singlet oxygen reacts with water to form the highly reactive ·OH in the so-called Haber-Weiss reaction (Fig. 8B). In addition, redox active transition metals such as Cu^+ and Fe^{2+} can convert H_2O_2 to the highly reactive ·OH molecule in a metal-catalyzed reaction known as the Fenton reaction (Fig. 8B) [87]. The ·OH molecule is one of the most reactive species known. Because of its ability to initiate radical chain reactions, it is very likely that this reaction is responsible for irreversible chemical modifications of various cellular components. Cellular damage by free radicals is observed in proteins, DNA, carbohydrates, and lipids [60,88]. ROS action on cell membranes results in the natural metabolic process of peroxidation of polyunsaturated fatty acids (PUFA) in membrane lipids (especially in chloroplast). This non-enzymatic reaction is initiated mainly by the most reactive oxygen species, OH and$\cdot O_2H$, which are more lipophilic than the non-protonated form, $\cdot O_2^-$, and thus able to penetrate the membranes more easily. Several laboratories and field examples of the heavy metal induced oxidative stress in plants and algae have been published [15,83,89,90]. Furthermore, chronic oxidative stress has been linked to the eradication of macroalgae in copper-polluted areas [35,54].

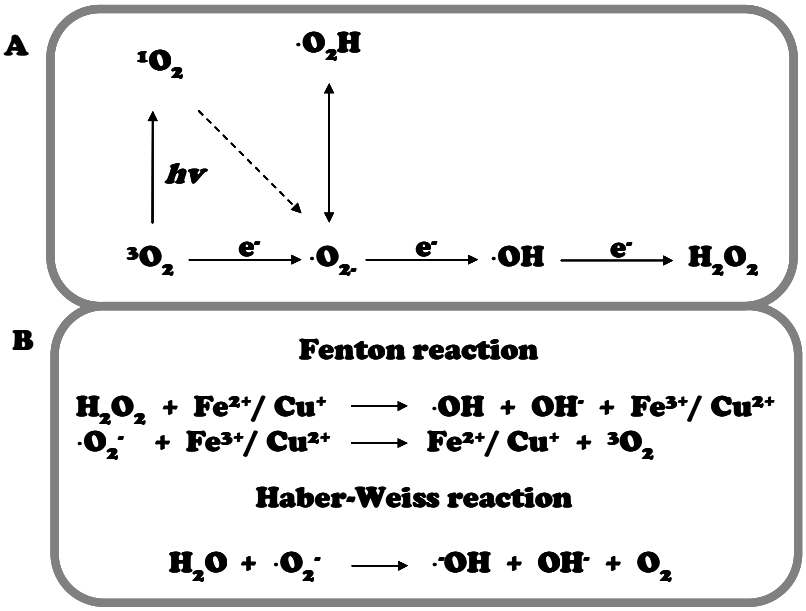

Figure 8. Non-enzymatic ROS production reactions**.** (A) Formation of different reactive oxygen species from molecular (triplet) oxygen (B) Chemical reactions involved in hydroxyl radical generation. Adapted from Dring 2006 [22].

1.2.4. Effect of copper on enzyme and protein activity

Copper is a transition metal with an incompletely filled δ-orbital as cation under physiological conditions. The physiological redox range of aerobic cells is situated around -420mV to +800mV. At these conditions, copper has a high redox potential of -0.26mV (Weast, 1984). This redox ability confers to copper some interacting features as electron carrier, illustrating why copper is the cofactor of several metalloproteins (Box 1) [91]. However, the qualities of copper can become its major default during uncontrolled excess. This metal has the ability to bind strongly to oxygen, nitrogen and sulphur atoms [92]. Copper has relatively high affinity for –SH groups, which can result in enzyme inactivation by binding to cystein residues involved in catalytic activity or by alteration of the structural integrality of the protein [93]. On the other side, excess metal uptake can induce deficiency of other essential elements and may therefore dramatically affect the cation balance at a subcellular level. This induction of other metal deficiency in metalloproteins can result in an enhanced substitution of copper for the essential metal [93]. Several examples accounting for

these processes are observed in land plants. The copper inhibition of Rubisco was explained by the interaction between Cu and SH- groups [94]. These authors have also explained this inhibition by the Cu^{2+}-induced displacement of Mg^{2+} which is essential for Rubisco activity. As previously exposed, inhibition of PSII by copper is marked by the inhibition of several metalloenzymes. In addition, Cu^{2+}-induced Mg^{2+} displacement has been proposed as a main factor of photosynthesis inhibition by copper in land plants and macroalgae [77].

1.2.5. Other alterations induced by copper excess

Excess of copper also seems to create competition for the uptake of other metals. In this context, copper can be unspecifically taken up, which affects dramatically the cation balance at subcellular levels [93,95]. In addition, copper excess can cause major ion leakage from cells. Cu excess caused increased efflux of essential ions such as K^+ in numerous land plants [96-98]. Such damage could result from various mechanisms including oxidation, thiol cross linking, ion transporter inhibition or changes in the composition and fluidity of membrane lipids [95,99]. Copper also interferes with ATP production. It has been observed in marine diatoms that copper excess induces a decrease in the ATP pool which was linked to the photosynthesis inhibition [100]. The pigment composition may also be affected by copper, particularly the chlorophyll. High concentrations of copper may lead to chlorosis by lipid peroxides or Fe uptake inhibition [101,102]. In addition Cu also affects the activity of several enzymes implicated in chlorophyll biosynthesis [93].

1.3. CELLULAR MECHANISMS OF COPPER HOMEOSTASIS AND AVOIDANCE IN VASCULAR PLANTS

1.3.1. Copper delivery into cells

In model organisms, mainly bacteria and yeast, major advances have been made during the past few years, in deciphering sophisticated homeostatic mechanisms which permit the acquisition and maintenance ofadequate intracellular copper concentrations [103,104]. These mechanisms have been subsequently found to be conserved among plants [62,105]. In seaweeds, almost nothing is known about the molecular mechanisms of copper homeostasis. Therefore, we will focus this short review on the copper delivery systems in vascular plants. Only transport systems with apparent relevance to copper will be discussed, explaining why other transition metal transporters such as CAX (calcium exchangers) of CDF (cation diffusion facilitator) have been excluded.

1.3.1.1. *Zrt-Irt-like proteins*

The Zrt-Irt-like (Zinc and Iron Regulated Transporter) proteins or ZIP, constitute a metal transporter family first identified in plants where they are capable of transporting a variety of divalent cations, including Cd, Fe, Cu, Mn and Zn [106,107]. Most ZIP proteins range from 309 to 476 aa in length, and the majority posses 8 TMDs with a variable region between TMD III and IV which is though to contain metal binding domain [107]. The ZIP family in *Arabidopsis* is composed of one iron-regulated (IRT1) and 14 zinc-regulated transporters [108]. Metal uptake experiments and growth assays in complemented yeast mutants suggest that IRT1 transports a broad range of divalent metal ions but not Cu [109]. On the other hand, the *Arabidopsis* ZIP2 and ZIP4 family members seem to be involved in the

uptake of Zn^{2+} and Cu^{2+}. Although the exact implication of ZIP transporters into Cu uptake is not yet clear, the expression of ZIP2 and ZIP4 is up-regulated in *Arabidopsis* by Cu deficiency [110].

1.3.1.2. *CTR family of high affinity copper transporters*

The conserved CTR family of Cu transport proteins mediates high-affinity Cu acquisition from the exterior into the cytoplasm of eukaryotic cells, ranging from yeast to mammals [62,104,105,111]. All CTR family members contain three putative transmembrane regions, with most of the aa similarity confined to a large hydrophobic stretch. The amino-terminal region is rich in methionine residues that are arranged as MXXM and MxM motifs. These motifs are thought to bind heavy metals [111]. The carboxy-terminal region is rich in charged amino acids and contains rather well conserved cystein and histidine residues. In plants, there are several CTR transporters that have been described to transport copper and therefore they were called Copper Transporter Protein (COPT). Some members are thought to be expressed in the plasma membrane whereas others are active in internal membranes, facilitating the release from intracellular stores (Fig. 9) [112]. The COPT1 transporter is likely to be active in the plasma membrane [104].

1.3.1.3. *NRAMP family of divalent cation transporters*

NRAMP proteins are a family of divalent metal transporters in eukaryotic organisms [113]. NRAMP stands for “Natural Resistance-Associated Macrophage Protein”, since Nramp1 was originally identified in mice as a gene conferring bacterial resistance [113]. These membrane proteins co-transport, by proton motive force, a variety of divalent metals including Cu^{2+}. They are characterized by a conserved hydrophobic core of ten transmembrane domains (TMDs) and either one or two non-conserved highly hydrophobic additional TMDs. In vascular plants NRAMP participate in plant intracellular Fe^{2+}

distribution [62]. In *Arabidopsis*, NRAMP1 over-expression confers increased Fe toxicity resistance and preferential root localization, suggesting its role in metal distribution [114]. NRAMP3 and NRAMP4 seem to be implicated in the Fe retrieveval from the vacuole [62]. In addition, they seem to transport other heavy metals sequestered in the vacuole such as Cd^{2+} [115]. Furthermore, in *Arabidopsis*, the transporter EIN2, a central signal transducer in the ethylene-signaling pathway, derives from the NRAMP family [116].

1.3.1.4. *Copper transporting P-type ATPases (HMA)*

P-type ATPases form a large family of transporter proteins which hydrolyze ATP for transporting a broad range of small cations, and possibly phospholipids, across cell membranes; they have been found in bacteria, fungi, yeast, animals and plants [104,105,117]. These pumps constitute the main heavy metal tolerance mechanism in bacteria [118]. In plants, five subfamilies have been determined according to their function [119]. The P1b subfamily is involved in the transport of heavy metals and these ATPases are therefore referred to as heavy-metal P-type ATPases [119]. They are also called HMA, because of their characteristic Heavy Metal Associated (HMA) motif consisting of a conserved MxCxxC aa motive. In *A. thaliana* 8 HMAs have been identified and separated into two groups according to their substrate specificity and sequence homology. A fist group is involved in the transport of monovalent ions such as Cu^{+}, and a second group is involved in divalent cation transport given their relation to their prokaryote homologues [112,117]. The Cu-transporting branch of the HMA family is characterized by the presence of a CPC aa ion transduction motif in the sixth predicted transmembrane domain, and by one or several HMA motifs. Some of theses proteins have been suggested as playing a role in plant copper detoxification, in particular AtHMA5 (Fig. 9) [120]. In *A. thaliana*, the expression of this transporter is predominant in roots, and is induced in response to copper excess. Moreover, *hma5* mutant displayed several defective copper-mediated processes and copper sensitivity [120]. On the other side,

enhanced ATP-dependent copper efflux across the root cell plasma membrane in copper-tolerant *Silene vulgaris* may be mediated by HMA ATPases [121].

1.3.1.5. *Copper chaperones*

Once inside the cell, the limited solubility and high reactivity of Cu requires the participation of specialized cellular factors named Cu chaperones. These factors are Cu binding soluble proteins that mediate intracellular Cu delivery to specific target to form biologically active Cu proteins [122]. Several independent Cu chaperones have been described in *S. cerevisiae*: Antioxidant 1 (Atx1) shuttles Cu to a P-type ATPase located within a post-Golgi compartment for translocation into the secretory pathway [123]; Cu chaperone for Cu/ZnSOD (Ccs1) is required for Cu insertion into the active site of cytosolic Cu/ZnSOD, and Cox17 is involved in Cu trafficking towards mitochondrial cytochrome *c* oxidase (COX) [104]. The *Arabidopsis* CCH protein was the first Cu chaperone described in plants [124]. This gene contains the conserved HMA motif (MxCxxC) that is related to copper binding. Although CCH expression is rather constitutive in plants [124], this chaperone could actively deliver copper to HMA ATPases upon stress conditions (Fig. 9). Cu chaperone for Cu/ZnSOD (CCS1) is required for Cu^{+} insertion into the active site of cytosolic Cu/ZnSOD [112]. As far as plant CCS are concerned, only one gene has been reported in *Arabidopsis*, although three CuZnSOD exist within three different compartments [62]. This underlines that copper delivery systems similar to metazoan ones may exist in plants. With respect to Cox17, it has been reported in green plants which is involved in Cu^{+} trafficking towards mitochondrial cytochrome c oxidase (COX) [125]. In addition, the *Arabidopsis* Atx1 homologue was shown to interact with RAN1 and HMA5 P-type ATPases metal-binding domains [120]. Finally, CutC are other chaperones also associated with cellular Cu^{+} and Cu^{2+} trafficking [126]. CutC were initially found in bacteria, then in mammals and chlorophyta (*Ostreocuccus sp*.). In bacteria, they play an important role for copper homeostasis [103].

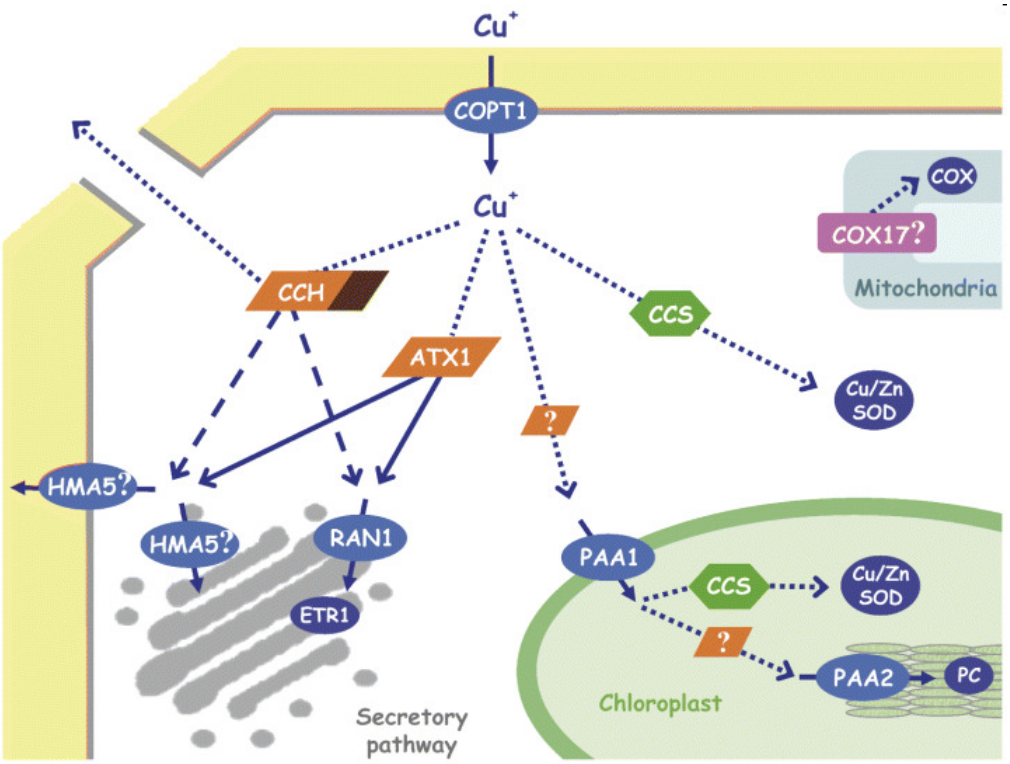

Figure 9. Subcellular distribution of copper by *Arabidopsis* metallochaperones. A speculative diagram showing subcellular distribution of copper in a generic plant cell is represented. Cu transporters and Cu proteins are represented in blue, while Cu chaperones are in orange, green and pink. Dotted lines indicate putative Cu delivery pathways; continuous lines represent interactions demonstrated by yeast two-hybrid, and discontinuous lines mean the lack of interaction unless the protein is processed. Question marks indicate unclear chaperones or steps. COPT, copper transporter; COX, cytochrome *c* oxidase; CCH, copper chaperone; ATX1, antioxidant 1; CCS, Cu chaperone for Cu/ZnSOD; SOD, superoxide dismutase; HMA, heavy metal P-type ATPase; RAN1, responsive-to-antagonist 1; PAA, P-type ATPase of *Arabidopsis*; PC, plastocyanin. Adapted from Puig *et al.* (2007) [62].

1.3.2. Cellular mechanism for copper avoidance

Tolerance to heavy metals in plants may be defined as the ability to survive in an environment that is toxic to other plants, and is manifested by an interaction between a genotype and its environment [58,127]. Nevertheless, the term is frequently used more widely in the literature to include changes that may occur experimentally in the sensitive response to heavy metals [128]. As explained in the previous chapter, uncontrolled copper excess cause damage that affect several physiological processes which can lead to cell death. In order to avoid these symptoms, plants have developed a range of potential mechanisms that are

involved in detoxification and tolerance of this type of metal stress. These mechanisms appear to be involved primarily in avoiding the build-up of toxic concentrations at sensitive sites of cells. Several strategies for metal avoidance exist (Fig. 10). They will be discussed from the extracellular levels toward subcelullar mechanisms.

1.3.2.1. *Mycorrhizal symbiosis*

Under natural conditions, roots of many plant species, especially those of trees, are associated with mycorrhizal symbionts. This association is of high importance for plant nutrition balance [129]. In addition, mycorrhization can significantly modify the response of plants to heavy metals, conferring enhanced tolerance [91]. The mycorrhizal species *Suillus bovinus* and *Thelephora terrestris* succeeded to protect *Pinus sylvestris* against copper toxicity, because the amount of Cu accumulated by the two fungi was considerable [130]. Extracellular and cellular mechanisms potentially involved in the tolerance of ectomycorrhizal fungi to heavy metal have recently been reviewed (Fig. 10) [131]. It appears that metal tolerance mechanisms employed by ectomycorrhizal fungal species are common to the systems found in non-mycorrizal fungi. This includes reduction in metal uptake, extracellular chelation by extruded ligands, and binding to cell wall components. Intracellular chelation involving glutathione and metallothioneins, and subcellular sequestrations are also involved in fungi tolerance. In relation to the role of ectomycorrhizas in metal tolerance by the host plant, most mechanisms which have been proposed involve various exclusion processes that restrict metal movements to the host roots. This includes absorption of metals by the hyphal sheath, reduced access to the apoplast due to the hydrophobicity of the fungal sheath, chelation by fungal exudates, and adsorption onto external mycelium [132].

1.3.2.2. *Cell wall binding*

The binding properties of the cell wall and its role in mechanisms of metal tolerance have been controversial. Earlier reports have been reviewed [133] and there are only a few more papers on this topic. Although the root cell wall is in direct contact with metals in the soil solution, adsorption onto the cell wall must be of limited capacity and thus have a limited effect on metal activity at the surface of the plasma membrane. It is also difficult to explain metal-specific tolerance by such a mechanism [133]. However Brigenzu *et al.* [134] reported that the heavy metal-tolerant *Silene vulgaris* accumulated a range of metals, including copper, along the epidermal cell walls, by a mechanism that is not well characterized. Root exudates have a variety of roles, including that of metal chelators, which may enhance the uptake of certain metals (Fig 10). These exudates of organic acids could also help to chelate and detoxify metals (see below).

1.3.2.3. *Repair of damaged structures*

Even if repairing systems are not the most important players in the establishment of tolerance, they can play a significant role in buffering deleterious effects of copper stress (Fig. 10). Some examples of these mechanisms are protein refolding, protein turnover, conjugation of fatty acid peroxidation products, or DNA repairing systems. Among these actors, Heat Shock Proteins (HSPs) are characteristically increased under several environmental stresses, including heavy metals [135,136]. These proteins are found in all groups of living organisms, and they are classified according to their molecular weight. They act as molecular chaperones in normal protein folding and assembly, but may also function in the protection and repair of proteins under stress conditions [136]. Several reports indicate the increase of these proteins under heavy metal stress in plants [137,138]. Cadmium stress was shown to up-regulate ten different HSP70 and one HSP60 in *Arabidopsis*. In Cu-rich soils, *Armeria maritima* actively expressed HSP17 in the roots. Beside HSPs, The GSTs (glutathione transferases) are

ubiquitous enzymes involved in the detoxification of a wide variety of hydrophobic substrates [139]. These enzymes conjugate damaged structures, such as altered (peroxidated) membrane fatty acids, to glutathione, and conjugates are then excreted by ABC transporters [140]. GSTs and glutathione involved enzymes have been demonstrated to be up-regulated in response to copper stress in plants [141]. Glutathione is a thiol tripeptide made out of cystein, glycine and glutamate [142]. It is the substrate for GSTs, but it is also the substrate for gluthathione peroxidase (see 1.5.1) and phytochelatin synthetases (see 1.3.2.5), which have a pivotal importance for ROS detoxification and metal chelation [68,143]. Therefore, the glutathione metabolism plays a fundamental role in cellular protection against copper toxicity.

1.3.2.4. *Plasma membrane active copper efflux and uptake inhibition*

In normal conditions, the lipid bilayer of plasma membrane constitutes an impermeable barrier for electrically charged ions such as Cu^{2+}. However, as previously discussed in this chapter, membrane function may be rapidly affected by copper excess and thus, active efflux of copper by heavy metal P1b-ATPases (HMA) may represent an important actor for maintaining Cu homeostasis. Vacuolar copper sequestration could also play a role into copper detoxification, involving transporters such as CDFs, Nramps and CAXs [128]. However, to our knowledge none of these latter proteins have been shown to be involved in plant copper transport [112]. As previously explained in this chapter, CTR transporters are a family-specific high affinity copper transporter. The COPT1 transporter is likely to be active in the cell membrane and its expression is negatively regulated by copper excess [112].

1.3.2.5. *Phytochelatins*

PCs are metal chelation polypeptides synthesized from glutathione by a specific γ-glutamylcysteine dipeptidyl transpeptidase commonly called PC synthase. PCs complex metals in the cytoplasm, from which they are pumped into the vacuole by ABC multidrug

resistance transporters, were they form high molecular weight complexes by sulphur addition [115]. Phytochelatins were first discovered in plants, and since then, their occurrence has also been reported in nematodes and in the slime mould *Dictyostelium discoideum* [144]. In normal non-hyperaccumulating plants, metals remain bound to PCs in the vacuole where they form high molecular weight complexes [144]. Although PCs have mostly been associated to Cd excess in plants, PC synthase induction was also shown in *S. cucubalus* upon copper excess [145]. However, these authors concluded that copper tolerance in *S. cucubalus* does not depend on the production of phytochelatins, but that it is related to the plant ability to prevent glutathione depletion resulting from copper-induced phytochelatin production, e.g. by restricting its copper uptake. This was confirmed by later studies showing that the blocking of PC synthesis does not affect the resistance of plants against copper [146]. Taking into account the affinity of copper to -SH, it is surprising to observe the reduced amount of literature accounting for the implication of PCs into copper stress tolerance.

1.3.2.6. *Metallothioneins*

Metallothioneins (MT) are small gene-encoded proteins that present two cystein rich domains and one spacer in between. These proteins are ubiquitously present in eukaryotes and prokaryotes, playing an important role in heavy metal detoxification and homeostasis. The high number of cysteine residues in MTs allow them to bind a variety of metals by mercaptide bonds. Four classes of MTs have been defined in green plants according to the Cys arrangements and the length of the spacer [144]. Class 1 and 2 are induced by copper treatment [147]. When genes MT1 and MT2b from *A. thaliana* were expressed in an MT-deficient yeast mutant, both genes confered high levels of resistance. Beside copper detoxification, MTs have been proposed to be involved in copper transport as chaperones in *A. thaliana*. To examine the tissue-specific expression of MT genes, GUS reporter gene activity driven by promoters of MT1a , MT2a , MT2b and MT3 was analysed in transgenic

Arabidopsis plants [148]. MT1a and MT2b are expressed in the phloem of all organs and are copper (Cu)-inducible; in contrast, MT2a and MT3 are expressed predominantly in mesophyll cells, and are also induced by Cu in young leaves and at root tips. Expression of MT genes is also highly induced by Cu in trichomes and increased during senescence. Expression of MT4 genes is restricted to seeds. Some studies proposed that plant MTs have distinct functions in heavy metal homeostasis, especially for Cu: MT1a and MT2b are involved in the distribution of Cu via the phloem, while MT2a and MT3 chelate excess metals in mesophyll cells and root tips [148].

1.3.2.7. *Organic acids*

The importance of metal-binding ligands, also called "phytosiderophores", in metal homeostasis is becoming clearer, as a number of small organic molecules have been identified as being required to fulfill roles as chelators for metal tolerance and uptake within plants. Only organic acids with a demonstrated role in copper uptake and tolerance will be discussed here. The non-proteogenic amino acid nicotinamine (NA) has been associated with Fe and Cu homeostasis [149]. NA is produced at much higher levels in the metallophyte *A. hallieri* rather than in the metal-sensitive *A. thaliana*, suggesting its role in metal tolerance [150]. Futhermore, NA may also be important for sequestration of metals such as Fe and Cu into the vacuoles; effectively, immuno-histochemical detection of NA in pea and tomato suggested that, under excess of Fe supply, NA concentrations increase and accumulate in vacuoles [151]. Free histidine was also found to be involved in copper uptake and transport [152]. This amino acid is highly excreted in xylem exudates of the metallophyte *Alyssum lesbiacum*, conferring high tolerance to nickel [153].

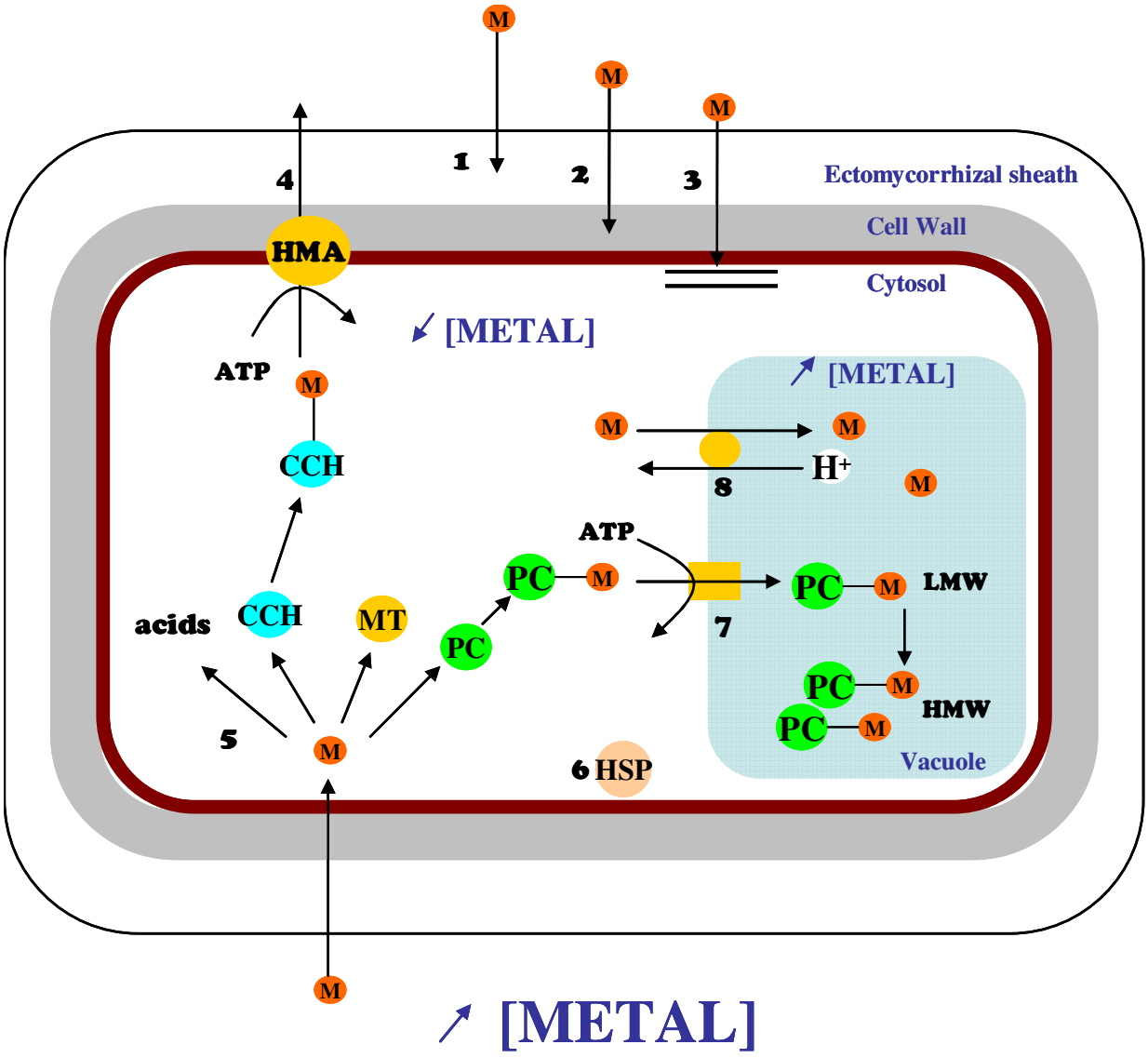

Figure 10. Summary of potential cellular mechanisms implicated in metal detoxification and tolerance in higher plants; modified from Hall (2002) [128].
1. Restriction of metal movement to roots by mycorrhizas.
2. Binding to cell wall and root exudates.
3. Reduced influx across plasma membrane.
4. Active efflux protection of plasma membrane under stress conditions.
5. Chelation in cytosol by various ligands.
6. Repair and protection of cellular structures under stress.
7. Transport and protection of PC-M complex into the vacuole.
8. Transport and accumulation of metals in vacuole.

1.4. CELLULAR MECHANISMS OF COPPER EXCESS AVOIDANCE IN BROWN ALGAE

1.4.1. Copper exclusion

Compared to the large body of literature in vascular plants, much less is known about the mechanisms responsible for copper detoxification in brown algae. Moreover, in some cases, results seem to be contradictory. Early studies in tolerant populations of *E. siliculosus* have explained its differential tolerance by enhanced copper exclusion mechanisms rather than extracellular exclusion of exudates [154]. On the other hand, later studies in the same species observed an enhanced liberation of metal-complexing exudates upon chronic copper excess [155]. However, the nature of these exudates was not determined.

1.4.2. Phytochelatins

Gekeler *et al* have first demonstrated the ability of brown algae to synthesize PCs in response to Cadmium [156]. Their structure was similar to PCs in vascular plants, presenting a structure $(\gamma\text{-Glu-Cys})_n$–Gly where n = 2-5. Furthermore, they discussed about previously published Cu and Cd-binding proteins in algae as probably being related to PCs. No further studies on brown algal PCs were carried out since, until recently. The PCs concentrations of naturally occurring *Fucus vesiculosus* and *F. serratus* populations were found to be correlated to their copper contamination history along the estuary of the Restronguet river in England [157]. In addition, PC-production was correlated with a high content of glutathione in populations originating from Cu-enriched areas. Furthermore, PCs lengths varied between the two *Fucus* species. Based on these results, Pawlik-Skowronska *et al.* concluded that metal detoxification and resistance in *Fucus* implies PC-based mechanisms. In addition, this

mechanism could partially explain the success of these species in natural copper-polluted areas. However, currently there is still no genomic data describing PC synthase in brown algae.

1.4.3. Metallothioneins

One MT gene was isolated in *F. vesiculosus* from a cDNA library constructed for populations adapted to elevated copper concentrations in the estuary of the Restronguet river in England [158]. The identified gene encoded for a 67 aa protein exhibiting several characteristic features of MT proteins, including two cystein-rich domains with 16 conserved cystein residues. Although the protein displays high degrees of identity with plant and invertebrate MTs, it contains a small different spacer (14 amino acid residues) between the putative cystein metal binding domains. Upon copper excess, high induction of *F. vesiculosus MT* gene was observed, accounting for its probable role in controlling intracellular copper excess. In addition, recombinant *F. vesiculosus* MT showed high affinity for Cd and Cu complexation. Further studies have also demonstrated the ability of MTs to chelate As [159].

1.4.4. Physode sequestration of heavy metals and phenolics chelation

Several studies have detected the enrichment of heavy metals, including copper, in the physodes [14,160]. Phlorotannins, packed within membrane-bound physodes, appear to play multiple roles in brown algae. These polyphenols have high affinity to heavy metals [160], therefore their function as heavy metal chelators has been proposed in the past [161]. On the other side, early studies have demonstrated that brown algae excrete polyphenols which are able to chelate divalent cations [162] However, a contradictory study shows no change in the phlorotannin content in the brown alga *Ascophyllum nodusum* upon copper excess [163].

1.4.5. Cell wall and polysaccharide heavy metal binding

In contrast with land plants, the brown algal cell wall matrix is composed of polyanionic charged polyshaccharides (alginates and fucoidan). For this reason, it is thought that cell wall can act as a primary ion filter by cation exchanger and ionic barrier, selecting ions that would be absorbed by algal cells [8,12]. In addition, the very high selectivity of alginates and fucoidan for heavy metal, in particular Cu^{2+}, has led to consideration of the use of these compounds for heavy metal pollution remediation [12]. It has been demonstrated in *Padina gymnospora* that heavy metals are strongly accumulated in granules that co-localize with cell wall charged polysaccharides such as fucans [14,164,165]. Furthermore, these heavy metal analysis revealed the presence of sulphur and oxygen association with heavy-metal granules, underlying their sequestration by sulphated polysaccharides [164].

1.4.6. Repair of damaged structures

Previous work in *L. digitata* showed the induction of several GSTs genes upon acute copper stress and by oxylipins [166]. Phylogenetic analysis showed that most of these enzymes were distinct from previously described GST classes, and were closely related to the Sigma class. Similar results were obtained in *E. siliculosus* [167].

1.5. HEAVY METAL-INDUCED ANTIOXIDANT DEFENSES IN PLANTS AND ALGAE

1.5.1. ROS scavenging mechanisms

If copper stress shifts the balance towards ROS accumulation, then oxidative stress can lead to the worst scenario of cell death [60]. Although antioxidant systems do not seem to be the most determinant factor for metal tolerance, these mechanisms play a fundamental role for buffering heavy metal ROS production in vascular plants and algae [35,89,90,168-170]. ROS scavenging and metal ion sequestering is thought to be important to prevent the formation of the highly toxic hydroxyl radical via the copper-dependent Haber-Weiss/Fenton reactions (Fig. 8) [68]. In this context, living organisms have established effective antioxidant mechanisms [42,68,86,88]. The ability of plants and seaweeds to combat these negative consequences resides in their antioxidant systems which are mainly separated into enzymatic and non-enzymatic ROS scavengers. Both of these systems act coordinately in order to avoid oxidative cell damage. Major ROS-scavenging pathways of plants and algae include the water-water cycle in chloroplasts; the ascorbate-glutathione cycle in chloroplasts, the cytosol, mitochondria, apoplast and peroxisomes; the glutathione peroxidase cycle (GPX) in almost all cellular compartments and catalase (CAT) in peroxisomes (Fig. 11A-D). SOD catalyzes the dismutation of superoxide radical to O_2 and H_2O_2. This enzyme is found in almost all cell compartments and it is defined as the first barrier to ROS production (Fig. 11) [68]. Several distinct forms of SOD have been found in photosynthetic organisms, incorporating different metals as cofactors [171]. The thylakoid membranes and cytosol of vascular plants and some algae contain CuZnSOD, whereas forms of SOD found in the stroma of the chloroplast contain FeSOD and those in the mithochondria and peroxisomes contain MnSOD [22]. It is

the activity of these various forms of SODs in plants that is thought to provide the major protection against the damaging effects of superoxide [15]. Moreover, their regulation is tightly dependent upon the mineral nutrition [62]. Scavenging of superoxide by SOD results in the production of H_2O_2 which, although less damaging than the superoxide radical, is far from harmless and especially in the presence of metals like copper. For this reason, H_2O_2 detoxification is of crucial importance. Three main redundant enzymatic systems can scavenge H_2O_2 with different affinities, suggesting that they belong to two different classes. One is responsible for accurate regulation of ROS when they are present at the µM range, the ascorbate peroxidase (APX); whereas the CAT system might be responsible for the removal of excess of ROS at the mM range upon oxidative stress [41,68]. CAT can directly detoxify H_2O_2 to produce O_2 (Fig 8d), while H_2O_2 is indirectly detoxified by the APX system which require ascorbate. This results in the oxidation of ascorbate, which is regenerated by the oxidation of glutathione, which is in turn regenerated by glutathione reductase (GR) using NADP. This cycle is known as the ascorbate-glutathione cycle. Besides, APX act in coordination with SOD to scavenge ROS produced by photosynthetic reactions [172]. Photoreduction of dioxygen in PSI of chloroplasts generates superoxide radicals as the primary product (Fig. 11A). In intact chloroplasts, the superoxide and the hydrogen peroxide (which is produced via the disproportionation of superoxide) are rapidly scavenged, which prevent ROS to inactivate the PSI complex, the stromal enzymes, or the scavenging system itself. This cycle is called “water-water”, because the radicals produced from water splitting during photosynthesis are reduced back to water through SOD and APX. On the other side, GPX also detoxifies H_2O_2 and requires glutathione, which is oxidized and subsequently regenerated in turn by glutathione reductase (GR) using NADP as well. This cycle is known as the glutathione peroxidase cycle (Fig. 8C). This ratio of GSH is maintained by glutathione reductase (GR), monodehydroascorbate dehydrogenase (MDAR), and Deshydroascorbate

deshydrogenase (DHAR) using NADPH as reducing power. The overall balance between different antioxidants has to be tightly controlled. Enhanced GSH biosynthesis in chloroplasts can result in oxidative damage to cells rather than their protection, possibly by altering the overall redox state of chloroplast. Besides enzymatic cycles, non-enzymatic ROS scavengers are also fundamental in controlling ROS concentrations. They encompass varied organic compounds such as GSH, ascorbate, flavonoids, tocopherols and carotenoids. In plants and algae, carotenoids have 2 distinct functionalities: they enlarge the photosynthetic light absorption spectrum, and they protect light harvesting pigments against photochemical damage caused by ROS [173,174]. Flavonoids are also important antioxidants in plants and algae, and are currently associated with the prevention of lipid peroxidation. They have been widely accepted as so-called “chain-breaking antioxidants” because they react very efficiently as radical scavengers and their aroxyl radicals are sufficiently stable to avoid propagating reactions [175]. In brown algae, phorotannins are thought to play important roles as ROS scavengers, therefore enhanced levels are observed in response to both biotic and abiotic stresses [13,160]. Ascorbate and glutathione are also of particular interest as direct ROS scavengers or as a substrate for antioxidant enzymes (see below) [15]. As mentioned previously in this chapter, iodide itself is an efficient, inorganic ROS savenger playing a pivotal role as inorganic ROS scavenger in the brown alga *L. digitata* (see 1.1.2) [19].

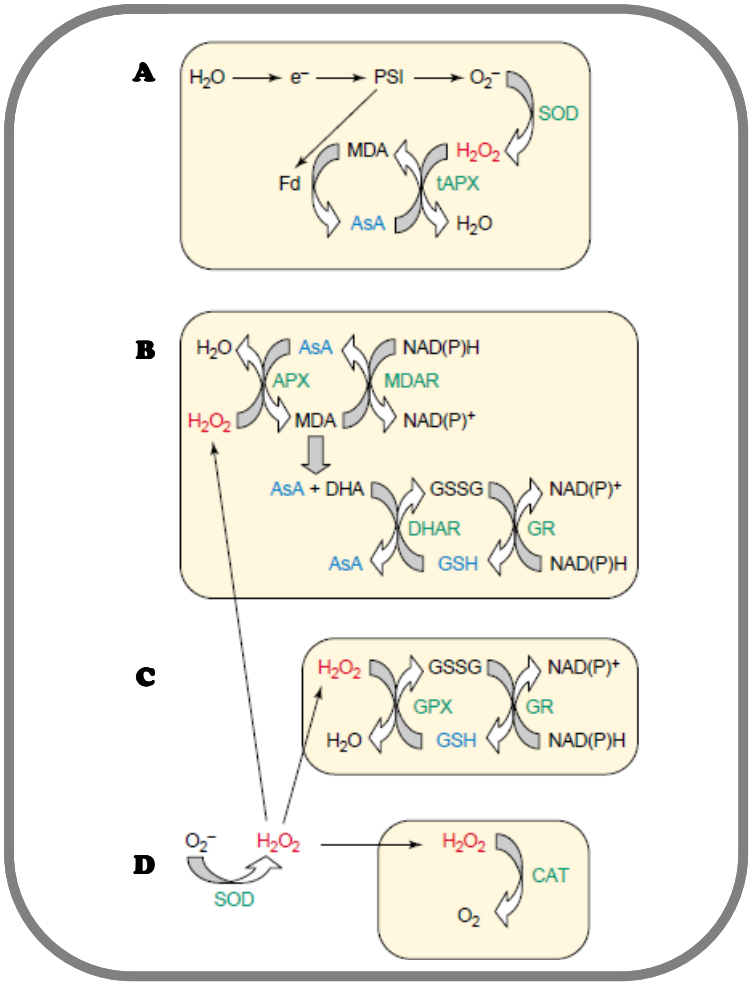

Figure 11. Pathways for reactive oxygen species (ROS) scavenging in plants. (A) The water–water cycle. (B) The ascorbate– glutathione cycle. (C) The glutathione peroxidase (GPX) cycle. (D) Catalase (CAT). Superoxide dismutase (SOD) acts as the first line of defense converting O_2 – into H_2O_2. Ascorbate peroxidases (APX), GPX and CAT then detoxify H_2O_2. In contrast to CAT (d), APX and GPX require an ascorbate (AsA) and/or a glutathione (GSH) regenerating cycle (A–C). This cycle uses electrons directly from the photosynthetic apparatus (A) or NAD(P)H (B,C) as reducing power. ROS are indicated in red, antioxidants in blue and ROI-scavenging enzymes in green. Abbreviations: DHA, dehydroascorbate; DHAR, DHA reductase; Fd, ferredoxin; GR, glutathione reductase; GSSG, oxidized glutathione; MDA, monodehydroascorbate; MDAR, MDA reductase; PSI, photosystem I; tAPX, thylakoid-bound APX. From Mittler *et al.* (2002) [68].

1.5.2. ROS signal transduction pathways

ROS were initially recognized as toxic by-products of aerobic metabolisms, which have to be detoxifid by antioxidant mechanisms. In the past years, it has become apparent that ROS also play an important role as signaling products in plants by modulating growth, cell

death, development, hormonal biosynthesis, as well as biotic and abiotic stress responses [41]. Recently, ROS-generating enzymes, such as NADPH oxidases, demonstrate that plants and algae can initiate and amplify ROS production in order to generate a signal [46,176]. ROS signaling is ephemerons; therefore, antioxidant systems must be actively coordinated in order to avoid damage by these compounds [41]. Although the receptors for ROS are unknown at present, it has been suggested that cells sense ROS via at least three different mechanisms: unidentified receptor proteins, redox-sensitive transcription factors, and direct inhibition of phosphatases by ROS. ROS sensing also interact with Ca^{2+} signaling in plants. In the brown alga *Fucus vesiculosus*, it is has been demonstrated that copper excess induces ROS production and subsequently variation of the Ca^{2+} content [177]. Moreover, ROS-induced Ca^{2+} signals activate mitogen-activated protein kinases (MAPK) cascades [178]. These mechanisms have been shown to occur under biotic and abiotic stresses, including copper stress in plants. This indicates that besides causing oxidative stress, copper can employ additional mechanisms to selectively activate particular MAPKs [178,179]. Next, these first signals trigger the accumulation of phytohormones such as the oxylipins of the family of jasmonates, which are generally regarded as key components in the coordination of plant responses [40,45,180,181]. These hormones are specifically up-regulated and orchestrate the plant response to various biotic and abiotic stresses [182,183].

1.6. OXYLIPIN METABOLISM IN MARINE ALGAE

ROS generation can trigger a variety of cellular responses through signaling events. One of these responses is the activation of fatty acids by the generation of oxygenated polyunsaturated fatty acids known as oxylipins. These molecules play a pivotal role during abiotic and biotic stress response in plants and metazoans. They are produced from polyunsaturated fatty acid (PUFA) oxidation, by incorporation of one, two or four atoms of oxygen. These reactions can be carried out non-enzymatically by direct oxidation of PUFAs by ROS, or catalyzed enzymatically (Fig. 12A). In mammals, oxylipins such as leukotrienes and prostaglandins are produced from the oxidation of C20 PUFAs by cyclooxygenases (COX), Lipoxygenases (LOX) or cytochromes P450 (CP450) (Fig. 12B). These compounds play a major role in inflammatory processes, allergy, and, in a broader sense, responses to infection, drugs, and xenobiotics [184]. In contrast, terrestrial plants have lost the ability to synthesize arachidonic acid, therefore they employ C18 and C16 PUFAs to synthesise oxylipins. These compounds have important functions in development, after wounding, and under pathogen and herbivore attacks [44,45,185].

In response to pathogen stimuli, biosynthesis of oxylipins in plants, red algae and mammals, is started by the release of PUFAs catalysed by phospholipases and galactolipases (Fig. 12A) [46,186,187]. Oxylipin enzymatic biosynthesis in plants is carried out mainly by LOX, cytochrome P450 and pathogen induced oxygenase (PIOX), even if the biological role of this last enzyme is not clear. LOXs catalyse the oxygenation of PUFA in order to create hydroperoxides, which, because of their high reactivity, are rapidly metabolized into secondary products, that can involve the activity of P450 family enzymes such as AOS in the jasmonic acid (JA) pahtway (Fig. 12C) [188,189]. Jasmonic acid, is known to play a key role in stress-mediated responses [45,185]. Although many examples of plants synthesizing and

accumulating oxidized fatty acid derivatives in response to biotic or abiotic stress have been reported [40,188,189], limited attention has been paid to the involvement of oxylipins in the stress response to heavy metals. The extensive literature on cross-talk mechanisms between biotic and abiotic stress suggest that compounds such as oxylipins could also be implicated in heavy metal detoxification mechanisms [43]. Maksymiec *et al*. showed the synthesis of JA upon copper stress in *Phaseolus coccineus* [190]. However, further studies in plants are still needed to characterize the involvement of this oxylipin in heavy metal stress.

In algae, a growing set of evidence account for the involvement of oxylipins in defense reactions set up during biotic stress [46,191]. Gerwick *et al.* have pointed out the originality of oxylipin metabolism in brown algae. Based on the function of some prostaglandins in mammals, these authors have suggested the involvement of marine algal oxylipins in ion transport and osmotic regulation. [192]. Marine algae are known to produce unique oxylipins, however little is known about their biosynthetic pathways [193].

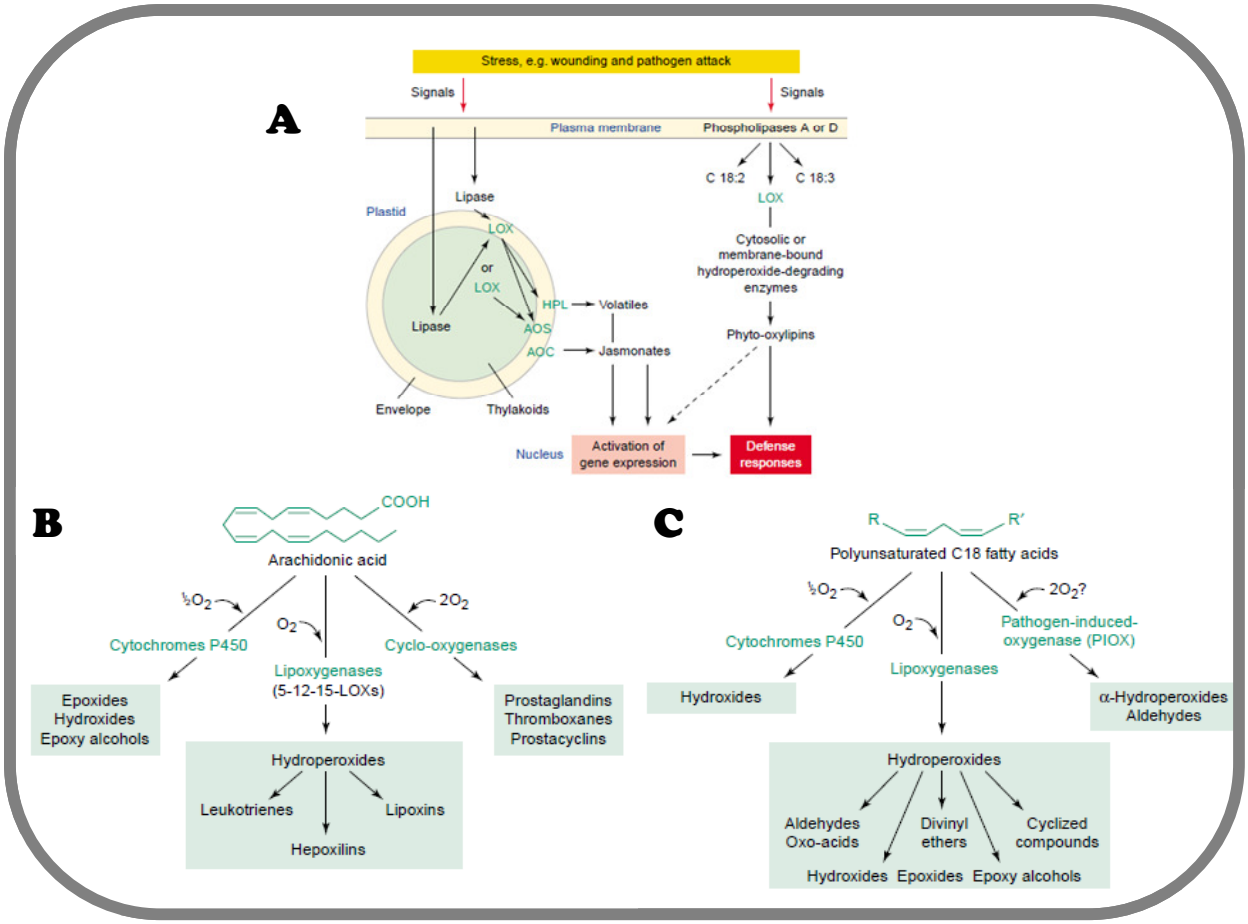

Figure 12. (A) Signaling pathways of plant oxylipins. Key signals that trigger the liberation of unsaturated fatty acids are poorly defined but might include ion fluxes, active oxygen species, protein phosphorylation cascades, plant hormones, peptide signals, glycans, volatile chemicals and electrical signals. Phyto-oxylipin cascades could begin in plastids, where unsaturated fatty acids are liberated from plastidial phospholipids or galactolipids by phospholipases A1 or by acyl hydrolases such as galactolipases. Then, hydroperoxides resulting from the oxygenation of these fatty acids by plastidial 13-lipoxygenase (LOX) could be transformed by the allene oxide synthase (AOS) or the hydroperoxide lyase (HPL) present in the plastid envelope. Alternatively, polyunsaturated fatty acids could be liberated from plasma membranes under the action of phospholipase A or D, then oxygenated by cytosolic 9-LOX or membrane-bound LOXs. Except for plastidial AOS and HPL, the localization of the other hydroperoxide-degrading enzymes is unknown, although most of them are thought to be membrane-bound proteins. 9-Hydroperoxide-derived signal molecules have not been identified. Abbreviations: AOC, allene oxide cyclase; DES, divinyl ether synthase; EAS, epoxy-alcohol synthase; HR, hydroperoxide reductase; POX, peroxygenase.
Oxidative metabolism of fatty acids in (B) mammals and (C) plants. Starting mainly from arachidonic acid in a mammalian system or from polyunsaturated octadecaenoic (C18) fatty acids in plants, both oxidative pathways involve oxygenation of these fatty acids by one, two or four atoms of oxygen. In addition, linoleic acid can be a substrate for mammalian lipoxygenases and C16:3 for plant allene oxide synthase. Adapted from Blée (2002) [189].

1.6.1. Lipase mediated free fatty acid liberation in algae

Existing evidence suggests that both red and brown algae start the synthesis of oxylipins by the liberation of free fatty acids (FFA) through lipase-like enzymes [47,194]. In brown algae, one study has reported that bacterial lipopolysaccharides (LPS), which trigger defense reactions in the brown algal kelp *L. digitata*, induce the release of PUFAs and the accumulation of oxylipins [194]. The gametophytes of the red alga *Chondrus crispus* showed significant accumulation of FFA when challenged with cell-free extracts from its endophyte *Acrochaete operculata* [47]. In addition, based on the inhibition of the FFA liberation in presence of LOX inhibitors, the authors have concluded that the synthesis of oxylipins in this alga occurred through enzymatic processes. Furthermore, lipase activity was found to be controlled through oxylipin feed back-loop regulation. In the red alga *Gracilaria chilensis*, FFA liberation was observed upon wounding, and it was suggested to happen through the action of a phospholipase A2 (PLA2). Free PUFAs were then shown to be used for the production of hydroxyl eicosatetraenoic acids [195]. In microalgae, PLA2 and galactolipases can be activated upon specific signaling, or can act immediately after rupture of cell compartments induced by wounding. In marine diatoms, chloroplast glycolipids are the main substrates for aldehyde biosynthesis, which have strong anti-proliferative properties [196]. This process also seems to be largely dependent upon PLA2 [197].

1.6.2. Oxylipin biosynthesis

Various unique oxylipins have been identified in red, green and brown algae, but their enzymatic biosynthesis has not been fully characterized so far. It is interesting to note that since the three algal groups have distinct evolutionary histories, different biosynthetic pathways may be involved in each of them.

1.6.2.1. *Red algae*

Red algae present the most varied range of oxylipins. These organisms produce several compounds which seem to derive from 12-hydroperoxide FAs (Fig. 13). These compounds encompass the 12*R*,13*S*-diHETE, 12*R*,13*S*-diHEPE which were found in *Gracilaria lemaneiformis*; as well as 12*S*-HETE, 12*S*-HEPE, and two lactones called "constanolactones" since they were isolated from *Constantinea simplex* [198]. The presence of these molecules suggests the occurrence of a 12-LOX in these organisms. Furthermore, in *Polyneura latissima*, the compounds 7*S*-hydroxy-8*S*,9*S*epETrE and 9*S*-HETE have been described [192]. Moreover, prostaglandins (PG) and leukotriene-like products have been reported in several species, such as *Rhodymenia pertusata* or in the genus *Gracilaria*, and they are thought to result from the action of a 5-LOX [199-201]. In addition, *Gracilaria asiatica* shows increased concentrations of 8-HETE and of the PGA2, B2 and LTB4 [202]. Despite the abundance of information in terms of oxylipins produced by several species of red algae, and the pharmacological interest surrounding these compounds, little attention has been paid to their biological significance until recently. Elicitation of red algae with pathogen extracts triggered oxylipin accumulation, and was followed by the set-up of defensive mechanisms [47]. Similar results were observed in the red alga *G. chilensis* that releases FFA, as well as hydoxylated eicosanoids, under epiphyte challenge [195]. In *C. crispus*, the synthesis of complex C_{18} cylcopentenones JA and MeJA, was reported to occur *in vitro* in elicited algal extracts containing FFA supplied exogenously [47]. However, the occurrence of jasmonates *in vivo* still needs to be established in *C. crispus*. On the other hand, the presence of MeJA has been reported in another red algae, *Gelidium latifolium* [203]. MeJa is taken up by *C. crispus*, and induces a dose-dependent production of C_{18} hydroperoxydes and C_{20} cyclopentenones such as prostaglandins [47,204]. Furthermore, pre-incubation of *Chondrus* gametophytes in presence of MeJA prevents their infestation by the endophyte *A. operculata,*

confirming the potential of MeJA to act as an elicitor of immune responses [47]. These observations were correlated with the activation of defense reactions involving the shikimate deshydrogenase and the phenylalanine ammonium lyase [47]. From a molecular point of view, microarray analysis of *C. crispus* incubated with MeJA permits to monitor the up-regulation of several stress-related genes such as glutathione S-transferases (GST), heat shock protein 20, a xenobiotic reductase, and phycocyanin lyase [205]. These genes are also important in abiotic stress responses, which underline, as in vascular plants, a possible MeJA cross-talk between mechanisms induced under different stress conditions. Further assessment of changes in expression of the GST and NADPH oxidase genes in *Chondrus* incubated with MeJA and 12-HpETE allowed to confirm their induction after treatment with both oxylipins [206]. Altogether, these results highlighted the importance of C_{18} and C_{20} oxylipins in Rhodophyta through pathogen-induced defenses and innate immunity reactions [46,191]. On the other hand, no studies have been carried about the involvement of these compounds in abiotic stress.

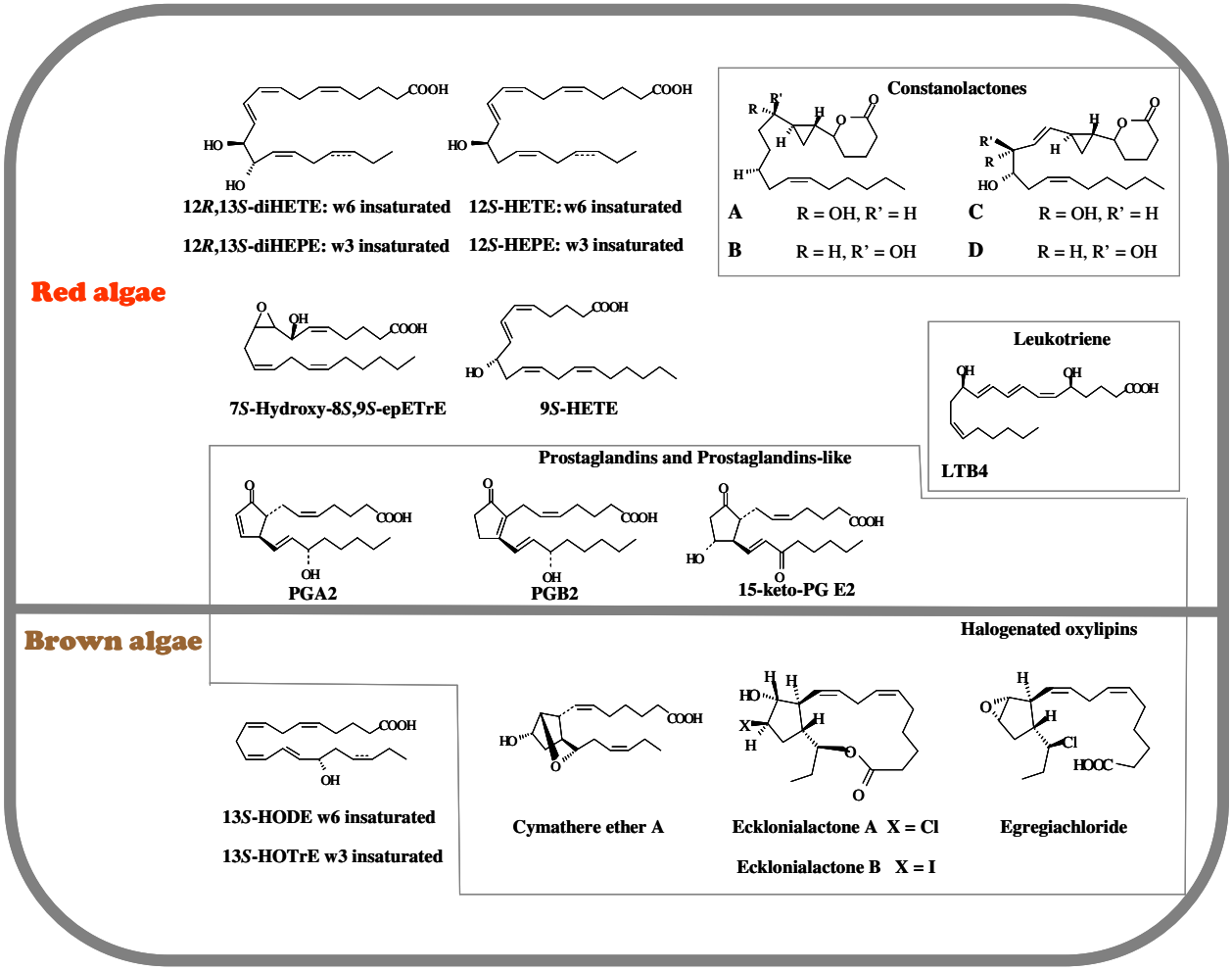

Figure 13. Summary of oxylipins from brown and red algae presenting original structures and/or special interest. 12*R*,13*S*-diHETE: 12*R*,13*S*-dihydroxi-5(*Z*),8(*Z*),10(*E*),14(*Z*)-eicosatetraenoic acid; 12*R*,13*S*-diHEPE: 12*R*,13*S*-dihydroxi-5(*Z*),8(*Z*),10(*E*),14(*Z*),17(*Z*)-eicosapentaenoic acid; 12*S*-HETE: 12*S*-hydroxieicosatetraenoic acid; 12*S*-HEPE: 12*S*-hydroxieicosapentaenoic acid ; constanolactones A, B, F, G; 7*S*-Hydroxy-8*S*,9*S*-epETrE: 7*S*-hydroxi-8*S*,9*S*-epoxy-5(*Z*),11(*Z*),14(*Z*)-eicosatrienoic acid; 9*S*-HETE: 9*S*-hydroxieicosatetraenoic acid ; PGA2: prostaglandin A2 ; PGB2 ; 15-keto-PG E2 ; LTB4: leukotriene B4; 13*S*-HODE: 13*S*-hydroxioctadecadienoic acid; 13*S*-HOTrE: 13*S*-hydroxioctadecatrienoic acid; cymathere ether A ; ecklonialactone A ; ecklonialactone B.

1.6.2.2. *Green algae*

Intensive studies have been carried out in the species *Acrosiphonia coalita* and *Cladophora columbiana*. These organisms seem to synthesise only octadecanoid derivatives, which is consistant with their evolutionary affiliation with the Chlorophyta [207,208] since these organisms are not able to produce C_{20} PUFAs. In addition, most products seem to derive

from a 9-LOX pathway, even if some consistent data for the presence of a 13-LOX pathway have been obtained from green microalgae [209].

1.6.2.3. *Brown algae*

Most brown algal studies dealing with oxylipins have been conducted in kelps (*Laminariales*). In *Laminaria sinclairii*, the eicosanoids 15*S*-HpETE and 15-HpEPE have been described, as well as the octadecanoids 13*S*-HODE and 13*S*-HOTrE (Fig. 13) [210]. An original compound deriving from stearidonic acid with a cyclopentane ring was isolated from *Cymathere triplicate*, and was called Cymathere ether [211]. Halide metabolism seems to interplay with oxylipins since several examples of halogenated oxylipins exist in the literature. *Eisenia bicyclis* synthesises "ecklonialactones" which contain an iodine or a chlorine, while *Egregia menzeisii* produces the egregiachloride A which is a homologue of a chlorinated prostaglandin [212]. Nevertheless, the biological activity and biosynthesis of these compounds is still unknown. Further research on volatile aldehydes was conducted in *Laminaria angustata* in order to detect flavour compounds for industrial applications. This alga synthesizes "cucumber smelling" C_9 aldehydes, exclusively from the C_{20} FA arachidonic acid, while C_6 aldehydes are derived either from C_{18} or from C_{20} FAs. The intermediates in these biosynthetic pathways were 15-LOX and 12-LOX products, the 12-HpETE and the 15-HpETE respectively [213,214]. These authors concluded that a hydroperoxide lyase may catalyze formation of C_9 aldehydes from 12*S*-HPETE.

Even more limited data than in red algae have been published on the biological role of oxylipins in brown algae. In diatoms, which belong to the Heterokonta like brown seaweeds, cell wounding triggers aldehyde production, which is then involved in indirect defense systems against grazing and distant cell signaling processes [215,216]. Brown algal aldehydes exhibit structures similar to those described in higher plants. Their involvement in biotic defensive mechanisms still remains to be proven. Elicitation by bacterial lipopolysaccharides

in *L. digitata* triggered the accumulation of products of 13- and 15-LOX such as 13-HOTrE and 15-HEPE respectively [194]. This provided evidence that pathogen-associated molecular patterns (PAMP) trigger the formation of oxylipins in brown algae. Moreover, MeJA was shown to induce the accumulation of phlorotannins in the brown alga *F. vesiculosus* during low tide [217]. Therefore, MeJA succeeded to recreate reactions stimulated by herbivore attack, suggesting the implication of oxylipins during the defense against grazing. Up to date MeJA has not been isolated in brown algae. No studies on endogenous oxylipin production under abiotic stress conditions have been published so far for brown algae.

1.7. PROTEOMICS AND TWO DIMENSIONAL ELECTROPHORESIS

1.7.1. From Genomics to Proteomics

It is obvious today that for understanding the biological functions of a cell, DNA sequence information alone is not sufficient. For that matter, post-genomic approaches such as proteomics are becoming a very attractive complement to genomics. The term proteome was first coined for the set of proteins encoded by the genome [218]. The concept of the proteome is fundamentally different to that of the genome: while the genome is virtually static and can be well-defined for an organism, the proteome continually changes in response to external and internal events. Therefore, the study of the proteome, called proteomics, now relates not only to all the proteins in any given cell, but also the interactions between them, their structural description, and their higher order complexes [219]. In the recent years, proteomics has experienced rapid development because of the apparition of new sensitive analytical tools and of the increasing complementary data from genomics. As a result, this field has become more popular and is now an important complement for functional genomics approaches such as microarray-based expression profiles, systematic genetics and small-molecule–based arrays. Moreover, the applications of these techniques concern a wide range of purposes, from molecular interactions to meta-population ecology [220,221]. The method commonly used to visualize the proteins that make up a proteome is the separation by two-dimensional electrophoresis (2-DE). It was developed in the 1970s by O'Farrell, and separates proteins according to their isoelectric point, pI (isoelectric focusing, the first dimension) and their molecular weight (SDS-PAGE, the second dimension) [222]. 2-DE allows the simultaneous visualization of up to thousands of proteins that appear as spots on a gel. Image analysis of the intensities of these spots can be compared between different treatments to yield information about the physiological response of an organism to specific conditions (Fig. 14).

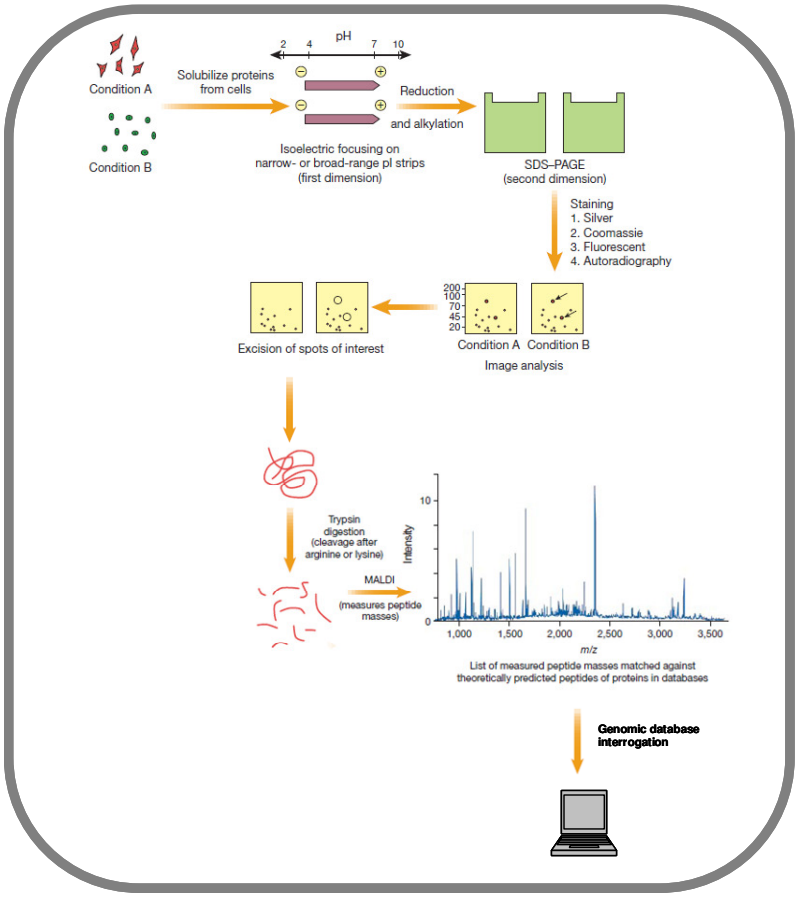

Figure 14. A sheme explaining the two dimensional gel approach. Cells (or tissue) derived from two different conditions, A and B, are harvested and the proteins solubilized. The crude protein mixture is then applied to a 'first dimension' gel strip that separates the proteins based on their isoelectric points. After this step, the strip is subjected to reduction and alkylation and applied to a 'second dimension' SDS–PAGE gel where proteins are denatured and separated on the basis of size. The gels are then fixed and the proteins can be visualized by various staining techniques. After staining, the resulting protein spots are recorded and quantified. Image analysis requires sophisticated software and remains one of the most labour-intensive parts of the two dimensional gel approach. The spots of interest are then excised and subjected to mass spectrometric analysis. The spectra peaks are then confronted to genomic database in order to obtain the protein identity. Adapted from Pandey and Mann (2000) [220].

Although 2-DE represents the inescapable first step of proteome analysis, this technique is representative of a limited total proteome spectrum because of incompatibilities attached to the protein extract degradation, solubility, pH range separation, and quantity. In spite, promising alternative or complementary technologies have been developed, e.g. multidimensional protein chromatographic technology, shotgun proteomics, stable isotope labeling, protein or antibody arrays. Nevertheless, 2-DE is currently the only technique that

can be routinely applied for parallel quantitative expression profiling of large sets of complex protein mixtures such as whole cell lysates. Today's 2-DE technology with IPGs (Immobilized pH Gradients) [223] has overcome the former limitations of carrier ampholyte based 2-DE [222], with respect to reproducibility, handling, resolution, and separation of very acidic and/or basic proteins. The development of IPGs between pH 2.5-12 has enabled the analysis of very alkaline proteins and the construction of the corresponding databases. Narrow-overlapping IPGs provide increased resolution (Deltapl = 0.001) and, in combination with pre-fractionation methods, allow the detection of low abundance proteins. Depending on the gel size and pH gradient used, 2-DE can resolve more than 5,000 proteins simultaneously (similar to 2,000 proteins routinely), and detect and quantify < 1 ng of protein per spot. Separation of these proteins is usually followed by identification of the protein spots of interest. The most significant breakthrough in proteomics has been the development of mass spectrometric (MS) identification of gel-separated proteins, which extends analysis beyond the mere display of proteins. MS has essentially replaced the classical technique of Edman degradation, offering several comparative advantages, such as better sensitivity, higher throughput, and it can deal with protein mixtures. In the past years, major advances have been made in the sensitivity and resolution for protein characterization, therefore a wide range of new MS instrumentation has emerged [224]. The mass spectrometric method that is used most frequently to identify proteins consists of an ionization source such as “matrix assisted laser desorption/ionization” (MALDI)) coupled with a “time-of-light mass spectrometry” (TOF MS). This method detects the molecular masses of the peptide fragments resulting from the enzyme digestion (usually trypsin). This yields a unique peptide-fragment mass fingerprint (PMF) for each protein analyzed, that can be used to search protein databases for matches [225]. This technique is routinely utilized today and it has even been automatized for high throughput analysis. The other technique consists in MALDI sources coupled with tandem

mass spectrometry (TOF-TOF MS), or "electrospray ionization" (ESI) source coupled with a tripe Quadrupole TOF (qTOF MS). These procedures are utilized for identification of ambiguous PMF. The method relies in protein fragmentation of individual peptides in the mixture to gain sequence information.

1.7.2. 2-DE based analysis of metal-stress related proteins in plants and algae

Proteome analysis in plants is becoming a powerful tool in the functional characterization of plants. The increasing genomic data, combined with the sensitive analytical tools (see previous section), have allowed to decipher subcellular fractions of specific organelles or whole organisms. The results in model plant organisms help to uncover complex physiological processes involved in germination, ectomychorrizhal symbiosis, plant–pathogen interactions, or abiotic stress [226,227]. 2-DE studies concerning heavy metal stress in plants are still relatively few, and they focus mostly on cadmium [138,228-231]. Common stress-related features appear in these studies such as the up-regulation of glutathione metabolism, antioxidant systems, or protein degradation and folding mechanisms. Photosynthesis and energetic processes also seem to be differentially regulated upon stress, in order to compensate damages caused on the photosynthetic apparatus and the increased energetic coast caused by the generated stress. Fewer studies in this domain concern copper stress. Some proteomic studies have focussed on GST family regulation upon copper excess [232]. Furthermore, the copper-binding proteins of *Arabidopsis* roots and seedlings have been explored by IMAC-MS [233]. A recent study in the cyanobacteria *Anabaena doliolum* showed that copper-acclimated strains display differential expression of transketolase, phycoerythrocyanin (photoxynthetic pigment), FeSOD and MnSOD. This study concluded that theses proteins were responsive for the copper acclimation in this species [234]. The root proteome of *Cannabis sativa* submitted to copper stress was also investigated by 2-DE

analysis [235]. The lack of genomic data in this species only allowed to identify a limited number of proteins of reduced interest. At the present time, no meaningful proteomic study exists in marine algae. This resides in the fact that no adapted technique for obtaining high quality protein extracts was available for these organisms. Previous work published on red algae proposed a method based on chloroform extraction, even if results were not conclusive [236]. In correlation to the work presented here, a recent publication proposes an alternative method for extracting soluble proteome extracts from brown algae [237].

1.8. OBJECTIVES

1.8.1. General objectives

Over 60 years of mining activities in northern Chile have generated a major decrease in biodiversity along coastal areas polluted by copper mines effluents. Few brown algal species are able to tolerate these conditions. Kelps are absent, leaving the space to metal-tolerant species such as *Ectocarpus sp.* and *Scytosiphon sp.*. There is only a limited amount of literature explaining how these organisms manage to tolerate copper. In this context, my main objective was to investigate the molecular and biochemical mechanisms leading to copper tolerance in brown algae. I have focused my research on two biological models, *L. digitata* and *E. siliculosus*. The first model has been used to analyze the putative involvement of oxylipins upon copper induced stress responses. The second species has represented my main research model. *E.siliculosus* strains were used to compare copper stress responses between isolates or from copper-impacted and non-impacted areas. This last topic was studied by an integrative approach, combining both genomic and proteomic analysis.

1.8.2. Specific objectives

- Study the possible implication of the oxylipin metabolism in the regulation of detoxification responses triggered by copper excess in the brown alga *L.digitata*.
- Determine the physiological response of different strains of *E. siliculosus* to copper excess, in order to select two strains presenting contrasting responses to metal tolerance.
- Establish a protocol for 2DE-proteomic analysis of *E. siliculosus*.
- Identify some of the mechanisms involved in the tolerance to copper stress in *E. siliculosus* by differential 2-DE analysis, and compare proteomic stress profiles between copper-tolerant and copper-sensitive strain.

- Annotation of the *E. siliculosus* genome, focusing on genes encoding enzymes related to copper homeostasis, and involved in detoxification and anti-oxidant responses.

The following chapters are based on two published scientific articles, two submitted manuscripts, and a last chapter on the *Ectocarpus* genome annotation and functional gene candidate characterization that will be enclosed as supplementary material in the genome publication. They represent the achievements of the original work which I developed independently or in collaboration with other scientists, mainly Sophie Goulitquer, PhD. Student in the Université de Bretagne Occidentale, Aaron Mann, PhD. Student at the Pontificia Universidad Católica de Chile (PUC) and Dr. Loretto Contreras, Post-doctoral researcher at the PUC.

BOX 1: Examples of the most important metalloproteins utilizing copper as cofactor (adapted from Küpper & Kroneck (2005) [61])

A Plastocyanin. This type-1 (blue) copper protein transfers electrons between the Rieske protein and PS I in all Chlorophyta (higher plants and green algae), Embryophyta, and most cyanobacteria [238]. In other groups of photosynthetic organisms, it is either absent (e.g., Rhodophyta, Phaeophyta, Euglenophyta), or its presence has not been shown unambiguously (e.g., Cryptophyta, Chlorarachniophyta, Dinophyta). In all organisms, where plastocyanin is absent, it is replaced by cytochrome c6, an iron-dependent electron carrier. In those organisms that can express both PC and cytochrome c6, the two soluble proteins can replace each other depending on the availability of iron and copper [238]. The crystal structures of plastocyanin from different organisms have been solved. The structure of poplar Cu(II)–plastocyanin (from Populus nigra var. italica) was first determined by Freeman and colleagues at 2.7 A ° resolution, and was further refined to 1.6 A °[239]. At the molecular level, its function in photosynthesis is to transfer electrons from the membrane-bound cytochrome b6 f complex in photosystem II to the membrane-bound reaction center of photosystem I [240]. The plastocyanin molecule is an eight-stranded beta-sandwich (cupredoxin fold). The Cu site is located near one end, conventionally described as the "northern" end of the barrel. Cu is coordinated by the side chains of His37, Cys84, His87, and Met92. Neither the Cu atom nor its ligands are accessible from the solvent, with the exception of the imidazole of the northern Histidine (His87). One edge of the imidazole ring is exposed to the solvent and probably forms the electron transfer pathway to the photooxidized chlorophyll dimer P700þ. There is another potential binding site for redox partners, the so-called acidic patch that is located around the conserved Tyr83 residue, 19 A ° away from the Cu atom vs. 6 A ° for the imidazole ring of His87. The overall structure of poplar plastocyanin and the coordination sphere of the Cu site apply with only minor qualifications to the known structures of plastocyanin from plants, green algae, and cyanobacteria. For a comprehensive review of the structural, spectroscopic, and functional properties of plastocyanin refer to Ref. [239].

B Superoxide dismutase (Cu,Zn SOD). A type-2 (non-blue) Cu center constitutes the redox-active site of this important metalloenzyme. Superoxide dismutases are ubiquitously distributed in all biological systems including prokaryotic, eukaryotic, and plant cells. In addition to the Cu,Zn enzyme, iron-, manganese-, and nickel-dependent SODs have been detected, since the early discovery of SOD. Cu,ZnSOD comes as a homodimer of 2 -16 kDa, in eukaryotes it is localized in the cytosol, in the intermembrane space, and in lysosomes, while a distinct Cu,Zn SOD is found as an extracellular form. In sequences derived from plants, two distinct forms have been detected, localized in the cytoplasm and in the chloroplast. Each subunit hosts a Cu,Zn pair responsible for the catalytic dismutation of the superoxide anion, O^-_2 [241]. As discussed in detail (including energetic aspects) by Raven et al. [238], Cu,Zn SOD detoxifies O^-_2 , generating H_2O_2 that is further processed by the iron-dependent enzyme catalase, or diffuses out of the cell. Under turnover conditions, the copper ion at the active site cycles between the Cu(II) and Cu(I) redox states, following successive interactions with the superoxide anion. The electron transfer between substrate and Cu is extremely efficient, the second-order catalytic rate for the enzymatic reaction being limited only by substrate diffusion [242]. In the first part of the reaction, Cu(II) becomes reduced by O^-_2 , dioxygen is then released and the Cu(I)-bridging histidine bond broken with concomitant protonation of this histidine. The reduced Cu(I) protein then reacts with a second superoxide radical to form H_2O_2 and the reoxidized enzyme.

C The first plant Cu enzyme that was isolated is the **laccase** from the Japanese lacqer tree. This multi-copper oxidase was isolated in 1938 by Keilin and Mann [243]; but only in 1958, finally, the redox role of Cu in this enzyme was demonstrated by Malmström et al. [244] by using EPR.

D The first plant enzyme in which Cu was shown to be the active center is the **cytochrome oxidase** (COX) of the respiratory electron chain. No crystal structure has been determined for any cyanobacterial or plant COX, but a cyanobacterial COX has been characterized biochemically and spectroscopically [245].

E The sensor for the plant hormone ethylene (ETR1) is a homodimeric protein that binds one Cu and is most likely located in the plasma membrane [246].

F A **multi-copper oxidase II** seems to be involved in iron uptake of green algae by reoxidation of Fe^{2+} during its uptake into the cell [247]. As discussed in these reports, reoxidation of the Fe^{2+} released from chelating agents may be necessary to prevent the generation of hydroxyl radicals via the Fenton reaction.

1.9. REFERENCES

[1] Mchugh, D.J. (2003) A guide to the seaweed industry. FAO Fisheries Technical Paper No. 441, 105p.

[2] van den Hoek, C., Mann, D.G. and Jahns, H.M. (1995) Algae: an introduction to phycology. Cambridge University press, 623pp.

[3] Baldauf, S.L. (2003) The Deep Roots of Eukaryotes. Science 300, 1703-1706.

[4] Barsanti, L. and Gualtieri, P. (2006), pp. 301 CRC Press.

[5] Charrier, B. et al. (2008) Development and physiology of the brown alga *Ectocarpus siliculosus*: two centuries of research. New Phytologist 177, 319-332.

[6] Lobban, C., Harrison PJ (1994) Seaweed ecology and physiology. Cambridge University Press, 366 pp.

[7] Valentin, K. and Zetsche, K. (1990) Rubisco Genes Indicate a Close Phylogenetic Relation between the Plastids of Chromophyta and Rhodophyta. Plant Molecular Biology 15, 575-584.

[8] Kloareg, B., Demarty, M. and Mabeau, S. (1987) Ion-Exchange Properties of Isolated Cell Walls of Brown Algae: The Interstitial Solution. Journal of Experimental Botany 38, 1652-1662.

[9] Kloareg, B. and Quatrano, R.S. (1988) Structure of the Cell-Walls of Marine-Algae and Ecophysiological Functions of the Matrix Polysaccharides. Oceanography and Marine Biology 26, 259-315.

[10] Kropf, D.L., Kloareg, B. and Quatrano, R.S. (1988) Cell-Wall Is Required for Fixation of the Embryonic Axis in *Fucus* Zygotes. Science 239, 187-190.

[11] Küpper, F.C., Kloareg, B., Guern, J. and Potin, P. (2001) Oligoguluronates Elicit an Oxidative Burst in the Brown Algal Kelp *Laminaria digitata*. Plant Physiol. 125, 278-291.

[12] Davis, T.A., Volesky, B. and Mucci, A. (2003) A review of the biochemistry of heavy metal biosorption by brown algae. Water Research 37, 4311-4330.

[13] Amsler, C.D. (2008) Algal chemical ecology. Springer-Verlang, 313pp.

[14] Salgado, L.T., Andrade, L.R. and Filho, G.M.A. (2005) Localization of specific monosaccharides in cells of the brown alga *Padina* gymnospora and the relation to heavy-metal accumulation. Protoplasma 225, 123-128.

[15] Pinto, E., Sigaud-kutner, T.C.S., Leitao, M.A.S., Okamoto, O.K., Morse, D. and Colepicolo, P. (2003) Heavy metal-induced stress in algae. Journal of Phycology 39, 1008-1018.

[16] Ragan, M.A. and K.W., G. (1986) Phlorotannins, brown algal polyphenols. Progress in Phycological Research 4, 129-241.

[17] Leblanc, C. et al. (2006) Iodine transfers in the coastal marine environment: the key role of brown algae and of their vanadium-dependent haloperoxidases. Biochimie 88, 1773-1785.

[18] Küpper, F.C., Schweigert, N., Ar Gall, E., Legendre, J.-M., Vilter, H. and Kloareg, B. (1998) Iodine uptake in Laminariales involves extracellular, haloperoxidase-mediated oxidation of iodide. Planta 207, 163-171.

[19] Küpper, F.C. et al. (2008) Iodide accumulation provides kelp with an inorganic antioxidant impacting atmospheric chemistry. Proceedings of the National Academy of Sciences 105, 6954-6958.

[20] Verhaeghe, E. et al. (2008) Microchemical imaging of iodine distribution in the brown alga *Laminaria digitata* suggests a new mechanism for its accumulation. Journal of Biological Inorganic Chemistry 13, 257-269.

[21] Bartsch, I. et al. (2008) The genus *Laminaria sensu lato*: recent insights and developments. European Journal of Phycology 43, 1 - 86.

[22] Dring, M.J. (2006) Stress resistance and disease resistance in seaweeds: The role of reactive oxygen metabolism. Advances in Botanical Research, Vol 43 43, 175-207.

[23] Davison, I.R. and Pearson, G.A. (1996) Stress tolerance in intertidal seaweeds. Journal of Phycology 32, 197-211.

[24] Crepineau, F., Roscoe, T., Kaas, R., Kloareg, B. and Boyen, C. (2000) Characterisation of complementary DNAs from the expressed sequence tag analysis of life cycle stages of Laminaria digitata (Phaeophyceae). Plant Molecular Biology 43, 503-513.

[25] Roeder, V., Collen, J., Rousvoal, S., Corre, E., Leblanc, C. and Boyen, C. (2005) Identification of stress gene transcripts in *Laminaria digitata* (Phaeophyceae) protoplast cultures by expressed sequence tag analysis. Journal of Phycology 41, 1227-1235.

[26] West, J.A. and G.T., K. (1996) *Ectocarpus siliculosus* from Hopkins River Falls, Victoria - the first record of a freshwater brown alga in Australia. Muelleria 9, 29-33.

[27] Russel, G. and Morris, O.P. (1970) Copper tolerance in marine fouling alga *Ectocarpus siliculosus*. Nature 228, 288-289.

[28] Medina, M., Andrade, S., Faugeron, S., Lagos, N., Mella, D. and Correa, J.A. (2005) Biodiversity of rocky intertidal benthic communities associated with copper mine tailing discharges in northern Chile. Marine Pollution Bulletin 50, 396-409.

[29] Peters, A.F., Scornet Delphine, and Muller Dieter G., K.B., Cock J . Mark (2004) Inheritance of organelles in arti.cial hybrids of the isogamousmulticellular chromist alga *Ectocarpus siliculosus* (Phaeophyceae). European Journal of Phycology 39, 235-242.

[30] Correa, J.A. et al. (1999) Copper, copper mine tailings and their effect on the marine algae in Northern Chile. Journal of Applied Phycology 11, 57-67.

[31] Livingstone, D.R. (2001) Contaminant-stimulated Reactive Oxygen Species Production and Oxidative Damage in Aquatic Organisms. Marine Pollution Bulletin 42, 656-666.

[32] Collen, J. and Davison, I.R. (1999) Reactive oxygen metabolism in intertidal *Fucus spp.* (Phaeophyceae). Journal of Phycology 35, 62-69.

[33] Collen, J. and Davison, I.R. (1999) Reactive oxygen production and damage in intertidal *Fucus spp.* (Phaeophyceae). Journal of Phycology 35, 54-61.

[34] Collén, J. and Davison, I.R. (1999) Stress tolerance and reactive oxygen metabolism in the intertidal red seaweeds *Mastocarpus stellatus* and *Chondrus crispus*. Plant, Cell and Environment 22, 1143-1151.

[35] Contreras, L., Moenne, A. and Correa, J.A. (2005) Antioxidant responses in *Scytosiphon lomentaria* (Phaeophyceae) inhabiting copper-enriched coastal environments. Journal of Phycology 41, 1184-1195.

[36] Collen, J. and Davison, I.R. (2001) Seasonality and thermal acclimation of reactive oxygen metabolism in *Fucus vesiculosus* (Phaeophyceae). Journal of Phycology 37, 474-481.

[37] Orr, H.A. (2005) The genetic theory of adaptation: a brief history. Nature Reviews Genetics 6, 119-127.

[38] Nielsen, H.D., Brownlee, C., Coelho, S.M. and Brown, M.T. (2003) Inter-population differences in inherited copper tolerance involve photosynthetic adaptation and exclusion mechanisms in *Fucus serratus*. New Phytologist 160, 157-165.

[39] Morris, O.P. and Russel, G. (1974) Inter-specific differences in response to copper by natural populations of *Ectocarpus*. Journal of British Phycology 9, 269-272.

[40] Farmer, E.E. and Davoine, C. (2007) Reactive electrophile species. Current Opinion in Plant Biology Special Issue on Biotic Interactions - Edited by Jane Glazebrook and Jurriaan Ton 10, 380-386.

[41] Mittler, R., Vanderauwera, S., Gollery, M. and Van Breusegem, F. (2004) Reactive oxygen gene network of plants. Trends in Plant Science 9, 490-498.

[42] Halliwell, B. (2006) Reactive Species and Antioxidants. Redox Biology Is a Fundamental Theme of Aerobic Life. Plant Physiology 141, 312-322.

[43] Mithofer, A., Schulze, B. and Boland, W. (2004) Biotic and heavy metal stress response in plants: evidence for common signals. FEBS Letters 566, 1-5.

[44] Farmer, E. and Schulze-Lefert, P. (2005) Biotic interactions: From molecular networks to inter-organismal communities. Current Opinion in Plant Biology Biotic interactions 8, 343-345.

[45] Farmer, E.E., Almeras, E. and Krishnamurthy, V. (2003) Jasmonates and related oxylipins in plant responses to pathogenesis and herbivory. Current Opinion in Plant Biology 6, 372-378.

[46] Cosse, A., Leblanc, C. and Potin, P. (2007) Dynamic Defense of Marine Macroalgae Against Pathogens: From Early Activated to Gene Regulated Responses Advances in Botanical Research. Academic Press, 221-266.

[47] Bouarab, K., Adas, F., Gaquerel, E., Kloareg, B., Salaun, J.P. and Potin, P. (2004) The innate immunity of a marine red alga involves oxylipins from both the eicosanoid and octadecanoid pathways. Plant Physiology 135, 1838-48.

[48] Duffus, J.H. (2002) "Heavy metals" - A meaningless term? (IUPAC technical report). Pure and Applied Chemistry 74, 793-807.

[49] Gledhill, M., Nimmo, M., Hill, S.J. and Brown, M.T. (1997) The toxicity of copper (II) species to marine algae, with particular reference to macroalgae. Journal of Phycology 33, 2-11.

[50] Bryan, G.W. and Langston, W.J. (1992) Bioavailability, Accumulation and Effects of Heavy-Metals in Sediments with Special Reference to United-Kingdom Estuaries - a Review. Environmental Pollution 76, 89-131.

[51] Stauber, J.L., Adams, M.S., Binet, M.T., Cook, L.S.J., Richardson, D.E., Parsons, T., Moore, N.J. and Kearney, P.S. (2001) Direct toxicity assessment of primary treated effluent from a newsprint mill. 55th Appita Annual Conference, Proceedings, 147-151.

[52] Castilla, J.C. (1983) Environmental-Impact in Sandy Beaches of Copper Mine Tailings at Chañaral, Chile. Marine Pollution Bulletin 14, 459-464.

[53] Castilla, J.C. and Nealler, E. (1978) Marine Environmental-Impact Due to Mining Activities of El-Salvador Copper Mine, Chile. Marine Pollution Bulletin 9, 67-70.

[54] Ratkevicius, N., Correa, J.A. and Moenne, A. (2003) Copper accumulation, synthesis of ascorbate and activation of ascorbate peroxidase in *Enteromorpha compressa* (Chlorophyta) from heavy metal-enriched environments in northern Chile. Plant Cell and Environment 26, 1599-1608.

[55] Correa, J., Gonzales, P., Sanchez, P., Munoz, J. and Orellana, M.C. (1996) Copper-algae interactions : inheritance or adaptation? Environmental Monitoring and Assessment 40, 41-54.

[56] Antonovics, J. (1971) Effects of a Heterogeneous Environment on Genetics of Natural Populations. American Scientist 59, 593-&.

[57] Baker, A.J.M. and Proctor, J. (1990) The influence of cadmium, copper, lead, and zinc on the distribution and evolution of metallophytes in the British Isles. Plant Systematics and Evolution 173, 91-108.

[58] Macnair, M.R. (1993) The Genetics of Metal Tolerance in Vascular Plants. New Phytologist 124, 541-559.

[59] Pauwels, M., Roosens, N.H., Frérot, H. and Saumitou-Laprade, P. (2008) When population genetics serves genomics: putting adaptation back in a spatial and historical context. Current Opinion in Plant Biology 11, 129-134.

[60] Halliwell, B., Gutterridge, John (1984) Oxygen toxicity, oxygen radicals, transition metals and disease. Biochem. J. 219, 1-14.

[61] Küpper, H. and Kroneck, P.M.H. (2005) Heavy metal uptake by plants and cyanobacteria. Metal Ions in Biological Systems 44, 97-144.

[62] Puig, S., Andres-Colas, N., Garcia-Molina, A. and Penarrubia, L. (2007) Copper and iron homeostasis in Arabidopsis: responses to metal deficiencies, interactions and biotechnological applications. Plant Cell and Environment 30, 271-290.

[63] Stromgren, T. (1980) Effect of Dissolved Copper on the Increase in Length of 4 Species of Inter-Tidal Fucoid Algae. Marine Environmental Research 3, 5-13.

[64] Ouzounidou, G. (1995) Cu-Ions Mediated Changes in Growth, Chlorophyll and Other Ion Contents in a Cu-Tolerant *Koeleria splendens*. Biologia Plantarum 37, 71-78.

[65] Maksymiec, W. and Baszynski, T. (1996) Different susceptibility of runner bean plants to excess copper as a function of the growth stages of primary leaves. Journal of Plant Physiology 149, 217-221.

[66] Maksymiec, W., Bednara, J. and Baszynski, T. (1995) Responses of Runner Bean-Plants to Excess Copper as a Function of Plant-Growth Stages - Effects on Morphology and Structure of Primary Leaves and Their Chloroplast Ultrastructure. Photosynthetica 31, 427-435.

[67] Gapper, C. and Dolan, L. (2006) Control of plant development by reactive oxygen species. Plant Physiology 141, 341-345.

[68] Mittler, R. (2002) Oxidative stress, antioxidants and stress tolerance. Trends in Plant Science 7, 405-410.

[69] Kossakowska, A., Falkowski, L. and Lewandowska, J. (1988) Effect of amino acids on the toxicity of havy metals to phytoplankton. Bulletin of Environemental Contamination and Toxicology 40, 532-538.

[70] Maksymiec, W. (1997) Effect of copper on cellular processes in higher plants. Photosynthetica 34, 321-342.

[71] Fernandes, J.C. and Henriques, F.S. (1991) Biochemical, Physiological, and Structural Effects of Excess Copper in Plants. Botanical Review 57, 246-273.

[72] Malaisse, F. and Brooks, R.R. (1982) Colonization of Modified Metalliferous Environments in Zaire by the Copper Flower *Haumaniastrum katangense*. Plant and Soil 64, 289-293.

[73] Contreras, L., Medina, M.H., Andrade, S., Oppliger, V. and Correa, J.A. (2007) Effects of copper on early developmental stages of *Lessonia nigrescens* Bory (Phaeophyceae). Environmental Pollution 145, 75-83.

[74] Yruela, I., Pueyo, J.J., Alonso, P.J. and Picorel, R. (1996) Photoinhibition of Photosystem II from Higher Plants. Effect of copper inhibition. Journal of Biological Chemistry 271, 27408-27415.

[75] Clijsters, H. and Vanassche, F. (1985) Inhibition of Photosynthesis by Heavy-Metals. Photosynthesis Research 7, 31-40.

[76] Küpper, H., Küpper, F. and Spiller, M. (1996) Environmental relevance of heavy metal-substituted chlorophylls using the example of water plants. Journal of Experimental Botany 47, 259-266.

[77] Küpper, H., Setlik, I., Spiller, M., Küpper, F.C. and Prasil, O. (2002) Heavy metal-induced inhibition of photosynthesis: targets of in vivo heavy metal chlorophyll formation. Journal of Phycology 38, 429-441.

[78] Yruela, I., Alfonso, M., Baron, M. and Picorel, R. (2000) Copper effect on the protein composition of photosystem II. Physiologia Plantarum 110, 551-557.

[79] Bernal, M., Roncel, M., Ortega, J.M., Picorel, R. and Yruela, I. (2004) Copper effect on cytochrome b559 of photosystem II under photoinhibitory conditions. Physiologia Plantarum 120, 686-694.

[80] Hsu, B.D. and Lee, J.Y. (1988) Toxic Effects of Copper on Photosystem-II of Spinach-Chloroplasts. Plant Physiology 87, 116-119.

[81] Patsikka, E., Aro, E.-M. and Tyystjarvi, E. (1998) Increase in the Quantum Yield of Photoinhibition Contributes to Copper Toxicity in Vivo. Plant Physiol. 117, 619-627.

[82] Mallick, N. and Mohn, F.H. (2003) Use of chlorophyll fluorescence in metal-stress research: a case study with the green microalga *Scenedesmus*. Ecotoxicology and Environmental Safety 55, 64-69.

[83] Luis, P., Behnke, K., Toepel, J. and Wilhelm, C. (2006) Parallel analysis of transcript levels and physiological key parameters allows the identification of stress phase gene markers in *Chlamydomonas reinhardtii* under copper excess. Plant, Cell & Environment 29, 2043-2054.

[84] Baker, C.J. and Orlandi, E.W. (1995) Active Oxygen in Plant Pathogenesis. Annual Review of Phytopathology 33, 299-321.

[85] Mittler, R. (2002) Oxidative stress, antioxidants and stress tolerance. Trends Plant Sci 7, 405-10.

[86] Asada, K. and Takahashi, M. (1987) in: *In* "Photoinhibition", pp. 227-297 Elsevier, New York.

[87] Halliwell, B. and Gutteridge, J.M.C. (1992) Biologically relevant metal ion-dependent hydroxyl radical generation An update. FEBS Letters 307, 108-112.

[88] Halliwell, B. and Gutteridge, J. (1989) Free Radicals in Biology and Medicine.

[89] Collén, J., Pinto, E., Pedersen, M. and Colepicolo, P. (2003) Induction of oxidative stress in the red macroalga *Gracilaria tenuistipitata* by pollutant metals. Archives of Environmental Contamination Toxicology 45, 337-42.

[90] Drazkiewicz, M., Skorzynska-Polit, E. and Krupa, Z. (2004) Copper-induced oxidative stress and antioxidant defence in *Arabidopsis thaliana*. Biometals 17, 379-387.

[91] Schutzendubel, A. and Polle, A. (2002) Plant responses to abiotic stresses: heavy metal-induced oxidative stress and protection by mycorrhization. Journal of experimental botany 53, 1351-65.

[92] Nieboer, E. and Richardson, D.H.S. (1980) The Replacement of the Non-Descript Term Heavy-Metals by a Biologically and Chemically Significant Classification of Metal-Ions. Environmental Pollution Series B-Chemical and Physical 1, 3-26.

[93] van Assche, F. and Clijsters, H. (1990) Effects of Metals on Enzyme-Activity in Plants. Plant Cell and Environment 13, 195-206.

[94] Stiborova, M., Doubravova, M. and Leblova, S. (1986) A Comparative-Study of the Effect of Heavy-Metal Ions on Ribulose-1,5-Bisphosphate Carboxylase and Phosphoenolpyruvate Carboxylase. Biochemie Und Physiologie Der Pflanzen 181, 373-379.

[95] Demidchik, V., Sokolik, A. and Yurin, V. (1997) The effect of Cu^{2+} on ion transport systems of the plant cell plasmalemma. Plant Physiology 114, 1313-1325.

[96] Devos, C.H.R., Schat, H., Dewaal, M.A.M., Vooijs, R. and Ernst, W.H.O. (1991) Increased resistance to copper-Induced damage of the root cell clasmalemma in copper tolerant *Silene cucubalus*. Physiologia Plantarum 82, 523-528.

[97] Wainwright, S.J. and Woolhouse, H.W. (1977) Some Physiological Aspects of Copper and Zinc Tolerance in *Agrostis tenuis* Sibth. Cell Elongation and Membrane Damage. Journal of Experimental Botany 28, 1029-1036.

[98] Alaoui-Sossé, B., Genet, P., Vinit-Dunand, F., Toussaint, M.-L., Epron, D. and Badot, P.-M. (2004) Effect of copper on growth in cucumber plants (*Cucumis sativus*) and its relationships with carbohydrate accumulation and changes in ion contents. Plant Science 166, 1213-1218.

[99] Meharg, A.A. (1993) The Role of the Plasmalemma in Metal Tolerance in Angiosperms. Physiologia Plantarum 88, 191-198.

[100] Cid, A., Herrero, C., Torres, E. and Abalde, J. (1995) Copper toxicity on the marine microalga *Phaeodactylum tricornutum*: effects on photosynthesis and related parameters. Aquatic Toxicology 31, 165-174.

[101] Amberger, A., Gutser, R. and Wunsch, A. (1982) Iron Chlorosis Induced by High Copper and Manganese Supply. Journal of Plant Nutrition 5, 715-720.

[102] Somashekaraiah, B.V., Padmaja, K. and Prasad, A.R.K. (1992) Phytotoxicity of Cadmium Ions on Germinating Seedlings of Mung Bean (*Phaseolus-Vulgaris*) -

Involvement of Lipid Peroxides in Chlorophyll Degradation. Physiologia Plantarum 85, 85-89.

[103] Rensing, C. and Grass, G. (2003) *Escherichia coli* mechanisms of copper homeostasis in a changing environment. Fems Microbiology Reviews 27, 197-213.

[104] Puig, S. and Thiele, D.J. (2002) Molecular mechanisms of copper uptake and distribution. Current Opinion in Chemical Biology 6, 171-180.

[105] Kim, B.E., Nevitt, T. and Thiele, D.J. (2008) Mechanisms for copper acquisition, distribution and regulation. Nature Chemical Biology 4, 176-185.

[106] Connolly, E.L., Fett, J.P. and Guerinot, M.L. (2002) Expression of the IRT1 metal transporter is controlled by metals at the levels of transcript and protein accumulation. Plant Cell 14, 1347-1357.

[107] Guerinot, M.L. (2000) The ZIP family of metal transporters. Biochimica et Biophysica Acta-Biomembranes 1465, 190-198.

[108] Maser, P. et al. (2001) Phylogenetic relationships within cation transporter families of *Arabidopsis*. Plant Physiology 126, 1646-1667.

[109] Korshunova, Y.O., Eide, D., Clark, W.G., Guerinot, M.L. and Pakrasi, H.B. (1999) The IRT1 protein from *Arabidopsis thaliana* is a metal transporter with a broad substrate range. Plant Molecular Biology 40, 37-44.

[110] Wintz, H., Fox, T., Wu, Y.-Y., Feng, V., Chen, W., Chang, H.-S., Zhu, T. and Vulpe, C. (2003) Expression Profiles of *Arabidopsis thaliana* in Mineral Deficiencies Reveal Novel Transporters Involved in Metal Homeostasis. Journal of Biological Chemistry 278, 47644-47653.

[111] Dancis, A., Yuan, D.S., Haile, D., Askwith, C., Eide, D., Moehle, C., Kaplan, J. and Klausner, R.D. (1994) Molecular characterization of a copper transport protein in *Saccharomyces cerevisiae* - an Unexpected Role for Copper in Iron Transport. Cell 76, 393-402.

[112] Pilon, M., Abdel-Ghany, S.E., Cohu, C.M., Gogolin, K.A. and Ye, H. (2006) Copper cofactor delivery in plant cells. Current Opinion in Plant Biology 9, 256-263.

[113] Nevo, Y. and Nelson, N. (2006) The NRAMP family of metal-ion transporters. Biochimica et Biophysica Acta-Molecular Cell Research 1763, 609-620.

[114] Curie, C., Alonso, J.M., Le Jean, M., Ecker, J.R. and Briat, J.F. (2000) Involvement of NRAMP1 from *Arabidopsis thaliana* in iron transport. Biochemical Journal 347, 749-755.

[115] Clemens, S. (2006) Toxic metal accumulation, responses to exposure and mechanisms of tolerance in plants. Biochimie 88, 1707-1719.

[116] Hirayama, T. and Alonso, J.M. (2000) Ethylene captures a metal! Metal ions are involved in ethylene perception and signal transduction. Plant and Cell Physiology 41, 548-555.

[117] Hanikenne, M., Kramer, U., Demoulin, V. and Baurain, D. (2005) A comparative inventory of metal transporters in the green alga *Chlamydomonas reinhardti*i and the red alga *Cyanidioschizon merolae*. Plant Physiology 137, 428-446.

[118] Silver, S. and Phung, L.T. (1996) Bacterial heavy metal resistance: New surprises. Annual Review of Microbiology 50, 753-789.

[119] Baxter, I., Tchieu, J., Sussman, M.R., Boutry, M., Palmgren, M.G., Gribskov, M., Harper, J.F. and Axelsen, K.B. (2003) Genomic Comparison of P-Type ATPase Ion Pumps in *Arabidopsis* and Rice. Plant Physiology 132, 618-628.

[120] Andrés-Colás, N., Sancenón, V., Rodríguez-Navarro, S., Mayo, S., Thiele Dennis J., Ecker, J.R., Puig, S. and Peñarrubia, L. (2006) The Arabidopsis heavy metal P-type ATPase HMA5 interacts with metallochaperones and functions in copper detoxification of roots. The Plant Journal 45, 225-236.

[121] van Hoof, N., Koevoets, P.L.M., Hakvoort, H.W.J., Ten Bookum, W.M., Schat, H., Verkleij, J.A.C. and Ernst, W.H.O. (2001) Enhanced ATP-dependent copper efflux across the root cell plasma membrane in copper-tolerant *Silene vulgaris*. Physiologia Plantarum 113, 225-232.

[122] O'Halloran, T.V. and Culotta, V.C. (2000) Metallochaperones, an Intracellular Shuttle Service for Metal Ions. Journal of Biological Chemistry 275, 25057-25060.

[123] Pufahl, R.A. et al. (1997) Metal ion chaperone function of the soluble Cu(I) receptor Atx1. Science 278, 853-856.

[124] Himelblau, E., Mira, H., Lin, S.-J., Cizewski Culotta, V., Penarrubia, L. and Amasino, R.M. (1998) Identification of a Functional Homolog of the Yeast Copper Homeostasis Gene ATX1 from Arabidopsis. Plant Physiol. 117, 1227-1234.

[125] Cobine, P.A., Pieffel, F. and Winge, D.R. (2006) Copper trafficking to the mitochondrion and assembly of copper metalloenzymes. Biochimica et Biophysica Acta-Molecular Cell Research 1763, 759-772.

[126] Li, J. et al. (2005) Identification and characterization of a novel Cut family cDNA that encodes human copper transporter protein CutC. Biochemical and Biophysical Research Communications 337, 179-183.

[127] Macnair, M.R., Tilstone, G.H. and Smith, S.E. (2000) The genetics of metal tolerance and accumulation in higher plants. Phytoremediation of Contaminated Soil and Water, 235-250.

[128] Hall, J.L. (2002) Cellular mechanisms for heavy metal detoxification and tolerance. Journal of Expperimental Botany 53, 1-11.

[129] Taiz, L. and Zeiger, E. (2002), pp. 690p Sinauer Associates, Inc., Suderland, MA USA.

[130] Van Tichelen, K.K., Colpaert, J.V. and Vangronsveld, J. (2001) Ectomycorrhizal protection of *Pinus sylvestris* against copper toxicity. New Phytologist 150, 203-213.

[131] Bellion, M., Courbot, M., Jacob, C., Blaudez, D. and Chalot, M. (2006) Extracellular and cellular mechanisms sustaining metal tolerance in ectomycorrhizal fungi. Fems Microbiology Letters 254, 173-181.

[132] Jentschke, G. and Goldbold, D.L. (2000) Metal toxicity and ectomycorrhizas. Physiologia Plantarum 109, 107-116.

[133] Ernst, W.H.O., Verkleij, J.A.C. and Schat, H. (1992) Metal Tolerance in Plants. Acta Botanica Neerlandica 41, 229-248.

[134] Bringezu, K., Lichtenberger, O., Leopold, I. and Neumann, D. (1999) Heavy metal tolerance of *Silene vulgaris*. Journal of Plant Physiology 154, 536-546.

[135] Feder, M.E. and Hofmann, G.E. (1999) Heat-shock proteins, molecular chaperones, and stress response: Evolutionary and Ecological Physiology. Annual Review of Physiology 61, 243-282.

[136] Lindquist, S. and Craig, E.A. (1988) The Heat-Shock Proteins. Annual Review of Genetics 22, 631-677.

[137] Tseng, T.S., Tzeng, S.S., Yeh, K.W., Yeh, C.H., Chang, F.C., Chen, Y.M. and Lin, C.Y. (1993) The Heat-Shock Response in Rice Seedlings - Isolation and Expression of Cdnas That Encode Class-I Low-Molecular-Weight Heat-Shock Proteins. Plant and Cell Physiology 34, 165-168.

[138] Sarry, J.-E. et al. (2006) The early responses of *Arabidopsis thaliana* cells to cadmium exposure explored by protein and metabolite profiling analyses. Proteomics 6, 2180-2198.

[139] Dixon, D., Lapthorn, A. and Edwards, R. (2002) Plant glutathione transferases. Genome Biology 3, reviews3004.1 -10.

[140] Murphy, R.C. and Zarini, S. (2002) Glutathione adducts of oxyeicosanoids. Prostaglandins & Other Lipid Mediators 68-69, 471-482.

[141] Xiang, C. and Oliver, D.J. (1998) Glutathione Metabolic Genes Coordinately Respond to Heavy Metals and Jasmonic Acid in *Arabidopsis*. Plant Cell 10, 1539-1550.

[142] Meister, A. and Anderson, M.E. (1983) Glutathione. Annual Review of Biochemistry 52, 711-760.

[143] Cobbett, C.S. (2000) Phytochelatin biosynthesis and function in heavy-metal detoxification. Current Opinion in Plant Biology 3, 211-216.

[144] Cobbett, C. and Goldsbrough, P. (2002) Phytochelatins and Metallothioneins: Roles in Heavy Metal Detoxification and Homeostasis. Annual Review of Plant Biology 53, 159-182.

[145] Devos, C.H.R., Vonk, M.J., Vooijs, R. and Schat, H. (1992) Glutathione depletion due to copper-induced phytochelatin synthesis causes oxidative stress in *Silene cucubalus*. Plant Physiology 98, 853-858.

[146] Schat, H., Llugany, M., Vooijs, R., Hartley-Whitaker, J. and Bleeker, P.M. (2002) The role of phytochelatins in constitutive and adaptive heavy metal tolerances in hyperaccumulator and non-hyperaccumulator metallophytes. Journal of Experimental Botany 53, 2381-2392.

[147] Murphy, A. and Taiz, L. (1995) Comparison of Metallothionein Gene Expression and Nonprotein Thiols in Ten Arabidopsis Ecotypes (Correlation with Copper Tolerance). Plant Physiol. 109, 945-954.

[148] Guo, W.J., Bundithya, W. and Goldsbrough, P.B. (2003) Characterization of the Arabidopsis metallothionein gene family: tissue-specific expression and induction during senescence and in response to copper. New Phytologist 159, 369-381.

[149] Haydon, M.J. and Cobbett, C.S. (2007) Transporters of ligands for essential metal ions in plants. New Phytologist 174, 499-506.

[150] Weber, M., Harada, E., Vess, C., von Roepenack-Lahaye, E. and Clemens, S. (2004) Comparative microarray analysis of *Arabidopsis thaliana* and *Arabidopsis halleri* roots identifies nicotianamine synthase, a ZIP transporter and other genes as potential metal hyperaccumulation factors. Plant Journal 37, 269-281.

[151] Pich, A., Manteuffel, R., Hillmer, S., Scholz, G. and Schmidt, W. (2001) Fe homeostasis in plant cells: Does nicotianamine play multiple roles in the regulation of cytoplasmic Fe concentration? Planta 213, 967-976.

[152] Liao, M., Hedley, M., Woolley, D., Brooks, R. and Nichols, M. (2000) Copper uptake and translocation in chicory (*Cichorium intybus* L. cv Grasslands Puna) and tomato (*Lycopersicon esculentum* Mill. cv Rondy) plants grown in NFT system. II. The role

of nicotianamine and histidine in xylem sap copper transport. Plant and Soil 223, 245-254.

[153] Kramer, U., CotterHowells, J.D., Charnock, J.M., Baker, A.J.M. and Smith, J.A.C. (1996) Free histidine as a metal chelator in plants that accumulate nickel. Nature 379, 635-638.

[154] Hall, A., Fielding A.H, Butler M (1979) Mechanisms of Copper Tolerancie in the Marine Fouling Alga *Ectocarpus siliculosus* - Evidence for an Exclusion Mechanism. Marine Biology 54, 195-199.

[155] Sueur, S., van den Berg, C.M.G. and Riley, J.P. (1982) Measurement of the metal complexing ability of exudates of marine macroalgae. Limnology and Oceanography 27, 536-543.

[156] Gekeler, W., Grill, E., Winnacker, E.L. and Zenk, M.H. (1988) Algae Sequester Heavy-Metals Via Synthesis of Phytochelatin Complexes. Archives of Microbiology 150, 197-202.

[157] Pawlik-Skowronska, B., Pirszel, J. and Brown, M.T. (2007) Concentrations of phytochelatins and glutathione found in natural assemblages of seaweeds depend on species and metal concentrations of the habitat. Aquatic Toxicology 83, 190-199.

[158] Morris, C.A., Nicolaus, B., Sampson, V., Harwood, J.L. and Kille, P. (1999) Identification and characterization of a recombinant metallothionein protein from a marine alga, *Fucus vesiculosus*. Biochem J 338 (Pt 2), 553-60.

[159] Merrifield, M.E., Ngu, T. and Stillman, M.J. (2004) Arsenic binding to *Fucus vesiculosus* metallothionein. Biochemical and Biophysical Research Communications 324, 127-132.

[160] Schoenwaelder, M.E.A. (2002) The occurrence and cellular significance of physodes in brown algae. Phycologia 41, 125-139.

[161] Karez, C.S. and Pereira, R.C. (1995) Metal contents in polyphenolic fractions extracted from brown alga *Padina gymnospora*. Botanica Marina 38, 151-155.

[162] Ragan, M.A., Ragan, C.M. and Jensen, A. (1980) Natural Chelators in Sea-Water - Detoxification of Zn^{2+} by Brown Algal Polyphenols. Journal of Experimental Marine Biology and Ecology 44, 261-267.

[163] Toth, G. and Pavia, H. (2000) Lack of phlorotannin induction in the brown seaweed *Ascophyllum nodosum* in response to increased copper concentrations. Marine Ecology Progress Series 192, 119-126.

[164] Andrade, L.R., Farina, M. and Amado Filho, G. (2002) Role of *Padina Gymnospora* (Dictyotales, Phaeophyceae) cell walls in cadmium accumulation. Phycologia 41, 39-48.

[165] Amado Filho, G., Karez, C.S., Pfeiffer, W., Y, Y.-V. and M, F. (1996) Accumulation effects on growth and ultrastructural localization of Zn in the brown alga *Padina gymnospora*. Hydrobiologia 326, 451-456.

[166] Hervé, C., de franco, P.-O., Groisillier, A., Tonon, T. and Boyen, C. (2008) New members of the glutathione transferase family discovered in red and brown algae. Biochem J 412, 535-544.

[167] de Franco, P.-O., Rousvoal, S., Tonon, T. and Boyen, C. (*In press*) Whole genome survey of the glutathione transferase family in the brown algal model *Ectocarpus siliculosus*. Marine Genomics.

[168] Tsang, E., Bowler, C., Herouart, D., Van Camp, W., Villarroel, R., Genetello, C., Van Montagu, M. and Inze, D. (1991) Differential Regulation of Superoxide Dismutases in Plants Exposed to Environmental Stress. Plant Cell 3, 783-792.

[169] Drazkiewicz, M., Skórzynska-Polit, E. and Krupa, Z. (2003) Response of the ascorbate-glutathione cycle to excess copper in *Arabidopsis thaliana* (L.). Plant Science 164, 195-202.

[170] Lombardi, L. and Sebastiani, L. (2005) Copper toxicity in *Prunus cerasifera*: growth and antioxidant enzymes responses of in vitro grown plants. Plant Science 168, 797-802.

[171] Alscher, R.G., Erturk, N. and Heath, L.S. (2002) Role of superoxide dismutases (SODs) in controlling oxidative stress in plants. Journal of Experimantal Botany 53, 1331-41.

[172] Asada, K. (1999) The water-water cycle in chloroplasts: Scavenging of active oxygens and dissipation of excess photons. Annual Review of Plant Physiology and Plant Molecular Biology 50, 601-639.

[173] Pinto, E., Van Nieuwerburgh, L., de Barros, M.P., Pedersen, M., Colepicolo, P. and Snoeijs, P. (2003) Density-dependent patterns of thiamine and pigment production in the diatom Nitzschia microcephala. Phytochemistry 63, 155-163.

[174] Woodall, A.A., Britton, G. and Jackson, M.J. (1997) Carotenoids and protection of phospholipids in solution or in liposomes against oxidation by peroxyl radicals: Relationship between carotenoid structure and protective ability. Biochimica et Biophysica Acta-General Subjects 1336, 575-586.

[175] Bors, W., Michel, C. and Stettmaier, K. (2001) Structure-activity relationships governing antioxidant capacities of plant polyphenols. Methods in Enzymology, pp. 166-180 (Packer, L., Ed.) Academic Press.

[176] Sagi, M. and Fluhr, R. (2006) Production of Reactive Oxygen Species by Plant NADPH Oxidases. Plant Physiology 141, 336-340.

[177] Nielsen, H.D., Brown, M.T. and Brownlee, C. (2003) Cellular responses of developing *Fucus* serratus embryos exposed to elevated concentrations of Cu^{2+}. Plant, Cell and Environment 26, 1737-1747.

[178] Pitzschke, A. and Hirt, H. (2006) Mitogen-activated protein kinases and reactive oxygen species signaling in plants. Plant Physiology 141, 351-356.

[179] Jonak, C., Nakagami, H. and Hirt, H. (2004) Heavy Metal Stress. Activation of Distinct Mitogen-Activated Protein Kinase Pathways by Copper and Cadmium. Plant Physiology 136, 3276-3283.

[180] Kwak, J.M., Nguyen, V. and Schroeder, J.I. (2006) The Role of Reactive Oxygen Species in Hormonal Responses. Plant Physiology 141, 323-329.

[181] Orozco-Cardenas, M.L., Narvaez-Vasquez, J. and Ryan, C.A. (2001) Hydrogen peroxide acts as a second messenger for the induction of defense genes in tomato plants in response to wounding, systemin, and methyl jasmonate. Plant Cell 13, 179-191.

[182] Fujita, M., Fujita, Y., Noutoshi, Y., Takahashi, F., Narusaka, Y., Yamaguchi-Shinozaki, K. and Shinozaki, K. (2006) Crosstalk between abiotic and biotic stress responses: a current view from the points of convergence in the stress signaling networks. Current Opinion in Plant Biology 9, 436-442.

[183] Zhao, J., Davis, L.C. and Verpoorte, R. (2005) Elicitor signal transduction leading to production of plant secondary metabolites. Biotechnology Advances 23, 283-333.

[184] Funk, C.D. (2001) Prostaglandins and Leukotrienes: Advances in Eicosanoid Biology. Science 294, 1871-1875.

[185] Weber, H. (2002) Fatty acid-derived signals in plants. Trends in Plant Science 7, 217-224.

[186] Parmentier, J.-H., Muthalif, M.M., Saeed, A.E. and Malik, K.U. (2001) Phospholipase D Activation by Norepinephrine Is Mediated by 12(S)-, 15(S)-, and 20-Hydroxyeicosatetraenoic Acids Generated by Stimulation of Cytosolic Phospholipase A2. Tyrosine phosphorylation of phospholipase D2 in response to norepinephrine. The Journal of biological chemistry 276, 15704-15711.

[187] Sasaki, Y. et al. (2001) Monitoring of Methyl Jasmonate-responsive Genes in Arabidopsis by cDNA Macroarray: Self-activation of Jasmonic Acid Biosynthesis and Crosstalk with Other Phytohormone Signaling Pathways. DNA research 8, 153-161.

[188] Howe, G.A. and Schilmiller, A.L. (2002) Oxylipin metabolism in response to stress. Current Opinion in Plant Biology 5, 230-236.

[189] Blee, E. (2002) Impact of phyto-oxylipins in plant defense. Trends in Plant Science 7, 315-322.

[190] Maksymiec, W., Wianowska, D., Dawidowicz, A.L., Radkiewicz, S., Mardarowicz, M. and Krupa, Z. (2005) The level of jasmonic acid in *Arabidopsis thaliana* and *Phaseolus coccineus* plants under heavy metal stress. Journal of Plant Physiology 162, 1338-1346.

[191] Weinberger, F. (2007) Pathogen-Induced Defense and Innate Immunity in Macroalgae. Biological Bulletin 213, 290-302.

[192] Gerwick, W.H., Roberts, M.A., Vulpanovici, A. and Ballantine, D.L. (1999) Biogenesis and biological function of matine algal oxylipins. Advances in experimental medicine and biology 447, 211-218.

[193] Potin, P., Bouarab, K., Salaun, J.-P., Pohnert, G. and Kloareg, B. (2002) Biotic interactions of marine algae. Current Opinion in Plant Biology 5, 308-317.

[194] Küpper, F.C., Gaquerel, E., Boneberg, E.-M., Morath, S., Salaun, J.-P. and Potin, P. (2006) Early events in the perception of lipopolysaccharides in the brown alga *Laminaria digitata* include an oxidative burst and activation of fatty acid oxidation cascades. Journal of Experimental Botany 57, 1991-1999.

[195] Lion, U., Wiesemeier, T., Weinberger, F., Beltran, J., Flores, V., Faugeron, S., Correa, J. and Pohnert, G. (2006) Phospholipases and galactolipases trigger oxylipin-mediated wound-activated defence in the red alga *Gracilaria chilensis* against epiphytes. Chembiochem 7, 457-462.

[196] Cutignano, A., d'Ippolito, G., Romano, G., Lamari, N., Cimino, G., Febbraio, F. and Fontana, A. (2006) Chloroplastic glycolipids fuel aldehyde biosynthesis in the marine diatom *Thalassiosira rotula*. Chembiochem 7, 450-456.

[197] Pohnert, G. (2002) Phospholipase A(2) activity triggers the wound-activated chemical defense in the diatom *Thalassiosira rotula*. Plant Physiology 129, 103-111.

[198] Gerwick, W.H., Proteau, P.J., Nagle, D.G., Wise, M.L., Jiang, Z.D., Bernart, M.W. and Hamberg, M. (1993) Biologically active oxylipins from seaweeds. Hydrobiologia 260-261, 653-665.

[199] Noguchi, T. et al. (1994) Poisoning by the red alga 'ogonori' (Gracilaria verrucosa) on the Nojima Coast, Yokohama, Kanagawa Prefecture, Japan. Toxicon 32, 1533-8.

[200] Gerwick, W.H., Roberts, M.A., Vulpanovici, A. and Ballantine, D.L. (1999) Biogenesis and biological function of marine algal oxylipins. Adv Exp Med Biol 447, 211-8.

[201] Jiang, Z.D., Ketchum, S.O. and Gerwick, W.H. (2000) 5-Lipoxygenase-derived oxylipins from the red alga *Rhodymenia pertusa*. Phytochemistry 53, 129-133.

[202] Sajiki, J. and Kakimi, H. (1998) Identification of eicosanoids in the red algae, *Gracilaria asiatica*, using high-performance liquid chromatography and electrospray ionization mass spectrometry. Journal of Chromatography A 795, 227-237.

[203] Krupina, M.V. and Dathe, W. (1991) Occurrence of Jasmonic Acid in the Red Alga *Gelidium latifolium*. Zeitschrift Fur Naturforschung C-a Journal of Biosciences 46, 1127-1129.

[204] Gaquerel, E., Herve, C., Labriere, C., Boyen, C., Potin, P. and Salaun, J.-P. (2007) Evidence for oxylipin synthesis and induction of a new polyunsaturated fatty acid hydroxylase activity in *Chondrus crispus* in response to methyljasmonate. Biochimica et Biophysica Acta - Molecular and Cell Biology of Lipids 1771, 565-575.

[205] Collén, J., Hervé, C., Guisle-Marsollier, I., Léger, J.J. and Boyen, C. (2006) Expression profiling of *Chondrus crispus* (Rhodophyta) after exposure to methyl jasmonate. J. Exp. Bot. 57, 3869-3881.

[206] Hervé, C., Tonon, T., Collén, J., Corre, E. and Boyen, C. (2006) NADPH oxidases in Eukaryotes: red algae provide new hints! Current Genetics 49, 190-204.

[207] Bernart, M.W., Whatley, G.G. and Gerwick, W.H. (1993) Unprecedented Oxylipins from the Marine Green-Alga Acrosiphonia-Coalita. Journal of Natural Products 56, 245-259.

[208] Gerwick, W.H. (1994) Structure and biosynthesis of marine algal oxylipins. Biochimica et Biophysica Acta - Lipids and Lipid Metabolism 1211, 243-255.

[209] Zimmerman, D.C. and Vick, B.A. (1973) Lipoxygenase in *Chlorella pyrenoidosa.* Lipids 8, 264-6.

[210] Proteau, P.J. and Gerwick, W.H. (1993) Divinyl ethers and hydroxy fatty acids from three species of *Laminaria* (brown algae). Lipids 28, 783-7.

[211] Proteau, P.J. and Gerwick, W.H. (1992) Cymathere ethers A and B: Bicyclic oxylipins from the marine brown alga *Cymathere triplicata*. Tetrahedron Letters 33, 4393-4396.

[212] Todd, J.S., Proteau, P.J. and Gerwick, W.H. (1994) The absolute configuration of ecklonialactones A, B, and E, novel oxylipins from brown algae of the genera *Ecklonia* and *Egregia*. J Nat Prod 57, 171-4.

[213] Boonprab, K., Matsui, K., Akakabe, Y., Yoshida, M., Yotsukura, N., Chirapart, A. and Kajiwara, T. (2006) Formation of Aldehyde Flavor (n-hexanal, 3Z-nonenal and 2E-nonenal) in the Brown Alga, *Laminaria Angustata*. Journal of Applied Phycology 18, 409-412.

[214] Boonprab, K., Matsui, K., Akakabe, Y., Yotsukura, N. and Kajiwara, T. (2003) Hydroperoxy-arachidonic acid mediated n-hexanal and (Z)-3- and (E)-2-nonenal formation in *Laminaria angustata*. Phytochemistry 63, 669-678.

[215] Ianora, A. et al. (2004) Aldehyde suppression of copepod recruitment in blooms of a ubiquitous planktonic diatom. Nature 429, 403-407.

[216] Pohnert, G. (2000) Wound-activated chemical defense in unicellular planktonic algae. Angewandte Chemie-International Edition 39, 4352-+.

[217] Arnold, T.M., Targett, N.M., Tanner, C.E., Hatch, W.I. and Ferrari, K.E. (2001) Evidence for methyl jasmonate-induced phlorotannin production in *Fucus vesiculosus* (Phaeophyceae). Journal of Phycology 37, 1026-1029.

[218] Wilkins, M.R. et al. (1996) From proteins to proteomes: Large scale protein identification by two-dimensional electrophoresis and amino acid analysis. Bio-Technology 14, 61-65.

[219] Tyers, M. and Mann, M. (2003) From genomics to proteomics. Nature 422, 193-197.

[220] Pandey, A. and Mann, M. (2000) Proteomics to study genes and genomes. Nature 405, 837-846.

[221] Biron, D.G., Loxdale, H.D., Ponton, F., Moura, H., Marche, L., Brugidou, C. and Thomas, F. (2006) Population proteomics: An emerging discipline to study metapopulation ecology. Proteomics 6, 1712-1715.

[222] O'Farrell, P.H. (1975) High resolution two-dimensional electrophoresis of proteins. J. Biol. Chem. 250, 4007-4021.

[223] Gorg, A., Boguth, G., Obermaier, C., Posch, A. and Weiss, W. (1995) 2-Dimensional Polyacrylamide-Gel Electrophoresis with Immobilized pH Gradients in the First Dimension (Ipg-Dalt) - the State-of-the-Art and the Controversy of Vertical Versus Horizontal Systems. Electrophoresis 16, 1079-1086.

[224] Domon, B. and Aebersold, R. (2006) Review - Mass spectrometry and protein analysis. Science 312, 212-217.

[225] Bengtsson, M. (2003), pp. 28 Department of Botany, Stockholm University.

[226] Qureshi, M.I., Qadir, S. and Zolla, L. (2007) Proteomics-based dissection of stress-responsive pathways in plants. Journal of Plant Physiology 164, 1239-1260.

[227] Canovas, F.M., Dumas-Gaudot, E., Recorbet, G., Jorrin, J., Mock, H.P. and Rossignol, M. (2004) Plant proteome analysis. Proteomics 4, 285-298.

[228] Ahsan, N. et al. (2008) Comparative proteomic study of arsenic-induced differentially expressed proteins in rice roots reveals glutathione plays a central role during As stress. Proteomics 8, 3561-3576.

[229] Ahsan, N., Lee, S.H., Lee, D.G., Lee, H., Lee, S.W., Bahk, J.D. and Lee, B.H. (2007) Physiological and protein profiles alternation of germinating rice seedlings exposed to acute cadmium toxicity. Comptes Rendus Biologies 330, 735-746.

[230] Gillet, S., Decottignies, P., Chardonnet, S. and Le Marechal, P. (2006) Cadmium response and redoxin targets in *Chlamydomonas reinhardtii*: a proteomic approach. Photosynthesis Research 89, 201-211.

[231] Yang, Q., Wang, Y., Zhang, J., Shi, W., Qian, C. and Peng, X. (2007) Identification of aluminum-responsive proteins in rice roots by a proteomic approach: Cysteine synthase as a key player in Al response. Proteomics 7, 737-749.

[232] Smith, A.P., DeRidder, B.P., Guo, W.J., Seeley, E.H., Regnier, F.E. and Goldsbrough, P.B. (2004) Proteomic analysis of *Arabidopsis* glutathione S-transferases from benoxacor- and copper-treated seedlings. Journal of Biological Chemistry 279, 26098-26104.

[233] Kung, C.-C.S., Huang, W.-N., Huang, Y.-C. and Yeh, K.-C. (2006) Proteomic survey of copper-binding proteins in *Arabidopsis* roots by immobilized metal affinity chromatography and mass spectrometry. Proteomics 6, 2746-2758.

[234] Bhargava, P., Mishra, Y., Srivastava, A.K., Narayan, O.P. and Rai, L.C. (2008) Excess copper induces anoxygenic photosynthesis in *Anabaena doliolum*: a homology based proteomic assessment of its survival strategy. Photosynthesis Research 96, 61-74.

[235] Bona, E., Marsano, F., Cavaletto, M. and Berta, G. (2007) Proteomic characterization of copper stress response in *Cannabis sativa* roots. Proteomics 7, 1121-1130.

[236] Wong, P.F., Tan, L.J., Nawi, H. and AbuBakar, S. (2006) Proteomics of the red alga, *Gracilaria changii* (Gracilariales, Rhodophyta). Journal of Phycology 42, 113-120.

[237] Nagai, K., Yotsukura, N., Ikegami, H., Kimura, H. and Morimoto, K. (2008) Protein extraction for 2-DE from the lamina of *Ecklonia kurome* (laminariales): Recalcitrant tissue containing high levels of viscous polysaccharides. Electrophoresis 29, 672-681.

[238] Raven, J.A., Evans, M.C.W. and Korb, R.E. (1999) The role of trace metals in photosynthetic electron transport in O_2 evolving organisms. Photosynthesis Research 60, 111-149.

[239] Freeman, H. and Guss, J. (2001) Handbook of metalloproteins. 1153-1169.

[240] Navarro, J.A., Hervas, M. and DelaRosa, M.A. (1997) Co-evolution of cytochrome c(6) and plastocyanin, mobile proteins transferring electrons from cytochrome b(6)f to photosystem I. Journal of Biological Inorganic Chemistry 2, 11-22.

[241] Bordo, D., Pesce, A., Bolognesi, M., Stroppolo, M., Falconi, M. and Desideri, A. (2001) Handbook of metalloptoteins. 1284-1300.

[242] Getzoff, E.D., Tainer, J.A., Weiner, P.K., Kollman, P.A., Richardson, J.S. and Richardson, D.C. (1983) Electrostatic Recognition between Superoxide and Copper, Zinc Superoxide-Dismutase. Nature 306, 287-290.

[243] Keilin, D. and Mann, T. (1939) Nature 143, 23-24.

[244] Malmstrom, B.G., Mosbach, R. and Vanngard, T. (1959) Electron Spin Resonance Study of the State of Copper in Fungal Laccase. Nature 183, 321-322.

[245] Pescheck (1999) Biochemica and biophysica acta 1275, 27-32.

[246] Rodriguez, F.I., Esch, J.J., Hall, A.E., Binder, B.M., Schaller, G.E. and Bleecker, A.B. (1999) A copper cofactor for the ethylene receptor ETR1 from *Arabidopsis*. Science 283, 996-998.

[247] Herbik, A., Bolling, C. and Buckhout, T.J. (2002) The involvement of a multicopper oxidase in iron uptake by the green algae *Chlamydomonas reinhardtii*. Plant Physiology 130, 2039-2048.

2 COPPER STRESS INDUCES BIOSYNTHESIS OF OCTADECANOID AND EICOSANOID OXYGENATED DERIVATIVES IN THE BROWN ALGAL KELP *Laminaria digitata*

Andrés Ritter, Sophie Goulitquer, Jean-Pierre Salaün, Thierry Tonon, Juan A. Correa and Philippe Potin

Abstract

- To better understand the toxicity and the orchestration of antioxidant defenses of marine brown algae in response to copper-induced stress, lipid peroxidation processes were investigated in the brown alga *Laminaria digitata*.
- The expression of genes involved in cell protection and anti-oxidant responses were monitored by semi-quantitative RT-PCR and the lipid peroxidation products were further characterized by profiling oxylipin signatures using HPLC-MS.
- Exposure to copper excess triggers lipoperoxide accumulation and upregulates the expression of stress related genes. It also increases the release of free polyunsaturated fatty acids, leading to an oxidative cascade through at least two distinct mechanisms. Incubations in presence of inhibitors of lipoxygenases and cycloxygenases showed that besides the ROS-mediated processes, copper stress induces the synthesis of oxylipins through enzymatic mechanisms. Among complex oxylipins, cyclopentenones from C18 and C20 fatty acids such as 12-oxo-PDA and prostaglandins were detected for the first time in brown algae, as well as unique compounds such as the 18-hydroxy-17-oxo-eicosatetraenoic acid.
- Our results suggest that lipid peroxidation participates in the toxic effects of copper and that lipid peroxidation derivatives may regulate protective mechanisms by employing plant-like octadecanoid signals but also eicosanoid oxylipins which are absent in vascular plants.

New Phytologist

Research

Copper stress induces biosynthesis of octadecanoid and eicosanoid oxygenated derivatives in the brown algal kelp *Laminaria digitata*

Andrés Ritter[1,2,4]*, Sophie Goulitquer[3]*, Jean-Pierre Salaün[3], Thierry Tonon[1,2], Juan A. Correa[4] and Philippe Potin[1,2]

[1]Université Pierre et Marie Curie-Paris 6, UMR 7139 Végétaux marins et Biomolécules, Station Biologique, F–29682, Roscoff, France; [2]CNRS, UMR 7139 Végétaux marins et Biomolécules, Station Biologique, F–29682, Roscoff, France; [3]Laboratoire de Biochimie 'Epissage, Cancer, Lipides et Apoptose', INSERM U613, Université de Bretagne Occidentale, Faculté de Médecine, F–29285 Brest, France; [4]Center for Advanced Studies in Ecology & Biodiversity, Departamento de Ecología, Facultad de Ciencias Biológicas, Pontificia Universidad Católica de Chile, Santiago, Chile

Author for correspondence:
Philippe Potin
Tel: +33 (0)298292375
Fax: +33 (0)298292324
Email: potin@sb-roscoff.fr

Received: *29 July 2008*
Accepted: *30 July 2008*

Summary

• To better understand the toxicity and the orchestration of antioxidant defenses of marine brown algae in response to copper-induced stress, lipid peroxidation processes were investigated in the brown alga *Laminaria digitata*.

• The expression of genes involved in cell protection and anti-oxidant responses were monitored by semi-quantitative reverse transcriptase polymerase chain reaction and the lipid peroxidation products were further characterized by profiling oxylipin signatures using high-pressure liquid chromatography–mass spectrometry.

• Exposure to copper excess triggers lipoperoxide accumulation and upregulates the expression of stress related genes. It also increases the release of free polyunsaturated fatty acids, leading to an oxidative cascade through at least two distinct mechanisms. Incubations in presence of inhibitors of lipoxygenases and cycloxygenases showed that in addition to the reactive oxygen species-mediated processes, copper stress induces the synthesis of oxylipins through enzymatic mechanisms. Among complex oxylipins, cyclopentenones from C18 and C20 fatty acids such as 12-oxo-PDA and prostaglandins were detected for the first time in brown algae, as well as unique compounds such as the 18-hydroxy-17-oxo-eicosatetraenoic acid.

• These results suggest that lipid peroxidation participates in the toxic effects of copper and that lipid peroxidation derivatives may regulate protective mechanisms by employing plant-like octadecanoid signals but also eicosanoid oxylipins which are absent in vascular plants.

Key words: brown algae, copper, heavy metal, kelp, *Laminaria digitata*, oxylipins, prostaglandins, stress.

New Phytologist (2008) **doi**: 10.1111/j.1469-8137.2008.02626.x

Introduction

Heavy metals such as copper remain among the most significant worldwide pollution factors in marine environments as a result of the wide range of human activities involving the use of this metal and their subsequent transfer to marine ecosystems. In these conditions, metals, which are essential components of global ecosystems, become a severe threat to coastal organisms (Correa *et al.*, 1999; Livingstone, 2001). Large brown seaweeds, such as kelps of the order Laminariales, are fundamental components of coastal benthic ecosystems and

*These authors contributed equally to this work.

dominate rocky shore natural assemblages. It was observed that they become absent in copper mine-affected areas of the coasts of Northern Chile (Medina *et al.*, 2005; Andrade *et al.*, 2006). However, compared with the large body of literature available for terrestrial higher plants or unicellular green algae, the effects of copper excess is poorly documented for these evolutionary distant photosynthetic organisms, which have evolved as an independent lineage for more than a billion yr in the division Heterokonta (Charrier *et al.*, 2008).

Although copper is an essential element for all living organisms as enzyme cofactor and key participant in several metabolic pathways, at elevated concentrations it becomes toxic (Gledhill *et al.*, 1997; Pinto *et al.*, 2003). An excess of this metal may lead to detrimental effects on photosynthesis, chlorophyll synthesis, fatty acid metabolism and carbohydrate synthesis (Fernandes & Henriques, 1991). Copper is known for its detrimental action on enzyme activity and reactive oxygen species (ROS) accumulation (Pinto *et al.*, 2003). When exposed to excess copper, photosynthetic organisms shift the balance of free radical metabolism toward an accumulation of H_2O_2, mainly caused by deleterious effects on the photosystems (Yruela *et al.*, 2000). In the presence of redox active transition metals such as Cu^{2+} and Fe^{2+}, H_2O_2 can be converted to highly reactive hydroxyl radicals via the Fenton reaction (Halliwell & Gutteridge, 1992; Mithöfer *et al.*, 2004). As a consequence, ROS can react with proteins, nucleic acids and lipids, causing deleterious effects on cell structure. At the same time ROS generation can trigger a variety of cellular responses through signaling events. One of these responses is the activation of fatty acids by the generation of oxygenated polyunsaturated fatty acids known as oxylipins, which play a pivotal role against abiotic and biotic stress in plants and metazoans. Oxylipins are subsequently produced via polyunsaturated fatty acid (PUFA) oxidation by incorporation of one, two or four atoms of oxygen. These reactions can be carried out nonenzymatically by direct oxidation of PUFA by ROS or catalysed by enzymes such as lipoxygenase (LOX), cytochrome P450 (CYP) or cycloxygenase (COX). In mammals, oxylipins such as leukotrienes and prostaglandins are produced from the oxidation of C20 PUFAs. These compounds play a major role in inflammatory processes, allergy and, in a broader sense, defensive stress responses to infection, drugs, and xenobiotics (Funk, 2001). In plants, their participation during wounding stress and pathogen and herbivore attacks has been recognized in the past and is still an active field of research (Farmer *et al.*, 2003; Farmer & Schulze-Lefert, 2005). In response to pathogen stimuli, biosynthesis of oxylipins in plants, red algae and mammals, is carried out by the release of PUFA with the involvement of phospholipases and galactolipases (Parmentier *et al.*, 2001; Sasaki *et al.*, 2001; Cosse *et al.*, 2007). Although many examples of plants synthesizing and accumulating oxidized fatty acid derivatives in response to biotic or abiotic stress have been reported (Blée, 2002; Howe & Schilmiller, 2002; Farmer & Davoine, 2007), limited attention has been paid to the involvement of oxylipins in stress responses to heavy metals.

Within the marine environment, brown algae deal with diverse abiotic stresses, including that caused by copper, by setting up specific defensive mechanisms (Contreras *et al.*, 2005). Previous work on brown algae has pointed to the originality of oxylipin metabolism in these organisms (Gerwick *et al.*, 1999). However, until recently, little was known about the involvement of oxylipins in the activation of cell-based induced defense responses. Only one study reported that bacterial lipopolysaccharides (LPS) triggered defense reactions in the brown algal kelp *Laminaria digitata*, involving an oxidative burst, a release of PUFAs and oxylipin accumulation (Küpper *et al.*, 2006). Therefore, the objective of this work was to examine lipid oxidation in *L. digitata* exposed to copper excess and the concomitant expression of genes involved in detoxification processes. By oxylipin profiling, we show that copper induces the enzyme-mediated synthesis of fatty acid hydroperoxides (FAHs) and prostaglandins, as well as the chemically mediated formation of various oxylipins.

Materials and Methods

Chemicals

Fatty acids (C14:0, C16:0, C18:1, C18:2, C18:3, C18:4, C20:4 and C20:5) and 12-OH-lauric acid were purchased from Sigma-Aldrich (St Louis, MO, USA); oxylipins 15*S*-hydroperoxy-5*Z*,8*Z*,11*Z*,13*E*-eicosatetraenoic acid (15(*S*)-HpETE), 15*S*-hydroxy-5Z,8Z,11Z,13E-eicosatetraenoic acid (15(*S*)-HETE), 13*S*-hydroperoxy-9*Z*,11*E*,15*Z*-octadecatrienoic acid (13(*S*)-HpOTrE), 13*S*-hydroxy-9*Z*,11*E*,15*Z*-octadecatrienoic acid (13(*S*)-HOTrE), (±)12(13)-epoxy-9*Z*-octadecenoic acid ((±)12(13)-EpOME)), 4-oxo-5*R*-(2*Z*)-2-pentenyl-2-cyclopentene-1*S*-octanoic acid (12-oxo-PDA) and prostaglandins A_2, B_2, E_1, D_1, E_2, D_2 and 15-keto-PGE_2 and arachidonic acid-d8 were purchased from Cayman Chemical (Spi-Bio, Montigny Le Bretonneux, France). Silylating reagent Sylon BFT (bis(trimethylsilyl)trifluoroacetamide :trimethylchlorosilane, 99:1) was purchased from Supelco (Bellefonte, PA, USA). All chemicals and solvents were obtained from Merck (Darmstadt, Germany).

Algal material and cultivation treatments

The marine brown alga *L. digitata* (Hudson) J.V. Lamouroux (Laminariales, Laminariaceae) was collected in the intertidal zone close to the Station Biologique de Roscoff in Brittany, France, during low tide. Young fronds of 10 cm (maximum length) were chosen and transported to the laboratory. After cleaning, they were separated and kept in separated flasks (200–900 mg FW of alga per flask) containing 1 l of 0.45 μm filtered seawater at 9–17°C, under constant aeration and photon flux density of 50–60 μmol photons m^{-2} s^{-1} with a

photoperiod of 10 h light : 14 h dark (L : D) for 1 wk. Just before the start of the experiment, three individuals were harvested as control material. The medium was then changed in the flasks and for copper exposure, a nominal concentration of 300 μg l^{-1} copper as $CuCl_2$ from Merck was applied. Algal samples were harvested after 6 h, 24 h, 48 h and 72 h of incubation in the presence or absence of copper. No nutrients were added during the experiment. For each kinetic point, three replicates were sampled. For pharmacological analyses, several inhibitors were used. Salicylhydroxamic acid (SHAM) at 1 mM final concentration and *n*-propylgallate (n-PGal) 100 μM final concentration were used because they are inhibitors of lipoxygenase (LOX) activity. Cycloxygenase (COX) inhibitor acetylsalicylate (AS) was applied at 1 mM of final concentration. Algae were treated for 20 min with these chemicals just before starting the treatments with copper excess. At the end of the experiment thalli were frozen in liquid nitrogen and kept at −80°C for analysis.

Analysis of lipid peroxidation by thiobarbituric acid reactive substances (TBARs)

Lipid peroxidation was quantified by determining the content of TBAR which reflects the malondialdehyde (MDA) equivalent (Collén *et al.*, 2003). Approximately 0.5 g fresh weight tissue were ground in liquid nitrogen, mixed with 3 ml of a solution of 20% trichloroacetic acid and 0.2% thiobarbituric acid, incubated for 30 min in boiling water, cooled on ice and centrifuged for 40 min at 5000 ***g***. The supernatant was then diluted to 1 : 10 and absorption was measured at 532 nm. A coefficient of 150 M^{-1} cm^{-1} was used to quantify lipoperoxides. Ultrapure water was included as control to remove the absorbance caused by the reagent.

Extraction of oxylipins and free fatty acids

Oxylipins and free fatty acids were extracted in *L. digitata* tissue according to Küpper *et al.* (2006). In each sample, 250 ng of 12-OH-lauric acid was added as an internal standard. The residue was dissolved in 100 μl of ethanol and 20 μl was used for the characterization of free fatty acid and their oxygenated derivatives by liquid chromatography coupled to mass spectrometry (LC–MS).

LC-MS analysis

Oxygenated derivates of fatty acids were resolved and characterized by reverse phase high-pressure liquid chromatography (RP-HPLC) coupled to a Navigator Thermo Finnigan LC/MS mass spectrometer (Thermo Electron, Bremen Germany), equipped with an ionization source at atmospheric pressure (APCI) running on the negative ion mode. Oxidized fatty acids were analysed using a 5 μm Ultrasphere C18 column 250 × 4.6 mm (Beckman Coulter, Fullerton CA, USA). The mobile phase (0.2% acetic acid in water–acetonitrile) program began with a 30-min linear gradient from 100 : 0 to 40 : 60 acetonitrile–water (v : v) to separate prostaglandins. For the rest of the oxylipins the elution was followed by a set of 40 : 60 (v : v) for 30 min. The run finished with the elution of fatty acids and sterols by applying a 5-min linear gradient to 5 : 95 (v : v). At the end of the run, the mixture was held for 20 min at flow rate of 1 ml min^{-1} before returning to the initial conditions. The source heater was at 150°C and the APCI heater at 350°C, with a cone voltage of 30 V for quantification and 40 V to increase fragmentation for identification. Detection of oxidized fatty acids was achieved by monitoring their expected carboxylate anions $[M\text{-}H]^-$. For complete identification, co-chromatography using standard compounds was employed to compare LC peak retention times and mass spectra fragmentation. Data were collected in both total ion (TIC, *m/z* 60–600) and selected ion monitoring (SIM) chromatograms. These compounds were then quantified by comparing their peak area with authentic standards.

Gas chromatography–mass spectrometry (GC-MS) analysis

For free fatty acids analysis, 50 ng of arachidonic acid-d8 were added to 20 μl of the FFA/oxylipin extract as internal standard. The solution was evaporated under a gentle stream of oxygen-free nitrogen and dissolved in 100 μl acetonitrile.

To form pentafluorobenzyl esters (PFB-esters), the carboxylic group reacted with 10 μl of 2,3,4,5,6-pentafluorobenzylbromide in the presence of 20 μl of *N,N*-diisopropylethylamine for 15 min at room temperature. The solvent was dried under a gentle stream of nitrogen and the residue was dissolved in 2 ml of water. Extraction was carried out twice with 2 ml ethyl acetate. At low concentration of oxylipins, the solution was dried under nitrogen gas and the residue was then dissolved in 100 μl hexane. Samples were analysed with a Hewlett-Packard 5873 Mass Selective Detector interfaced to a Hewlett-Packard 6890 Series+ gas chromatograph (Agilent, Les Ullis, France). A 2 μl sample was injected into a capillary column (HP-5MS; J & W Scientific, Folsom CA, USA) of 0.25 mm internal diameter, 30 m length and 0.25 mm-film thickness. The temperature of injection port and interface was 250°C and 280°C respectively. The oven temperature was set at 60°C for 5 min, increased at the rate of 10°C min^{-1} to 230°C, then set at 290°C at a rate of 1°C min^{-1} and held for 5 min at 290°C. Temperatures of the ion source and analyser of the mass spectrometer were 250°C and 100°C, respectively. The compounds were ionized by negative ion chemical ionization (NICI) using methane as reagent gas at 40 ml min^{-1} ionization energy and the trap current was at 123 eV and 49 μA respectively. For oxylipin identification, GC-MS analyses were carried out in a HP 5890 Series II gas chromatograph equipped with a

Table 1 Specific primer, annealing temperatures and total numbers of amplification cycles used for reverse transcriptase polymerase chain reaction (RT-PCR) analysis of gene expression

Gene	Primer sequence (5′–3′)	Number of amplification cycles	Amplified fragment size (bp)	*Laminaria digitata* database matches and EST accession number
LdHSP70	CAAGGAGAACAAGATCACCATC ACACTAGCCTAGTCGATCTCCTC	25	486	Heat shock protein 70 CN466643.1
LdGST2	ATGGCTCCCACCACATCTTTG TTACTTGTTGGTGGTCTCTGA	25	639	Glutathione *S*-transferase CN467141.1
LdTRX1	GAAGTAGACGGAGCACGATGG CAAGTGCTCGTCGAGCCTTC	30	348	Thioredoxin CN467319.1
LdTRX3	CAAGTTCAACGTCAAGGTCATCAG CGCGATTTCCAGAAGCACGTC	30	448	Thioredoxin CN467552.1
LdTRX4	GGAGTACGCTCGATCCACAGC GTCCTCCAAGAACAACTTCTCGATAG	25	468	Thioredoxin CN467295.1
LdSOD	CAGGATCACGAGGAGCGATG GTGCTCCAGCACAGCGTTTAGCT	30	209	Mn super oxide dismutase AW401234.1
LdPRX	CTCATGACAGATTGGTGGATGTG CGATGTCTGACAAGAGCGTCAT	30	374	Peroxyredoxin CN466553.1
LdMSR1	ACGAGGTTTGGGATCGCATC GTAACAGCGTATGTTCGTTGTGTCT	25	275	Methionine sulphoxide Reductase CN468288.1
LdMSR2	GAATATTCGCCGCAGCTGCT GTTGTTCCGTGCAGACTCCTG	25	133	Methionine sulphoxide Reductase AW400923.1
LdRPL14	TCCCGAAACCGTCAACCTT GTTATGGTCGCTCGCAAGC	25	248	Ribosomal protein 14 AW400923.1
LdEF	TCATGCTCGACACCGAAGTCAAGT GGAACAGAGGAGAGAAGGAACGA	25	647	Elongation factor CN467521.1

Fragment size of amplified products and their correspondent Blast match result with the expressed sequence tags (EST) GenBank accession number.

fused silica capillary column (as described earlier) coupled to a quadrupole mass-selective detector (HP 5971A; Agilent Technology). Mass spectra (E.I. mode) were recorded at 70 eV. Analyses were performed after silylation for 1 h at 60°C, in order to obtain trimethylsilyl derivatives for compounds containing a hydroxyl group (Pinot *et al.*, 1992). Compounds were dissolved in 1 ml of hexane and 2 µl were injected in the splitless mode at 60°C. After 5 min at 60°C, the oven temperature was increased to 200°C at 50°C min^{-1} and then linearly ramped to 280°C at 2°C min^{-1}, which was stabilized for 10 min before returning to initial conditions.

RNA extraction and cDNA synthesis

Total RNA was extracted according to Apt *et al.* (1995) with an additional step consisting of ethanol based polysaccharide precipitation (Fang *et al.*, 1992). For each condition, three replicates were treated independently. After treatment with RNase-free DNase (Qiagen, Hilden, Germany), RNA was purified through on column digestion using the RNeasy Mini Kit (Qiagen). From each RNA sample, 1 µg of total RNA was employed to synthesize cDNA using the SuperScript Double-Stranded cDNA Synthesis Kit (Invitrogen, Carlsbad, CA, USA) as recommended by the manufacturer.

Gene expression analysis

Semi-quantitative reverse transcriptase polymerase chain reaction (RT-PCR) was carried to perform gene expression analyses. Three independent replicates were examined. Nucleotide sequences presenting high similarity to genes coding for the genes manganese superoxide dismutase (*LdSOD*), sigma class glutathione S-transferase (*LdGST2*), peptide methionine sulphoxide reductases (*LdMSR1, LdMSR3*), heat shock protein 70 (*LdHSP70*), thioredoxins (*LdTRX1, LdTRX3*) and peroxiredoxin (*LdPRX*) were identified through analysis of four expressed sequences tag (EST) libraries from *L. digitata* containing a total of 3479 ESTs (Crépineau *et al.*, 2000; Roeder *et al.*, 2005). Expression of the genes encoding for elongation factor (*LdEF*) and ribosomal protein 14 (*LdRPL14*) were used as controls (Table 1). Specific primers sets were designed using the software VECTOR NTI ADVANCE 10.3.0 (Invitrogen). Reactions were carried out in a final volume of 25 µl of the following reaction mix: 2 µl cDNA, 1× GoTaq Reaction Buffer (1.5 mM $MgCl_2$) (Promega, Madison, WI, USA) with 0.2 mM dNTP, 1.25 units of GoTaq DNA polymerase (Promega) and 0.2 µM gene-specific primers (Eurogentec, Seraing, Belgium). PCRs were carried on a GenAmp PCR System 2700 (Applied Biosystems Foster City, LA, USA) The cycling program for PCR was run as follows: initial

New Phytologist

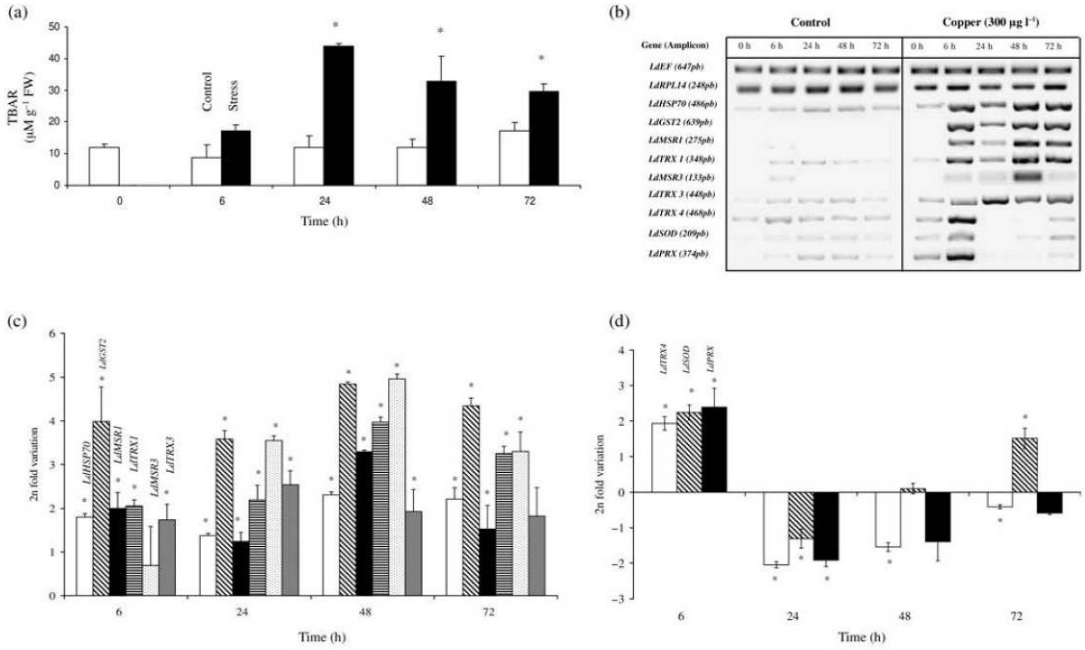

Fig. 1 Evidence for copper stress in *Laminaria digitata* juveniles. (a) Lipid peroxidation measured by thiobarbituric acid (TBA) assay following 0, 6, 24, 48 and 72 h of exposure to copper (300 μg l^{-1}). Controls are carried out following the same harvesting times. Values represent means of three independent replicates and bars represents the SE; *, significantly different from the control group ($P < 0.05$). (b) Simultaneous study of stress related gene expression by semi-quantitative reverse transcriptase polymerase chain reaction (RT-PCR) analysis. Reference gene expression level was assayed by studying genes encoding for ribosomal protein 14 (RPL14) and the elongation factor (EF). Results are representative of three independent replicates (see the Supporting Information, Fig. S1). The relative genes expression ratios were determined as described in materials and methods. (c) Transcript accumulation profiles of genes presenting upregulation throughout the copper treatments. (d) Transcript accumulation profiles of genes presenting upregulation at early stress stages. Values are the means of three independent replicates; bars, SE; *, significantly different from the control group ($P < 0.05$).

denaturation 5 min at 94°C, 25 to 35 cycles of 30 s at 95°C, 30 s at 55°C and 1 min at 72°C, and final elongation for 7 min at 72°C. For each gene examined, 10 μl of PCR product was loaded in a 2% agarose gel electrophoresis and run at 100 V for 30 min in the presence of ethidium bromide (0.07 μg ml^{-1}). Gel images were obtained using a Biovision 1000/26M (Vilber Lourmat, Marne-la-Vallée, France). In each condition, one representative image of each replicate was selected to be displayed. The expression levels were assessed by quantifying the gel bands using IMAGEQUANT v.5.2 software (Molecular Dynamics, GE Healthcare, Piscataway, NJ, USA). The Elongation Factor gene (*LdEF*) was used as internal control. The relative changes in expression among genes were calculated as *x*-fold changes to the appropriate control treatments.

Statistical analysis

Statistically significant differences among treatments were determined by the nonparametric Mann–Whitney U-test run on STATISTICA v.5.1 software (StatSoft, Tulsa, OK, USA). All conclusions are based on at least 5% level of significance ($P < 0.05$).

Results

Effect of copper excess on lipid peroxidation and gene stress marker regulation

No significant difference in the level of lipoperoxides was observed after 6 h of copper excess (Fig. 1a). However, after 24 h exposure to copper excess, the levels of lipoperoxides were almost four times higher than values recorded in the controls. These high levels declined toward the end of the experiment, but mean values remained significantly higher than controls (Fig. 1a). To further investigate the responses to this oxidative stress, we monitored the expression of diverse genes selected as markers because of their role on cell repair and detoxification. These genes exhibited different expression patterns with respect to control genes (*LdEF* and *LdRPL14*), providing evidence for regulation under copper stress conditions

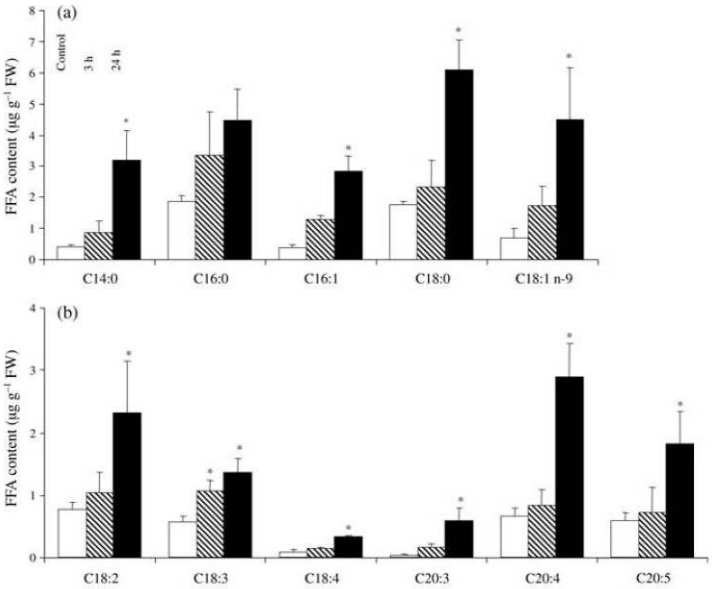

Fig. 2 Effect of copper on free fatty acids (FFAs) release in *Laminaria digitata*. Kelp juveniles were kept in seawater as control (open columns) and compared with individuals treated with 300 μg l^{-1} of copper for 3 h (hatched columns) and 24 h (closed columns). (a) Free saturated/monounsaturated FA. (b) Polyunsaturated FFAs. FFAs from C:14 to C:20 were quantified by gas chromatography–mass spectrometry. Values are the means of three independent replicates; bars, SE; *, significantly different from the control group ($P < 0.05$).

(Fig. 1b and Supporting information, Fig. S1). For a first set of genes, including *LdHSP70*, *LdGST2*, *LdMSR1* and *LdTRX1*, the transcripts levels increased two- to eightfold after 6 h of exposure to copper excess and remained high to the end of the experiment (Fig. 1c). A second set of genes, *LdSOD*, *LdPRX* and *LdTRX4*, displayed fourfold upregulation at 6 h followed by downregulation after 24 h of exposure to copper excess (Fig. 1d). The *LdMSR3* gene showed enhanced upregulation from 24 h onward (Fig. 1c).

Free fatty acid release is induced by copper

The effects of copper-induced oxidative stress and concomitant lipid peroxidation in *L. digitata* sporophytes were further investigated by monitoring their free fatty acid composition. After 3 h of incubation, significant changes in the FFA level were only observed for 18:3 (Fig. 2). In contrast, the 24 h treatment induced the release of significant levels of PUFA, representing four times the overall quantity compared with control conditions. All FFA types analysed, except palmitic acid (16:0) (Fig. 2a), exhibited significant increases after 24 h of exposure to copper excess. Among these compounds, C18 and C20 polyunsaturated FFA such as linoleic acid (C18:2), arachidonic acid (C20:4), dihomo-γ-linolenic acid (C20:3) and eicosapentaenoic acid (C20:5) increased significantly (Fig. 2b).

Copper stress induces FFA release and oxylipin synthesis

The extent of the FFA release simultaneous with high levels of lipoperoxides detected using the TBAR test at 24 h prompted us to monitor additional changes among oxygenated derivatives, oxylipins that could constitute signals in *L. digitata* sporophytes exposed to copper excess. The LC–MS profile shows an overall tenfold lipoperoxide increase after 24 h of treatment, compared with the corresponding controls (Fig. 3a,b). In order to identify enzymatic signatures, we focused on upstream derivatives such as hydroperoxides and hydroxyls FA. Results showed that copper stressed *L. digitata* produced a wide variety of EPA, AA and LA hydroxyls and hydroperoxide derivatives (Fig. 3c, Table 2). When stressed, amounts of 13-HpOTrE (309 *m/z* $[M-H]^{(-)}$, Rt 33.38 min) and 13-HOTrE (293 *m/z* $[M-H]^{(-)}$, Rt 39.11 min) increased significantly, representing 80% of the overall octadecanoids. For eicosanoid derivatives, significant increases were recorded for 15-HETE (319 *m/z* $[M-H]^{(-)}$, Rt 46.17 min), 15-HpEPE (333 *m/z* $[M-H]^{(-)}$, Rt 31.71 min) and 15-HEPE (317 *m/z* $[M-H]^{(-)}$, Rt 40.71 min). Other uncommon hydroperoxides and hydroxide FAs such as the 11-HpOTrE (309 *m/z* $[M-H]^{(-)}$, Rt 31.78 min), 12-HpOTrE (309 *m/z* $[M-H]^{(-)}$, Rt 32.67 min), 15-HpOTrE (309 *m/z* $[M-H]^{(-)}$, Rt 30.14 min), 12-HpETE (309 *m/z* $[M-H]^{(-)}$, Rt 32.67 min) and 16-HEPE (317 *m/z* $[M-H]^{(-)}$, Rt 50.39 min), were also detected, although at much lower levels. Among complex downstream oxylipins, C18 ketols and epoxides (Fig. 3d, Table 2) such as the 12,13-EpOME (*m/z* 295 $[M-H]^{(-)}$, Rt 44.09 min) and the 13-hydroxy-12-oxo-monoenoic acid (13-H-12oxo-OME *m/z* 311 $[M-H]^{(-)}$, Rt 29.87 min) exhibited significant increase after 3 h of exposure to copper excess. It was observed that copper triggered the synthesis of PUFA derivatives with identical characteristics to enzymatic cyclic cyclopentenones such as the C18 jasmonic acid precursor 12-oxo-PDA (291 *m/z* $[M-H]^{(-)}$, Rt 36.28 min)

New Phytologist

Table 2 Summary of the structure of oxylipins that were identified in *Laminaria digitata* during this study

Compound		[M-H]$^-$ (*m*/*z*)	Compound		[M-H]$^-$ (*m*/*z*)
11-HpOTrE	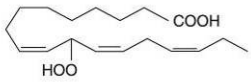	309	**PGE_1**	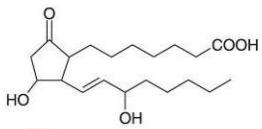	353
12-HpOTrE	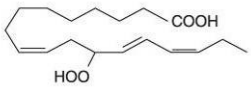	309	**PGD_1**	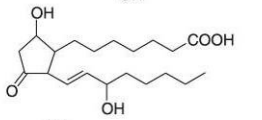	353
13-HpOTrE	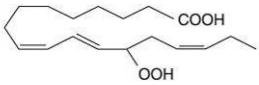	309	**15-Keto-$PGF_{2\alpha}$**	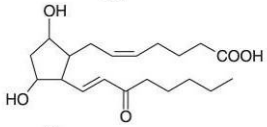	351
13-HOTrE	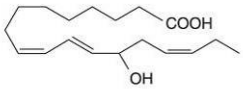	293	**PGE2**	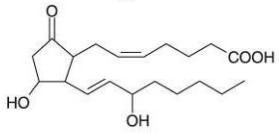	351
15-HpOTrE	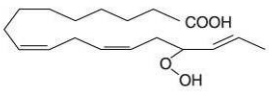	309	**15-Keto-PGE2**	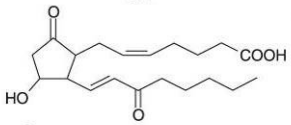	349
12-HpETE	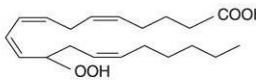	335	**PGA2**	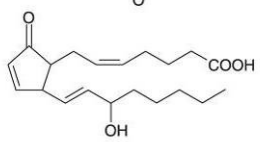	333
15-HpETE	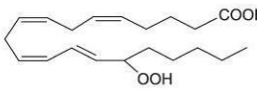	335	**PGB2**	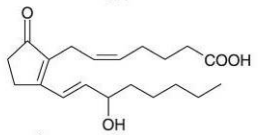	333
15-HETE	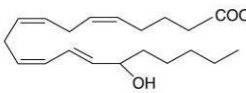	319	**PGJ2**	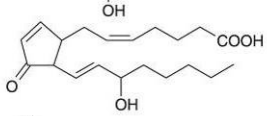	333
15HpEPE	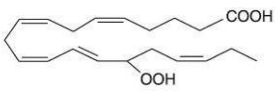	333	**12-oxo-PDA**	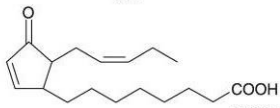	291
15-HEPE	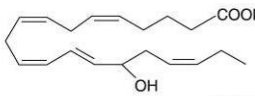	317	**12,13-EpOME**	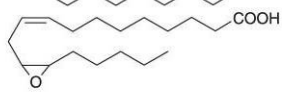	295
16-HEPE	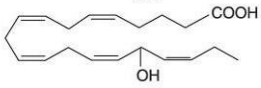	317	**13-H-12-oxo-OME**	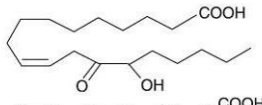	311
			18H-,17-oxo-ETE	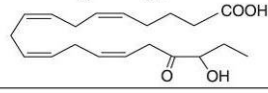	333

For each compound, the current short name, the structure and the *m*/*z* value are specified.

New Phytologist

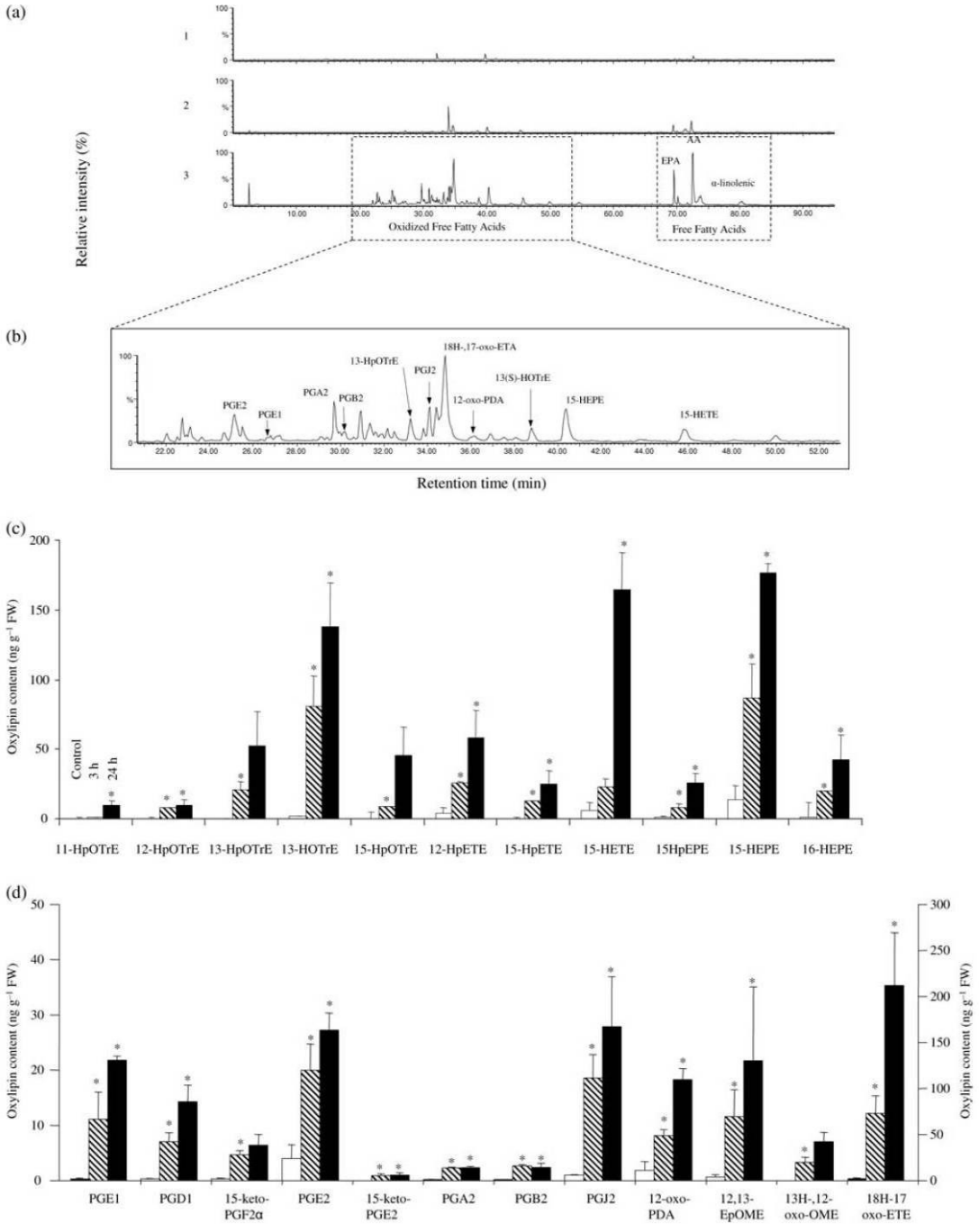

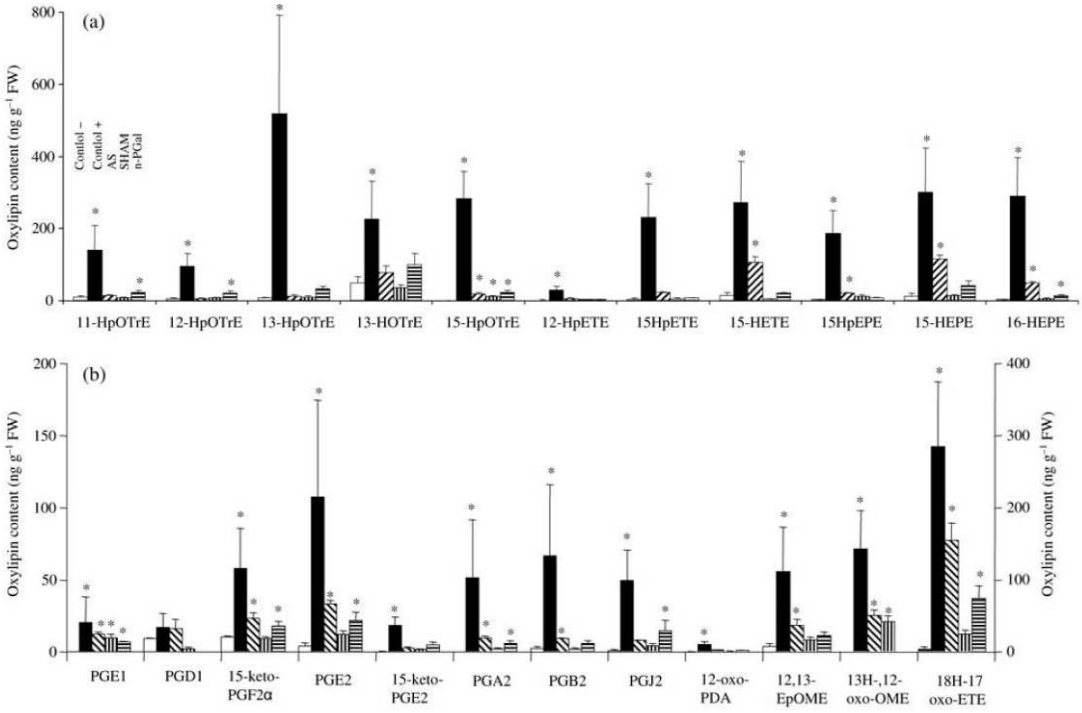

Fig. 4 Effect of inhibitors on the free fatty acid (FFA) oxygenation products after 24 h of copper exposure in *Laminaria digitata*. Kelp juveniles were kept 24 h in seawater as negative control and treated with 300 μg l^{-1} of copper at 24 h as positive control. Using the same stress conditions and period of time, individuals were incubated with: 1 mM AS, 1 mM SHAM, and 100 μM *n-n*-PGal. Results are sorted by (a) enzymatic hydroxyls and hydroperoxides and (b) noncomplex oxylipins. The right *y*-axis only applies to the content of 12,13-EpOME, 13-H-12-oxo-OME and 18-H-17-oxo-ETE. Values are the means of three independent replicates; bars, SE; *, significantly different from the control group ($P < 0.05$).

and C20 prostaglandins (PG). Two types of PGs were observed: type 1 derived from C20:3 and type 2 derived from C20:4. For type 1 we identified the PGE_1 (353 *m/z* $[M-H]^{(-)}$, Rt 26.30 min) and PGD_1 (353 *m/z* $[M-H]^{(-)}$, Rt 27.07 min). For type 2, results indicate the presence of PGJ_2 (333 *m/z* $[M-H]^{(-)}$, Rt 33.59 min) and a set of derived structures such as PGE_2 (351 *m/z* $[M-H]^{(-)}$, Rt 25.47 min), 15-keto-$PGF_{2\alpha}$ (351 *m/z* $[M-H]^{(-)}$, Rt 23.88 min), 15-keto-PGE_2 (349 *m/z* $[M-H]^{(-)}$, Rt 29.11 min), PGA_2 (333 *m/z* $[M-H]^{(-)}$, Rt 29.49 min) and PGB_2 (333 *m/z* $[M-H]^{(-)}$, Rt 29.73 min). Treatments with both inhibitors of LOX, particularly SHAM, were highly efficient in modifying oxylipin signatures, including LOX as well as COX-like derivatives (Fig. 4a,b). By contrast, AS was shown to be less effective in decreasing the levels of oxylipins.

Fig. 3 Effect of copper on the synthesis of oxidized fatty acids (FA) in *Laminaria digitata*. Kelp juveniles were kept in seawater as control (open columns) and compared with individuals treated with 300 μg l^{-1} of copper for 3 h (hatched columns) and 24 h (closed columns). (a) The FA profile was monitored by liquid chromatography–mass spectrometry (LC-MS) on individuals submitted to early (3 h) and late (24 h) stages of copper stress. (b) The magnification of the oxylipin window at 24 h of copper stress shows the appearance of high oxylipin diversity corresponding to octadecanoid and eicosanoid derivatives. (c) Quantification of hydroxyls and hydroperoxides FFA coming from a FFA mixture induced by 24 h of copper exposure. (d) Characterization and quantification of complex oxylipins on stressed individuals of *L. digitata* at 3 h and 24 h of copper exposure. The right y-axis only applies to the content of 18-H-17oxoETE. Values are the means of three independent replicates; bars, SE; *, significantly different from the control group ($P < 0.05$).

18-H-17oxo-ETE is generated by copper stress

Laminaria digitata stressed by copper generated an original polar compound displaying a RP-LC retention time at 34.19 min: 18-hydroxy-17-oxo-eicosatetraenoic acid (18-H-17oxo-ETE, *m/z* 333 $[M-H]^{(-)}$), that was identified by the mass spectra fragmentation in the negative APCI mode (Fig. 5a) and in the EI mode as a TMS derivative (Fig. 5b). The molecule underwent $APCI^{(-)}$ cleavage resulting in informative signals with ions at *m/z* 317 $[M-H-O]^{(-)}$, 297 $[M-H-2H_2O]^{(-)}$, 289 $[M-H-CO_2]^{(-)}$, 271 $[M-H-H_2O-CO_2]^{(-)}$, and in two characteristic fragments from the keto-alcohol function at

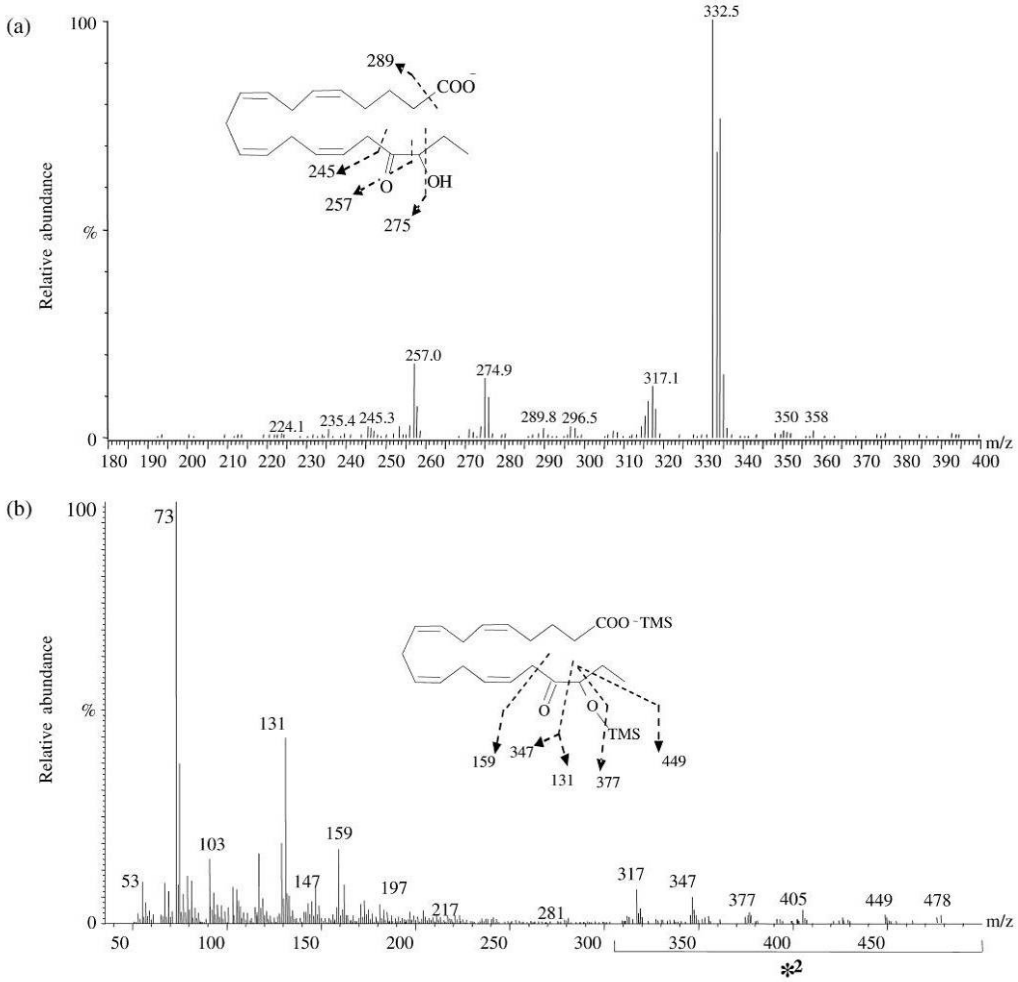

Fig. 5 Evidence for the production of 18-Hydroxy-17-oxo-eicosatetraenoic acid (18-H-17-oxo-ETE, *m/z* 333 [M-H]$^-$) in *Laminaria digitata* after 24 h of exposure to copper (300 µg l^{-1}). (a) Mass spectrum in the negative APCI mode 18-H-17-oxo-ETE obtained after liquid chromatography–mass spectrometry analysis; characteristic fragments from the keto-alcohol function are *m/z* 275 [M-H-CH_2OH-CH_2-CH_3]$^{(-)}$ and 257 [M-H-H_2O-CH_2OH-CH_2-CH_3]$^{(-)}$. The same fraction was monitored by gas chromatography–mass spectrometry analysis after TMS derivatization. (b) Mass spectrum of 18H-17-oxo-ETE in the EI mode as a TMS derivative (*m/z* 478 [M]$^+$) displaying characteristic fragments owing to the position of the keto-alcohol at *m/z* 347 [M-CH(O-TMS)-CH_2-CH_3]$^{(+)}$, 159 [C(O)-CH(O-TMS)-CH_2-CH_3]$^{(+)}$ and 131 [CH(O-TMS)-CH_2-CH_3]$^{(+)}$.

m/z 275 [M-H-CH_2OH-CH_2-CH_3]$^{(-)}$ and 257 [M-H-H_2O-CH_2OH-CH_2-CH_3]$^{(-)}$. 18-H-17oxo-ETE was also characterized by its fragmentation patterns, in the EI mode (70 eV), displaying fragments at *m/z* 478 [M]$^{(+)}$, 405 [M-TMS]$^{(+)}$, 449 [M-CH_2-CH_3]$^{(+)}$, 377 [M-CH_2-CH_3-TMS]$^{(+)}$ and characteristic fragments owing to the position of the keto-alcohol at *m/z* 347 [M-CH(O-TMS)-CH_2-CH_3]$^{(+)}$, 159 [C(O)-CH(O-TMS)-CH_2-CH_3]$^{(+)}$ and 131 [CH(O-TMS)-CH_2-CH_3]$^{(+)}$.

Discussion

In order to maintain cellular homeostasis, organisms have developed sophisticated environmental sensors and signaling mechanisms. In the context of signaling, oxylipins play a key role inducing accurate responses to biotic and abiotic stressors. Our results show that lipid peroxidation in *L. digitata* was induced by copper excess, indicating that after 24 h of exposure

to the metal, an oxidative stress condition is established in the alga. Lipid peroxidation is concomitant with the release of free PUFAs and is followed by the formation of oxylipins through oxidative cascades. Previous studies in brown algae (Contreras *et al.*, 2005) demonstrated a link between oxidative stress indicated by lipid peroxidation and the launch of antioxidant defenses. In agreement with those results, we demonstrated the regulation of copper-induced cell protection mechanisms at transcriptional level. The antioxidant related genes *LdSOD, LdPRX* and *LdTRX4* showed strong upregulation after 6 h, possibly as a result of the activation of early defensive systems against ROS (Tsang *et al.*, 1991; Broin *et al.*, 2002; Gelhaye *et al.*, 2005). However, a second set of genes involved in cell repair and detoxification – *LdHSP70, LdGST2, LdMSR1, LdMSR3, LdTRX1* and *LdTRX3* – showed upregulation throughout, or at late stages, of the copper treatments. This regulation results from stress-generated damage (Feder & Hofmann, 1999; Dixon *et al.*, 2002; Weissbach *et al.*, 2002). The occurrence of oxidative stress damage at 24 h is correlated with the occurrence of oxylipins (Table 2). In addition, high levels of FFA are released, suggesting the involvement of lipases. In the presence of ROS FFA provoked oxidative cascades reactions generating lipid peroxidation. Taking into account the role played by transition metals, such as copper ions, in accelerating lipid peroxidation, it is possible that the observed compounds 11-HpOTrE,12-HpOTrE,15-HpOTrE,12-HpETE and 16-HEPE derived from nonenzymatic ROS-mediated reactions (Halliwell & Gutteridge, 1989; Montillet *et al.*, 2004). However, our results suggest the coexistence of the above with enzymatic oxylipin pathways. Some of the compounds observed, such as 13-HOTrE, 15-HETE and 15-HEPE have already been described in *Laminaria* (Gerwick *et al.*, 1993; Küpper *et al.*, 2006), where it was proposed the occurrence of hydroxyl FAs resulted from ω-6 lipoxygenase metabolism. Another compound detected that had not previously been described in *Laminaria*, the 12,13-EpOME, was also induced by copper. This oxylipin was reported in the red alga *Chondrus crispus* when challenged with pathogen extracts (Bouarab *et al.*, 2004). In addition, epoxy allelic carbocation structures have been postulated to provide a key intermediate in the biogenesis of diverse marine algal oxylipins (Gerwick *et al.*, 1999). The major product detected in this study is the rare C20:5 derivative 18-H-17-oxo-ETE. Until now, no enzyme is known to synthesize this product. However, previous studies have reported close relatives to this oxylipin, such as the 18-hydroxy-eicosatetraenoic acid from *Leptomis lacteus*, an oomycete phylogenetically related to brown algae (Fox *et al.*, 2000). Another closely related structure, the 17(*R*),18(*S*)-epoxyeicosatetraenoic acid, results from a CYP activity in humans and the nematode *Caenorhabditis elegans* (Schwarz *et al.*, 2004; Kulas *et al.*, 2008). In mammals, this compound acts as a highly potent BK channel activator in vascular smooth muscle cells (Lauterbach *et al.*, 2002). Among the complex oxylipins, we report here cyclopentenone structures, never before found in brown algae. These oxylipins displayed MS spectra identical to those of plant C18 allene oxide synthase derivative 12-oxo-PDA and the animal C20 cycloxygenase derivatives known as prostaglandins. Cyclopentenones are well known as key components in a wide variety of metabolic pathways in mammals (Funk, 2001), invertebrates (Rowley *et al.*, 2005) and plants (Farmer *et al.*, 2003) exposed to biotic and/or abiotic stress conditions. In Phaeophyceae, the presence of C18 cyclopentenone ether structures was reported in *Cymathere triplicate* (Proteau & Gerwick, 1992), and no further findings have been reported since. In the case of plants, the C18 cyclopentenones, known as jasmonates, are classically known to be involved in pathogenesis, herbivore innate-immune responses and abiotic stress responses (Howe & Schilmiller, 2002; Farmer *et al.*, 2003; Farmer & Schulze-Lefert, 2005; Maksymiec *et al.*, 2005). Although the enzymes involved in oxylipin synthesis in brown algae remain unknown, the reduced efficiency of AS to inhibit the synthesis of COX-like derivatives suggests that prostanoids could derive through an alternative pathway. In mammals, prostaglandins constitute effective lipid mediators in almost all organs for a wide number of metabolic pathways including pyrogenicity, vasodilatation, hyperalgesic response and salt–water balance (Funk, 2001). In invertebrates, Rowley *et al.* (2005) reported the occurrence of prostanoids not only of mammal types, but also in the form of proper invertebrate prostanoids. These molecules are of common occurrence in red algae but no function has yet been described (Bouarab *et al.*, 2004; Gaquerel *et al.*, 2007). Based on the function of some prostaglandins in mammals, previous authors (Gerwick *et al.*, 1999) have suggested the involvement of marine algal oxylipins in ion transport and osmotic regulation. Our observations underline the high potential of brown algae as models for oxylipin research. In addition, they raise several questions regarding the physiological role of the oxylipins and the importance of the unusual oxygenated metabolites generated in copper-stressed *L. digitata* sporophytes. Taken together, our results suggest that the toxic effects of copper in brown algae are buffered by protective mechanisms, likely triggered by octadecanoid and eicosanoid oxylipin-mediated pathways. In plants and red algae, cyclopentenones such as jasmonates mediate transcriptional reprogramming of metabolism (Collén *et al.*, 2006; Pauwels *et al.*, 2008). Based on this fact, it is possible to speculate that brown algae also use hormone-like compounds (Table 2) to regulate their defensive responses. In higher plants, detoxification processes such as the ascorbate–glutathione cycle, TRXs, PRXs or GSTs are regulated in response to both biotic and abiotic stress (Mauch & Dudler, 1993; Mittler, 2002). These defensive mechanisms can be mimicked by MeJA or other structurally related cyclopentenones such as 12-OPDA (Wagner *et al.*, 2002; Farmer *et al.*, 2003; Loeffler *et al.*, 2005; Pauwels *et al.*, 2008). Furthermore, the increasing expression of *LdGTS2* in *L. digitata* could be related to a detoxification mechanism against toxic nonenzymatic lipoperoxides, as previously described

in higher plants (Murphy & Zarini, 2002) or as suggested in red algae (Gaquerel *et al.*, 2007; Hervé *et al.*, 2008).

In conclusion, our findings underline the importance of the oxylipin metabolism in the regulation of the responses to copper excess in brown algae. There is no doubt that the completion of the genome sequencing of the brown alga *Ectocarpus siliculosus* will promote future oxylipin research in phaeophycean heterokonts. We expect that the development of new techniques on this model for transcriptomic, proteomic (Contreras *et al.*, in press) and metabolomic analyses, coupled with the extensive knowledge of its genetic, reproductive and stress biology (Charrier *et al.*, 2008), will allow a better understanding of copper tolerance and resistance mechanisms.

Acknowledgements

We thank C. Henriquez for her help during the TBAR test and gene expression experimentation, and F. Thomas for supplying algal material. This work has been partially funded by Marine Genomics Europe NoE 7 (EU contract n° GOCE-CT-2004-505403) and a Programme de Recherche d'Intérêt Régional (STRESS) from the Conseil Régional de Bretagne (France) and by the French Embassy and the CONICYT of Chile and the Ministère de l'Enseignement Supérieur et de la Recherche through PhD fellowships to A.R. and S.G., respectively. This work was supported by the Laboratoire International Associé 'Dispersal and Adaptation of Marine Species' (LIA DIAMS) PUC, Chile and CNRS-UPMC, France.

References

Andrade S, Contreras L, Moffett JW, Correa JA. 2006. Kinetics of copper accumulation in *Lessonia nigrescens* (Phaeophyceae) under conditions of environmental oxidative stress. *Aquatic Toxicology* **78**: 398–401.

Apt KE, Clendennen SK, Powers DA, Grossman AR. 1995. The gene family encoding the fucoxanthin chlorophyll proteins from the brown alga *Macrocystis pyrifera*. *Molecular and General Genetics* **246**: 455–464.

Blée E. 2002. Impact of phyto-oxylipins in plant defense. *Trends in Plant Science* 7: 315–322.

Bouarab K, Adas F, Gaquerel E, Kloareg B, Salaun JP, Potin P. 2004. The innate immunity of a marine red alga involves oxylipins from both the eicosanoid and octadecanoid pathways. *Plant Physiology* **135**: 1838–1848.

Broin M, Cuine S, Eymery F, Rey P. 2002. The plastidic 2-cysteine peroxiredoxin is a target for a thioredoxin involved in the protection of the photosynthetic apparatus against oxidative damage. *Plant Cell* **14**: 1417–1432.

Charrier B, Coelho SM, Le Bail A, Tonon T, Michel G, Potin P, Kloareg B, Boyen C, Peters AF, Cock JM. 2008. Development and physiology of the brown alga *Ectocarpus siliculosus*: two centuries of research. *New Phytologist* **177**: 319–332.

Collén J, Hervé C, Guisle-Marsollier I, Léger JJ, Boyen C. 2006. Expression profiling of *Chondrus crispus* (Rhodophyta) after exposure to methyl jasmonate. *Journal of Experimental Botany* **57**: 3869–3881.

Collén J, Pinto E, Pedersen M, Colepicolo P. 2003. Induction of oxidative stress in the red macroalga *Gracilaria tenuistipitata* by pollutant metals. *Archives of Environmental Contamination Toxicology* **45**: 337–342.

Contreras L, Moenne A, Correa JA. 2005. Antioxidant responses in *Scytosiphon lomentaria* (Phaeophyceae) inhabiting copper-enriched coastal environments. *Journal of Phycology* **41**: 1184–1195.

Contreras L, Ritter A, Dennett G, Boehmwald F, Guitton N, Pineau C, Moenne A, Potin P, Correa JA. (in press). Two-dimensional gel electrophoresis analysis of brown algal protein extracts. *Journal of Phycology*, in press.

Correa J, Castilla J, Ramirez M, Varas M, Lagos N, Vergara S, Moenne A, Roman D, Brown MT. 1999. Copper, copper mine tailings and their effect on the marine algae in Northern Chile. *Journal of Applied Phycology* **11**: 57–67.

Cosse A, Leblanc C, Potin P. 2007. Dynamic defense of marine macroalgae against pathogens: from early activated to gene-regulated responses. *Advances in Botanical Research* **12**: 221–266.

Crépineau F, Roscoe T, Kaas R, Kloareg B, Boyen C. 2000. Characterisation of complementary DNAs from the expressed sequence tag analysis of life cycle stages of *Laminaria digitata* (Phaeophyceae). *Plant Molecular Biology* **43**: 503–513.

Dixon D, Lapthorn A, Edwards R. 2002. Plant glutathione transferases. *Genome Biology* **3**: reviews3004.1–10.

Fang G, Hammar S, Grumet R. 1992. A quick and inexpensive method for removing polysaccharides from plant genomic DNA. *Biotechniques* **13**: 52–54, 56.

Farmer E, Schulze-Lefert P. 2005. Biotic interactions: from molecular networks to inter-organismal communities. *Current Opinion in Plant Biology Biotic Interactions* **8**: 343–345.

Farmer EE, Almeras E, Krishnamurthy V. 2003. Jasmonates and related oxylipins in plant responses to pathogenesis and herbivory. *Current Opinion in Plant Biology* **6**: 372–378.

Farmer EE, Davoine C. 2007. Reactive electrophile species. *Current Opinion in Plant Biology* **10**: 380–386.

Feder ME, Hofmann GE. 1999. Heat-shock proteins, molecular chaperones, and stress response: evolutionary and ecological physiology. *Annual Review of Physiology* **61**: 243–282.

Fernandes JC, Henriques FS. 1991. Biochemical, physiological and structural effects of excess copper in plants. *Botanical Reviews* **57**: 246–73.

Fox S, Akpinar A, Prabhune A, Friend J, Ratledge C. 2000. The biosynthesis of oxylipins of linoleic and arachidonic acids by the sewage fungus *Leptomitus lacteus*, including the identification of 8R-hydroxy-9Z,12Z-octadecadienoic acid. *Lipids* **35**: 23–30.

Funk CD. 2001. Prostaglandins and leukotrienes: advances in eicosanoid biology. *Science* **294**: 1871–1875.

Gaquerel E, Hervé C, Labrière C, Boyen C, Potin P, Salaün J-P. 2007. Evidence for oxylipin synthesis and induction of a new polyunsaturated fatty acid hydroxylase activity in *Chondrus crispus* in response to methyljasmonate. *Biochimica et Biophysica Acta (BBA) – Molecular and Cell Biology of Lipids* **1771**: 565–575.

Gelhaye E, Rouhier N, Navrot N, Jacquot JP. 2005. The plant thioredoxin system. *Cellular and Molecular Life Sciences* **62**: 24–35.

Gerwick WH, Proteau PJ, Nagle DG, Wise ML, Jiang ZD, Bernart MW, Hamberg M. 1993. Biologically active oxylipins from seaweeds. *Hydrobiologia* **260–261**: 653–665.

Gerwick WH, Roberts MA, Vulpanovici A, Ballantine DL. 1999. Biogenesis and biological function of matine algal oxylipins. *Advances in Experimental Medicine and Biology* **447**: 211–218.

Gledhill M, Nimmo M, Hill SJ, Brown MT. 1997. The toxicity of copper (II) species to marine algae, with particular reference to macroalgae. *Journal of Phycology* **33**: 2–11.

Halliwell B, Gutteridge J. 1989. *Free radicals in biology and medicine.* Oxford, UK: Clarendon Press.

Halliwell B, Gutteridge JMC. 1992. Biologically relevant metal ion-dependent hydroxyl radical generation An update. *FEBS Letters* **307**: 108–112.

Hervé C, de Franco P-O, Groisillier A, Tonon T, Boyen C. 2008. New members of the glutathione transferase family discovered in red and brown algae. *Biochemical Journal* **412**: 535–544.

Howe GA, Schilmiller AL. 2002. Oxylipin metabolism in response to stress. *Current Opinion in Plant Biology* **5**: 230–236.

Kulas J, Schmidt C, Rothe M, Schunck W-H, Menzel R. 2008. Cytochrome P450-dependent metabolism of eicosapentaenoic acid in the nematode *Caenorhabditis elegans*. *Archives of Biochemistry and Biophysics* **472**: 65–75.

Küpper FC, Gaquerel E, Boneberg E-M, Morath S, Salaün J-P, Potin P. 2006. Early events in the perception of lipopolysaccharides in the brown alga *Laminaria digitata* include an oxidative burst and activation of fatty acid oxidation cascades. *Journal of Experimental Botany* **57**: 1991–1999.

Lauterbach B, Barbosa-Sicard E, Wang MH, Honeck H, Kärgel E, Theuer J, Schwartzman ML, Haller H, Luft FC, Gollasch M *et al.* 2002. Cytochrome P450-dependent eicosapentaenoic acid metabolites are novel BK channel activators. *Hypertension* **39** (Part II): 609–613.

Livingstone DR. 2001. Contaminant-stimulated reactive oxygen species production and oxidative damage in aquatic organisms. *Marine Pollution Bulletin* **42**: 656–666.

Loeffler C, Berger S, Guy A, Durand T, Bringmann G, Dreyer M, von Rad U, Durner J, Mueller MJ. 2005. B1-Phytoprostanes trigger plant defense and detoxification responses. *Plant Physiology* **137**: 328–340.

Maksymiec W, Wianowska D, Dawidowicz AL, Radkiewicz S, Mardarowicz M, Krupa Z. 2005. The level of jasmonic acid in *Arabidopsis thaliana* and *Phaseolus coccineus* plants under heavy metal stress. *Journal of Plant Physiology* **162**: 1338–1346.

Mauch F, Dudler R. 1993. Differential induction of distinct glutathione-S-transferases of wheat by xenobiotics and by pathogen attack. *Plant Physiology* **102**: 1193–1201.

Medina M, Andrade S, Faugeron S, Lagos N, Mella D, Correa JA. 2005. Biodiversity of rocky intertidal benthic communities associated with copper mine tailing discharges in northern Chile. *Marine Pollution Bulletin* **50**: 396–409.

Mithöfer A, Schulze B, Boland W. 2004. Biotic and heavy metal stress response in plants: evidence for common signals. *FEBS Letters* **566**: 1–5.

Mittler R. 2002. Oxidative stress, antioxidants and stress tolerance. *Trends in Plant Science* **7**: 405–410.

Montillet J-L, Cacas J-L, Garnier L, Montane M-H, Douki T, Bessoule J-J, Polkowska-Kowalczyk L, Maciejewska U, Agnel J-P, Vial A *et al.* 2004. The upstream oxylipin profile of *Arabidopsis thaliana:* a tool to scan for oxidative stresses. *Plant Journal* **40**: 439–451.

Murphy RC, Zarini S. 2002. Glutathione adducts of oxyeicosanoids. *Prostaglandins & Other Lipid Mediators* **68–69**: 471–482.

Parmentier J-H, Muthalif MM, Saeed AE, Malik KU. 2001. Phospholipase D activation by norepinephrine is mediated by 12(s)-, 15(s)-, and 20-hydroxyeicosatetraenoic acids generated by stimulation of cytosolic phospholipase A2. Tyrosine phosphorylation of phospholipase D2 in response to norepinephrine. *The Journal of Biological Chemistry* **276**: 15704–15711.

Pauwels L, Morreel K, De Witte E, Lammertyn F, van Montagu M, Boerjan W, Inze D, Goossens A. 2008. Mapping methyl jasmonate-mediated transcriptional reprogramming of metabolism and cell cycle progression in cultured *Arabidopsis* cells. *Proceedings of the National Academy of Sciences, USA* **105**: 1380–1385.

Pinot F, Salaün J-P, Bosch H, Lesot A, Mioskowski C, Durst F. 1992. ω-Hydroxylation of Z9-octadecenoic, Z9,10-epoxystearic and 9,10-dihydroxystearic acids by microsomal cytochrome P450 systems from *Vicia sativa*. *Biochemical and Biophysical Research Communications* **184**: 183–193.

Pinto E, Sigaud-Kutner TCS, Leitao MAS, Okamoto OK, Morse D, Colepicolo P. 2003. Heavy metal-induced stress in algae. *Journal of Phycology* **39**: 1008–1018.

Proteau PJ, Gerwick WH. 1992. Cymathere ethers A and B: bicyclic oxylipins from the marine brown alga *Cymathere triplicata*. *Tetrahedron Letters* **33**: 4393–4396.

Roeder V, Collen J, Rousvoal S, Corre E, Leblanc C, Boyen C. 2005. Identification of stress gene transcripts in *Laminaria digitata* (Phaeophyceae) protoplast cultures by Expressed Sequence Tag analysis. *Journal of Phycology* **41**: 1227–1235.

Rowley AF, Vogan CL, Taylor GW, Clare AS. 2005. Prostaglandins in noninsectan invertebrates: recent insights and unsolved problems. *The Journal of Experimental Biology* **208**: 3–14.

Sasaki Y, Asamizu E, Shibata D, Nakamura Y, Kaneko T, Awai K, Amagai M, Kuwata C, Tsugane T, Masuda T *et al.* 2001. Monitoring of methyl jasmonate-responsive genes in *Arabidopsis* by cDNA macroarray: self-activation of jasmonic acid biosynthesis and crosstalk with other phytohormone signaling pathways. *DNA Research* **8**: 153–161.

Schwarz D, Kisselev P, Ericksen SS, Szklarz GD, Chernogolov A, Honeck H, Schunck W-H, Roots I. 2004. Arachidonic and eicosapentaenoic acid metabolism by human CYP1A1: highly stereoselective formation of 17(R),18(S)-epoxyeicosatetraenoic acid. *Biochemical Pharmacology* **67**: 1445–1457.

Tsang E, Bowler C, Herouart D, Van Camp W, Villarroel R, Genetello C, van Montagu M, Inze D. 1991. Differential regulation of superoxide dismutases in plants exposed to environmental stress. *Plant Cell* **3**: 783–792.

Wagner U, Edwards R, Dixon DP, Mauch F. 2002. Probing the diversity of the *Arabidopsis* glutathione-S-transferase gene family. *Plant Molecular Biology* **49**: 515–532.

Weissbach H, Etienne F, Hoshi T, Heinemann SH, Lowther WT, Matthews B, St. John G, Nathan C, Brot N. 2002. Peptide methionine sulfoxide reductase: structure, mechanism of action, and biological function. *Archives of Biochemistry and Biophysics* **397**: 172–178.

Yruela I, Alfonso M, Baron M, Picorel R. 2000. Copper effect on the protein composition of photosystem II. *Physiologia Plantarum* **110**: 551–557.

Supporting Information

Additional supporting information may be found in the online version of this article.

Fig. S1 Simultaneous study of stress-related gene expression by semi-quantitative reverse transcriptase polymerase chain reaction (RT-PCR) analysis in the three independent replicates.

Please note: Wiley-Blackwell are not responsible for the content or functionality of any supporting information supplied by the authors. Any queries (other than missing material) should be directed to the *New Phytologist* Central Office.

SUPPLEMENTARY MATERIAL

Figure S1

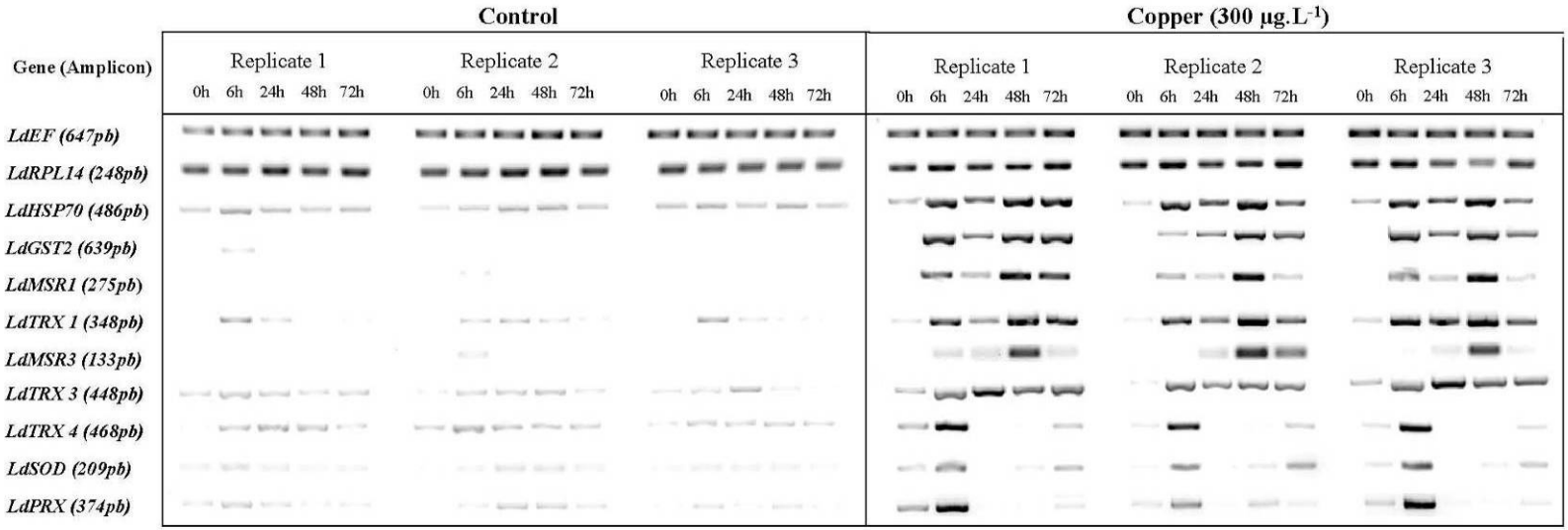

Figure S1.

Simultaneous study of stress related gene expression by semi-quantitative RT-PCR analysis. Figure displays the relative expression by gel analyses of 3 independent biological replicates for the control and the stress conditions for 9 targeted genes. Reference gene expression level was assayed by studying genes encoding for ribosomal protein 14 (RPL14) and the elongation factor (EF).

3 RELEASE OF VOLATILE ALDEHYDES BY THE BROWN ALGAL KELP *Laminaria digitata* IN RESPONSE TO BOTH BIOTIC AND ABIOTIC STRESSES

Submitted to Chembiochem

Sophie Goulitquer, Andrés Ritter, François Thomas , Jean-Pierre Salaün and Philippe Potin

Abstract

In higher plants it is well established that short-chain aldehydes, produced via hydroperoxydelyase (HPL), are important flavor compounds, and also play a role in response to wounding. In recent years some aldehydes have been found in diatoms and algae after mechanical wounding and fatty acid incubation. A GC/MS on the NICI mode method was develop to monitor *O*-pentafluorobenzyl (*O*-PFB) oxime derivatives in both sea water and air fraction. Here we demonstrate that under stress conditions such as oligoguluronate (GG) elicitation or low tide, in a natural environment, the brown kelp *Laminaria digitata* produce a large panel of aldehydes. Formation of C6- and C9-aldehydes, and 9-oxo-nonanoic acid was observed. Mono- and poly-unsaturated aldehydes were also detected, either as 4-hydroxy-(*E*)-2-alkenals. The release of volatile was detected in the hour after elicitation. A pharmacological approach suggested that these compounds are formed enzymatically by lipases and lipoxygenases (LOX) pathways. Malonaldehyde (MDA) a reactive electrophile specie which can potentially affect gene expression has also been found in large amounts. Algal derived aldehydes could be important molecules for both signaling within and between kelps and marine invertebrates.

DOI: 10.1002/cbic.200((will be filled in by the editorial staff))

Stress-induced aldehyde release by kelps

Release of volatile aldehydes by the brown algal kelp *Laminaria digitata* in response to both biotic and abiotic stresses

Sophie Goulitquer [c], Andrés Ritter [a,b,d], François Thomas [a,b], Cyrille Ferec [c], Jean-Pierre Salaün [a,c] and Philippe Potin*[a]

((Dedication, optional))

Reminiscent of the important role in wound healing and pest resistance of the so-called fresh green odour caused by volatile C6 and C9 aldehydes in higher plants [1], the occurrence of volatile polyunsaturated aldehydes (PUAs) has also been reported in several marine diatoms [2-5] and other planktonic algae [5, 6]. These organisms seem to use (*E,E*)-2,4,7-octatrienal, (*E,E,Z*)-2,4,7-decatrienal and (*E,E*)-2,4-decadienal as signal molecules related to defence mechanisms [7] and as a stress alarm system [8]. Moreover, in the brown marine alga *Laminaria angustata* the capacity to enzymatically produce long- and short-chain aldehydes has also been demonstrated [9, 10]. The precursors of these aldehydes are n-6 fatty acids such as linoleic and arachidonic acids. In spite of numerous studies that had demonstrated that PUAs could be produced enzymatically by algae, these experiments were done by sonicating cells, to partially wound the alga, or by incubating algal extracts with polyunsaturated fatty acids (PUFAs). Only, a recent report indicates that the diatom *Skeletonema marinoi* releases PUAs at some growth phases in culture conditions [11]. Therefore, to better establish that PUAs act as infochemicals in the marine environment, there is a need to evidence their release from intact algae in their natural environment.

[a] *A. Ritter, F.Thomas, Dr J-P Salaün, Dr P. Potin* CNRS, UMR 7139 Végétaux marins et Biomolécules, Station Biologique, F 29682, Roscoff, France. Fax: (+) 33+ 298292385 E-mail: potin@sb-roscoff.fr*

[b] *A. Ritter, F.Thomas, Dr P. Potin* Université Pierre et Marie Curie-Paris6, UMR 7139 Végétaux marins et Biomolécules, Station Biologique, F 29682, Roscoff, France.*

[c] *S. Goulitquer, C. Ferec, Dr J-P Salaün Laboratoire de Biochimie « Epissage, Lipides, Cancer et Apoptose », INSERM U613, Faculté de Médecine, F-29285 Brest, France*

[d] *A Ritter , Center for Advanced Studies in Ecology & Biodiversity, LIA-DIAMS, Departamento de Ecología, Facultad de Ciencias Biológicas, Pontificia Universidad Católica de Chile, Santiago, Chile.*

In this context, the brown alga kelp, *Laminaria digitata* provides a model to investigate aldehyde release in a physiological context. The objective of this work was therefore to address aldehyde release by *L. digitata* in stress conditions. First, when algae are subjected to oligoguluronate (GG) treatment that mimic a biotic stress by inducing an oxidative burst [12, 13]. Second, when exposed to a copper excess as an abiotic stressor [14, 15]. And finally, when naturally submitted to the effects of low tide that increases UV exposure, salinity and temperature [16].

We first address the hypothesis that an oxidative burst-mediated peroxidation of lipids should involve the release of PUAs and other aldehydes in the surrounding seawater medium of young *L. digitata* sporophytes upon challenge with GG. As shown by GC-MS analyses, on the NICI mode of *O*-pentafluorobenzyl (*O*-PFB) oxime derivatives, the production of aldehydes extracted from both seawater and air was increased after GG treatment (Figure 1). Compared to control *L. digitata* sporophytes, challenging plantlets with GG elicitors indeed dramatically changed the emission of a bouquet of more than 16 compounds, ranging from the formaldehyde to the 4-Hydroxy-dodecadienal (4-HDDE) (Figure 1). The concentrations of (*E*)-2-hexenal and 4-HHE produced or released by elicited *L. digitata* sporophytes were 2 and 24 fold higher in the water phase than in controls, respectively. Few compounds such as hexanal, 4-hydroxy-(*E*)-2-nonenal (4-HNE), 4-HDDE, were much more abundant in the air-phase, whereas (*E*)-2-hexenal, 4-hydroxy-(*E*)-2-hexenal (4-HHE) and very short chain aldehydes were more abundant in the water phase. Differences were observed in the content of 4-HHE that was 2.5 times more abundant in the aqueous phase than in the volatile fraction. In contrast, 4-HNE was 6 times more abundant in the volatile fraction. Such variations could be explained by difference of aldehyde stability in seawater, which lead to the accumulation of short-chain aldehydes.

The presence of two peaks for each aldehyde-*O*-PFB on the chromatograms was due to the presence of *syn*- and *anti*-stereoisomers (suppl. inf., Figure S1). C6-aldehydes were characterized as hexanal (*m/z* 275 $[M\text{-}HF]^-$, Rt 17.90 min - 17.98 min), (*E*)-2-hexenal (*m/z* 273 $[M\text{-}HF]^-$, Rt 18.96 min - 19.10 min), and 4-HHE (*m/z* 361 $[M\text{-}HF]^-$, Rt 22.17 min - 22.28 min). C9-aldehydes were also detected in large amount, nonanal (*m/z* 317 $[M\text{-}HF]^-$, Rt min 21.68- 22.17 min), (*E*)-2-nonenal (*m/z* 315 $[M\text{-}HF]^-$, Rt 22.99 min – 23.19 min), (*E,E*)-2,4-nonadienal (*m/z* 313 $[M\text{-}HF]^-$, Rt 24.08 min - 24.11 min) and 4-HNE (*m/z* 403 $[M\text{-}HF]^-$, Rt 25.03 min - 25.40 min). Other PUAs were detected such as C7:2 ((*E,E*)-2,4-heptadienal) (*m/z* 285 $[M\text{-}HF]^-$, Rt 21.75 min – 21.57 min), C8:2 (2,4-Octadienal) (*m/z* 299 $[M\text{-}HF]^-$, Rt 22.46 min – 22.51 min) and C8:3 (2,4,7-Octatrienal) (*m/z* 297 $[M\text{-}HF]^-$, Rt 23.19 min – 23.32 min). We also detected 9-oxo-nonanoic acid (*m/z* 419 $[M\text{-}HF]^-$, Rt 27,89 min- 27,93 min), which is known as a by-product of HPL action on fatty acid hydroperoxide [17]. Malonaldehyde (MDA) put aside, (*E*)-2-nonenal is the most abundant aldehyde (9.85 ± 2.46 $ng.mL^{-1}$ seawater).

In *L. digitata*, GG elicitation induces a rapid regulation of the synthesis of aldehydes which should occur probably in the first

minutes following challenge, as also observed for the release of iodide stores [18] and the concomitant emission of molecular iodine and volatile halocarbons that occurs during oxidative burst [19]. This is reminiscent of oligosaccharide elicitor-induced modification in the emissions of aldehydes and of other volatile organic compounds (VOCs) recently reported in the plant model *Medicago trunculata* [20].

Generation of aldehydes is known to be both mediated by enzyme reactions and chemically via oxidative mechanisms [17, 21, 22]. Quinacrine and chlorpromazine-HCl, that were previously shown to interfere with the GG-induced oxidative burst in *L. digitata* [12], affected aldehyde production suggesting the involvement of the oxidative burst in the lipoperoxidation process (Figure 2). However, chlorpromazine-HCl is also known to interfere with lipases and its strong inhibitory effect on the release of aldehydes is likely to reflect the limitation of PUFA release to fuel a putative lipoxygenase (LOX) pathway. Not surprisingly, SHAM, a known non specific inhibitor of LOXs in mammals and higher plants also repressed aldehyde formation. These preliminary inhibitor studies suggest that aldehydes are not only formed chemically but also via enzymatic pathways. Some of the observed compounds such as the (*E*)-2-nonenal, (*E*)-2-hexenal and (*E,E*)-2,4-heptadienal have already been described in *L. angustata*, in which synthesis of PUAs is proposed to derive from HPL metabolism [17]. Production of 4-hydroxy-(*E*)-2-alkenals, 4-HHE, 4-HNE and 4-HDDE, was also strongly induced during GG elicitation. 4-HDDE is a biomarker of the 12-lipoxygenation of arachidonic acid in human plasma [21]. Our data suggest that *L. digitata* generates aldehydes via both enzymatic and non-enzymatic pathways. Despite biosynthetic pathways of brown algal aldehydes was hardly investigated, the synthesis of pheromones was proposed to involve the same steps as aldehyde synthesis in diatoms [23]. Previous studies on diatoms have suggested that the biosynthesis of aldehydes is the result of the breakdown of cellular compartments and the subsequent mixture of pre-existing enzymes with their respective substrates. A process which occurs after wounding of diatoms cells by sonication [2, 6] or copepod grazing [7]. Similarly, this biosynthesis of aldehydes was only observed in crude algal extracts of the brown macroalga *L. angustata* or during incubation with exogenous PUFAs [10]. Our results might provide a signal transduction pathway triggered by GG with the activation of lipase- and lipoxygenase-like enzymes in a physiological response.

Within marine environment brown algae do not only cope with biotic stresses, but also deal with abiotic stresses, such as heavy metal exposure and modification of physical factors of the environment (UV, salinity, temperature) associated to low and high tides. Copper stress was recently shown to induce the enzyme-mediated synthesis of fatty acid hydroperoxides and prostaglandins in *L. digitata*, as well as the chemically mediated formation of various oxylipins [15]. The present study further show that treatment of this kelp species with 100 $\mu g.L^{-1}$ $CuCl_2$ enhanced the early release of a bouquet of more than 16 compounds including hexanal, (*E*)-2-nonenal, and 4-hydroxy-alkenals such as 4-HHE and 4-HNE (Figure 3), whereas low amount was observed in control sporophytes. In the water phase, 4-HHE and dodecadienal concentrations were 37 and 10 fold higher than in the control, respectively. Within 60 min after addition of copper, the (*E*)-2-nonenal, MDA and hexanal concentrations produced by *L. digitata* sporophytes in the air phase were 10, 4 and 3 fold higher than in the control, respectively. Hexanal has been described to derive from C18:2 n-6 and C20:4 n-6 fatty acids in the brown alga *L. angustata* [17]. Interestingly, no (*E*)-2-hexenal could be detected after copper stress in both air and water phase.

In addition, the ecological significance of volatile emissions was tested in field conditions by monitoring aldehyde fingerprints in rock pools, which are colonized by *L. digitata* submitted to environmental stress. The partial emersion of algae during spring tides involves desiccation, exposure to UV and ozone, and rapid variations of temperature and salinity leading to lipid peroxidation and oxidative stress [16, 24, 25].

Results of some aldehyde measurements, over a 2.5-hour field experiment, are summarized in Figure 4. Concentrations of C6 aldehydes, particularly (*E*)-2-hexenal, increased dramatically 1h after low tide. Levels of C9 aldehydes, (*E*)-2-nonenal and (*E,E*)-2,4-nonadienal were also significantly increased. As expected, the levels of the corresponding 4-hydroxy-(*E*)-2-alkenals was significantly increased with emersion time. MDA concentrations behave similarly with a maximum of 3.25 +/- 0.50 $ng.mL^{-1}$ 1 hour after low tide. Concentrations of all compounds decreased dramatically when the sea rised. This decrease could be attributed to a dilution effect when the seawater flooded the pool.

In contrast with mammals [26], higher plants [1] and even diatoms [4] the function of aldehydes in macroalgae have been hardly investigated. Their potential role as feeding attractants was suggested from bio essays using an essential oil of the green alga *Ulva pertusa*, which is known to contain some of these aldehydes [27]. The biological significance of aldehyde emission in *L. digitata* was therefore investigated by asking whether these compounds induce metabolic responses in the alga. Thalli of *L. digitata* were therefore exposed to stress-induced aldehydes by adding pure compounds in the surrounding seawater. Hexanal, nonanal, (*E*)-2-nonenal, 4-HHE, 4-HNE, (*E*,*E*)-2,4-nonadienal, (*E*,*E*)-2,4-decadienal were individually tested at both 1 $\mu g.mL^{-1}$ and 100 $ng.mL^{-1}$. Both endogenous oxylipin signatures and aldehyde profiles in seawater were monitored by GC-MS in the NICI mode. Only 4-hydroxy-(*E*)-hexenal (4-HHE), a C6 hydroxylated aldehyde, induced modifications of both aldehyde and oxylipin profiles (Figure 5). The analysis of the seawater medium revealed that (*E*)-2-hexenal was predominantly released after treatment with 4-HHE at 1 $\mu g.mL^{-1}$ and 100 $ng.mL^{-1}$. (*E*)-2-hexenal production was 75 fold higher in treated algae with 4-HHE at 1 $\mu g.mL^{-1}$ than in control. This release could not be attributed to a chemical modification of 4-HHE because, in the absence of algae, the (*E*)-2-hexenal was not formed in the seawater medium (data not shown). A release of 13-HOTrE was also induced after 24 hours incubation. Interestingly, this oxylipin derives from the pathway leading to the production of 12-oxo-phytodienoic acid, wich was recently characterized in copper-stressed *L.digitata* [15] and of jasmonate in higher plants [28]. Therefore, its early synthesis may similarly involve the activation of a signaling cascade leading to late-defence mechanisms in *L. digitata*.

To our knowledge, this is the first report showing that some aldehydes may induce the synthesis of oxylipins in algae and therefore act as inducers of metabolic responses. This is reminiscent of the early regulation of cell-protective mechanisms suggested for reactive electrophile species in higher plants [29]. By analogy with higher plants [30-33] and diatoms [8], these

results strongly suggest that the release of aldehydes may play the role of an external and/or internal emergency signal in *L. digitata* confronted with physical modifications of their environment and exposed to pollutants.

In conclusion, we have shown that the brown algal kelp *L. digitata* naturally emits volatile aldehydes in response to both biotic and abiotic stress in laboratory conditions and in their natural environment. Together with previous reports showing temperature-dependent, species-dependent and light-dependent isoprene emissions in macro-algae, including *L. digitata [34]* and the increased emission of iodinated and brominated VOCs in response to oligoguluronates, ozone and H_2O_2 in *L. digitata* [19], our results extend the repertoire of VOCs naturally emitted by kelps during both biotic and abiotic stress to saturated, mono and polyunsaturated and hydroxylated aldehydes. In addition, this is the first study which quantifies the production of PUAs by algae in their natural field (Figure 4). Interestingly, previous knowledge about the release into seawater of oxidized fatty acid-derived compounds from brown algae was limited to sexual pheromones [25].

These findings also raise the questions of which enzymes are involved with the generation of fatty acid aldehydes in brown algae, either hydroperoxide lyase CYP74 enzymes like in plants [1] and / or lipoxygenases like in the moss *Physcomitrella patens* [35] or, else, an enzyme machinery specific to the phylum of Heterokont as suggested by recent results on diatoms [36]. Recent access to whole genomes of brown algae [37] and diatoms [38, 39] provides new opportunities to express the cDNA of the conserved sequences and to characterize the products of the respective recombinant enzymes as conducted in the green lineage [1, 35].

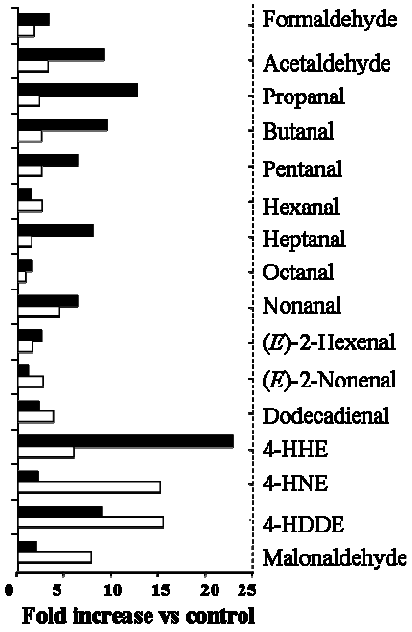

Figure 1. Comparative productions of aldehydes by *L. digitata,* in both the surrounding seawater and, the headspace after elicitation by 150 µg.mL^{-1} oligoguluronates. Aldehyde levels in seawater (black) and in air (white) were determined after 1 hour incubation. Results are expressed as a fold increase vs. control samples.

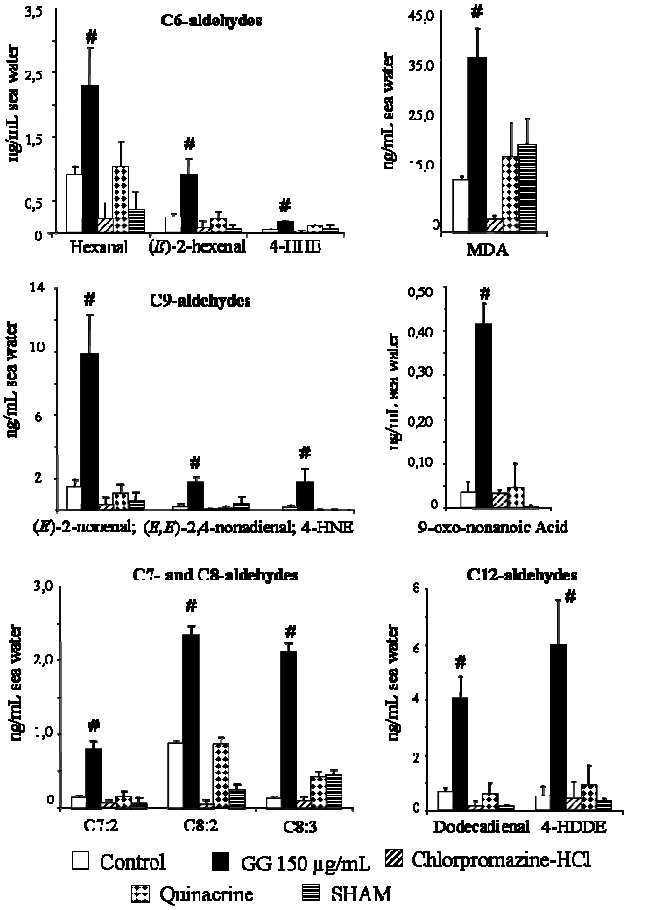

Figure 2. Aldehyde concentration and effect of inhibitors after GG treatment for 1 hour of *L. digitata*. Algae were kept 1 h in seawater as control and treated during 1 hour with 150 µg.mL^{-1} GG. Individuals were pre-incubated with: 20 µM chlorpromazine-HCl, 20 µM Quinacrine and 1 mM SHAM and subjected to GG treatment. Values represent means of three independent replicates and bars represents SD. # Significantly different from control ($p < 0.05$).

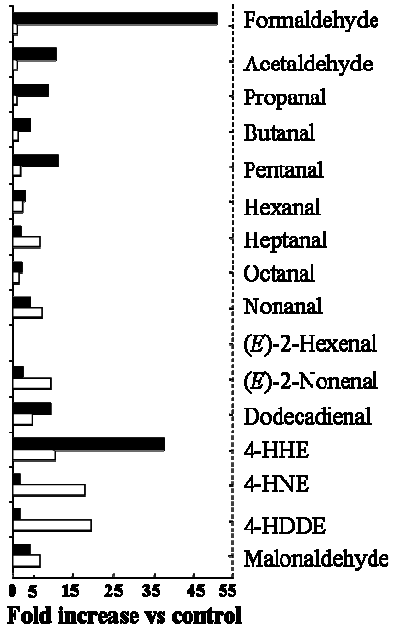

Figure 3. Comparative productions of aldehydes by *L. digitata* in both the headspace and the surrounding seawater after exposure to 100 µg.L^{-1} copper chloride. Aldehyde levels in seawater (black) and in air (white) were determined after 1 hour incubation. Results are expressed as a fold increase vs. control samples.

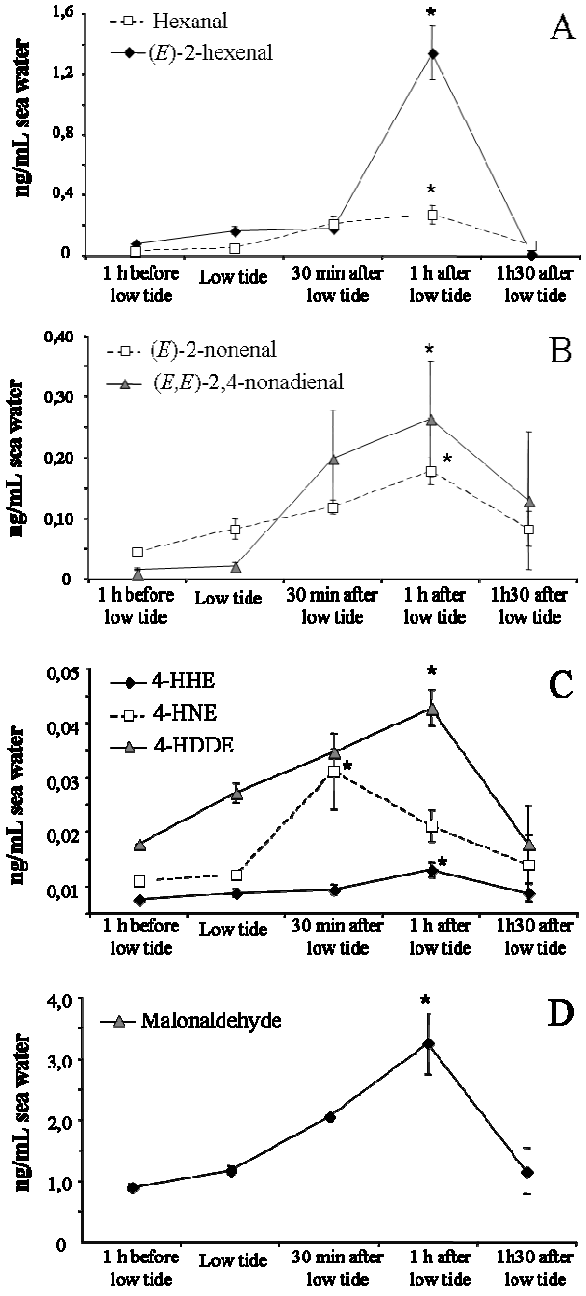

Figure 4. Variability of the emission of various aldehydes during emersion of *L.digitata* at low tide. 20mL seawater were sampled at 1 hour before low tide, at low tide and at 30 min, 1 hour and 1 h 30 min after low tide. (A) C6 aldehydes, (B) C9-aldehydes, (C)-4-hydroxy-alkenals and (D) malonaldehyde (MDA). Aldehydes were extracted in the field. * Significantly different from values at 1 hour before low tide ($p < 0.05$).

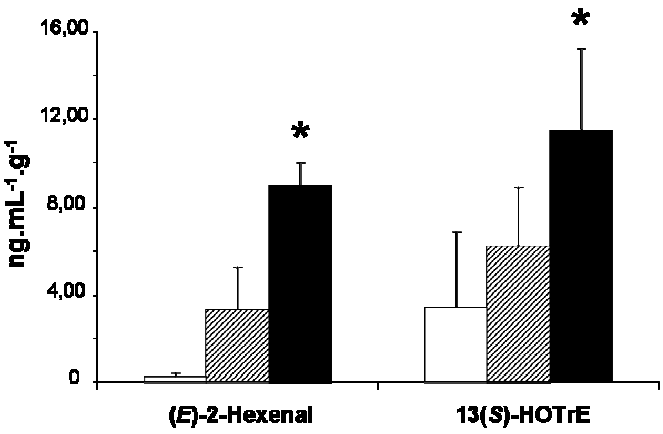

Figure 5. (*E*)-2-hexenal and 13(*S*)-HOTrE release after treatment of *L. digitata* by 4-HHE. Both aldehyde and oxylipin signature modification were monitored by GC/MS. Treatments by 100 ng.ml^{-1} (hatched) and 1 µg.ml^{-1} (black) of 4-HHE were compared to controls (white). n= 3. * Significantly different from control ($p < 0.05$)

Experimental Section

Material and treatment conditions: The marine brown alga *Laminaria digitata* V. Lamouroux (Laminariales, Laminariaceae) was collected in the intertidal zone close to the Station Biologique de Roscoff in Brittany, France, during low tide. Young fronds (2 to 15 cm in length) were chosen and transported to the laboratory. They were kept in cultivation tanks with seawater as described [15].

Seawater analyses: Seawater medium was transferred into a funnel containing 20 mL ethyl acetate and 50 ng of 4-HNE-d3 as internal standard. After a vigorous shaking of the mixture, water phase was discarded and the organic phase was recovered and gently dried in vacuum conditions (Rotary evaporator). The residues were dissolved with 2 mL MeOH containing PFBHA-HCl 0.05 M, transferred into a sylilated glass tube and incubated for 2 hours at room temperature. Solvent was evaporated under a gentle stream of nitrogen (free of oxygen) and residues were dissolved into 100 µL CH_3CN and 200 µL Sylon BFT. The mixture was further incubated for 1 hour at 60 °C to form TMS derivatives, dried under a stream of nitrogen gas and the residues dissolved in 100 µL of hexane.

Trapping of volatile compounds: The trapping protocol of aldehydes was similar to that described by Engelberth and co-workers to trap the methyl jasmonate [40]. *L. digitata* plantlets (1 g blotted fresh weight) were incubated in a 50 mL flask containing 20 mL of fresh filtered seawater (suppl. inf., Figure S2). A Super Q filter trap, containing about 30 mg of adsorbent, and a Teflon vent tubing were connected to a vacuum source at a flow rate of 500 mL.min^{-1}. A magnetic bar maintained constant agitation. Oligoguluronates were injected via a septum by a 200 µL syringe. The compounds were eluted from the Super Q with 600 µL MeOH containing PFBHA-HCl 0.05 M and incubated for 2 hours at room temperature. TMS-derivatization was then carried out as described above.

Tide pool measurements: Experiment took place at the Pointe Sainte-Barbe close to the CNRS Institute of Roscoff. A tide pool containing 102 thalli of *L. digitata* and only exposed at very high coefficient of tide was chosen for the experiment. During the whole experiment pH, temperature, salinity, brightness and O_2 were monitored. A five-point study was done at 1 hour before low tide, at low tide and 30 min, 1 hour and 1 hour 30 min after low tide. In this last point, the sea raised and flooded the pond. With a glass pipette, 20 mL seawater samples collected in triplicates were transferred into a Pyrex bottle containing 20 mL of ethyl acetate and 50 ng 4-HNE-d3 and the mixture was vigorously shaken. Samples were cooled on ice and rapidly analysed in the laboratory as describe above (see "seawater analyses").

GC-MS-NCI Analyses : Aldehyde samples were analyzed by using a HP 5873 MSD interfaced to a HP 6890 Series+ gas chromatograph (Agilent, Les Ullis, France). A 2 µL volume of sample was injected into a capillary column (HP-5MS, J & W Scientific) with 0.25 mm i.d., 30 m length and 0.25 mm-film thickness. The temperature of injection port and interface was 250 °C and 280 °C respectively. The oven temperature was set at 60 °C for 5 min, increased at the rate of 8 °C/min to 300 °C and held for 5 min. The compounds were ionized by negative ion chemical ionization (NICI) using methane as reagent gas at 40 mL/min. For aldehydes identification, sample GC-MS analysis was carried out in both NICI and EI mode (70 eV) in the total ion current (TIC) mode. Calibration curves were prepared with increasing amounts of standards in distilled water analyzed by GC-MS in the NICI mode. The sample were extracted and derivatized as described in the "seawater analyses" section. The calibration curves were constructed by plotting the areas ratios of each analyte relative to the internal standard against the concentration of the analyte. For quantification of 2,4,7-octatrienal and 2,4,7-decadienal, the calibration curve of the commercially available 2,4-dienals were used, which were assumed to behave similarly during derivatization [41], for 4-HDDE quantification, the calibration curve of 4-HNE was similarly used. Standard curves were linear ($r^2 > 0.95$) from 0.5 ng to 50 ng injected.

Acknowledgements

This work has been partially funded by a Programme de Recherche d'Intérêt Régional (STRESS) from the Conseil Régional de Bretagne (France) and by the ECOKELP program (ANR 06 BDIV 012), funded by the French Agence Nationale de la Recherche (ANR). PhD fellowships to S.G., F.T. and A.R. were awarded by the Ministère de l'Enseignement Supérieur et de la Recherche and the French Embassy and the CONICYT of Chile, respectively. This work was conducted within the Laboratoire International Associé 'Dispersal and Adaptation of Marine Species' (LIA DIAMS) PUC, Chile and CNRS-UPMC, France.

Keywords: marine alga · aldehyde · biotic stress · abiotic stress · volatiles

[1] K. Matsui, A. Minami, E. Hornung, H. Shibata, K. Kishimoto, V. Ahnert, H. Kindl, T. Kajiwara and I. Feussner, *Phytochemistry* **2006**, *67*, 649-57.
[2] G. d'Ippolito, O. Iadicicco, G. Romano and A. Fontana, *Tetrahedron Letters* **2002**, *43*, 6137-6140.
[3] A. Miralto, G. Barone, G. Romano, S. A. Poulet, A. Ianora, G. L. Russo, I. Buttino, G. Mazzarella, M. Laabir, M. Cabrini, et al., *Nature* **1999**, *402*,
[4] G. Pohnert, *Chembiochem* **2005**, *6*, 946-59.
[5] T. Wichard, S. A. Poulet, C. Halsband-Lenk, A. Albaina, R. Harris, D. Liu and G. Pohnert, *J Chem Ecol* **2005**, *31*, 949-58.
[6] G. Pohnert, *Angew. Chem. Int. Ed.* **2000**, *39*, 4352-4354.
[7] A. Ianora, A. Miralto, S. A. Poulet, Y. Carotenuto, I. Buttino, G. Romano, R. Casotti, G. Pohnert, T. Wichard, L. Colucci-D'Amato, et al., *Nature* **2004**, *429*, 403-7.
[8] A. Vardi, F. Formiggini, R. Casotti, A. De Martino, F. Ribalet, A. Miralto and C. Bowler, *PLoS Biol* **2006**, *4*, e60.
[9] Y. Akakabe, K. Matsui and T. Kajiwara, *Bioorg Med Chem* **2003**, *11*, 3607-9.
[10] K. Boonprab, K. Matsui, Y. Akakabe, N. Yotsukura and T. Kajiwara, *Phytochemistry* **2003**, *63*, 669-78.
[11] C. Vidoudez and G. Pohnert, *Journal of Plankton Research* **2008**, *DOI:10.1093/plankt/fbn085*,
[12] F. C. Küpper, B. Kloareg, J. Guern and P. Potin, *Plant Physiol* **2001**, *125*, 278-91.
[13] F. C. Küpper, D. G. Muller, A. F. Peters, B. Kloareg and P. Potin, *J Chem Ecol* **2002**, *28*, 2057-81.
[14] L. Contreras, M. H. Medina, S. Andrade, V. Oppliger and J. A. Correa, *Environ Pollut* **2007**, *145*, 75-83.
[15] A. Ritter, S. Goulitquer, J. P. Salaun, T. Tonon, J. A. Correa and P. Potin, *New Phytol* **2008**, *180*, 809-821.
[16] M. J. Dring, *Adv. Bot. Res.* **2005**, *43*, 175-207.
[17] K. Boonprab, K. Matsui, Y. Akakabe, M. Yoshida, N. Yotsukura, A. Chirapart and T. Kajiwara, *J Appl Phycol* **2006**, *18*, 409-412.
[18] F. C. Küpper, L. J. Carpenter, G. B. McFiggans, C. J. Palmer, T. J. Waite, E. M. Boneberg, S. Woitsch, M. Weiller, R. Abela, D. Grolimund, et al., *Proc Natl Acad Sci U S A* **2008**, *105*, 6954-8.
[19] C. J. Palmer, T. L. Anders, L. J. Carpenter, F. Kupper and G. B. McFiggans, *Environ. Chem.* **2005**, *2*, 282-290.
[20] M. Leitner, R. Kaiser, M. O. Rasmussen, H. Driguez, W. Boland and A. Mithofer, *Phytochemistry* **2008**, *69*, 2029-40.
[21] M. Guichardant, N. Bernoud-Hubac, B. Chantegrel, C. Deshayes and M. Lagarde, *Prostaglandins Leukot Essent Fatty Acids* **2002**, *67*, 147-9.
[22] C. Schneider, N. A. Porter and A. R. Brash, *J Biol Chem* **2008**,
[23] G. Pohnert and W. Boland, *Nat Prod Rep* **2002**, *19*, 108-22.
[24] J. Collen and I. A. Davison, *J. Phycol.* **1999**, *35*, 54-61.
[25] G. A. Pearson and I. A. Davison, *J. Phycol.* **1994**, *30*, 257-267.
[26] P. J. O'Brien, A. G. Siraki and N. Shangari, *Crit Rev Toxicol* **2005**, *35*, 609-62.
[27] Y. Akakabe and T. Kajiwara, *J. App. Phycol.* **2007**, *DOI : 10.1007/s10811-007-9309-x*,
[28] E. Blée, *Prog Lipid Res* **1998**, *37*, 33-72.
[29] E. E. Farmer and C. Davoine, *Curr Opin Plant Biol* **2007**, *10*, 380-6.
[30] I. T. Baldwin, A. Kessler and R. Halitschke, *Curr Opin Plant Biol* **2002**, *5*, 351-4.
[31] Z. Chen, H. Silva and D. F. Klessig, *Science* **1993**, *262*, 1883-6.
[32] A. Levine, R. Tenhaken, R. Dixon and C. Lamb, *Cell* **1994**, *79*, 583-93.
[33] M. L. Orozco-Cardenas, J. Narvaez-Vasquez and C. A. Ryan, *Plant Cell* **2001**, *13*, 179-91.
[34] W. J. Broadgate, G. Malin, F. Kupper, A. Thompson and P. S. Liss, *Marine Chemistry* **2004**, *88*, 61-73.
[35] M. Stumpe, J. Bode, C. Gobel, T. Wichard, A. Schaaf, W. Frank, M. Frank, R. Reski, G. Pohnert and I. Feussner, *Biochim Biophys Acta* **2006**, *1761*, 301-12.
[36] A. Barofsky and G. Pohnert, *Org Lett* **2007**, *9*, 1017-20.
[37] B. Charrier, S. M. Coelho, A. Le Bail, T. Tonon, G. Michel, P. Potin, B. Kloareg, C. Boyen, A. F. Peters and J. M. Cock, *New Phytol* **2008**, *177*, 319-32.
[38] E. V. Armbrust, J. A. Berges, C. Bowler, B. R. Green, D. Martinez, N. H. Putnam, S. Zhou, A. E. Allen, K. E. Apt, M. Bechner, et al., *Science* **2004**, *306*, 79-86.
[39] C. Bowler, A. E. Allen, J. H. Badger, J. Grimwood, K. Jabbari, A. Kuo, U. Maheswari, C. Martens, F. Maumus, R. P. Otillar, et al., *Nature* **2008**, *456*, 239-44.
[40] J. Engelberth, E. A. Schmelz, H. T. Alborn, Y. J. Cardoza, J. Huang and J. H. Tumlinson, *Anal Biochem* **2003**, *312*, 242-50.
[41] T. Wichard, S. A. Poulet and G. Pohnert, *J Chromatogr B Analyt Technol Biomed Life Sci* **2005**, *814*, 155-61.

Received: ((will be filled in by the editorial staff))
Published online: ((will be filled in by the editorial staff))

Supplementary material

Chemicals : 4-hydroxy-(*E*)-2-Hexenal (4-HHE); 4-hydroxy-(*E*)-2-nonenal-d3 (4-HNE-d3) and 4-oxo-(*E*)-2-nonenal-d3 were purchased from Cayman Chemical (Spi-Bio, Montigny Le Bretonneux, France); 9-oxo-nonanoic acid was from Larodan Fine Chemicals (Malmö, Sweden). Silylating reagent Sylon BFT (bis(trimethylsilyl)trifluoro-acetamide : trimethyl-chlorosilane, 99:1) was from Supelco (Bellefonte, PA, USA). All other chemicals and solvents were from Merck (Darmstadt, Germany) and Sigma (St Louis, MO, USA). MDA was synthesized as described in Vollenweider and co-workers (Vollenweider et al., 2000).

Elicitors : Copper treatment medium consisted in filtered seawater with addition of the nominal concentration of 100 μgL^{-1} copper as $CuCl_2$ from Merck (Darmstadt, Germany). Each treatment included three replicates.Alginate oligosaccharides with a polymerization degree ranging from 15 to 25 (Heyraud et al., 1996) were prepared in the laboratory according to Haug and co-workers (Haug et al., 1974) using sodium alginate from *Laminaria hyperborea* stipes (provided by B. Larsen, Trondheim University, Norway) and yielding three categories of alginate oligosaccharides (GG, MM, and MG blocks). In elicitation experiments, GG were added to the seawater at final concentrations of 150 $\mu g\ mL^{-1}$ (3 mg). Incubation period was 1 hour. At the end of the experiment thalli were frozen in liquid nitrogen and kept at -80 °C until further analyses.

Inhibitors : Several compound were screened for their potential to inhibit enzyme activity possibly involved in the synthesis of aldehydes: quinacrine (20 µM; target, flavin-dependent redox enzymes, in particular oxidases), and chlorpromazine-HCl (20 µM; target, phospholipase A) from stock solutions dissolved in ethanol, Salicylhydroxamic acid (SHAM) at 1 mM final concentration (LOX activities). Plantlets were preincubated in seawater added with inhibitors dissolved in ethanol or ethanol alone during 30 min. Incubation medium was completely removed and algae rinsed with fresh filtered sea water. 20 mL of newly fresh filtered seawater was added in the flask prior to oliguluronates addition.

Algae treatment by aldehydes: Hexanal, nonanal, (*E*)-2-nonenal, 4-HHE, 4-HNE, (*E*,*E*)-2,4-nonadienal, (*E*,*E*)-2,4-decadienal were individually tested at both 1 $\mu g.mL^{-1}$ and 100 $ng.mL^{-1}$ by addition into the surrounding seawater. After 1 hour, the seawater was extracted as described in "seawater analyses" for aldehydes analyses. 20 mL of newly fresh filtered seawater was added in the flask. After 23 hours at room temperature (24 hours incubation), thalli were frozen in liquid nitrogen and kept at -80 °C until oxylipin extraction.

Oxylipin extraction and GC-MS-EI analysis : Oxylipins were extracted in *L. digitata* tissue according to (Küpper et al., 2006). In each sample, 250 ng of 12-OH-lauric acid was added as an internal standard. The residue was dissolved in 100 µl of hexane.

Methyl esters were prepared by treatment with an excess of ethereal diazomethane. Silylation was achieved by treatment with a mixture of BSTFA (*N,N*-bistrimethylsilyl-trifluoroacetamide)/TMCS (1% trimethyl-chlorosilane) for 1 hour at 60 °C, in order to obtain trimethylsilyl derivatives for compounds containing hydroxyl group.
GC-MS analyses were carried out on a HP 5890 Series II gas chromatograph equipped with a fused silica capillary column (HP-5MS 5% phenyl methyl siloxane; 30 m × 0.32 mm I.P, film thickness 0.25 µm) and combined to a quadrupole mass-selective detector (HP 5971A, Agilent Technology). Mass spectra (EI mode) were recorded at 70 eV. 2 µL were injected in the splitless mode at 60 °C. After 5 min at 60 °C, the oven temperature was increased to 200 °C at 50 °C min^{-1} and then linearly ramped to 280 °C at 2 °C min^{-1} that became stable for 10 min before returning to initial conditions. 13-HOTrE was identified using authentic standard and was quantified from standard curves.

Statistical analyses : Data analysis was performed using the Mann & Whitney non-parametric test with Prism 4.0 software (GraphPad, Inc., San Diego, CA, USA). Data are presented as the mean ± SD.

Supplementary figures :

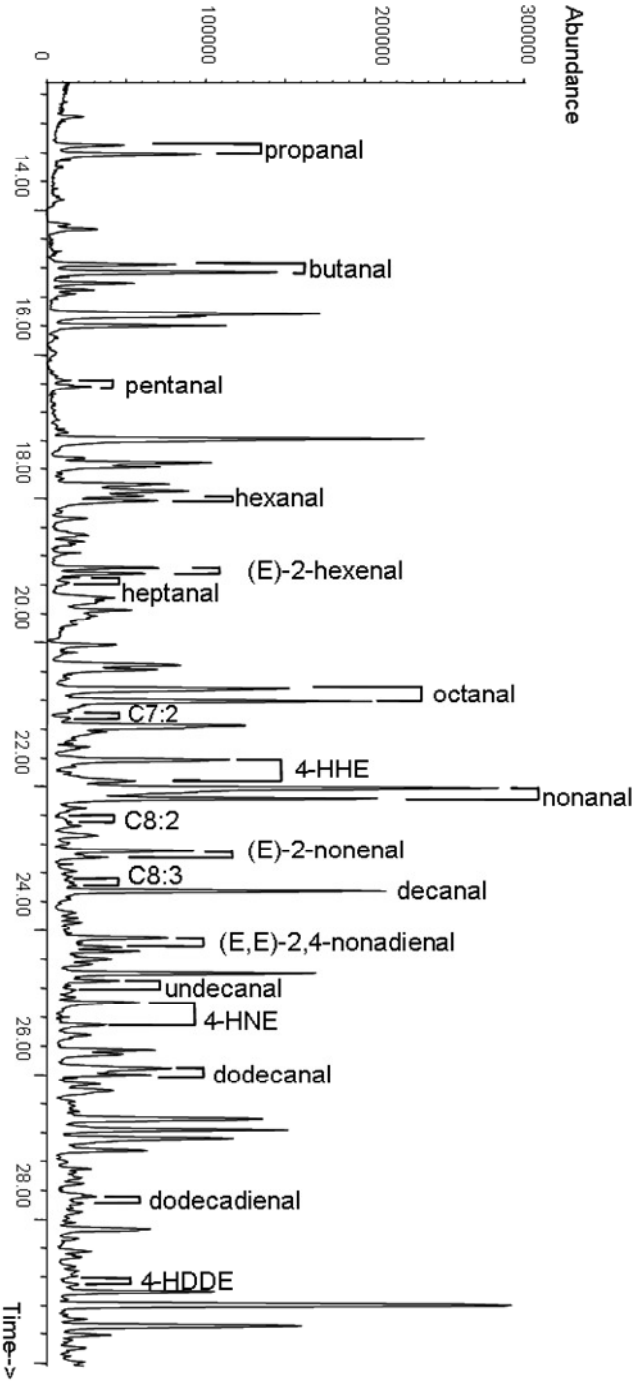

Figure S1. *m/z* 181 chromatogram obtained by GC-MS in the NICI mode for aldehydes extracted from 20 mL filtered seawater containing *L. digitata* elicited by 150 $\mu g.mL^{-1}$ oligoguluronates. Aldehydes were monitored as PFB-oximes/TMS-ethers. *m/z* 181 is the corresponding ion for the fragment $[CH_2\text{-}C_6F_5]$ loss by all aldehydes-*O*-PFB.

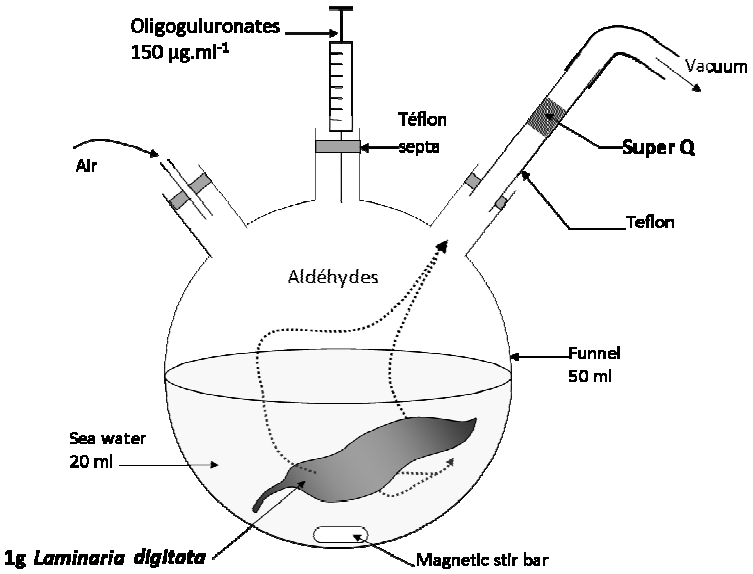

Figure S2. Trapping of volatile compounds emitted by *Laminaria digitata* on Super Q adsorbent in response to oligoguluronates (150 µg.mL^{-1}) elicitation. Both the head space and the surrounding sea water medium were submitted to PFB-oximation and TMS-etherification previous GC/MS analysis in the NCI mode.

COMMUNICATION

Stress-induced aldehyde release by kelps. In response to biotic and abiotic stresses, the brown algal kelp *Laminaria digitata* releases volatile fatty aldehydes in laboratory conditions and in its natural environment (red). In response to 4-HHE treatment, *L. digitata* releases (*E*)-2-hexenal and synthesizes 13(S)-HOTrE (green). These results support the hypothesis that by analogy with higher plants or diatoms these compounds may mediate kelp responses to stress.

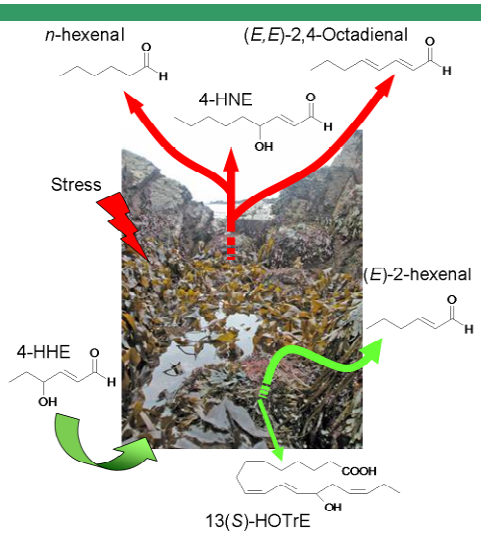

*Sophie Goulitquer, Andrés Ritter, François Thomas, Cyrille Ferec, Jean-Pierre Salaün, Philippe Potin**

Page No. – Page No.

Release of volatile aldehydes by the brownalgal kelp *Laminaria digitata* in response to both biotic and abiotic stresses

4 TWO-DIMENSIONAL GEL ELECTROPHORESIS ANALYSIS OF BROWN ALGAL PROTEIN EXTRACTS

Loretto Contreras, Andrés Ritter, Geraldine Dennett, Freddy Boehmwald, Nathalie Guitton, Charles Pineau, Alejandra Moenne, Philippe Potin, and Juan A. Correa

Abstract

High quality protein extracts are required for proteomic studies, a field that is poorly developed in marine macroalgae. A reliable phenol extraction protocol using *Scytosiphon gracilis* and *Ectocarpus siliculosus* (Phaeophyceae) as algal models resulted in high quality protein extracts. The performance of the new protocol was tested against four methods available for vascular plants and a seaweed. The protocol, which includes an initial step to remove salts from the algal tissues, allowed the use of highly resolving 2-DE protein analyses, providing the opportunity to unravel potentially novel physiological processes unique to this group of marine organisms.

J. Phycol. **44,** 1315–1321 (2008)

DOI: 10.1111/j.1529-8817.2008.00575.x

TWO-DIMENSIONAL GEL ELECTROPHORESIS ANALYSIS OF BROWN ALGAL PROTEIN EXTRACTS[1]

Loretto Contreras[2,3]

Center for Advanced Studies in Ecology & Biodiversity, Departamento de Ecología, Facultad de Ciencias Biológicas, Pontificia Universidad Católica de Chile, Santiago, Chile

Andrés Ritter[3]

Center for Advanced Studies in Ecology & Biodiversity, Departamento de Ecología, Facultad de Ciencias Biológicas, Pontificia Universidad Católica de Chile, Santiago, Chile

CNRS, Université Pierre et Marie Curie, UMR 7139, Station Biologique, Roscoff, France

Geraldine Dennett

Center for Advanced Studies in Ecology & Biodiversity, Departamento de Ecología, Facultad de Ciencias Biológicas, Pontificia Universidad Católica de Chile, Santiago, Chile

Freddy Boehmwald

Departamento de Biología, Facultad de Química y Biología, Universidad de Santiago, Santiago, Chile

Nathalie Guitton, Charles Pineau

High-Throughput Proteomics Platform OUEST-genopole®, UPRES JE 2459, INSERM, U625, Campus de Beaulieu F-35042, France

Alejandra Moenne

Departamento de Biología, Facultad de Química y Biología, Universidad de Santiago, Santiago, Chile

Philippe Potin

CNRS, Université Pierre et Marie Curie, UMR 7139, Station Biologique, Roscoff, France

and Juan A. Correa

Center for Advanced Studies in Ecology & Biodiversity, Departamento de Ecología, Facultad de Ciencias Biológicas, Pontificia Universidad Católica de Chile, Santiago, Chile

High-quality protein extracts are required for proteomic studies, a field that is poorly developed for marine macroalgae. A reliable phenol extraction protocol using *Scytosiphon gracilis* Kogame and *Ectocarpus siliculosus* (Dillwyn) Lyngb. (Phaeophyceae) as algal models resulted in high-quality protein extracts. The performance of the new protocol was tested against four methods available for vascular plants and a seaweed. The protocol, which includes an initial step to remove salts from the algal tissues, allowed the use of highly resolving two-dimensional gel electrophoresis (2-DE) protein analyses, providing the opportunity to unravel potentially novel physiological processes unique to this group of marine organisms.

Key index words: **2-DE; algae; Phaeophyceae; protein extraction methods; proteomics**

Abbreviations: **2-DE, two-dimensional gel eletrophoresis; ACN, acetonitrile; CHAPS, 3-[(3-cholamidopropyl)dimethyl-amonio]-1-propanesulfonate; IEF, isoelectric focusing; IPG, immobilized pH gradient; kDa, kilodalton (molecular mass); MALDI, matrix-assisted laser desertion/ionization; M_r, relative molecular mass; MS, mass spectrometry; MS/MS, tandem mass spectrometry; p*I*, isoelectric point; ppm, parts per million; PVP, polyvinylpyrrolidone; TCA, trichloroacetic acid; TFA, trifluoroacetic acid; TOF, time of flight**

The development of postgenomic approaches, such as proteomics and transcriptomics, has become an inescapable step to understand how organisms physiologically adapt to abiotic and biotic stresses. Among the available proteomic tools, 2-DE, established by O'Farrell (1975), is an effective technology for protein analysis of complex biological samples.

[1]Received 21 November 2007. Accepted 14 March 2008.
[2]Author for correspondence: e-mail lcontrer@puc.cl.
[3]These authors contributed equally to the work.

Sample preparation, in particular the quality of protein extraction, is critical to the successful resolution of the 2-DE pattern. Important changes have been introduced in proteomic methods in recent years to provide standard protocols for a wider diversity of cells, organs, and organisms (Unlu et al. 1997, Gygi et al. 2000, Jacobs et al. 2001, Beranova-Giorgianni 2003, Yan et al. 2006). However, in comparison to other organisms, available protein extraction methods have proved to be incapable of producing high-quality extracts for marine algae.

Brown algae (Phaeophyceae) are of interest for a number of reasons, ranging from their major ecological importance to their phylogenetic position within eukaryotes. In the latter context, they represent one of the five eukaryotic lineages that independently evolved complex multicellularity. Nevertheless, this class of organisms has been poorly studied compared to other plant and animal lineages. Thus, proteome analyses are expected to help unravel the physiological bases of the ecological success of this group. Few proteomic studies have been undertaken in other species of algae, and, in addition, those studies deal only with evolutionarily distant microalgal groups, such as *Haematococcus* (Wang et al. 2004a,b), *Euglena* (Hoffmeister et al. 2004), *Nannochloropsis* (Kim et al. 2005), and *Chlamydomonas* (Stauber et al. 2003).

Electrophoretic separation of brown algal proteins, as those of plants, is often difficult because of their relatively low concentration and by the coextraction of contaminants, such as anionic polysaccharides, polyphenols, salts, and pigments, which are highly concentrated in the tissue extracts (Cremer and Van de Walle 1985, Flengsrub and Kobro 1989, Rabilloud 1996, Mechin et al. 2003, Chinnasamy and Rampitsch 2006). These contaminants pose a significant difficulty for 2-DE because they cause horizontal and vertical streaking, smearing, and a reduction in the number of distinctly resolved protein spots. In addition, algal tissues are often rich in proteases that severely interfere with downstream protein separation and analysis. The difficulty in obtaining high-quality 2-DE gels from macroalgae was recently highlighted by Wong et al. (2006), who obtained algal proteins from *Gracilaria* (Rhodophyta) using several extraction methods, including the phenol/chloroform combination. Nevertheless, the quality of the 2-DE profiles was poor due to the presence of a significant amount of interfering substances accompanied by low protein yield. In this context, and as part of ongoing work focused on unraveling the metabolic processes occurring in physiologically stressed brown macroalgae, we developed a new method for protein extraction that minimized the coextraction of nonprotein compounds using the two structurally distinct brown algal species *S. gracilis* (Contreras et al. 2007) and *E. siliculosus* (Peters et al. 2004). We tested and compared different protein extraction methods available in the literature and identified the protein spots present in the gels.

MATERIALS AND METHODS

Algal sampling and culture. Individual thalli of *S. gracilis* were collected during low tide in the locality of Maitencillo (32°39.5′ S, 71°26.6′ W), central Chile. Three replicates of 40–60 individuals each were kept in plastic bags containing seawater and transported to the laboratory in a cooler at 15°C. Material of *E. siliculosus* was obtained from cultures of strain 32 (from southern Peru) kept as a stock in the Laboratory Collection at the Marine Biology Station in Roscoff, France. To produce enough biomass, inoculates from the unialgal stock were cultivated in 10 L Provasoli-enriched natural seawater (PES) medium (Starr and Zeikus 1993) in polycarbonate tanks, at 15°C, 10–30 $\mu mol \cdot m^{-2} \cdot s^{-1}$ photon fluence rate, and a photoperiod of 10:14 light:dark (L:D).

Protein extraction methods. A total of 5–7 g (fresh tissue) of *S. gracilis* and 300 mg of *E. siliculosus* were used for testing each of the methods selected for comparisons. Tissues were rinsed with filtered seawater and cleaned using an ultrasonic bath (Ultrasonic cleaner; Model 575T, Cortland, NJ, USA) for 30 s. Tissues were then pulverized in liquid nitrogen using a mortar and pestle before homogenization in the corresponding extraction buffer. Five methods were tested to select the one producing the most consistent results.

Method 1 (urea extraction and acetone precipitation): This method was based on Wang et al. (2003a) and Förster et al. (2006). Pulverized tissue was resuspended in 15 mL of 2-DE-standard lysis buffer (9 M urea, 4% w/v 3-[(3-cholamidopropyl)dimethyl-amonio]-1-propanesulfonate [CHAPS], 60 mM diothiothreitol [DTT], 40 mM Tris–HCl pH 7.4), 1% w/v carrier ampholytes pH 3–10 (immobilized pH gradient [IPG] buffer, Amersham Biosciences, Uppsala, Sweden) and complete protease inhibitor cocktail (Roche Diagnostics Ltd., Lewes, UK [1 tablet · 50 mL^{-1} extraction buffer]). The mixture was homogenized and centrifuged (Hettich Zentrifugen; Universal 32R, Tuttlingen, Germany) at 10,000*g* for 20 min. Proteins were precipitated with five volumes of 80% v/v ice-cold acetone with 20 mM DTT during 2 h at −20°C and pelleted by centrifugation at 10,000*g* for 20 min.

Method 2 (urea extraction, ultracentrifugation, and acetone precipitation): The extraction followed the same steps described in Method 1. However, an additional step was incorporated: after homogenization and centrifugation at 10,000*g* for 20 min, the liquid phase was ultracentrifuged at 100,000*g* for 1 h.

Method 3 (urea extraction, ultracentrifugation, and trichloroacetic acid (TCA)/acetone precipitation): The extraction followed that used in Method 2, although in this case, the proteins were precipitated overnight in 10% v/v TCA in 100% ice-cold acetone, pelleted by centrifugation at 10,000*g* for 20 min, and rinsed seven times in four volumes of 80% ice-cold acetone.

Method 4 (phenol extraction): Proteins were extracted using the phenol extraction method according to available protocols used for recalcitrant plants (Wang et al. 2003b, Saravanan and Rose 2004, Carpentier et al. 2005). The main modifications were the concentration of reagents and their inclusion in the extraction buffer. Once pulverized, tissue was resuspended in 5–15 mL of extraction buffer (1.5% w/v polyvinylpyrrolidone [PVP], 0.7 M sucrose, 0.1 M KCl, 0.5 M Tris–HCl pH 7.5, 250 mM EDTA, 1 tablet for 50 mL extract of complete protease inhibitor cocktail, 2% v/v β-mercaptoethanol, and 0.5% w/v CHAPS) and homogenized at 4°C for 20 min. Then, an equal volume of Tris–HCl pH 7.5–saturated phenol was added, and the mixture was rehomogenized for 20 min at 4°C. The mixture was centrifuged at 10,000*g* for 20 min, and the upper phenol phase was removed. The lower

phase was reextracted using the same volume of phenol as above. Proteins in the phenol phase were precipitated by addition of five volumes of 0.1 M ammonium acetate dissolved in methanol and incubated at −20°C for 3 h. The extract was centrifuged at 10,000*g* for 20 min, the supernatant was discarded, and the protein pellet was rinsed in ammonium acetate (0.1 M in methanol) for 20 min at −20°C. Subsequently, the protein pellet was rinsed seven times in four volumes of 80% ice-cold acetone and once in cold acetone containing 20 mM DTT.

Method 5 (phenol extraction and desalting steps): To remove salt excess, the tissue was rinsed four times with Milli Q water (Barnstead International, Easy pure II, RF ultra pure water system, Dubuque, IA, USA; 15–20 s) and four times with 50 mM Tris–HCl pH 8.8 (15–20 s). Afterward, the algal tissue was blotted dry, weighed, and stored at −80°C. After tissue pulverization in liquid nitrogen, the proteins were extracted using the phenol method. Furthermore, after protein precipitation in ice-cold acetone, a final cleaning step was incorporated using the 2-D Clean-up Kit (Amersham Biosciences, Piscataway, NJ, USA). Finally, protein extracts were stored at −80°C.

SDS-PAGE and isoelectric focusing (IEF). Regardless of the extraction method, protein concentrations were quantified using the BCA™ protein assay kit (Pierce, Rockford, IL, USA), with BSA as standard. For one dimension SDS-PAGE (1-DE) analysis, the protein pellet was dissolved in Laemmli (1970) buffer, and for 2-DE, the pellet was dissolved in Tris–HCl 40 mM pH 7.5. Electrophoresis trials for 1-DE (30 µg protein per lane) were run in 12.5% w/v SDS-PAGE gels, using SDS electrophoresis buffer (25 mM Tris pH 8.3, 192 mM glycine, and 0.1% w/v SDS) and a Mini-Protean® 3 cell apparatus (Bio-Rad, Hercules, CA, USA) at 30 mA for ~45 min (PowerPac Universal™ power supply; Bio-Rad). Three extracts were prepared from each tissue, and electrophoresis was run for each of them. For the IEF step, 500 µg of the protein pellet was suspended in 340 µL of IEF buffer (6 M urea, 2 M thiourea, 4% w/v CHAPS, 1% w/v DTT, 1% w/v carrier ampholytes pH 3–10 or pH 4–7 [IPG buffer; Amersham Biosciences]) and maintained at room temperature for 1 h. IPG strips (Immobiline™ DryStrip 18 cm pH 3–10 or pH 4–7; Amersham Biosciences) were actively rehydrated for 15 h in IEF buffer containing the proteins, focused into a Protean IEF Cell (Bio-Rad) at 20°C with the following successive steps: a linear increase from 0 to 250 V for 15 min, a gradient phase from 250 V to 10,000 V for 4 h, and then a hold at 10,000 V for a total of 60 kVh. After focusing, the proteins were reduced by incubating the IPG strips for 10 min at room temperature, under gentle stirring, in an equilibration buffer (6 M urea, 30% w/v glycerol, 2% [w/v] SDS, 50 mM Tris–HCl pH 8.8), containing 65 mM DTT. Strips were then alkylated for an additional 10 min in 10 mL of the same solution containing 4.5% w/v iodoacetamide and a few grains of bromophenol blue. Upon equilibration, the strips were directly applied onto a 12.5% w/v SDS-PAGE gel, and the electrophoresis was done using the Protean® II xi Cell (Bio-Rad) system at 50 mA for 3–4 h.

Gel analyses. Gels (1-DE and 2-DE) were stained with ProtoBlue Safe Coomassie Stain G-250 (National Diagnostics, Atlanta, GA, USA) and scanned using the Precision Scan Pro 3.02 software (Hewlett Packard, Palo Alto, CA, USA). Molecular masses were estimated using a broad-range standard (Bio-Rad) co-migrating in the SDS-PAGEs. The Precision Scan Pro 3.02 software was used to capture gel images at 600 dpi. The 2-DE images were analyzed using the Z3 2-DE gel analysis software (Compugen, Tel Aviv, Israel) according to the manufacturer's instructions.

Protein identification. For mass spectrometry (MS) analyses, Coomassie blue-stained protein spots were excised from 2-DE gels and processed using an Ettan™ Spot Handling Workstation (GE Healthcare, Uppsala, Sweden). Gel plugs were first rinsed three times in MilliQ water, once in 50% methanol/50 mM ammonium bicarbonate, and once in 75% acetonitrile (ACN) and were then dried. Gel pieces were then rehydrated by incubation for 120 min with 8.3 $\mu g \cdot mL^{-1}$ sequencing grade modified porcine trypsin (Promega, Charbonnières-les-bains, France) in 20 mM ammonium bicarbonate. Extraction was performed in two successive steps, by adding 50% ACN and 0.1% trifluoroacetic acid (TFA). Digests were dried and dissolved in 2 $mg \cdot mL^{-1}$ α-cyano-4-hydroxycinnamic acid in 70% ACN/0.1% TFA, before spotting onto matrix-assisted laser desertion/ionization (MALDI) targets (384 Scout MTP 600 µm AnchorChip™; Bruker Daltonics, Bremen, Germany). Mass fingerprints were acquired using a MALDI–time of flight (TOF)/TOF mass spectrometer (Ultraflex™, Bruker Daltonics, Bremen, Germany) and processed using the FlexAnalysis™ software (version 2.2; Bruker Daltonics). Following internal calibration with trypsin autodigestion peptides, the monoisotopic masses of tryptic peptides were used to query NCBInr sequence databases (4,848,770 sequences; 1,676,932,316 residues) using the Mascot (Mascot server version 2.1.04; http://www.matrixscience.com) and ProFound (http://prowl.rockefeller.edu/prowl-cgi/profound.exe). Search conditions were as follows: an initially permissive mass window of 100–70 ppm for internal calibration, 200 ppm for external calibration, allowing a single missing cleavage, modification of cysteines by iodoacetamide, methionine oxidation, and N-terminal pyroglutamylation as variable modifications. To ascertain unambiguous identification, each was carefully checked as previously described (Com et al. 2003).

RESULTS

Qualitative comparisons of proteins extracts obtained from *S. gracilis* and *E. siliculosus* using the five methods are displayed in Figure 1A. In *S. gracilis*, protein extraction was more effective using the phenol method (Method 4). However, the addition of a desalting step (Method 5) gave the best results in terms of quality and resolution of the proteins in one-dimensional SDS-PAGE gels (1-DE). Proteins extracted using this method were resolved into distinct bands from 200 to 19 kDa (Fig. 1A). Approximately 30 polypeptides appeared neatly identifiable over a pale background resulting from a low level of contaminants. In *E. siliculosus*, on the other hand, protein extraction was adequate with all the methods tested, and as with *S. gracilis*, more than 30 polypeptides appear clearly resolved in 1-DE (Fig. 1A).

Extracts using Method 1 yielded no spots in 2-DE from *S. gracilis*, and only a few were observed after ultracentrifugation was included in the protocol. These 2-DE patterns demonstrate the incapacity of the proteins to migrate into the gel and the high electrophoretical resistance (Fig. 1B). It is important to highlight that 2-DE was more effective in *E. siliculosus* than in *S. gracilis*. However, 2-DE patterns in the former showed higher background and band distortion, although proteins were well resolved in 1-DE. On the other hand, protein maps obtained for *S. gracilis* and *E. siliculosus* by 2-DE using the phenol method showed high levels of resolution and reproducibility (Fig. 2). Representative 2-DE protein patterns in the p*I* region of 3–10 showed

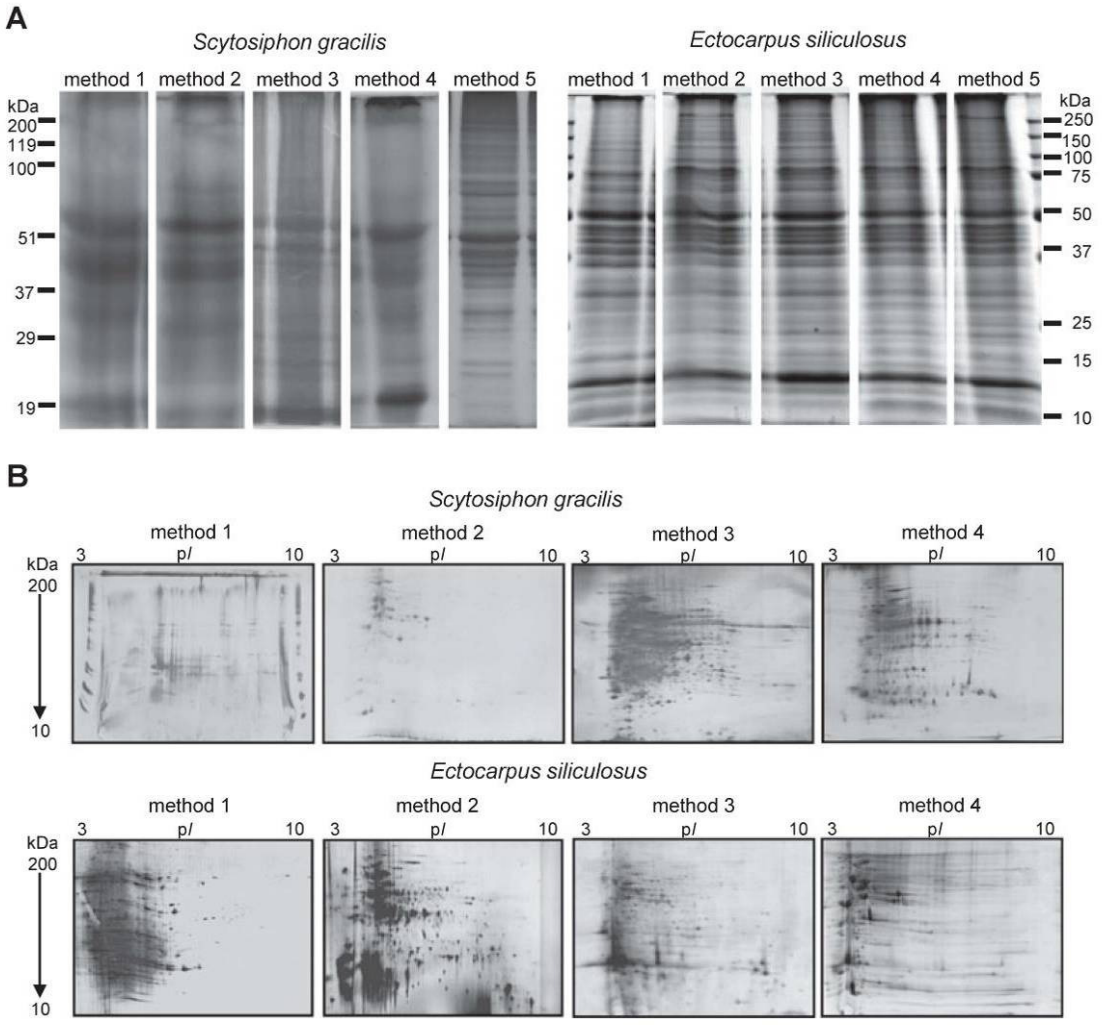

FIG. 1. (A) Representative SDS-PAGE gels of proteins (30 μg proteins) from *Scytosiphon gracilis* and *Ectocarpus siliculosus* extracted by method 1 (urea extraction and acetone precipitation), method 2 (urea extraction, ultracentrifugation, and acetone precipitation), method 3 (urea extraction, ultracentrifugation, and TCA/acetone precipitation), method 4 (phenol extraction), and method 5 (phenol extraction and desalting). (B) Representative 2-DE patterns of proteins from *S. gracilis* and *E. siliculosus* extracted using methods 1–4. The first dimension was done on linear gradient IPG strip of pH 3–10 using 500 μg of total proteins. The 12.5% SDS-PAGE gels were stained with colloidal Coomassie blue. Molecular masses of protein standards are indicated. IPG, immobilized pH gradient.

~1,100 protein spots for *S. gracilis* and *E. siliculosus* (Fig. 2A and B). Interestingly, at pH 4–7, well-resolved 2-DE protein patterns were also obtained (Fig. 2, C and D).

We selected 46 spots from *S. gracilis* and 150 from *E. siliculosus* corresponding to neutral, basic, and acidic proteins with high and low relative molecular mass (M_r) for identification by MS. Ten of the selected spots from *S. gracilis* and 14 of those from *E. siliculosus* matched with known proteins already present in available databases. The identified proteins are labeled on the gels (Fig. 2) and listed in Table 1. Their theoretical and experimental p*I*, M_r values, and matching amino acid sequences are also indicated. Using cross-species identification, only a small number of spots (12%) could be identified because of the limited genomic data available for these species. Of the identified proteins, ~54% were similar to plant and algal database entries. The identified proteins appeared to be involved in several primary metabolic pathways, including carbon fixation, protein

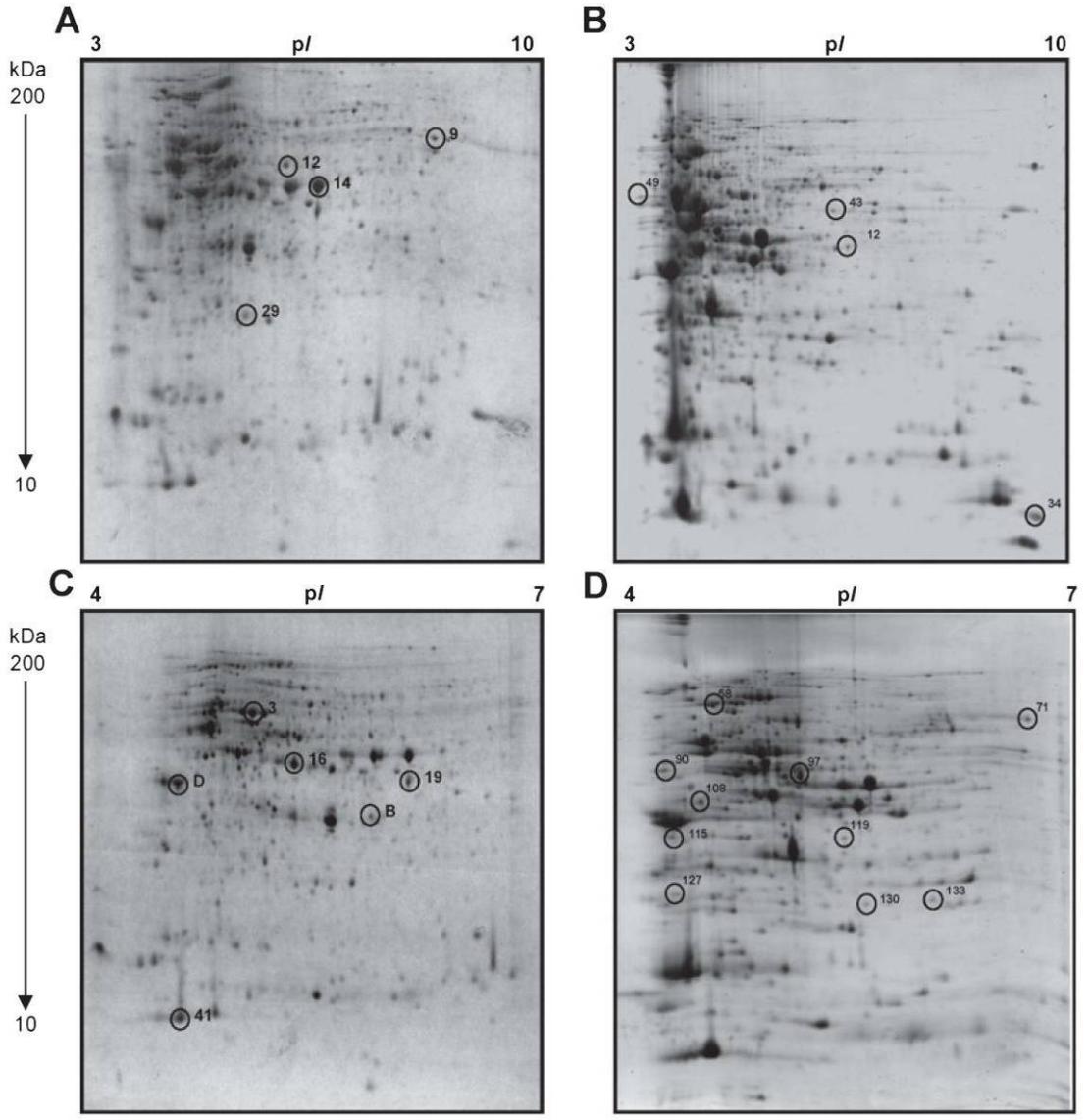

FIG. 2. Representative 2-DE patterns of proteins extracted from *Scytosiphon gracilis* (A, C) and *Ectocarpus siliculosus* (B, D) using the phenol method with desalting (Method 5). The first dimension was performed on a linear gradient IPG strip of pH 3–10 (A, B) and pH 4–7 (C, D) using 500 µg of total proteins. The 12.5% SDS-PAGE gels were stained with colloidal Coomassie blue. Molecular masses of protein standards are indicated on the left. Labeled spots designate the proteins identified by mass spectrometry (see Table 1). IPG, immobilized pH gradient.

synthesis, and oxidative phosphorylation. An additional analysis was performed with the selected spots of *E. siliculosus*, this time using an unpublished expressed sequence tag (EST) library from *E. siliculosus* containing >26,000 sequences. In this case, 85 sequences were identified for 65 distinct proteins (data not shown), including proteins involved in stress responses, such as glutathione-S-transferase and peroxiredoxins, and heat-shock proteins (protein folding).

DISCUSSION

Brown algae contain high levels of compounds that interfere with protein fractionation. These compounds, combined with proteins, lead to

TABLE 1. Results from mass spectra and database searching of different proteins from *Scytosiphon gracilis* and *Ectocarpus siliculosus*.

Spot[a]	Protein identification	Accession number (NCBI)	No. peptides[b]	Sequence coverage (%)[c]	Estimated M_r (kDa)	Observed/ theoretical p*I*
Scytosiphon gracilis						
3	Elongation factor TU [*Pylaiella littoralis*]	AAN62452	11	37	36	5.2/4.8
9	Actin [*Bangia fuscopurpurea*]	CAI56206	7	26	37	6.4/5.8
12	6-phosphogluconate deshydrogenase [*Porphyra yezoensis*]	AAL76325	4	18	43	5.6/5.4
14	Ribulose-1,5-bisphosphate carboxylase/ oxygensase LSU [*Himantothallus grandifolius*]	CAC67484	8	20	46	5.7/6.0
16	Elongation factor 1β gamma 1 [*Crithidia fasciculata*]	AAS55634	6	25	43	5.3/5.2
19	Phosphoglycerate kinase [*Euglena gracilis*]	AAU11484	6	20	39	5.5/5.7
29	Glycerol kinase [*Phytomonas* sp.]	AAF66150	6	48	25	5.4/5.3
41	Ribulose 1,5 bisphosphate carboxylase/ oxygenase SSU [*Scytosiphon gracilis*]	AAL47754	3	100	6	4.8/4.4
B	Inosine triphosphatase [*Griffithsia japonica*]	AAM93951	3	47	32	5.6/8.1
D	Indole-3-glycerol-phosphatesynthase [*Phaeodactylum tricornutum*]	AAL79536	5	32	37	4.8/5.4
Ectocarpus siliculosus						
12	CsgA Rossman fold oxidoreductase [*Polynucleobacter* sp. QLW-P1DMWA-1]	116269538	8	41	25	6.5/8.8
34	Unnamed protein product [*Paramecium tetraurelia*]	124427131	12	26	68	9.4/9.1
43	BP915190 [*Adiantum capillus-veneris*]	67224063	9	71	19	6.4/8.5
49	ATP synthase subunit beta [*Pylaiella littoralis*]	114561	16	40	52	4.4/5.0
58	Nesprin-3 isoform alpha [*Mus musculus*]	111607453	16	26	112	5.0/5.9
71	DB603843 [*Halocynthia roretzi*]	117743848	9	61	27	9.1/6.3
90	ATP-dependent DNA ligase [*Methanosarcina mazei*]	21228816	10	37	63	6.0/4.4
97	Actin [*Saccharina japonica*]	ABB02445.1	20	31	69	8.7/5.3
108	Hypothetical protein-fission yeast [*Schizosaccharomyces pombe*]	11359091	9	47	40	8.6/4.8
115	Peptidase U62 [*Nitrobacter winogradskyi* Nb-255]	75674420	13	34	50	5.7/4.5
119	Hypothetical protein Chro.60608 [*Cryptosporidium hominis* TU502]	67582251	5	100	5	5.9/5.6
127	Cullin, E3 ubiquitin ligase subunit [*Anopheles gambiae* str. PEST]	118783970	14	29	88	6.6/4.6
130	Diguanylate cyclase [*Geobacter lovleyi* SZ]	118746586	10	57	27	5.6/5.7
133	RGS family member [*Arabidopsis thaliana*]	9279616	9	35	35	6.0/6.2

[a]The number corresponds to the protein spots indicated in Figure 1 that were analyzed by mass spectrometry.
[b]Number of peptides matching the protein sequence.
[c]Percentage of the protein sequence covered by the matching peptides.

precipitation of insoluble polymers. In this context, the pattern of proteins obtained from tissues of *S. gracilis* extracted with urea and including ultracentrifugation and TCA/acetone treatments show high background, band distortion, and more importantly, very low protein dissolution. Using these methods, high molecular weight proteins of *S. gracilis* were lost during extraction, likely due to coprecipitation with polysaccharides and/or phenolic compounds as well as to the presence of cell membrane fragments. In addition, low molecular weight proteins were either not detected or when bands were observed, they appeared poorly defined. Even though the same protein concentration was used in the SDS-PAGEs, the intensity of the bands in the gels varied, likely due to underestimation of the real protein content in the extracts resulting from cross-reaction of the reagents of the protein assay kit with contaminants.

The low efficiency and poor quality of the *S. gracilis* protein extracts using these methods become evident in the 2-DE patterns. A possible explanation is that interfering charged polysaccharides and polyphenols, present in the protein extracts of *S. gracilis*, are much more abundant than in *E. siliculosus* simply because of the different structure of the thallus. Indeed, the thallus of *S. lomentaria* is complex and includes a cortical layer and a relatively thick medulla whose cells have bulky cell walls rich in polysaccharides. In contrast, *E. siliculosus* is a uniseriate filament. The phenol method including the cleaning step (Method 5) results in consistently high-quality protein extractions and electrophoresis runs in both species, conciliating suitable quality and reliability for 2-DE gels and its downstream analyses.

The advantage of using phenol as an extracting agent resides in its capacity to disrupt membranes,

leaving most of the water-soluble molecules in the aqueous phase. As a result, proteins in the phenol phase were efficiently purified and concentrated with the subsequent ammonium acetate/methanol precipitation. In addition, PVP was shown to be effective in chelating and precipitating existing polyphenolic compounds. Following these steps, the TCA/acetone precipitation permitted the removal of the remaining contaminants that copurified with proteins. Another advantage of the phenol extraction is that it minimized the degradation of proteins. We also demonstrated that initial desalting is of major importance to eliminate interference by inorganic compounds. The identification of several proteins in both species demonstrates the efficiency of the method and accounts for its suitability in identifying proteins involved in stress responses using differential 2D-PAGE. In fact, this method has already been successfully employed with *S. gracilis* extracts to monitor responses to copper stress (L. Contreras, unpublished observations). This method comes as an encouraging improvement, as brown algal protein identification is becoming an active field and since the entire genome of *E. siliculosus* is currently being sequenced and will be available during 2008. The viability of the genome will represent a major advance in the knowledge of multicellular Heterokonta and will facilitate protein identification through direct MALDI-MS profiling.

This work supported by Marine Genomics Chile (CONICYT) to J. A. C. and A. M., FONDAP 1501-0001 subprogram 7 from CONICYT and ICA to J. A. C. and by DICYT-USACH to A. M. This work is part of the NoE in Marine Genomics (Europe). Protein identification was done at the high-throughput proteomic platform of OUEST-genepole® (Rennes, France). Our thanks go to M. Vasquez for providing several 2-DE equipment and to M. Cock for providing access to the *E. siliculosus* EST database. This study was conducted within the framework of the Laboratoire International Associe Dispersal and Adaptation in Marine Species (DIAMS).

Beranova-Giorgianni, S. 2003. Proteome analysis by two dimensional gel electrophoresis and mass spectrometry: strengths and limitations. *Trends Anal. Chem.* 22:273–81.

Carpentier, S. C., Witters, E., Laukens, K., Deckers, P., Swennen, R. & Panis, B. 2005. Preparation of protein extracts from recalcitrant plant tissues: an evaluation of different methods for two-dimensional gel electrophoresis analysis. *Proteomics* 5:2497–507.

Chinnasamy, G. & Rampitsch, C. 2006. Efficient solubilization buffers for two-dimensional gel electrophoresis of acidic and basic proteins extracted from wheat seeds. *Biochem. Biophys. Acta* 1764:641–4.

Com, E., Evrard, B., Roepstorff, P., Aubry, F. & Pineau, C. 2003. New insights into the rat spermatogonial proteome: identification of 156 additional proteins. *Mol. Cell Proteomics* 2:248–61.

Contreras, L., Dennett, G., Palma, E., Moenne, A. & Correa, J. A. 2007. Molecular and morphologically distinct *Scytosiphon* species (Scytosiphonales, Phaeophyceae) display similar antioxidant capacities. *J. Phycol.* 43:1320–8.

Cremer, F. & Van de Walle, C. 1985. Method for extraction of proteins from green plant tissues for two-dimensional polyacrylamide gel electrophoresis. *Anal. Biochem.* 147:22–6.

Flengsrub, R. & Kobro, G. 1989. A method for two-dimensional electrophoresis of proteins from green plant tissues. *Anal. Biochem.* 177:33–6.

Förster, B., Mathesius, U. & Pogson, B. J. 2006. Comparative proteomics of high light stress in the model alga *Chlamydomonas reinhardtii*. *Proteomics* 6:4309–20.

Gygi, S. P., Corthals, G. L., Zhang, Y., Rochon, Y. & Aebersold, R. 2000. Evaluation of two-dimensional gel electrophoresis-based proteome analysis technology. *Proc. Natl. Acad. Sci. U. S. A.* 97:9390–5.

Hoffmeister, M., van der Klei, A., Rotte, C., van Grinsven, K. W. A., van Hellemond, J. J., Henze, K., Tielens, A. G. M. & Martin, W. 2004. *Euglena gracilis* rhodoquinone:ubiquinone ratio and mitochondrial proteome differ under aerobic and anaerobic conditions. *J. Biol. Chem.* 279:22422–9.

Jacobs, D. I., van Rijssen, M. S., van der Heijden, R. & Verpoorte, R. 2001. Sequential solubilization of proteins precipitated with trichloroacetic acid in acetone from cultured *Catharanthus roseus* cells yields 52% more spots after two-dimensional electrophoresis. *Proteomics* 1:1345–50.

Kim, Y. K., Yoo, W. I., Lee, S. H. & Lee, M. Y. 2005. Proteomic analysis of cadmium-induced protein profile alterations from marine alga *Nannochloropsis oculata*. *Ecotoxicology* 14:589–96.

Laemmli, U. K. 1970. Cleavage of structural proteins during the assembly of the head of bacteriophage T4. *Nature* 227:680–5.

Mechin, V., Consoli, L., Guilloux, M. L. & Damerval, C. 2003. An efficient solubilization buffer for plant proteins focused in IPGs. *Proteomics* 3:1299–302.

O'Farrell, P. H. 1975. High resolution two-dimensional electrophoresis of proteins. *J. Biol. Chem.* 250:4007–21.

Peters, A. F., Marie, D., Scornet, D., Kloareg, B. & Cock, J. M. 2004. Proposal of *Ectocarpus siliculosus* as a model organism for brown algal genetics and genomics. *J. Phycol.* 40:1079–88.

Rabilloud, T. 1996. Solubilization of proteins for electrophoretic analysis. *Electrophoresis* 17:813–29.

Saravanan, R. S. & Rose, J. K. C. 2004. A critical evaluation of sample extraction techniques for enhanced proteomic analysis of recalcitrant plant tissues. *Proteomics* 4:2522–32.

Starr, R. C. & Zeikus, J. A. 1993. UTEX-The culture collection of algae at the University of Texas at Austin. *J. Phycol.* 29(Suppl.):1–106.

Stauber, E. J., Fink, A., Markert, C., Kruse, O., Johanningmeier, U. & Hippler, M. 2003. Proteomics of *Chlamydomonas reinhardtii* light-harvesting proteins. *Eukaryot. Cell.* 2:978–94.

Unlu, M., Morgan, M. E. & Minden, J. S. 1997. Difference gel electrophoresis: a single gel method for detecting changes in protein extracts. *Electrophoresis* 18:2071–7.

Wang, S. B., Chen, F., Sommerfeld, M. & Hu, Q. 2004a. Proteomic analysis of molecular response to oxidative stress by the green alga *Haematococcus pluvialis* (Chlorophyceae). *Planta* 220:17–29.

Wang, S. B., Hu, H., Sommerfeld, M. & Chen, F. 2003a. An optimized protocol for isolation of soluble proteins from microalgae for two-dimensional gel electrophoresis analysis. *J. Appl. Phycol.* 15:485–96.

Wang, S. B., Hu, Q., Sommerfeld, M. & Chen, F. 2004b. Cell wall proteomics of the green alga *Haematococcus pluvialis* (Chlorophyceae). *Proteomics* 4:692–708.

Wang, W., Scali, M., Vignani, R., Spadofora, A., Sensi, E., Mazzuca, S. & Cresti, M. 2003b. Protein extraction for two-dimensional electrophoresis from olive leaf, a plant tissue containing high levels of interfering compounds. *Electrophoresis* 24:2369–75.

Wong, P. F., Tan, L.-J., Nawi, H. & AbuBakar, S. 2006. Proteomics of the red alga, *Gracilaria changii* (Gracilariales, Rhodophyta). *J. Phycol.* 42:113–20.

Yan, S., Zhang, Q., Tang, Z., Su, W. & Sun, W. 2006. Comparative proteomic analysis provides new insights into chilling stress responses in rice. *Mol. Cell. Proteomics* 5:484–96.

4.1 SUPPLEMENTARY MATERIAL

Following the development of a reliable protocol for 2-DE analysis in *E. siliculosus*, we have selected 150 spots in order to create a first proteome map for this species (Fig S1). Proteins spots were identified with the *Ectocarpus* EST database genomic resources accessible at http://www.sb-roscoff.fr/UMR7139/ectocarpus/transcriptomics/design.html and by public database searches. At this time the *Ectocarpus* EST database was not released. Therefore only proteins identified in public databases were presented in the published paper. On the other side, we have identified over 85 matched spots consisting in 63 fully identified proteins (Table S1-2). Among these results, we have found proteins from diverse metabolisms (Fig. S2), including stress related actors such as GSTs and HSP (Table S1-2). These results demonstrated that this technique was adapted for the identification of stress related mechanisms, which encouraged us to carry out 2-DE analysis upon copper stress in *Ectocarpus*.

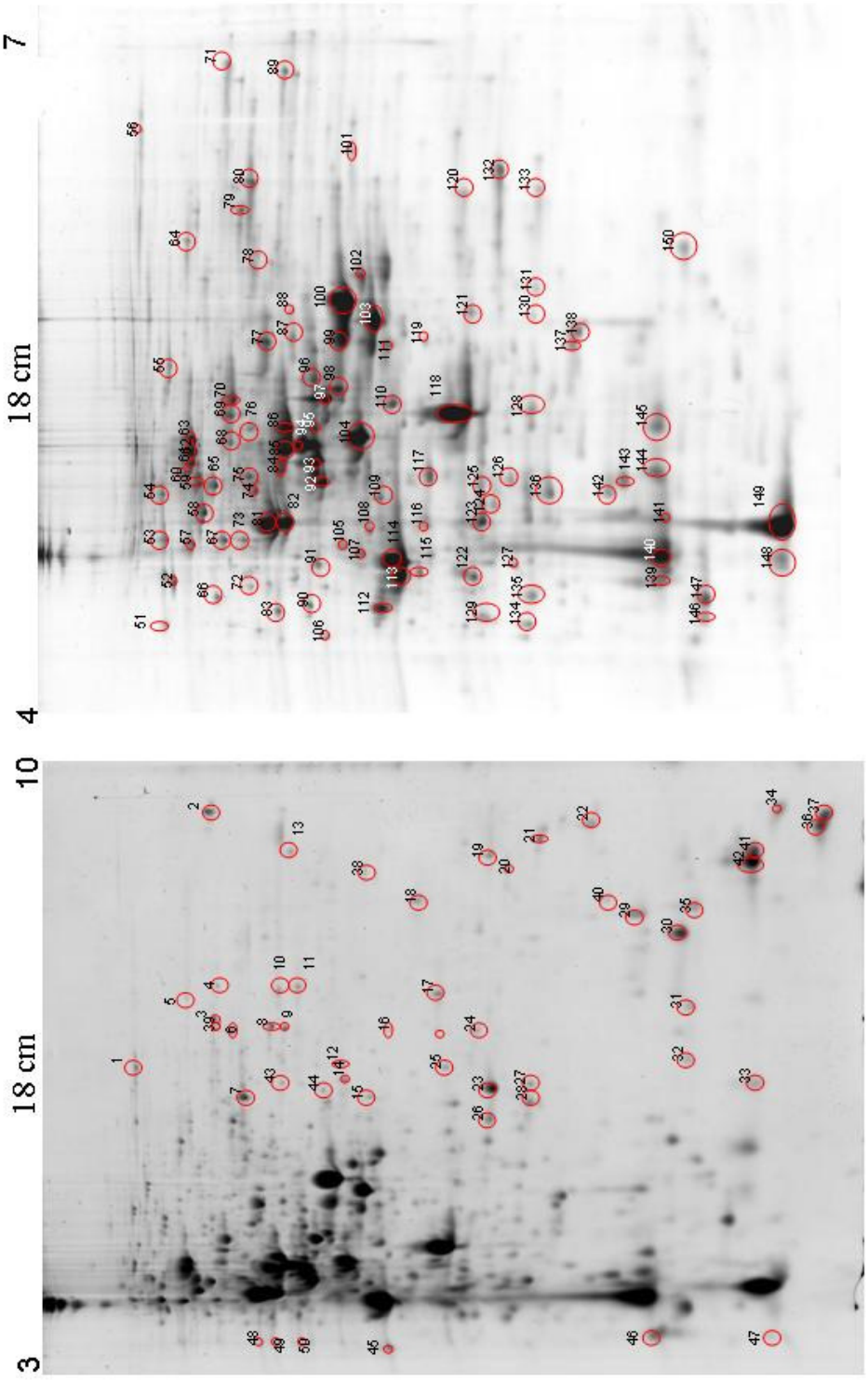

Figure S1. Representative 2-DE patterns of proteins extracted from *Ectocarpus siliculosus* using the phenol method with desalting (Method 5). The first dimension was performed on a linear gradient of pH 3–10 (A,) and pH 4–7 (B) using 500 µg of total proteins. The 12.5% SDS-PAGE gels were stained with colloidal Coomassie blue. Labelled spots designate the proteins identified by mass spectrometry (see Table S1) using *E. siliculosus* genomic livery.

Table S1. Results from mass spectra and *E. siliculosus* EST database searches of different proteins from *Ectocarpus siliculosus.* The number corresponds to the protein spots indicated in Figure S1 that were analyzed by mass spectrometry.

Spot	Protein identification	Accession Number (NCBI)	Number of peptides	Sequence coverage (%)	estimated Mw (Da)	Observed pI
1	translation elongation factor 2 [*Spodoptera exigua*]	AAL83698.1	22/60	21	128 292	7,82
6	glucose-6-phosphate 1-dehydrogenase [*Branchiostoma belcheri*]	BAD17954.1	12/48	37	49 320	8,59
7	Pyruvate kinase (PK) [*Eimeria tenella*]	AAC02529.1	24/49	43	72 842	7,57
8	hydroxymethyltransferase [*Arabidopsis thaliana*]	NP_193129.1	20/60	54	53 317	6,46
9	putative alanine aminotransferase [*Arabidopsis thaliana*]	NP_974122.1	12/44	58	28 389	8,29
11	chloroplast geranylgeranyl reductase/hydrogenase [*Isochrysis galbana*]	AAW79317.1	18/47	35	67 539	9,14
12	CsgA Rossman fold oxidoreductase [*Polynucleobacter sp.*]	116269538	8/50	41	25 357	8,81
15	similar to Nucleoside-diphosphate-sugar epimerases [*Trichodesmium erythraeum*]	EAO27596.1	20/59	40	47 174	7,29
17	receptor for activated protein kinase C [*Oreochromis mossambicus*]	AAQ91574.1	9/52	23	53 846	8,55
23	cytochrome c peroxidase, putative [*Aspergillus fumigatus Af293*]	XP_751914.1	15/66	39	47 519	8,94
25	Diacetyl/L-xylulose reductase [*Apis mellifera*]	XP_397008.1	10/53	30	42 493	7,57
28	Carbonic anhydrase [*Cytophaga hutchinsonii*]	ZP_00309906.1	17/46	27	77 018	6,84
34	unnamed protein product [Paramecium tetraurelia]	124427131	12/52	26	68 421	9,1
38	sperm associated antigen 1 [*Mus musculus*]	AAF06160.1	9/29	18	60 947	9,34
39	glucose-6-phosphate isomerase [*Phytophthora infestans*]	AAP51067.1	12/61	29	53 445	5,93
42	hypothetical protein CwatDRAFT_3021 [*Crocosphaera watsonii WH 8501*]	EAM49893.1	8/30	20	38 620	9,61
43	BP915190 [Adiantum capillus-veneris]	67224063	9/46	71	19 994	8,54
44	putative alanine aminotransferase [*Arabidopsis thaliana*]	AAK59635.1	8/45	40	27 277	8,92
49	ATP synthase subunit beta	114561	16/61	40	52 050	5,03
52	heat shock protein, putative [*Plasmodium falciparum 3D7*]	AAN37030.1	14/77	29	82 821	4.99
53	heat shock protein Hsp90 [*Achlya ambisexualis*]	AAM90675.1	26/83	33	94 458	5,54
54	elongation factor EfG [*Bartonella bacilliformis*]	AAL79907.1	12/76	70	21 146	4,96
57	glucose regulated protein /BiP [*Phytophthora cinnamomi*]	CAA53369.1	13/75	73	28 116	5,5
58	translation elongation factor 2 [*Spodoptera exigua*]	AAL83698.1	25/73	53	65 501	5.08
59	heat shock protein 70 [*Phytophthora nicotianae*]	AAR21577.1	21/79	45	69 830	5.13
60	glycolaldehydetransferase [*Dictyostelium discoideum*]	XP_644368.1	16/49	21	89 199	6,22
71	DB603843 [*Halocynthia roretzi*]	117743848	9/45	61	27 508	9,14
73	Glutathione S-Transferase family member (gst-11) [*Caenorhabditis elegans*]	AAA82318.1	6/38	37	26 055	11,27
74	protein disulfide isomerase [*Ancylostoma caninum*]	AAS84454.1	14/47	27	83 625	6,15
75	acetohydroxy acid reductoisomerase; ketol-acid reductoisomerase [*Spinacia oleracea*]	CAA40356	7/48	41	24 185	5,78
77	putative mitochondrial ATP synthase alpha subunit precursor [*Toxoptera citricida*]	AAU84946.1	16/48	28	76 015	9,23

Table S2. Results from mass spectra and *E. siliculosus* EST database searches of different proteins from *Ectocarpus siliculosus.* The number corresponds to the protein spots indicated in Figure S1 that were analyzed by mass spectrometry.

Spot	Protein identification	Accession Number (NCBI)	Number of peptides	Sequence coverage (%)	estimated Mw (Da)	Observed pI
82	ATP synthase beta chain, mitochondrial precursor [*Cyprinus carpio*]	BAA82837.1	21/50	59	43 496	5,08
83	Calreticulin precursor [*Prunus armeniaca*]	AAD32207.1	11/41	22	76 627	4,97
84	6-phosphogluconate dehydrogenase [*Laminaria digitata*]	CAB61332.1	13/77	24	75 503	5.27
85	ATP synthase subunit beta [*pylaiella littoralis*]	114561	22/58	47	52 050	5,03
89	hydroxymethyltransferase [*Arabidopsis thaliana*]	AAM16248.1	17/63	45	53 317	6,46
90	ATP-dependent DNA ligase [Methanosarcina mazei]	21228816	10/52	37	63 316	6.08
92	phosphoribulokinase precursor [*Spinacia oleracea*]	AAA34036.1	9/53	35	38 991	6,6
93	phosphoglycerate kinase [*Laminaria digitata*]	CAB61334.1	9/40	44	31 550	8,98
94	glutamine synthetase [*Phytophthora infestans*]	AAN31463.1	24/66	35	57 361	7,97
96	glutamate 1-semialdehyde 2,1-aminomutase [*Bigelowiella natans*]	AAP79194.1	12/70	36	38 991	5.36
97	actin [*Saccharina japonica*]	ABB02445.1	20/59	31	69 737	8.78
98	Myo-inositol 2-dehydrogenase [*Solibacter usitatus*]	EAM54088.1	26/80	39	58 442	8.57
99	glyceraldehyde-3-phosphate dehydrogenase isoform 2 [*Gonyaulax polyedra*]	AAD01871.1	18/50	25	73 735	9,16
102	glyceraldehyde-3-phosphate dehydrogenase [*Achlya bisexualis*]	AAF44719.1	22/63	58	52 946	8,05
103	chloroplast ferredoxin NADP(+) reductase [*Isochrysis galbana*]	AAW79315.1	14/41	21	71 772	9,37
104	putative aldolase [*Arabidopsis thaliana*]	AAG40366.1	9/40	30	66 245	8,74
108	Hypothetical protein [*Schizosaccharomyces pombe*]	11359091	9/43	47	40 889	8,67
111	coproporphyrinogen III oxidase precursor [*Chlamydomonas reinhardtii*]	AAD28474.1	16/75	20	80 522	8,7
112	sedoheptulose-1,7-bisphosphatase precursor [*Oryza sativa*]	AAO22558.1	17/46	34	59 867	6,05
115	peptidase U62 [*Nitrobacter winogradskyi*]	75674420	13/65	34	50 719	5,72
118	oxygen-evolving enhancer 1 [*Heterosigma akashiwo*]	AAN11311.1	14/40	26	64 528	9,08
119	hypothetical protein Chro.60608 [*Cryptosporidium hominis*]	67582251	5/55	100	5 012	5,98
120	similar to Diacetyl/L-xylulose reductase [*Apis mellifera*]	XP_397008.1	10/55	34	42 493	7,57
125	cyclophilin [*Cucumis sativus*]	AAX94775.1	12/65	40	43 573	6,24
127	ENSANGP00000011815 [*Anopheles gambiae*]	118783970	14/54	29	88 895	6,67
129	14-3-3 [*Fucus vesiculosus*]	1433_FUCVE	16/63	33	53 747	5,15
130	diguanylate cyclase [*Geobacter lovleyi*]	118746586	10/52	57	27 126	5,69
132	cytochrome c peroxidase, putative [*Aspergillus fumigatus*]	XP_751914.1	16/73	40	47 519	8,94
133	hypothetical protein [*Neurospora crassa*]	EAA30440.1	20/56	31	77 018	6.84
136	ribulose-phosphate 3-epimerase (pentose-5 phosphate 3-epimerase) (PPE) (R5P3E) [*Photorhabdus luminescens*]	CAE12381.1	10/40	37	39 687	6,23
146	Alkyl hydroperoxide reductase/ Thiol specific antioxidant/ Mal allergen [*Sphingopyxis alaskensis*]	EAN45705.1	13/55	35	37 455	7,12
150	Description: Nucleoside diphosphate kinase 1 (Nucleoside diphosphate kinase I) (NDK I) (NDP kinase I) (NDPK I) (PP18) [*Saccharum officinarum*]	AAB40609.1	12/43	30	39 186	9,46

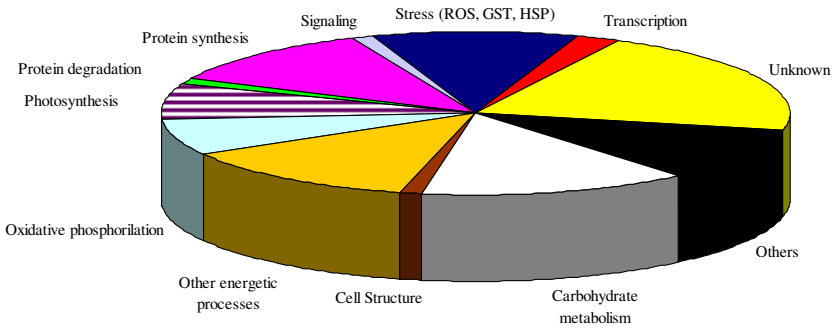

Figure S2. Graphic representation of the systematic protein identification in *E. siliculosus*. Proteins are sorted by their metabolic classes

5 COPPER STRESS PROTEOMICS HIGHLIGHTS LOCAL ADAPTATION OF TWO STRAINS OF THE MODEL BROWN ALGA *Ectocarpus siliculosus*

To be submitted to Proteomics

Andrés Ritter[1-2-4], Martin Ubertini[1-2], Sarah Romac[3], Fanny Gaillard[3], Ludovic Delage[1-2], Jessica Beltran[4], Aaron Mann[4], Thierry Tonon[1-2], Juan A. Correa[4] and Philippe Potin[1-2*]

[1] *UPMC Univ Paris 6, UMR 7139 Végétaux Marins et Biomolécules, Station Biologique, Place Georges Teissier, BP74, F 29682, Roscoff, France.*

[2] *CNRS, UMR 7139 Végétaux Marins et Biomolécules, Station Biologique, Place Georges Teissier, BP74, F 29682, Roscoff, France.*

[3] *Computer and Genomics resource Centre, FR 2424, Station Biologique, Place Georges Teissier, BP74, F 29682 Roscoff, France.*

[4] *Center for Advanced Studies in Ecology & Biodiversity, Departamento de Ecología, Facultad de Ciencias Biológicas, Pontificia Universidad Católica de Chile, Santiago, Chile.*

Abstract

Ectocarpus siliculosus is a cosmopolitan brown alga with a capacity to thrive in copper-enriched environments. In this study, we have characterized through physiological approaches two strains of *E. siliculosus* isolated from i) an uncontaminated coast in southern Peru (strain Es32) and ii) a copper polluted beach in northern Chile (strain Es524). Analysis of copper toxicity in both strains indicated that Es32 was more sensitive than Es524, with toxicity detected at 50 µg/L Cu, whereas Es524 displayed negative effects of copper excess only when exposed to 250 µg/L Cu. Differential soluble proteome profiling between control and copper stress conditions for each strain allowed to identify the induction of proteins related to processes such as energy production, glutathione

metabolism, phenolics biosynthesis and HSPs (Heat Shock Proteins) accumulation. In addition, the inter-strain comparison of stress related proteomes led to identify features related to copper tolerance in Es524. This strain presented a striking expression of the PSII Mn-stabilising protein and Fucoxanthine cholophyll a-c binding protein. In addition, Es524 expressed specific stress-related enzymes such as RNA helicases from the DEAD box families involved in RNA folding and maturation, and a vanadium dependent bromoperoxidase. These observations were supported by RT-qPCR analysis and enzyme activity assays. Therefore, two different phenotypes at proteomic level strongly suggest that persistent copper stress may have driven selective force leading to the development of strains genetically adapted to copper contaminated sites.

* Corresponding author e-mail: potin@sb-roscoff.fr; fax 33-2-98292324.

Keywords: Algae / Stress / Heavy metal / 2-DE / Bromoperoxidase

Abreviations: afc% percentage of autofluorescent cells; **LC_{50}**, median (50%) lethal concentration; **LHC**, Light Harvesting Complex; **OEC**, Oxygen Evolving Complex

5.1 Introduction

The release of heavy metals, including copper, by a wide range of human activities, remains a major threat for marine ecosystems, impacting benthic flora and fauna assemblages [1-3]. Copper is a vital micronutrient essential for all forms of life, acting as cofactor for many enzymatic systems and participating in crucial physiological processes including photosynthesis and respiration. However, copper is extremely toxic at high concentrations, particularly affecting photosynthetic organisms which suffer effects on chlorophyll structure, synthesis and function, on fatty acid metabolism, and on carbohydrate synthesis [4-6]. In addition, copper can catalyze the synthesis of the highly reactive hydroxyl radical in presence of H_2O_2 via the Fenton reaction, a process that causes oxidative stress [7-8].

Some local geographic areas that have been chronic recipients of heavy metal containing wastes (i.e. mine wastes) constitute a persistent stressful environment that acts as a selective force leading, in some cases, to the generation of tolerant strains genetically adapted [9-11]. In northern Chile, copper mine wastes discharges were, for almost seventy years, a major and only source of coastal pollution at Chañaral bay and surroundings, where local disturbances included the creation of large tailing beaches and the disappearance of most of the seaweeds and invertebrates [1-12]. The process of biological recovery, expected to follow after tighter legislation were implemented, and after the building of a sedimentation dam close to the mine operations, is far from being complete and many key ecological species, such as the brown kelp *Lessonia nigrescens* [12], are still absent. Among the few species recorded in this area, the filamentous brown alga *Ectocarpus siliculosus* is a persistent inhabitant, thriving in tide pools [12]. Early studies on *E. siliculosus* have identified copper tolerant populations, isolated from the hulls of ships treated with copper-based antifouling paints [13-16]. Although copper exclusion mechanisms were proposed for explaining this differential tolerance, analytical methods did not allow identifying genetically distinct population traits and/or characterizing the molecular bases leading to this differential tolerance. Nowadays,

major advances have been made in vascular plants towards understanding copper homeostasis and tolerance [17-19]. Vascular plants have evolved a number of general detoxification mechanisms, the best known of them being complexation by strong ligands such as phytochelatins (PCs) and metallothioneins (MTs) [20]. Other plant chelating mechanisms employ organic acids such as histidine, proline or nicotianamine [18-19-21]. Active metal exclusion mediated by P-type ATPases may also act for detoxification of copper in *Arabidopsi*s [22]. Compared to the large body of literature available for vascular plants, much less is known about the mechanisms responsible for copper detoxification in brown algae. In the genus *Fucus,* MTs and PCs are induced by copper excess [23-24]. Phenolic compounds have also been proposed as metal chelators, however results seem to be contradictory among species [25-28]. In addition, charged sulphated polysaccharides of the cell wall could play an important role acting as primary ion filter of algal cells [26-29]. Once inside the cell, it is well documented that metals in general, and copper in particular, activate antioxidant mechanisms in seaweeds [30-31]. Moreover, Cu-induced ROS production in brown algae seems to trigger oxylipin signaling pathways that could be related to detoxification mechanisms [32]. Brown algae (Class Phaeophyceae) belong to the Division Heterokonta, which evolved as an independent lineage more than a billion years ago [33]. Based on their particular evolutionary history, it is likely that original physiological mechanisms have evolved in these organisms in order to adapt to the various and highly fluctuating habitats they colonize. Consistent with this, a recent study underlined a unique antioxidant system based on iodide metabolism in the kelp *Laminaria digitata* [34]. Because of this particular evolutionary history, a consortium of laboratories initiated a project to sequence the genome of *Ectocarpus siliculosus* in 2004, which is currently being annotated (Cock et al., 2009; http://www.genoscope.cns.fr/externe/English/Projets/). The pertinence of using *E. siliculosus* as a metallophyte, its easy handling in the laboratory, and the current efforts to developing this species

as a model organism for Phaeophyceae [35], make it an attractive candidate for studying metal tolerance through global approaches such as proteomics.

At the proteomic level, whereas several studies on plant responses to heavy metal stress exist, they are mostly restricted to the exposure to arsenic, cadmium, and zinc [36-37]. Fewer studies on this domain concern copper stress. Some proteomic studies have focused on GST family regulation caused by copper excess [38], and the copper-binding proteins of *Arabidopsis* roots and seedlings have been explored by IMAC-MS [39]. Recently, the molecular effects of copper on the root proteome of *Cannabis sativa* was investigated by 2-DE based analysis [40]. At the present time no meaningful proteomic study does exist in marine algae. This was probably due to the fact that until recently no adequate technique for obtaining high quality protein extracts was available for these organisms [41]. In this work, copper tolerance of two *E. siliculosus* strains, originating from habitats with contrasting histories of copper levels, was analyzed by a comparative 2-DE proteomic approach. Differentially expressed protein patterns were compared within and between the two strains to better identify several cellular processes potentially involved in copper stress response and tolerance.

5.2 Materials and Methods

5.2.1 Plant material and cultivation treatments

E. siliculosus (Ectocarpales, Phaeophyceae) unialgal strains 32 (CCAP accession 1310/4, origin San Juan de Marcona, Peru 15°22'S, 75°10'W) and 524 (origin Caleta Palito, Chile 26°15'S, 70°40'W) were cultivated in 10 L plastic flasks in a culture room at 14 °C using 0.22 µm filtered seawater enriched in Provasoli nutrients [42]. Light was provided by Philips daylight fluorescence tubes at a photon flux density of 40 µmol m^{-2} s^{-1} for 14 h per day. Cultures were aerated with filtered (0.22 µm) compressed air to avoid CO_2 depletion.

Two days before exposing the algae to copper excess experiments, tissues were transferred into 1 L of seawater free of organic matter prepared with 0.22 µm filtered natural SW treated overnight with 0.2 g/L activated charcoal (Merk, Germany). Treated water was then filtered at 0.45 µm to remove charcoal excess. Culture flasks used during the experiments were washed overnight with 1 % HCl to limit copper adsorption by glass. Copper stress was triggered by changing the algae to fresh seawater free of organic matter and enriched with $CuCl_2$ (Merk, Germany) at nominal final concentrations of 50, 150, 250 and 500 µg/L. The term "acute stress" was employed for high copper concentrations exposure (250-500 µg/L) during reduced amounts of time (4-8 h). On the other side, chronic stress defines the exposure to lower sub-lethal copper concentrations (50-150 µg/L) during long periods of time (6-10 days). No nutrients were added during the experiment. For each kinetic point, three replicate algal samples were harvested. At the end of the experiment, thalli were frozen in liquid nitrogen and kept at -80 °C for analysis.

5.2.2 Copper toxicity bioassay

Individual *E. siliculosus* filaments of ~ 0.2 mm were transferred into separate dishes containing 5 mL of seawater enriched with copper. The concentrations tested were 0, 20, 25, 32, 40, 50, 65, 80, 100, 200, 500, and 1000 µg/L of nominal copper during 10 days. The medium was

changed every 2 days to prevent changes in the concentrations of the metal during the experiment. Then, filaments were transferred into 0.22 µm filtered seawater during 1 week, period after which mortality was estimated by microscopic observation. Filaments (n= 10 for each copper concentration) were classified as dead when all cells were bleached, or alive when pigmented cells appeared normally distributed along the plants.

5.2.3 *In vivo* fluorescence measurements and observations

To monitor the intensity of the stress in the algal tissues caused by the copper treatments we measured the quantum yield, a fluorometric marker for photosynthesis efficiency, using a Walz Phyto-PAM (Waltz, Germany) and default parameters (actinic light intensity 3, saturation pulse intensity 10 for 200ms) before harvesting the cultures for subsequent analysis. Since photosynthesis is stress sensitive, the quantum yield decreased under sub-optimal (stressful) conditions. Simultaneously to PAM measurements, chloroplasts autofluorescence was monitored using an Olympus BX60 (Olympus, Japan) epifluorescence microscope and images were obtained using a digital camera (DIAGNOSTIC instruments model 2.1.1). The number of fluorescent cells was estimated and represented as % of fluorescent cells.

5.2.4 Protein extraction and 2-DE separation

Global soluble proteome extraction followed the protocol developed by Contreras et al. [41]. The total protein concentration was assayed by the use of the 2-D quant kit (GE Healthcare, USA). For each replicate, 500 µg of total protein extract was loaded into a 17 cm non linear ReadyStrip pH range 4-7 (Biorad, USA). The 2-DE proteome separation and gel staining was carried out as described elsewhere [41].

5.2.5 Image analysis

Gel images were obtained using an Image scanner UMAX Powerlook III (UMAX Technologies, USA) at 300 dpi resolution and the analyses were done with the Melanie version 5.0

software (Swiss Institute of Bioinformatics, Switzerland). After automated detection and matching, manual editing and normalization were done. Spot quantification was based on spot volume (integration of spot density over spot area) as percentage of the total spot volumes of the gel to normalize for possible staining differences between gels. Gel annotations and matching fidelity were checked manually to eliminate matching errors caused by the software. Three gels representing independent biological samples were analyzed for each condition.

5.2.6 Protein Mass Fingerprints (PMF)

Coomassie blue-stained protein-bearing gel slices were cut into small pieces, washed with distilled water, and de-stained with acetonitrile. The cysteine residues were reduced by 100 µL of 10 mM DTT at 56°C and alkylated by 150 µL of 55 mM iodoacetamide at room temperature. The iodoacetamide solution was replaced by 100 µL of 100 mM NH_4HCO_3 and gel dehydration was achieved with acetonitrile. After evaporation in Speed-Vac (Thermo, USA), proteins were digested overnight at 37°C in a solution containing 0.9 µg of a modified bovine trypsin sequencing grade (Roche, Germany) prepared in 25 mM NH_4HCO_3. Finally, a double extraction was done, first with 5% (v/v) formic acid solution and subsequently with 100% (v/v) acetonitrile. The resulting peptide mixture was extracted and dried under vacuum, re-suspended in 1% formic acid solution and desalted using a ZipTipTM (Millipore, USA) C-18 reverse phase micro column. After evaporation, the desalted peptide mixture was re-suspended in 10 µl of 1% formic acid solution. PMF by MALDI-TOF MS was performed using a Voyager DE-STR MALDI-TOF mass spectrometer (Applied Biosystems, USA). One µL of tryptic digest was mixed with an equal volume of CHCA matrix (Sigma; 10 mg/L in 50% ACN, 0.1% TFA) and spotted onto the MALDI target. Spectra were acquired in positive ion reflector mode under 20 kV accelerating voltage and a mass range of 800–4000 Da. Internal calibration was performed using trypsin autolysis fragments at *m/z* 1433.70, 2163.05, and 2289.1. The monoisotopic masses of tryptic peptides were used to query NCBI nucleotide and amino acid sequences non redundant databases, specific *Ectocarpus siliculosus*

EST collection (contigs and singletons accessible at http://www.sb-roscoff.fr/UMR7139/ectocarpus/transcriptomics/design.html, Dittami *et al.* submitted) and the proteins deduced from the genome sequence (version 1 of the genome accessible at http://bioinformatics.psb.ugent.be/webtools/bogas) using Mascot version 2.1. Search conditions were as follow: an initially permissive mass window of 200 ppm for external calibration, then 100-50 ppm was applied for internal calibration with trypsin autodigestion fragments, allowing double missing cleavage, modification of cysteines by iodoacetamide, methionine oxidation and N-terminal pyroglutamylation as variable modifications.

5.2.7 RNA extraction and RT-qPCR analysis

The RNA extraction, quantification, cDNA synthesis and RT-qPCR reactions followed the protocol described by Le Bail et al. [43]. For each gene, a specific pair of oligonucleotide sequences in the 3' coding sequence (Table S1) was designed using Beacon designer 5.00 (Premier biosoft international, USA). The qPCR reactions were done in a Chromo4 apparatus (Biorad, USA) with a SYBR Green reaction mix AB-1162/B from ABgene (ABgene, UK). A dilution series ranging from 91 to 121312 copies of the *E. siliculosus* genome was prepared. The Dynein gene was used as internal control as previously described [43]. The relative variations in gene expression were calculated as *x*-fold changes to the appropriate control treatments.

5.2.8 Bromoperoxidase activity assay

Total protein extracts were obtained from of 0.2-0.5g of fresh weight tissue, grounded in liquid nitrogen and mixed with 0.4 mL of extraction buffer containing 25 mM MOPS pH 7.2, 15 mM $MgCl_2$, 15 mM EGTA, 1 mM DTT, 0.5 % PVP and antiproteases cocktail at a concentration specified by the manufacturer (Roche, France). Extracts were homogenized for 1 h at 4 °C, centrifuged at 10,000 *g* for 30 min and the supernatant collected. Vanadate was added to the extracts at 1 mM final concentration, followed by an incubation at 4° for at least 1 h prior to the

analysis. The total amount of proteins were quantified using the Bradford assay [44], and 20 µg were loaded on the gel. Bromoperoxidase enzymatic assays were conducted on non-denaturing gels as described by Colin et al. [45]. The activity levels using band density in the gels were assessed by the ImageQuant v5.2 software (Molecular Dynamics, GE Healthcare, USA). The relative changes among conditions were calculated as Volume Intensity and quantified in arbitrary units (AU).

5.2.9 Statistical analysis

Statistically significant differences among treatments were determined by the non-parametric Mann-Whitney U test run on Statistica version 5.1 software (StatSoft, USA). All conclusions are based on at least 5% level of significance ($P<0.05$).

5.3 Results

5.3.1 Copper toxicity tests in strains Es32 and Es524

The toxicity of copper was assessed in the two strains by observations of chlorophyll autofluorescence monitored by epifluorescence microscopy coupled with mortality assays. The dose-response relationships between Cu concentrations and mortality differed between strains after 10 days of exposure to copper excess (Table 1). LC_{50} for Es32 was 50 µg/L whereas for Es524 it was higher than 200 µg/L. Images presented in Fig. 1A show clearly a dramatic loss of fluorescence in numerous cells of strain Es32 after 10 days of exposure to 250 µg/L Cu. In comparison, Es524 displayed a higher proportion of autofluorescent cells at the same copper concentration. Cell counting in Es32 revealed a dose-response relationship between copper concentrations and the number of cells loosing chlorophyll red fluorescence (Fig. 1B). After 1 day of exposure, significant differences ($P<0.05$) were observed for this strain at 250 and 500 µg/L. After 2 days of exposure, all concentrations triggered a significant decline in the percentage of chlorophyll autofluorescent cells (%afc). Finally, 10 days of exposure caused chlorophyll damage in a proportion of cells higher than 50% for thalli exposed at 50 µg/L, 75% at 250 µg/L and 90% at 500 µg/L. On the other hand, strain Es524 showed no significant differences in %afc up to 150 µg/L. After 10 days, the values of %afc decreased by 25 % and 90 % in presence of 250 µg/L and 500 µg/L of copper, respectively. In agreement with these observations, photosynthetic yields (Fv/Fm) of both strains were negatively affected by Cu excess (Fig. 1C). After 10 days, a significant decline in the yield was observed in strain Es32 when copper concentration was higher than 50 µg/L, with Fv/Fm decreasing in a dose-dependent manner. After the same time of incubation, Es524 displayed significant changes in Fv/Fm only for Cu concentrations higher than 150 µg/L. Like in Es32, a significant decrease in Fv/Fm was observed in a dose dependent manner

from 250 µg/L on. These results allowed to select the best concentrations to expose each isolate to non-lethal conditions of copper stress, required for differential soluble proteome analyses.

5.3.2 Analyses of the proteins induced by chronic copper stress in Es32

To identify proteins specifically regulated under chronic copper stress conditions, the most sensitive strain (Es32) was exposed to 10 days at 50 µg/L nominal Cu. The 2-DE profiles of soluble proteome fractions were compared between control and treated thalli. Coomassie blue staining provided an average yield of 790 spots per gel (Fig. S1). Image analysis of the gels produced over 560 reproducible spot groups considering the two experimental conditions (Fig. 2A), with 58 statistically variable spots (fold–change > 1.5). Among these spots, 3 down-regulated and 16 up-regulated proteins were selected for MS identification because they presented enough intensity to be located and excised manually (Fig. 2A). PMF spot identifications are described in Table 2. For most of the identified spots, the 2-DE observed molecular mass and pI values are in agreement with the theoretical values obtained from the corresponding protein hits in the genomic database. Among the identified enzymes, a transketolase (TKT) and an enoyl-CoA hydratase (ECH) belong to energy metabolism. The cell wall polysaccharide biosynthesis enzyme, mannose-6-phosphate isomerase (ManA), was up-regulated. Several enzymes involved in amino acid metabolism were also identified. Two nitrogen related enzymes, glutamine synthase (GS) and glutamate synthase (GOGAT) were up-regulated in thalli exposed to copper excess. In addition, Cu enhanced the accumulation of serine hydroxymethyl transferase (SHMT) and cysteine synthase, involved in the biosynthesis of glycine and cystein respectively. Related to this, the nucleotide metabolism enzyme S-adenosylmethionine synthetase (SAM) was also increased. Protein folding and turnover processes were induced as well by copper since proteins corresponding to a HSP10 and the proteasome subunit alpha were more abundant in stressed individuals. Finally, whereas the chaperones Metacaspase (MC) and Calreticulin (CALR) were

down-regulated by copper excess, the phenolics- related aryl sulfotransferase accumulated in response to the metal.

5.3.3 Analyses of the proteins induced by chronic copper stress in Es524

The tolerant strain Es524 was exposed during 10 days to 50 µg/L and 150 µg/L of copper. Protein extracts from Es524 were analyzed with identical criteria as for Es32. The analysis of gel images obtained under the control condition and after treatment with 50 µg/L yield over 423 matched spot groups. Spot intensity analysis showed 32 differentially expressed spots (fold–change > 1.5). Among these spots, 20 were up-regulated and 12 down-regulated. On the other hand, comparisons of control thalli with those exposed to 150 µg/L of copper produced 494 reproducible groups, from which 58 presented significant changes (Fig. 2B). For PMF, a first group of 6 spots corresponding to proteins accumulated under both treatments with copper excess was considered (639, 734, 745, 941, 1174, and 1176). Then a second group was selected with 9 spots only regulated by exposure at 150 µg/L, corresponding to 8 proteins up-regulated (814, 897, 1192, 584, 1089, 1167, 768 and 1184) and 1 down-regulated (1252). PMF results are presented in Table 3. One enzyme involved in energy metabolism, ECH, was identified. The enhancement of a potential C18 fatty acid desaturase accounted for the activation of lipid metabolism. As for Es32, copper excess caused differential expression of amino acid biosynthesis and nucleotide metabolism related enzymes. Metal excess triggered the enhancement of a GS and a glutaminyl-tRNA synthetase (GlnS). The SAM showed an up-regulation as well. The two protein folding chaperones HSP70 and HSP40 were also markedly increased by copper excess. Copper caused accumulation of the same aryl sulfotransferase than the one identified in stressed Esi32. Interestingly, among the new spots up-regulated in Es524, we found some proteins related to the cell rescue process, i.e. two RNA helicases from the DEAD box family. In addition, one specific brown algal antioxidant related enzyme, the vanadium dependent Bromoperoxidase (vBPO), was also identified in this set of proteins.

5.3.4 Inter-strain differences in protein expression caused by copper excess

Finally, patterns of proteome expression were compared between Es32 and Es524 exposed to 50 µg/L of copper after 10 days. Over 406 spots matched on reproducible groups between both strains, whereas 93 proteins were differentially expressed at a fold-change higher than 2 (Fig. 2C). From these, in Es524, we selected 11 markedly increased and 2 decreased spots with respect to Es32 and subsequently identified them (PMF identification in Table 4). Two spots, corresponding to the same locus Esi0002_0327 encoding for a potential TKT, showed contrasting regulation in the two strains: increased in Es524 and decreased in Es32. Several energy-related enzymes are markedly increased in Es524: a phosphoribulokinase (PKK), a glyceraldehyde-3-phosphate dehydrogenase (GAPD), and a fructose 1,6-bisphosphate aldolase (SMALDO). Concerning the amino acid metabolism, a GS (different from the GS up-regulated in Es32) was highly increased in Es524. Photosynthesis-related processes were also stimulated in Es524. For instance, The PSII Mn-stabilizing protein of the oxygen evolving complex (OEC33) was over-expressed in Es524, whereas in Es32 it was not detectable. Similar results were obtained for the light harvesting complex protein Fucoxanthine cholophyll a-c binding protein B (Fcp).

5.3.5 Expression analysis of selected key genes by RT-qPCR under acute and chronic stress conditions

Four genes, encoding proteins identified through proteomic analyses, *vBPO*, *HSP70*, *HSP10* and *SAM,* were chosen for RT-qPCR experiments in order to compare changes in their level of expression during acute and chronic stress. Algal cultures were exposed to acute copper stress consisting in 250 µg/L and 500 µg/L and harvested after 4h and 8h of treatment. For chronic copper stress, final concentrations of 50 and 150 µg/L of Cu were applied for 6 and 10 days. Interestingly, *vBPO* is the gene whose expression levels were the most altered under stress. Its expression was induced under all the tested conditions in both strains, and more specifically, this gene was the most up-regulated under chronic stress. Accumulation of *HSP70* transcripts was

observed under all acute stress conditions in Es32 and Es524. However, during chronic stress, the transcription of this gene was up-regulated only in Es524 at 150 µg/L after 10 days. Significant changes in HSP10 gene expression were monitored only under acute stress, mainly in Es32. Slight induction of this gene was observed after incubation of Es524 for 4h in presence of 250 µg/L copper. SAM gene was down-regulated in most of the conditions tested.

5.3.6 Bromoperoxidase activity assay

In order to assess the importance of vBPO in the regulation of the oxidative stress created by Cu in Es32 and Es524, changes in enzymatic activity were followed on native PAGE gels. No visible activity was detected in Es32 under the control condition (Fig. 4A), while an intense band appeared under stress conditions, with an estimated molecular mass of ~140 KDa. The band intensity quantification showed an increase to 4E+6 AU in stressed Es32 (Fig. 4B). Protein extract from Es524 incubated in absence of copper showed only a slight coloration, indicating a low basal bromoperoxidase activity (Fig. 4C-D). After treatment with 50 or 150 µg/L, a band similar to that observed in extracts from stressed Es32 was identified, demonstrating an increase in bromoperoxidase activity. The quantification of the signal of this band was estimated at 3E+6 AU on all individuals and for both copper treatments. Similar results were obtained when replacing potassium bromide by potassium iodide during the revelation of the gels, indicating that the protein identified in *E. siliculosus* exhibit a true vBPO activity (data not shown).

5.4 Discussion

Studies of differential protein expression mapping are still uncommon to marine algae. Proteomics allowed us to analyze responses to acute and chronic stress in 2 strains of the marine brown alga *E. siliculosus* isolated from contrasting habitats. Exposure of these isolates to chronic copper stressful conditions allowed identifying the isolate Es524 from Caleta Palito as copper tolerant, whereas the isolate Es32 from San Juan de Marcona was more sensitive to copper. Epifluorescence microscopy observations in Es32 showed dramatic loss in chlorophyll autofluorescence when this strain was exposed to the lowest tested concentration (50 µg/L). Küpper *et al*. [46] suggested that the loss of chlorophyll autofluorescence in *E. siliculosus* was generated by Cu^{2+} substitution of Mg^{2+} in chlorophyll bounded predominantly to the light harvesting complexes (LHC). In contrast, after 10 days of treatment, Es524 showed only minor losses in %afc, regardless the concentration of the metal, illustrating its special capability to prevent damage in the LHC when exposed to copper excess.

5.4.1 Common protein expression features between the two isolates exposed to copper

Surprisingly, the marked differences in tolerance to copper between the two isolates were not accompanied by major differences in protein expression patterns. Exposure to sub-lethal copper concentrations induced the expression of common proteins in both strains, underlining the crucial importance of certain metabolic pathways during the stress response. Copper induced the accumulation of proteins involved in pathways related to energy production such as the pentose phosphate pathway and the beta-oxidation. These observations are in agreement with the correlation established between alteration of the photosynthesis and the ATP pool depletion in the diatom *Phaeodactylum tricornutum* [47]. Also, as in vascular plants [37], heavy metal stress induced the onset of repairing and detoxification systems, which represent an additional energetic cost for the cells, and therefore, it should not be a surprise to observe accumulation of enzymes

involved in energy production in both isolates. In addition, inhibition of nitrogen uptake due to copper toxicity has been observed in marine cyanobacteria [48]. Therefore, the accumulation of glutamate synthase and glutamine synthetase supports an increase in the activity of the GOGAT/GS cycle in order to compensate the apparent decrease in nitrogen uptake caused by copper in both strains. In this context, a recent study showed an increase in the activities of these enzymes under stress in the copper-acclimated cyanobacterium *Anabaena doliolum,* which conferred an improved resistance to several abiotic stresses [49]. In relation to nitrogen uptake, copper stress activated several enzymes implicated in amino acid metabolism. These enzymes encompassed SHMT and CS, linked to the biosynthesis of glycine and cystein respectively. These two enzymes, plus the GS mentioned above, are essential for the production of amino acid precursors used for the biosynthesis of glutathione (GSH). GSH plays a pivotal role in protecting living organisms from environmental stresses [50-51], by detoxifying ROS and toxins [8-52-53]. The GSH polymers phytochelatins (PCs) are fundamental for chelating metal excess in vascular plants [20]. Recently, concentrations of PCs and GSH in the brown algae *Fucus vesiculosus* and *F. serratus* have been correlated with the history of copper contamination of the sampling sites [23]. The enhanced GSH biosynthesis could also be related to the activity of the detoxification enzymes Glutathion-S-Transferases (GSTs). Theses enzymes are particularly abundant in *E. siliculosus*, and some of them have been shown recently to be induced by copper stress [54]. Theses findings, together with our results, highlight the involvement of thiol peptides to maintain the homeostasis in brown algae under metal stress, as well as in detoxification processes. In addition, SAM, which synthesizes S-adenosyl-methionine, was also up-regulated in both strains. Previous proteomic work in vascular plants and animals have also demonstrated that this enzyme is up-regulated under a condition of stress by heavy metals [37-55]. This enzyme belongs to the methyl cycle that interacts with GSH biosynthetic pathway, specifically at the level of the SHMT enzyme. In

vascular plants, S-adenosyl methionine is the direct precursor for nicotianamine, which is involved in copper complexation [56].

Both strains showed also up-regulation of enzymes involved in protein folding and turn-over. These proteins are important for the recycling of stress-damaged proteins, justifying their accumulation in response to stress. HSPs, known to be induced by a variety of stress conditions and important players in protecting cells against protein degradation [57-58], were increased in both strains. Additional data obtained through gene expression analysis in Es32 showed a strong up-regulation of *HSP70* and *HSP10* in response to acute copper-caused stress. In contrast, level of expression of *HSP10* was not regulated in Es524, which is in agreement with the proteomic results. In both strains, *HSP 70* was a mainly induced under acute exposures to copper excess, with a higher expression in Es32 than in ES524, suggesting an involvement in rapid stress responses rather than in adaptation. Accumulation of the same aryl sulfotransferase was also observed in both strains. This enzyme is known to catalyze the sulfate conjugation of phenolic compounds, and uses 3-phosphoadenylyl phospho-sulfate (PAPS) as cofactor. Phenolic compounds are particularly abundant in brown algae [59] and are thought to play an important role in attenuating the negative effects of both biotic and abiotic stresses in these organisms [60]. Phenolics are known as ROS scavengers, and have high affinity for metals [28]. In addition, previous work suggests the heavy metal-polyphenols complexes seem to be sequestrated in the physodes [26-28]. Based on the putative biochemical function of this aryl sulphotransferase, it is likely that sulphation of phenolics may substitute the reactive hydroxyl groups, therefore preventing the oxidation and the condensation of phenolics.

5.4.2 Strain-specific responses

Several individual proteins exhibited inter-strain qualitative or quantitative differences in expression. The protein chaperones, ML and CALR, were down-regulated only in Es32. These proteins are implicated in cell-death mechanisms in several organisms, under a variety of stress,

including metal ions [61-62], however further studies must be carried to fully characterize their role in *Ectocarpus*.

We discussed above the capability of Es524 to resist Cu excess by avoiding LHC degradation. In agreement with this observation, an increased expression of Fcp was observed. The enhanced turn-over of this protein could contribute to the maintenance of the LHC integrity in this strain. In addition, our physiological measurements recorded a diminished autofluorescence, which is reportedly associated with chlorophyll degradation [63]. Other damage can affect directly the PSII of the photosynthetic apparatus. Indeed, the effect of copper on the Fv/Fm is a well documented phenomenon in vascular plants and algae [47-64-65]. Copper excess can damage directly PSII and create an oxidative stress as a result of the PS dysfunction [5-8-66-68]. Es524 exhibited unchanged Fv/Fm values up to 250 µg/L copper, in contrast to Es32 whose values were affected by concentrations higher than 50 µg/L. This result highlights the capacity of Es524 to maintain the integrity of PSII when exposed to copper excess. In agreement with this, a marked increase in OEC33 was observed in Es524 when compared to Es32. This could account for an enhanced turnover of OEC33, which constitutes a major copper toxicity target in PSII [67-69]. As in *Ectocarpus*, copper adapted populations of the brown alga *F. serratus* showed better photosynthetic performance when stressed with copper than populations non-exposed to this metal [70]. Besides, the cell detoxification enzymes, DEAD box helicases and vBPO were increased under copper stress in Es524 but not in Es32. RNA helicases from the DEAD box family are found in almost all organisms and have important roles in RNA metabolism. They are associated with many cellular processes including ribosome biogenesis, pre-mRNA splicing, mRNA export, translation initiation, organellar gene expression and RNA decay [71]. Moreover, these enzymes have been reported to play important roles in resistance to abiotic stress in vascular plants [72-73]. Two DEAD box helicases were accumulated under stress in Es524, indicating the involvement of these enzymes in response to copper-mediated stress. On the other side, vBPOs are original

peroxidases of brown and red algae, which are absent in vascular plants or metazoans [74]. They catalyze the oxidation of bromide, as well as iodide, in the presence of hydrogen peroxide to generate oxidized halogens which is thought to be related to iodine uptake [75]. Recent studies in the kelp *L. digitata* showed that iodine was mainly stored in the apoplasmic region as iodide [34-76]. Küpper *et al.* presented iodide as a powerful scavenger for a wide variety of ROS because of its high reducing capacity [34]. Furthermore, these authors propose vBPO for catalyzing this process. Gene expression analysis showed a strong induction of *vBPO* in both strains under all conditions of copper excess, which underlines the importance of vBPO in stress responses. In agreement with these results, in-gel activity assays clearly showed the increase of vBPO activity in relation to chronic stress. Iodide metabolism is not well characterized in *E. siliculosus* and thereby this is, to our knowledge, the first study describing vBPO and its regulation under stress in this species. Based on our results and previous work in brown algae, it is likely that vBPO plays a mayor role in the processes leading to ROS detoxification [34-77]. In addition, if significant amounts of I^- are released upon stress, it could be possible that a complexation with Cu^{2+} occurs, leading to a non bioavailable form of copper. However, additional research is required to prove this hypothesis.

5.4.3 Concluding remarks

In this work we have characterized two strains of *E. siliculosus* presenting different copper tolerance (Es32 and Es524). The availability of these different strains paves the way for the study of genetic bases of adaptative traits in seaweeds. Global proteome profiling led us to identify several pathways involved in the tolerance to copper and helped us to better understanding the differential metal tolerance between strains. In this context, photosynthesis-related proteins seem to be crucial for copper tolerance. In addition, we suggest the occurrence of an original antioxidant response of brown algae, based on halide metabolism and involving vanadium-dependent bromoperoxidases.

Acknowledgments

We thank Santiago Andrade for his help and advice concerning metal handling and during toxicity assays. This work has been partially funded by Marine Genomics Europe NoE 7 (EU contract n° GOCE-CT-2004-505403) and by the French Embassy and the CONICYT of Chile through PhD fellowships to A.R. This work was supported by the Laboratoire International Associé 'Dispersal and Adaptation of Marine Species' (LIA DIAMS) PUC, Chile and CNRS-UPMC, France. Additional support came from FONDAP 1501-0001 (Program 7) and ICA research grant, both to J.A.C.

5.5 References

[1] Correa, J.A. et al. (1999) Copper, copper mine tailings and their effect on the marine algae in Northern Chile. Journal of Applied Phycology 11, 57-67.

[2] Livingstone, D.R. (2001) Contaminant-stimulated Reactive Oxygen Species Production and Oxidative Damage in Aquatic Organisms. Marine Pollution Bulletin 42, 656-666.

[3] Gledhill, M., Nimmo, M., Hill, S.J. and Brown, M.T. (1997) The toxicity of copper (II) species to marine algae, with particular reference to macroalgae. Journal of Phycology 33, 2-11.

[4] Maksymiec, W. (1997) Effect of copper on cellular processes in higher plants. Photosynthetica 34, 321-342.

[5] Yruela, I., Pueyo, J.J., Alonso, P.J. and Picorel, R. (1996) Photoinhibition of Photosystem II from Higher Plants. Effect of copper inhibition. Journal of Biological Chemistry 271, 27408-27415.

[6] Fernandes, J.C. and Henriques, F.S. (1991) Biochemical, Physiological, and Structural Effects of Excess Copper in Plants. Botanical Review 57, 246-273.

[7] Halliwell, B. and Gutteridge, J.M.C. (1992) Biologically relevant metal ion-dependent hydroxyl radical generation An update. FEBS Letters 307, 108-112.

[8] Halliwell, B. (2006) Reactive Species and Antioxidants. Redox Biology Is a Fundamental Theme of Aerobic Life. Plant Physiology 141, 312-322.

[9] Baker, A.J.M. and Proctor, J. (1990) The influence of cadmium, copper, lead, and zinc on the distribution and evolution of metallophytes in the British Isles. Plant Systematics and Evolution 173, 91-108.

[10] Macnair, M.R. (1993) The Genetics of Metal Tolerance in Vascular Plants. New Phytologist 124, 541-559.

[11] Pauwels, M., Roosens, N.H., Frérot, H. and Saumitou-Laprade, P. (2008) When population genetics serves genomics: putting adaptation back in a spatial and historical context. Current Opinion in Plant Biology 11, 129-134.

[12] Medina, M., Andrade, S., Faugeron, S., Lagos, N., Mella, D. and Correa, J.A. (2005) Biodiversity of rocky intertidal benthic communities associated with copper mine tailing discharges in northern Chile. Marine Pollution Bulletin 50, 396-409.

[13] Hall, A. (1981) Copper accumulation in copper-tolerant and non-tolerant populations of the marine fouling alga *Ectocarpus siliculosus* (Dillw.) Lyngbye. Botanica Marina 24, 223-228.

[14] Hall, A. (1980) Heavy metal Co-tolerance in a copper tolerant population of the marine fouling alga, *Ectocarpus siliculosus* (Dillw.) Lyngbye. New Phytologist 85, 73-78.

[15] Russel, G. and Morris, O.P. (1970) Copper tolerance in marine fouling alga *Ectocarpus siliculosus*. Nature 228, 288-289.

[16] Morris, O.P. and Russel, G. (1974) Inter-specific differences in response to copper by natural populations of *Ectocarpus*. Journal of British Phycology 9, 269-272.

[17] Puig, S., Andres-Colas, N., Garcia-Molina, A. and Penarrubia, L. (2007) Copper and iron homeostasis in Arabidopsis: responses to metal deficiencies, interactions and biotechnological applications. Plant Cell and Environment 30, 271-290.

[18] Küpper, H. and Kroneck, P.M.H. (2005) Heavy metal uptake by plants and cyanobacteria. Metal Ions in Biological Systems 44, 97-144.

[19] Hall, J.L. (2002) Cellular mechanisms for heavy metal detoxification and tolerance. Journal of Expperimental Botany 53, 1-11.

[20] Cobbett, C. and Goldsbrough, P. (2002) Phytochelatins and Metallothioneins: Roles in Heavy Metal Detoxification and Homeostasis. Annual Review of Plant Biology 53, 159-182.

[21] Clemens, S. (2006) Toxic metal accumulation, responses to exposure and mechanisms of tolerance in plants. Biochimie 88, 1707-1719.

[22] Andrés-Colás, N., Sancenón, V., Rodríguez-Navarro, S., Mayo, S., Thiele Dennis J., Ecker, J.R., Puig, S. and Peñarrubia, L. (2006) The Arabidopsis heavy metal P-type ATPase HMA5 interacts with metallochaperones and functions in copper detoxification of roots. The Plant Journal 45, 225-236.

[23] Pawlik-Skowronska, B., Pirszel, J. and Brown, M.T. (2007) Concentrations of phytochelatins and glutathione found in natural assemblages of seaweeds depend on species and metal concentrations of the habitat. Aquatic Toxicology 83, 190-199.

[24] Morris, C.A., Nicolaus, B., Sampson, V., Harwood, J.L. and Kille, P. (1999) Identification and characterization of a recombinant metallothionein protein from a marine alga, *Fucus vesiculosus*. Biochem J 338 (Pt 2), 553-60.

[25] Toth, G. and Pavia, H. (2000) Lack of phlorotannin induction in the brown seaweed *Ascophyllum nodosum* in response to increased copper concentrations. Marine Ecology Progress Series 192, 119-126.

[26] Salgado, L.T., Andrade, L.R. and Filho, G.M.A. (2005) Localization of specific monosaccharides in cells of the brown alga *Padina* gymnospora and the relation to heavy-metal accumulation. Protoplasma 225, 123-128.

[27] Sueur, S., van den Berg, C.M.G. and Riley, J.P. (1982) Measurement of the metal complexing ability of exudates of marine macroalgae. Limnology and Oceanography 27, 536-543.

[28] Karez, C.S. and Pereira, R.C. (1995) Metal contents in polyphenolic fractions extracted from brown alga *Padina gymnospora*. Botanica Marina 38, 151-155.

[29] Andrade, L.R., Farina, M. and Amado Filho, G. (2002) Role of *Padina Gymnospora* (Dictyotales, Phaeophyceae) cell walls in cadmium accumulation. Phycologia 41, 39-48.

[30] Contreras, L., Moenne, A. and Correa, J.A. (2005) Antioxidant responses in *Scytosiphon lomentaria* (Phaeophyceae) inhabiting copper-enriched coastal environments. Journal of Phycology 41, 1184-1195.

[31] Pinto, E., Sigaud-kutner, T.C.S., Leitao, M.A.S., Okamoto, O.K., Morse, D. and Colepicolo, P. (2003) Heavy metal-induced stress in algae. Journal of Phycology 39, 1008-1018.

[32] Ritter, A., Goulitquer, S., Salaün, J.-P., Tonon, T., Correa, J.A. and Potin, P. (2008) Copper stress induces biosynthesis of octadecanoid and eicosanoid oxygenated derivatives in the brown algal kelp *Laminaria digitata*. New Phytologist 180, 809-821.

[33] Baldauf, S.L. (2003) The Deep Roots of Eukaryotes. Science 300, 1703-1706.

[34] Küpper, F.C. et al. (2008) Iodide accumulation provides kelp with an inorganic antioxidant impacting atmospheric chemistry. Proceedings of the National Academy of Sciences 105, 6954-6958.

[35] Charrier, B. et al. (2008) Development and physiology of the brown alga *Ectocarpus siliculosus*: two centuries of research. New Phytologist 177, 319-332.

[36] Requejo, R. and Tena, M. (2005) Proteome analysis of maize roots reveals that oxidative stress is a main contributing factor to plant arsenic toxicity. Phytochemistry 66, 1519-1528.

[37] Sarry, J.-E. et al. (2006) The early responses of *Arabidopsis thaliana* cells to cadmium exposure explored by protein and metabolite profiling analyses. Proteomics 6, 2180-2198.

[38] Smith, A.P., DeRidder, B.P., Guo, W.J., Seeley, E.H., Regnier, F.E. and Goldsbrough, P.B. (2004) Proteomic analysis of Arabidopsis glutathione S-transferases from benoxacor- and copper-treated seedlings. Journal of Biological Chemistry 279, 26098-26104.

[39] Kung, C.-C.S., Huang, W.-N., Huang, Y.-C. and Yeh, K.-C. (2006) Proteomic survey of copper-binding proteins in *Arabidopsis* roots by immobilized metal affinity chromatography and mass spectrometry. Proteomics 6, 2746-2758.

[40] Bona, E., Marsano, F., Cavaletto, M. and Berta, G. (2007) Proteomic characterization of copper stress response in *Cannabis sativa* roots. Proteomics 7, 1121-1130.

[41] Contreras, L. et al. (2008) Two-dimesional gel electrophoresis analyses of brown algal protein extracts. Journal of Phycology 44, 1315-1321.

[42] Starr, R.C. and Zeikus, J.A. (1993) UTEX-THE CULTURE COLLECTION OF ALGAE AT THE UNIVERSITY OF TEXAS AT AUSTIN 1993 LIST OF CULTURES. Journal of Phycology 29, 1-106.

[43] Le Bail, A., Dittami, S., de Franco, P.-O., Rousvoal, S., Cock, M., Tonon, T. and Charrier, B. (2008) Normalisation genes for expression analyses in the brown alga model *Ectocarpus siliculosus*. BMC Molecular Biology 9, 75.

[44] Bradford, M.M. (1976) Rapid and Sensitive Method for Quantitation of Microgram Quantities of Protein Utilizing Principle of Protein-Dye Binding. Analytical Biochemistry 72, 248-254.

[45] Colin, C., Leblanc, C., Michel, G., Wagner, E., Leize-Wagner, E., Dorsselaer, A.V. and Potin, P. (2005) Vanadium-dependent iodoperoxidases in *Laminaria digitata*, a novel biochemical function diverging from brown algal bromoperoxidases. Journal of Biological Inorganic Chemistry 10, 156-166.

[46] Küpper, H., Setlik, I., Spiller, M., Kupper, F.C. and Prasil, O. (2002) Heavy metal-induced inhibition of photosynthesis: targets of in vivo heavy metal chlorophyll formation. Journal of Phycology 38, 429-441.

[47] Cid, A., Herrero, C., Torres, E. and Abalde, J. (1995) Copper toxicity on the marine microalga *Phaeodactylum tricornutum*: effects on photosynthesis and related parameters. Aquatic Toxicology 31, 165-174.

[48] Kashyap, A.K. and Gupta, S.L. (1982) Effect of lethal copper concentrations on nitrate uptake reduction and nitrite release in *Anacystis nidiculans*. Zeitung Pflanzenphysiologie 107, 289-294.

[49] Thapar, R., Srivastava, A.K., Bhargava, P., Mishra, Y. and Rai, L.C. (2008) Impact of different abiotic stresses on growth, photosynthetic electron transport chain, nutrient uptake and enzyme activities of Cu-acclimated *Anabaena doliolum*. Journal of Plant Physiology 165, 306-316.

[50] Xiang, C. and Oliver, D.J. (1998) Glutathione Metabolic Genes Coordinately Respond to Heavy Metals and Jasmonic Acid in Arabidopsis. Plant Cell 10, 1539-1550.

[51] Meister, A. and Anderson, M.E. (1983) Glutathione. Annual Review of Biochemistry 52, 711-760.

[52] Alscher, R.G. (1989) Biosynthesis and antioxidant function of glutathione in plants. Physiologia Plantarum 77, 457-464.

[53] Dixon, D., Lapthorn, A. and Edwards, R. (2002) Plant glutathione transferases. Genome Biology 3, reviews3004.1 -10.

[54] de Franco, P.-O., Rousvoal, S., Tonon, T. and Boyen, C. (*In press*) Whole genome survey of the glutathione transferase family in the brown algal model *Ectocarpus siliculosus*. Marine Genomics.

[55] Lee, S.-E., Yoo, D.-h., Son, J. and Cho, K. (2006) Proteomic evaluation of cadmium toxicity on the midge *Chironomus riparius* Meigen larvae. Proteomics 6, 945-957.

[56] Liao, M., Hedley, M., Woolley, D., Brooks, R. and Nichols, M. (2000) Copper uptake and translocation in chicory (*Cichorium intybus* L. cv Grasslands Puna) and tomato (*Lycopersicon esculentum* Mill. cv Rondy) plants grown in NFT system. II. The role of nicotianamine and histidine in xylem sap copper transport. Plant and Soil 223, 245-254.

[57] Vierling, E. (1991) The Roles of Heat Shock Proteins in Plants. Annual Review of Plant Physiology and Plant Molecular Biology 42, 579-620.

[58] Lindquist, S. and Craig, E.A. (1988) The Heat-Shock Proteins. Annual Review of Genetics 22, 631-677.

[59] Mashek, J.A. and Baker, B.J. (2008) Chemistry of algal secondary metabolism, pp. 1-24 (Springer-Verlag, Ed.) Springer-Verlang, Heildelberg.

[60] Schoenwaelder, M.E.A. (2002) The occurrence and cellular significance of physodes in brown algae. Phycologia 41, 125-139.

[61] Mazzoni, C. and Falcone, C. (2008) Caspase-dependent apoptosis in yeast. Biochimica et Biophysica Acta - Molecular Cell Research 1783, 1320-1327.

[62] Panaretakis, T. et al. (2008) The co-translocation of ERp57 and calreticulin determines the immunogenicity of cell death. Cell Death & Differentiation 15, 1499-1509.

[63] Ciscato, M., Valcke, R., Loven, K., Clijsters, H. and Navari-Izzo, F. (1997) Effects of in vivo copper treatment on the photosynthetic apparatus of two *Triticum durum* cultivars with different stress sensitivity. Physiologia Plantarum 100, 901-908.

[64] Patsikka, E., Aro, E.-M. and Tyystjarvi, E. (1998) Increase in the Quantum Yield of Photoinhibition Contributes to Copper Toxicity in Vivo. Plant Physiol. 117, 619-627.

[65] Mallick, N. and Mohn, F.H. (2003) Use of chlorophyll fluorescence in metal-stress research: a case study with the green microalga Scenedesmus. Ecotoxicology and Environmental Safety 55, 64-69.

[66] Halliwell, B., Gutterridge, John (1984) Oxygen toxicity, oxygen radicals, transition metals and disease. Biochem. J. 219, 1-14.

[67] Yruela, I., Alfonso, M., Baron, M. and Picorel, R. (2000) Copper effect on the protein composition of photosystem II. Physiologia Plantarum 110, 551-557.

[68] Bernal, M., Roncel, M., Ortega, J.M., Picorel, R. and Yruela, I. (2004) Copper effect on cytochrome b559 of photosystem II under photoinhibitory conditions. Physiologia Plantarum 120, 686-694.

[69] Henmi, T., Miyao, M. and Yamamoto, Y. (2004) Release and Reactive-Oxygen-Mediated Damage of the Oxygen-Evolving Complex Subunits of PSII during Photoinhibition. Plant Cell Physiology 45, 243-250.

[70] Nielsen, H.D., Brownlee, C., Coelho, S.M. and Brown, M.T. (2003) Inter-population differences in inherited copper tolerance involve photosynthetic adaptation and exclusion mechanisms in *Fucus serratus*. New Phytologist 160, 157-165.

[71] Rocak, S. and Linder, P. (2004) DEAD-box proteins: the driving forces behind RNA metabolism. Nature Reviews Molecular Cell Biology 5, 232-241.

[72] Sanan-Mishra, N., Pham, X.H., Sopory, S.K. and Tuteja, N. (2005) Pea DNA helicase 45 overexpression in tobacco confers high salinity tolerance without affecting yield. Proceedings of the National Academy of Sciences of the United States of America 102, 509-514.

[73] Luo, Y., Liu, Y.B., Dong, Y.X., Gao, X.-Q. and Zhang, X.S. (2008) Expression of a putative alfalfa helicase increases tolerance to abiotic stress in Arabidopsis by enhancing the capacities for ROS scavenging and osmotic adjustment. Journal of Plant Physiology.

[74] Leblanc, C. et al. (2006) Iodine transfers in the coastal marine environment: the key role of brown algae and of their vanadium-dependent haloperoxidases. Biochimie 88, 1773-1785.

[75] Küpper, F.C., Schweigert, N., Ar Gall, E., Legendre, J.-M., Vilter, H. and Kloareg, B. (1998) Iodine uptake in Laminariales involves extracellular, haloperoxidase-mediated oxidation of iodide. Planta 207, 163-171.

[76] Verhaeghe, E. et al. (2008) Microchemical imaging of iodine distribution in the brown alga *Laminaria digitata* suggests a new mechanism for its accumulation. Journal of Biological Inorganic Chemistry 13, 257-269.

[77] Roeder, V., Collen, J., Rousvoal, S., Corre, E., Leblanc, C. and Boyen, C. (2005) Identification of stress gene transcripts in *Laminaria digitata* (Phaeophyceae) protoplast cultures by Expressed Secuence Tag analysis. Journal of Phycology 41, 1227-1235.

5.6 FIGURES

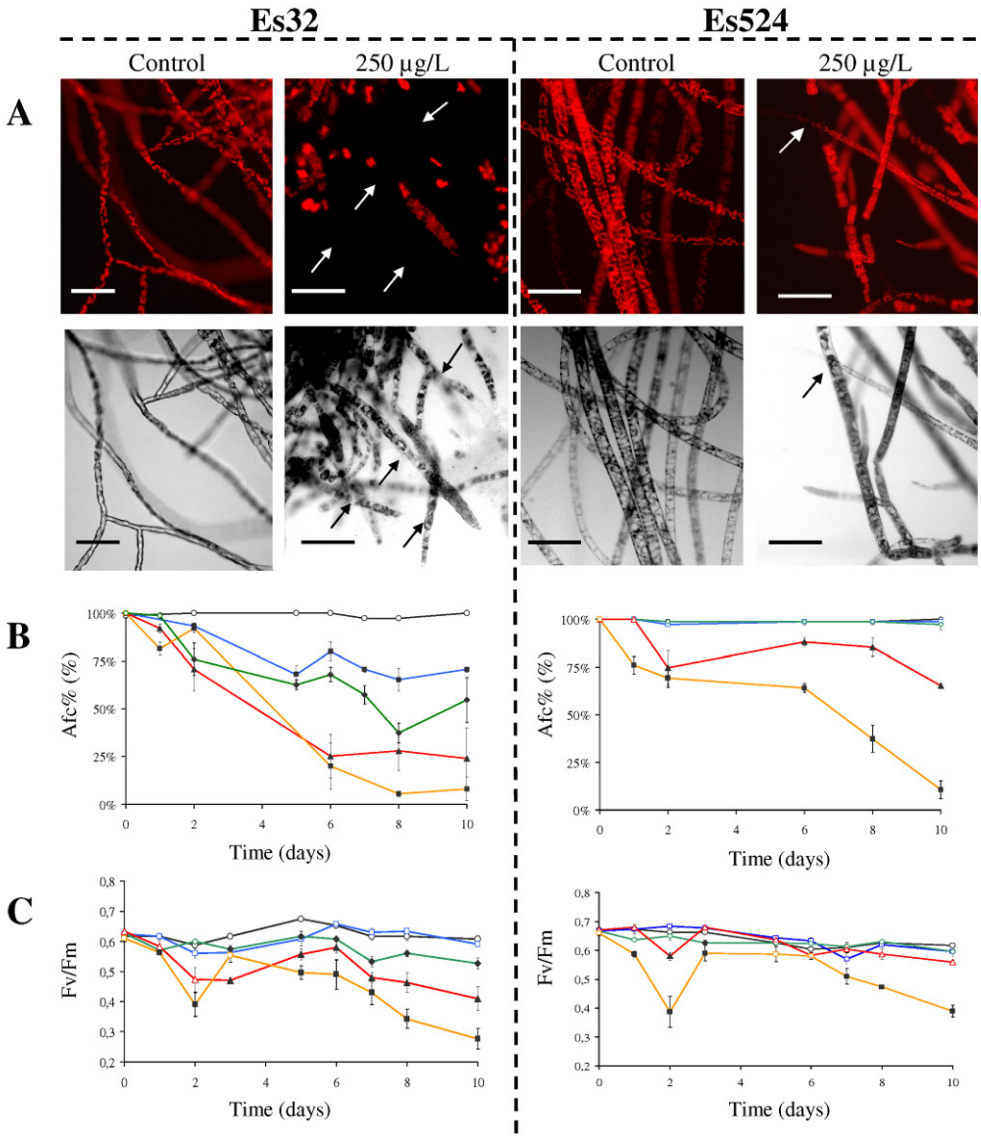

Figure 1. Physiological effects of copper toxicity on the *E. siliculosus* strains Es32 and Es524. (A) Comparison of epifluorescence and transmission microscopic photographs of Es32 and Es524 after 10 days of copper treatment. Top images represent the green cut-off filter fluorescence images with their correspondent transmission images at the bottom. For each strain, the images are organized as follow: control condition (left) and 250 µg/L of copper (right). The bars represent 0.1mm. (B) Effect of different copper concentrations on the percentage of remaining auto-fluorescent cells in Es32 and Es524 thalli during 10 days. Control seawater (black), and different concentrations of copper: 50 µg/L (blue), 150 µg/L (green), 250 µg/L (red) and 500 µg/L (orange). Values represent means of three independent replicates and bars represent the SE. Black-filled spots represent a significantly different condition from the control group ($P< 0.05$). (C) Changes in the photosynthetic yield of Es32 and Es524 treated with different concentrations of copper during 10 days. Control seawater (black), and different concentrations of copper: 50 µg/L (blue), 150 µg/L (green), 250 µg/L (red), 500 µg/L (orange). Values represent means of three independent replicates and bars represent the SE. Black-filled spots represent a significantly different condition from the control group ($P< 0.05$).

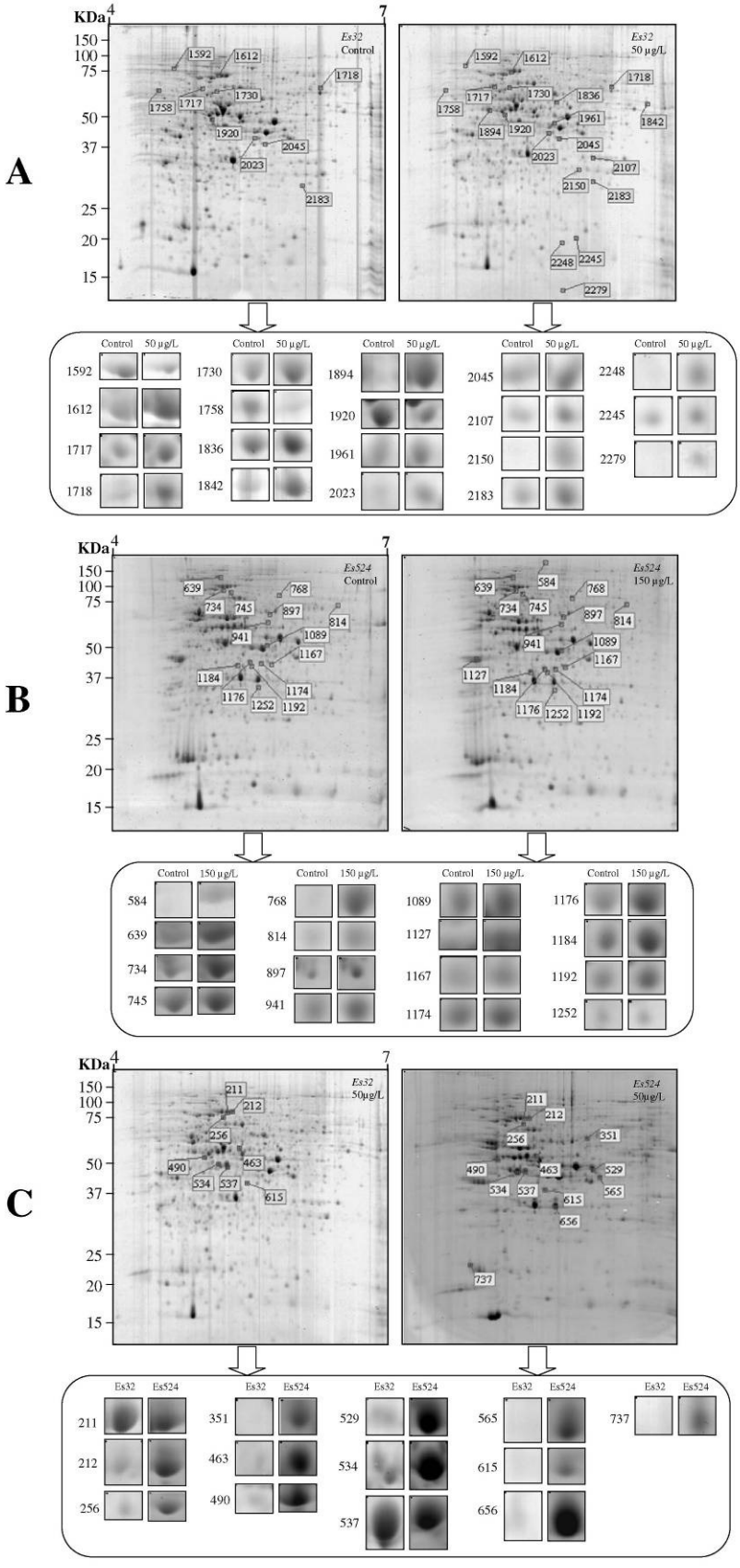
A
KDa
4
7
150
100
75
50
37
25
20
15
Es32
Control
Es32
50 µg/L
1592
1612
1718
1717
1730
1758
1920
2045
2023
2183
1836
1842
1894
1961
2107
2150
2248
2245
2279
Control
50 µg/L
B
Es524
Control
Es524
150 µg/L
639
768
734
745
897
814
941
1089
1167
1184
1176
1174
1252
1192
584
1127
150 µg/L
C
Es32
50µg/L
Es524
50µg/L
211
212
256
490
463
534
537
615
351
529
565
656
737
Es32
Es524

Figure 2. Proteomic profiling of *E. siliculosus* strains Es32 and Es524 in response to copper stress. (A) Representatives 2-DE gels using a non-linear gradient of p*I* 4-7 of total soluble proteome fractions of Es32 under control condition (left gel) and 50 µg/L of nominal Cu, for 10 days under (right gel). Differentially expressed spots (fold-change < 1.5) are highlighted on the bottom panel. Spot identification numbers are listed on the left side of the images. (B) Representative 2-DE gels using a non-linear gradient of p*I* 4-7 of total soluble proteome fractions of Es524 under control condition (left gel) and 150 µg/L nominal Cu, for 10 days under (right gel). Differentially expressed spots (fold-change < 1.5) are highlighted on the bottom panel. (C) Representative 2-DE using a non-linear gradient of p*I*4-7 gels comparing total soluble proteomes between Es32 and Es524 submitted to 50µg/L nominal Cu for 10 days. Differentially expressed proteins (fold-change < 1.5) are highlighted on the bottom panel.

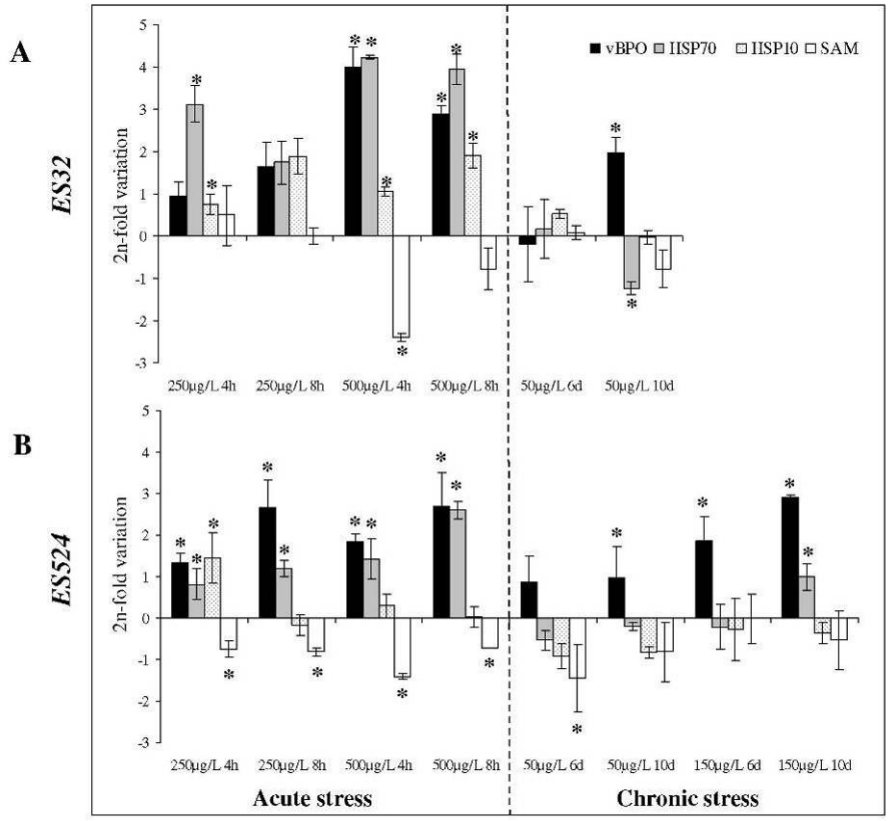

Figure 3. Changes in gene expression of *E. siliculosus* strains Es32 and Es524 submitted to acute and chronic stresses monitored by RT-qPCR. (A) Expression profile of *vBPO*, *HSP70*, *HSP10* and *SAM* transcripts from Es32 submitted to acute Cu stresses (250 µg/L and 500 µg/L for 4 and 8 h) at the left and chronic Cu stresses (50 µg/L for 6 and 10 days) at the right. (B) Expression profile of *vBPO, HSP70, HSP10* and *SAM* transcripts from Es524 submitted to acute Cu stresses (250 µg/L and 500 µg/L for 4 and 8 hours idem 2 lignes au-dessus) at the left and chronic Cu stresses (50 µg/L and 150 µg/L for 6 and 10 days) at the right. The relative gene expression ratios was calculated as 2n-fold variation as described in Materials and Methods. Results are means ± SE for two determinations from three independent biological samples. * Significantly different from the control group (P<0.05).

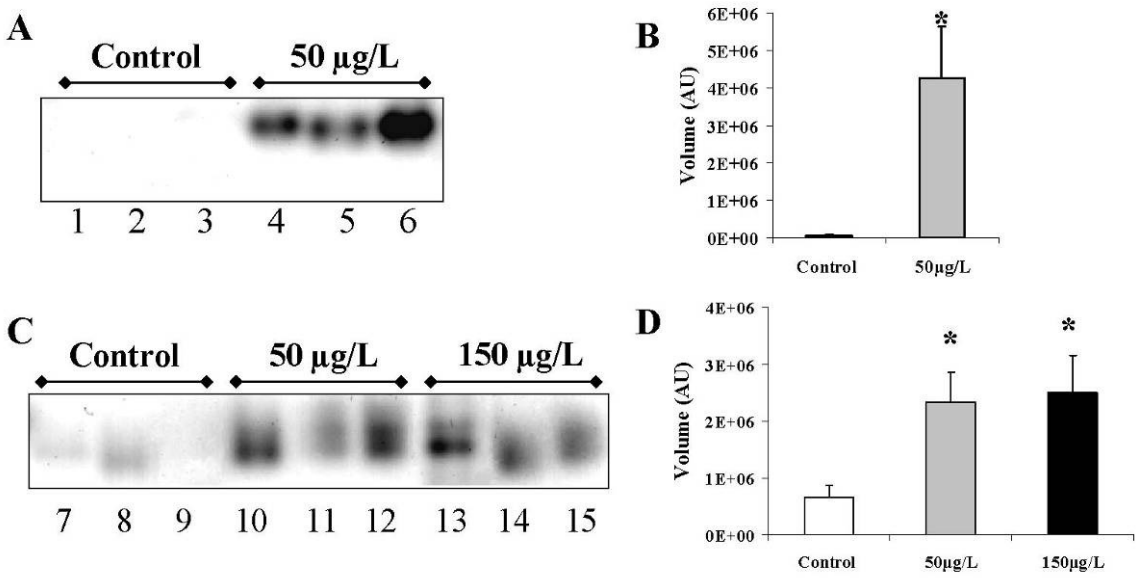

Figure 4. Native-PAGE bromoperoxidase activity staining assay from *E. siliculosus* strains Es32 and Es524 submitted to 10 days of copper excess. Twenty µg of each total protein extract were loaded into the gel for testing BPO activity as described in materials and methods. (A) Lines 1-3: Es32 controls; lines 4-6: Es32 treated with 50 µg/L of nominal copper. (B) Image band quantification of Es32 controls and 50 µg/L Cu treated individuals. Values (AU) represent the mean of the three replicates and bars the SE. * Significantly different from the control group (P<0.05). (C) Lines 7-9: Es524 controls; lines 10-12: Es524 treated with 50 µg/L of copper; lines 13-15: Es524 treated with 150 µg/L of nominal copper. (D) Image band quantification of Es524 controls, 50 µg/L and 150 µg/LCu treated individuals. Values (AU) represent the mean of the three replicates and bars the SE. *Significantly different from the control group (P<0.05).

Table 1. Mortality rates of *E. siliculosus* strains Es524 and Es32 exposed 10 days to different copper concentrations. Values are representative of 10 individuals (n=10).

[Nominal Cu]	Es32	Es524
0	0	0
20	0	0
25	0	0
32	0	0
40	20	0
50	50	0
65	100	0
80	100	0
100	100	0
200	100	0
500	100	
1000	100	100

Table 2. Proteins identified in Es32 whose level of expression changed between control and copper stress.*

Spot n°	**Functional category** Protein name	Ectocarpus genomic database accession code	Expression under Stress	Theo/obs MW (KDa)	Theo/obs p*I*	Mean % Vol ±SD Control / Stress	Fold – change
	Energy metabolism						
2183	Vacuolar ATP synthase subunit E	Esi0062_0090	Up	15/30	5.0/6.2		1.5
1612	Transketolase (TKT)	Esi0002_0327	Up	83/80	5.6/5.3		2.0
2150	Short chain enoyl-CoA hydratase (ECH)	Esi0030_0175	Up	31/30	8.1/6.2		>10
	Polysaccharide metabolism						
1717	Mannose-6-phosphate isomerase, type I (ManA)	Esi0000_0208	Up	59/68	5.5/5.2		2.3
	Amino acid metabolism						
1730	Glutamate synthase small chain (GOGAT)	Esi0029_0131	Up	62/67	5.2/5.3		1.5
1842	Serine hydroxymethyltransferase 2 (SHMT)	Esi0148_0037	Up	53/53	8.3/6.7		1.5
1894	Glutamine synthetase (GS)	Esi0072_0092	Up	45/53	4.9/5.0		5.8
2023	Cysteine synthase (CS)	Esi0008_0179	Up	35/35	8.5/5.6		2.4
	Nucleotide metabolism						
2245	Uridylate Kinase (UMPK)	Esi0064_0085	Up	27/21	11.9/6.0		1.8
1836	S-adenosylmethionine synthetase (SAM)	Esi0175_0026	Up	33/54	5.2/5.6		2.1
	Protein turnover						
2107	Proteasome alpha subunit	Esi0003_0161	Up	27/31	5.9/6.2		1.6
	Protein folding and stabilization						
2279	Heat shock protein 10kDa (HSP 10)	Esi0000_0403	Up	11/11	6.2/5.8		>10
1758	Calreticulin (CALR)	Esi0363_0006	Down	48/64	4.2/4.8		-1.9
1920	Metacaspase (ML)	Esi0414_0015	Down	40/45	4.9/5.2		-1.5
2248	Immunophilin FKBP type (FKBP11)	Esi0148_0072	Up	17/25	5.7/5.7		>10
	Cell recue and detoxification						
2045	Aryl Sulphotransferase	Esi0197_0023	Up	38/39	6.4/5.7		2.3
	Unknown / hypothetical proteins						
1592	Hypothetical protein	Esi0173_0035	Down	64/90	4.5/4.9		-1.9
1718	hypothetical protein TP04_0059	Esi0174_0047	Up	58/64	6.0/54.8		2.3
1961	Conserved hypothetical protein	Esi0175_0006	Up	39/40	7.6/5.6		2.0

Table 3. Proteins identified in Es524 whose level of expression changed between control and chronic copper stress (50 and 150 µg/L Cu for 10 days)*.

Spot n°	**Functional category** Protein homologue name	Ectocarpus genomic database accession code	Condition Stress/Control	Theo/obs MW (KDa)	Theo/obs *pI*	Mean % Vol ±SD Control / Stress	Fold – change
1192	**Energy metabolism**						
	Enoyl coenzyme A hydratase (ECH)	Esi0136_0023	Up	27/33	4.9/4.8		1.5
814	**Fatty acid metabolism**						
	C18 Fatty acid desaturase	Esi0207_0012	Up	49/66	5.8/5.7		1.7
	Amino acid metabolism						
584	Glutamate synthase (GOGAT)	Esi0103_0010	Up	185/140	5.9/5.7		>10
1089	Glutaminyl-tRNA Synthetase (GlnS)	Esi0138_0058	Up	53/44	5.9/5.7		1.6
	Nucleotide metabolism						
941	S-adenosylmethionine synthetase (SAM)	Esi0175_0026	Up	33/55	5.2/5.7		1.5
	Protein turnover						
1252	30S Ribosomal protein	Esi0012_0045	Down	42/32	6.4/5.7		-2.2
	Protein folding and stabilization						
734	Heat Shock protein 70 KDa (HSP 70)	Esi0379_0027	Up	72/75	5.0/5.1		2.0
1184	Heat shock protein 40 KDa (HSP 40)	Esi0048_0108	Up	38/33	6.6/5.4		2.3
	Cell rescue and detoxification						
1167	Aryl Sulphotransferase	Esi0197_0023	Up	38/38	6.4/5.8		1.6
768	vanadium dependent Bromoperoxidase (vBPO)	Esi0009_0080	Up	70/70	5.9/5.8		2.8
745	DEAD box helicase 1	Esi0033_0067	Up	112/71	5.5/10.0		1.6
897	DEAD box helicase 2	Esi0028_0100	Up	45/59	5.7/6.0		1.7
	Unknown or other hypothetical proteins						
639	Conserved hypothetical protein	Esi0061_0045	Up	102/102	9.2/4.9		1.5
1176	Hypothetical Acid phosphatase/vanadium-dependent haloperoxidase domain	Esi0067_0058	Up	37/38	9.7/5.7		1.7
1174	Hypothetical protein: Fatty acid desaturase subdomain	Esi0806_0003	Up	27/37	8.9/5.7		1.5
1127	Hypothetical protein: Legume lectin, beta domain	Esi0024_0144	Up	32/40	4.6/4.6		>10

Table 4. Proteins identified in Es524 proteins whose expression levels showed changes compared to Es32 at 50 µg/L of copper for 10 days*.

Spot n°	**Functional category** Protein homologue name	Ectocarpus genomic database accession code	Condition Es524/Es32	Theo/obs MW (KDa)	Theo/obs *pI*	Mean % Vol ±SD Es524/Es32	Fold – change Es524/Es32
	Energy metabolism						
537	Fructose-1,6-biphosphate aldolase (SMALDO)	Esi0183_0065	Down	54/41	5.9/5.5		-1.5
534	*Fructose-1,6-biphosphate aldolase (SMALDO)*	Esi0183_0065	Up	54/41	5.9/5.4		8.9
529	Glyceraldehyde-3-phosphate deshydogenase (GAPD)	Esi0240_0024	Up	41/43	5.2/5.8		7.8
351	ATP synthetase subunit beta	Esi0327_0021	Up	60/64	5.6/5.8		>10
211	Transketolase (TKT)	Esi0002_0327	Down	83/82	5.6/5.5		-1.5
212	*Transketolase (TKT)*	Esi0002_0327	Up	83/82	5.6/5.6		4.4
490	Phosphoribulokinase (PKK)	Esi0000_0466	Up	48/50	5.6/5.0		>10
	Amino acid metabolism						
463	Glutamine synthetase, catalytic region (GS)	Esi0188_0004	Up	45/51	5.5/5.6		14
	Cell rescue, repair and defense						
256	DEAD box helicase 1	Esi0033_0067	Up	112/77	10.0/5.5		>10
	Photosynthesis						
656	Manganese-stabilising protein (PsbO)	Esi0155_0030	Up	34/35	5.3/5.7		>10
737	Fucoxhantin chlorophyll a-c binding protein b (Fcp)	Esi0492_0001	Up	21/21	5.3/4.2		>10
	Unknown or hypothetical proteins						
615	Hypothetical Acid phosphatase/vanadium-dependent haloperoxidase domain	Esi0067_0058	Up	37/38	9.7/5.7		2.8
565	AKR7A2 protein	Esi0341_0018	Up	39/40	5.0/5.8		3.4

Footnote: *Tryptic peptides obtained from isolated spots were considered for MALDI-TOF-MS analysis, and their profile/pattern were compared with the proteins sequences generated from the *E. siliculosus* genomic resources using MASCOT. Proteins are listed by their individual spot numbers, identification name and their accession number in the version 1 of the genome. Further indications are included, on the protein regulation under the stress condition, the observed and theoretical MW, the observed and theoretical p*I* values, the relative spot expression (% Vol ± SD), and the x fold-change ratio. All proteins listed present significant differences in their accumulation under control and stress condition ($P<0.05$).

Table S1: Specific characteristics of the primers utilized for gene expression analyses by reverse transcriptase quantitative polymerase chain reaction (RT-qPCR).

Gene	Primer sequence (5'-3')	Tm	Amplified fragment size (bp)	*E. siliculosus* genome database matches and Accession Number
EsvBPO	AGTGGCCCAGAAAAAGAGTACG AGTCAAGGCAGAGGTGCACC	59.4 58.7	101	vanadium dependent Bromoperoxidase Esi0009_0080
EsHSP70	CGTGAGCGTGCTGACCATC GCAAGAAGTAGTCCACCATCCG	58.2 58.5	110	Heat Shock protein 70 Esi0379_0027
EsHSP10	GGCGAGGTTGTTGCGGTTG CGGCAGAAGCACAGTTTCCC	58.2 58.5	93	Heat shock protein 10kDa Esi0000_0403
EsSAM	CCGTGGCGTACAAGGAGGAG TCGTGCTGCGTGGAGATGAC	59.3 58.9	76	S-Adenosylmethionine synthetase Esi0175_0026

6 ANNOTATION OF THE *E. siliculosus* GENOME

6.1 A SURVEY FOR GENES INVOLVED IN COPPER HOMEOSTASIS, DETOXIFICATION AND ANTI-OXIDANT RESPONSES

6.1.1 INTRODUCTION

At elevated concentrations, Cu is a toxic element, and organisms utilize homeostatic mechanisms to tightly control both intracellular concentration and activity of Cu, as well as other general detoxification systems. Molecular mechanisms for this tolerance were not fully deciphered for brown algae by the approaches developed in Chapter 2 and Chapter 5. Therefore, in order to draw new hypotheses and develop alternative approaches, I took the opportunity of the sequencing of the *Ectocarpus* genome (Cock *et al.* 2009) to conduct a genome-wide survey of proteins involved directly in metal uptake; of several chaperones, as well as proteins involved in the synthesis of metal-binding ligands (see general introduction). I also mined for homologues from various eukaryotes or bacteria enzymes which are involved in main anti-oxidative processes such as superoxide dismutase, catalase as well as the vascular plant water-water cycle, the glutathione-ascorbate cycle and the gluthathione peroxidase cycle [1]. As developed in the general introduction (see 1.3), a number of molecular mechanisms are employed by organisms in order to maintain copper homeostasis. In this study, exploration of the *E. siliculosus* genome was directed to provide insights into the mechanisms which regulate its copper stress response.

6.1.2 METHODS

A database with annotation interface was created for the manual annotation of the *Ectocarpus* genome and additional annotations were entered manually for the predicted genes (http://bioinformatics.psb.ugent.be/webtools/bogas/). Genes of interest were selected either using key-word searches or by tBlastn (BLOSUM62) searches against the *E. siliculosus* genome in the respective database at Bogas. Targeted sequences from plants and metazoans for blast searches were identified by key-word searches on GenBank (http://www.ncbi.nlm.nih.gov/Genbank). The identified *E. siliculosus* genes of interest were subsequently blasted (blastp) against the Uniprot database [2] (http://services.uniprot.org/) and NCBI database (http://blast.ncbi.nlm.nih.gov/Blast.cgi) where only genes presenting identity higher than 30%, and a blast score higher than 80 were considered. Further characterization was carried out by searching specific protein features on interpro or prosite websites (http://www.ebi.ac.uk/interpro/ and http://www.expasy.ch/prosite/ respectively). For membrane proteins, α-helix transmembrane domains (TMD) were searched in TMHMM, (http://www.cbs.dtu.dk/services/TMHMM/) based in hidden Markov prediction model [3]. Enzymes Gene Ontology [4] (GO) and the enzymes KOG number were determined by the websites AmiGO and KOGnitor (http://amigo.geneontology.org/ ; http://www.ncbi.nlm.nih.gov/COG/grace/kognitor.html). Signal peptides were searched using HECTAR (Heterokont Subcellular Targeting software [5]. ClustalW sequences alignments were carried out using on vector NTI software [6].

6.1.3 RESULTS

6.1.3.1 Copper homeostasis

I searched the genomic data of *E. siliculosus* to look for genes involved in copper uptake and transport (Table 1). Several families of transporters were detected.

6.1.3.1.1 Zrt-Irt-like proteins

The Zrt-Irt-like proteins or ZIPs, constitute a metal transporter family first identified in plants and capable of transporting a variety of divalent cations, including Cd, Fe, Cu, Mn and Zn [7,8]. In *E. siliculosus*, four ZIP gene orthologs were identified by sequence similarity in the genome database (Table 1). Although most ZIP transporters present 8 transmembrane domains (TMDs), *Ectocarpus* ZIP proteins seem to present only 7 TMDs. EsZIP1, EsZIP2 and EsZIP4 present conserved topology with variable region after TMD III (Fig S1;2;4). On the other side, EsZIP3 present divergent topology with respect to typical ZIP topology (Fig S3) [8]. The ZIP family in *Arabidopsis* counts one iron-regulated (IRT1) and forteen zinc-regulated transporters [9]. Metal uptake experiments and growth assays in yeast suggested that IRT1, despite acting as a broad range divalent metal ion transporter, do not transport Cu [10]. On the other hand, the *Arabidopsis* ZIP2 and ZIP4 family members seem to be involved in the uptake of Zn and Cu [11].

6.1.3.1.2 Ctr family of high affinity copper transporters

The copper transporter (Ctr) family of Cu^+ uptake systems are well conserved within eukaryotes and mediates high-affinity Cu acquisition from the extracellular medium into the cytoplasm of eukaryotic cells [12-15]. In *E. siliculosus*, one gene presenting sequence similarity to a Ctr gene was identified (Table 1). Its sequence showed highest similarity to yeast Ctr genes [15]. Characteristic methionine motifs MXXM in the N-terminal part and C/H

rich region in the C-terminal part are conserved [15]. In addition, the three TMDs are also conserved, accounting for the characteristic Ctr topology (Fig S5). In conclusion, this gene is thought to constitute an important component for copper uptake in *E. siliculosus* from the outer cellular region into the cytoplasm.

6.1.3.1.3 Copper transporting P-type ATPases

Copper P-ATPases are important copper transporter systems mediating active extracellular efflux and subcellular compartimentation. In *E. siliculosus,* three genes with sequence similarity to ATPases referred to as heavy-metal P-type ATPases (HMA) were annotated (Table 1) [16]. The three sequences are quite divergent, indicating probable different origins. The EsHMA1 sequence shows over 50% similarity to cyanobacterial P-type ATPase. This protein has conserved P-type ATPase features such as one HMA motif in the N-terminal end (N-ter), an E1-E2 ATPase domain, and a haloacid dehalogenase domain (HAD) in the C-terminal end (C-ter) (Fig. 1). On the other side, a hydropathy test showed only 3 TMDs, whereas P-type ATPases have 8 characteristic TMDs (Fig. S6). This result may indicate that the original protein function may have diverged. In addition, only 1 EST supports this gene model, which could either mean a wrong gene prediction, or that this gene is transcribed at a very low level. EsHMA2 displays high similarity with vascular plant HMAs such as AtHMA5, underlining its probable homologous function in copper homeostasis and detoxification in *Ectocarpus*. The enzyme topology showed a conserved HMA motif in the N-ter cytoplasmic region, E1-E2 ATPase domain and a HAD in C-ter (Fig. 1). Hydopathy test showed the presence of the 8 conserved P-ATPase TMDs (Fig. S7). EsHMA3 displays similarity with slime mold (*Dictyostelium discoideum)* P-type ATPases. Although general P-ATPase topology is conserved, such as N-ter HMA motif, E1-2 ATPase domain and C-ter HAD domains, some features are uncommon. Only 7 TMDs were observed. In addition, this enzyme has a long (575aa in contrast to ~150 commonly observed) N-ter cytosolic region

containing 5 HMA motifs (Heavy metal binding motifs) (Fig. 1). This feature diverges from normal P-ATPases that display ~ 170 pb region with 2 HMA domains [12,13,16], and may account for special copper efflux ability under metal stress conditions.

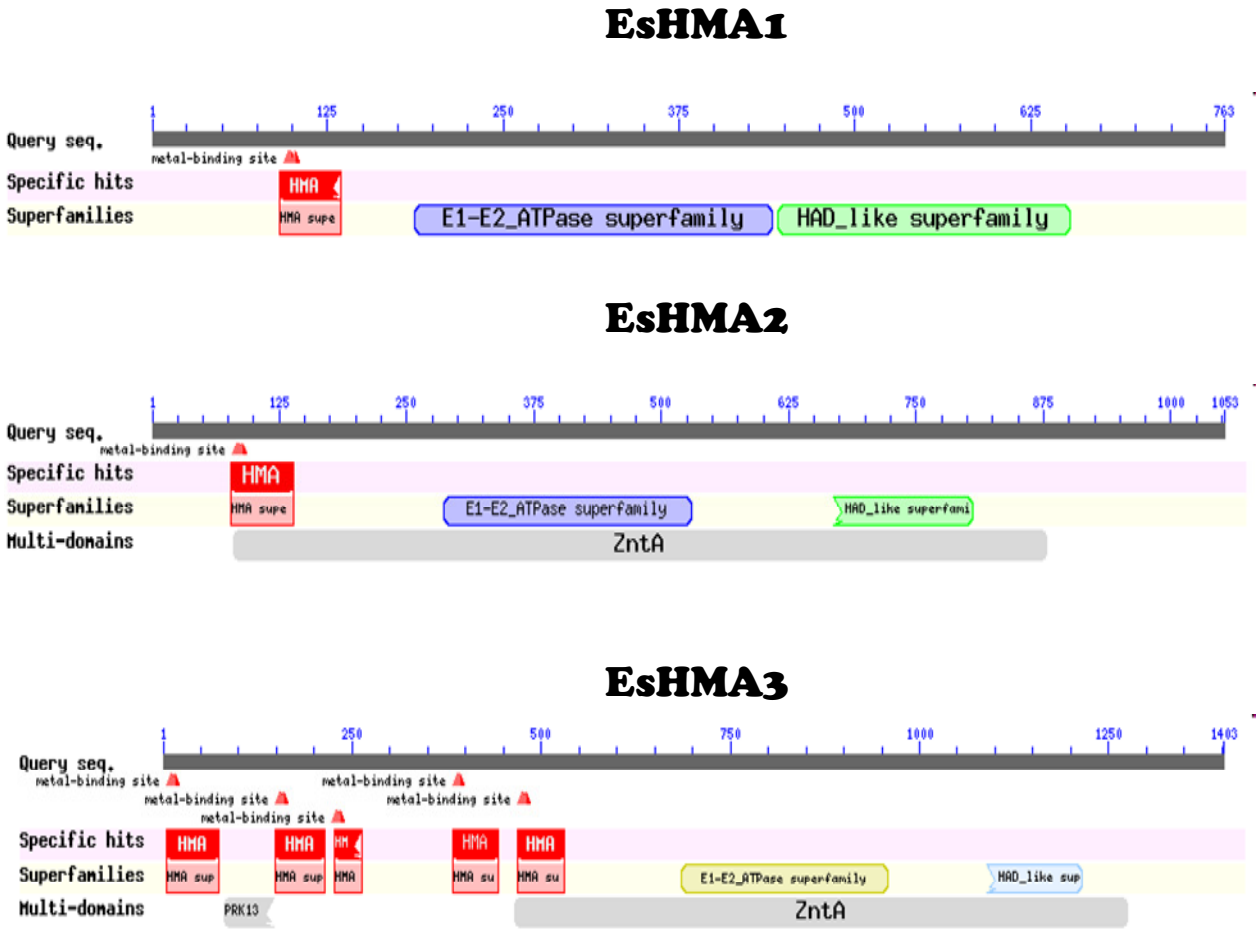

Figure 1. Summary of *E. siliculosus* P-ATPase features. All three enzymes contain the conserved metal-binding HMA motives, the E1-E2 ATPase superfamily domain, and the haloacid dehydrogenase domain. EsHMA3 exhibits an uncommon repetition of HMA motive. Each diagram was obtained by amino acid sequence analysis carried out at the NCBI website (http://blast.ncbi.nlm).

6.1.3.1.4 NRAMP divalent cation transporters

The NRAMP (Natural Resistance-Associated Macrophage Protein) is a family of divalent metal-ions transporters in eukaryotes (Table 1). One sequence presenting high similarity to the NRAMP family was identified showing high degree of identity to metazoan DMT (Divalent Metal Transporters) proteins. These proteins cotransport a variety of divalent metals including Cu^{2+} by proton motive force, mediating ion subcellular compartment distribution or uptake from out-cellular space (see General Introduction) [17]. EsNRAMP1 shows a conserved NRAMP domain with 12 TMDs which are a common feature of this family. The subcellular localisation is not clear. Based on higher plant examples, this transporter could mediate metal transport from the vacuole into the cytoplasm, regulating cytosolic metal concentrations [12].

6.1.3.1.5 Copper chaperones

The known copper chaperones in vascular plants are divided into four functional groups: Atx1-like chaperones (CCH), the copper chaperones for superoxide dismutase (CCS), the copper chaperones for cytochrome c oxidase and copper chaperones CutC like (COX17) [18] (see general introduction). The *E. siliculosus* genome presented one Atx1-like gene, showing high homology to plant-type CCH chaperones (Table1). This gene contains the conserved HMA motive (MxCxxC) that is related to copper binding. In addition, a mitochondrial chaperone sequence (Cox17) was identified. EsCOX17 contained a conserved active site for Cu(I) binding as two conserved residues Cys23 and Cys26 [19]. The presence of this protein confirms the existence of a conserved copper delivery mechanism to mitochondria in brown algae. No sequence with homology to CCS was found in the genome while one CutC gene was identified. This sequence showed high homology to bacterial CutC proteins. Blast results indicate that the *Ectocarpus* protein belongs to the CutC superfamily.

6.1.3.2 Metal chelating mechanisms

6.1.3.2.1 Metallothioneins

Metallothioneins (MT) are ubiquitous small proteins that present two cystein rich domains and one spacer in between *E. siliculosus* genome contains 2 MTs (Table 1). Both, of them EsMT1 and EsMT2, contained Cys residues which are highly conserved among plant, animal and algal sequences (Fig. 2). EsMT1 is highly similar to *Fucus* MT (FvMT), with over 60% of identity. EsMT1 shows a 16 aa spacer and a total of six CXC motives distributed equally among the two Cys domains, which allow to classify it as a type I MTs [20]. However, like in the *Fucus* MT, the spacer region is smaller than other MTs from class I [21]; therefore, this feature could be characteristic of brown algal MTs. EsMT2 is smaller than EsMT1, and shows similarity to small plant-type I MTs. This protein has an extremely reduced spacer with CXC motives along the Cys-rich regions as well, which is similar to plant small MTs (Fig. 2). In addition, 40 ESTs are related to EsMT2 gene illustrating its high transcription rate. (Table 1). MTs of type I and II appear to be important chelation actors in vascular plants [22]. In addition, the expression of MT in *F. vesiculosus* is induced by copper excess, and its recombinant protein showed a greater affinity for Cu than for Cd [21]. The pH required for dissociation of Cd from FvMT was approximately 2 pH units higher than for a recombinant human MT. Moreover, a role of MTs in recycling metals has been suggested in plants, in particular for free copper after degradation of metalloproteins [20]. Therefore, taking into account all the functions encountered by MT in vascular plants and brown algae, it is likely that MTs play a role in copper homeostasis.

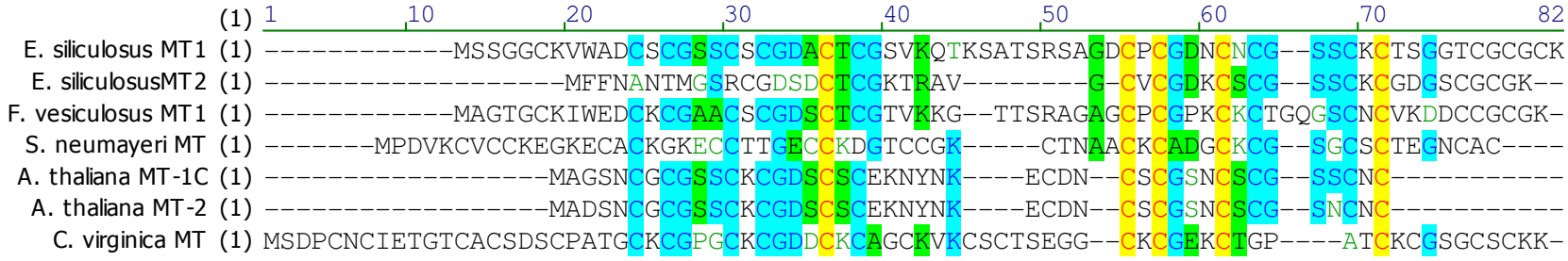

Figure 2. Amino acid alignment between the *E. siliculosus* Metallothioneins (MT) and MTs from *Fucus vesiculosus*, *Sterechinus neumayeri, Arabidopsis thaliana and Crassostea virginica.* Conserved Cys motifs are observed along the MT family and highlighted in yellow. The alignment was produced with ClustalW.

6.1.3.2.2 Phytochelatin synthetase

Phytochelatin synthetase (PCS) catalyses the production of phytochelatins which are short polypeptides synthesized from glutathione that play a pivotal role in metal tolerance. PCS possess a conserved N-terminal region among organisms while the C-terminal part is more variable [23]. In addition, the C-ter region contains several Cys residues [20]. *E. siliculosus* displayed one PCS gene (EsPCS), which is comparable to the situation in plants and animals [24] (Table 1). The sequence analysis of EsPCS showed over 60% of identity with plant PCS (Fig. 3), whereas much lower similarity was observed with a putative *Thalassiosira pseudonana* PCS (18% of identity). Interestingly, the conserved N-ter region among plant PCS corresponded to the C-ter region of EsPCS and the N-ter region of the algal sequence did not present Cys residues. A number of 11 ESTs support the EsPCS model, which account for its active transcription. As previously exposed, the presence of phytochelatins has been reported in brown algae [25,26] in response to copper stress, suggesting that PCS plays an active role in metal resistance.

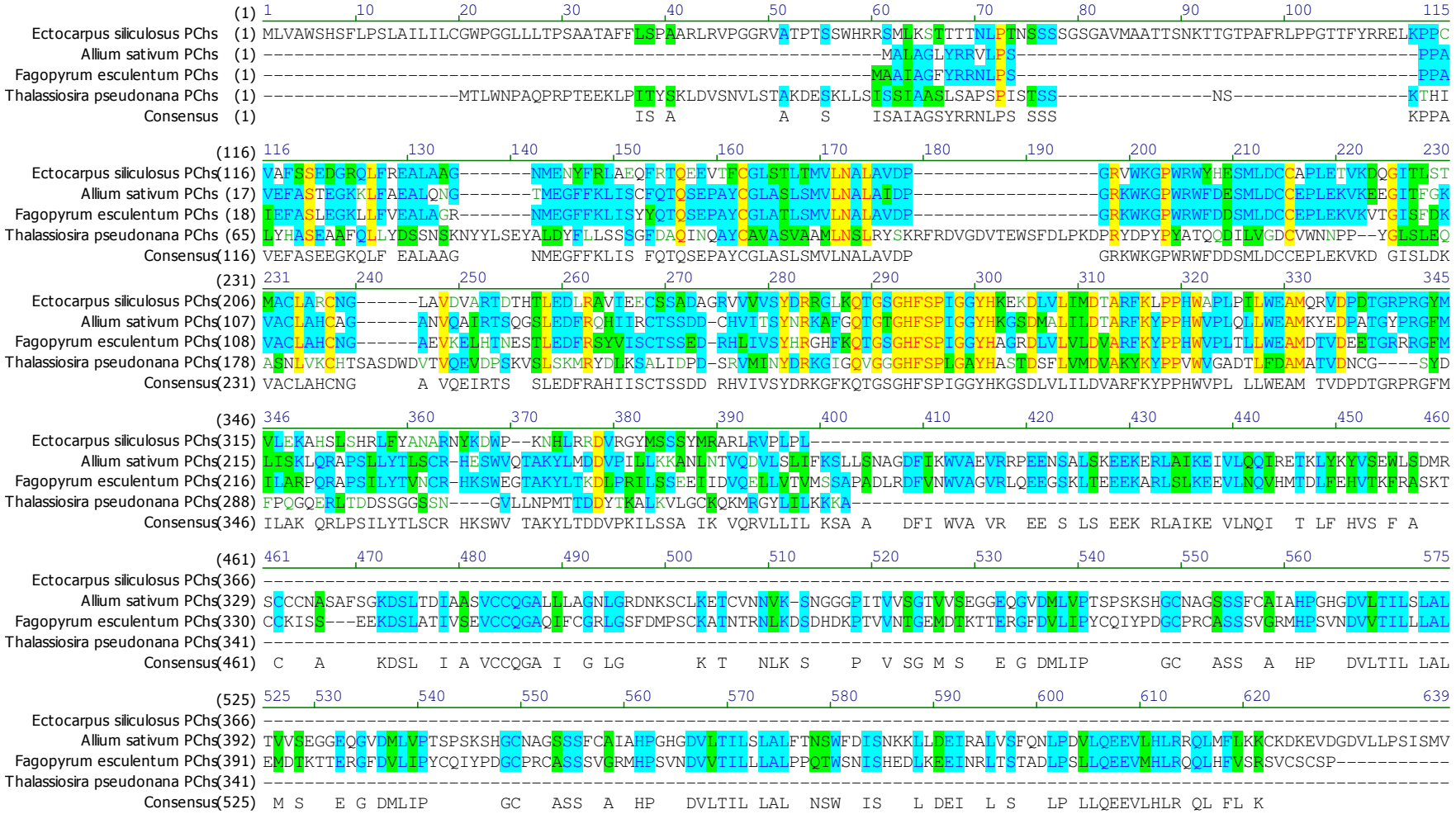

Figure 3. Amino acid sequences alignment (ClustalW) of Phytochelatin synthases (PCS) that compares the *Ectocarpus* PCS to the vascular plants *Allium sativum*, *Fagopyrum esculentum* and heterokont *Thalassiosira pseudonana*.

6.1.3.2.3 Phytochelatin vacuolar ABC transporter

Once PC chelates metals, the complexes are stored in the vacuole. This transport is mediated by a multidrug ABC type transporter [27]. One gene presenting 25% similarity to PC ABC transporter was identified (Table 1). Sequence features typical of a multidrug transporter are conserved, such as 9 TMDs, and a P-loop N-ATPase domain with an ABC transporter motive (Fig. S10). This multidrug ABC transporter could mediate the transport of PC into the vacuole. In addition, this protein presents a signal peptide that may target it to the vacuole. However, there are several other ABC transporters in the *Ectocarpus* genome that could mediate this transport, indicating that further studies must be carried out to confirm this prediction.

Table 1. Annotated *E. siliculosus* genes coding for proteins involved in copper homeostasis and chelation mechanisms

Family	Name	Genome database accession code	Theoretical localisation	Signal peptide	Signal anchor	AA	TMD	EST	% Identity Blast	KOG	Description	Coments
ZIP	EsZIP1	Esi0016_0180	Plasma membrane	No	Yes	400	7	3	29%	KOG1558	Divalent cation uptake transporter (classical Zn/Fe-transporter)	AtZIP4, paralog to EsZIP2 Variable region after IIITMD
	EsZIP2	Esi0016_0179	Plasma membrane	Yes	Yes	354	7	0	34%	KOG1558	Divalent cation uptake transporter (classical Zn/Fe-transporter)	AtZIP4, paralog to EsZIP1, Variable region ater III TMD
	EsZIP3	Esi0444_0001	Plasma membrane	No	No	277	7?	4	30%	KOG2474	Divalent cation uptake transporter (classical Zn/Fe-transporter)	Present similarity with AtZIP, however, this protein lack tipicall ZIP structure, High silmilarity with predicted transporter in P. tricornutom (see supplementary data)
	EsZIP4	Esi0111_0079	Plasma membrane	Yes	Yes	430	7or 8	15	36%	KOG1558	Divalent cation uptake transporter (classical Zn/Fe-transporter)	Present ZIP structure. Similar to Chlamydomonas ZIPs (see supplementary data)
Ctr	EsCtr1	Esi0021_0108	Plasma membrane	No	No	152	3	6	34%	KOG3386	High affinity copper transporter	Conserved Nter MXXM motifs and Cter Cys/His domains, 3 TMD
HMA	EsHMA1	Esi0125_0069	Plasma membrane/ Golgy apparatus	No	No	896	6?	1	42%	KOG0207	Copper Transporting P-type ATPase	Nter HMA and CPx mtifs are conseved. Sequens display similarity to Cyanobacterial P-ATPase, however 8 TMD in this family seem not to be respected.
	EsHMA2	Esi0023_0054	Plasma membrane / Golgy apparatus	No	No	1053	8	3	42%	KOG0207	Copper Transporting P-type ATPase	Nter HMA and CPC motifs are conseved, high similiarity with AtHMA5, 8 TMD are conseved HMA ATPase topology is conserved
	EsHMA3	Esi0009_0037	Plasma membrane / Golgy apparatus	No	No	1403	7	8	40%	KOG0208	Copper Transporting P-type ATPase	5 repeated Nter HMA domains in Nter E-ATPase motifs close to dyctiostellum pATPase, HMA Topology is not conserved
NRAMP	EsNRAMP1	Esi0141_0009	Vacuole	No	No	629	12	0	49%	KOG1291	Divalent metal transporter, mostlyFe(II)	Conserved 12 TMDs, Topology of RAN transported is conserved
HMT	EsHMT1	Esi0060_0030	Vacuole	Yes	no	905	9	0	25%		Multidrug ABC transporter	
ATX-like	EsCCH	Esi0188_0038	Cytoplasm	No	No	75	0	1	40%	KOG1603	Intracelular Cu(I) transport	Heavy Metal Associated (HMA) domain 1
CutC	EsCutC	Esi0059_0052	Cytoplasm	No	No	226	0	0	53%	KOG4013	Intracelular Cu(I) transport	
Cox17	EsCox17	Esi0079_0019	Mitochondria	No	No	84	0	1	43%	KOG3496	Mitochondrion cytochrome C Cu(I) delivery	All Blast matches related to green plants Cox17. Topoligy an lengthe are well conserved
PCS	EsPCS	Esi0399_0022	Cytoplasm	No	No	503	0	11	53%	KOG0632	PCS catalyse the biosynthesis of phytochelatins from GSH	In the opposite form other PCs, the Cter is conserved but not Nter
MT	EsMT1	Esi0351_0016	Cytoplasm	No	No	69	0	4	54%		Metal chelating peptides	Two Cys rich domains are conserved and a small linker, Close to *Fucus vesiculosus* MT, thus may be specific MT family form brown algae
	EsMT2	Esi0075_0040	Cytoplasm	No	No	51	0	40	47%		Metal chelating peptides	High number of ESTs. Linker between 2 cys domains is very reduced. Close to mollusks and *F. vesiculosus* MT

6.1.3.3 Oxidative stress

Like all photosynthetic organisms, *E. siliculosus* has to cope with the normal excessive generation of reactive oxygen species (ROS) during photosynthesis and aerobic metabolism. In addition, copper toxicity causes an unbalanced cellular redox status which induces are increased production of ROS. In order to avoid oxidative stress, effective antioxidant systems must be set up by *Ectocarpus*. We have listed and commented below on key conserved components of antioxidant pathways such as the superoxide dismutase, catalase, the enzymes of the plant water water cycle, the ascorbate glutathione cycle, the glutathione peroxidase cycle (Table 2-3).

6.1.3.3.1 Superoxide Dismutase (SOD)

The *E. siliculosus* genome has 6 genes encoding for enzymes of the Mn/FeSOD family (Table 2). All of them have a conserved metal binding motive DVWEHAYY. In some cases, the determination of the exact metal co-factor can not be based on sequence analysis prompting us to annotate 3 of these candidates as Mn/FeSODs.

On the other hand, much conserved blast results allowed me to identify two proteins as MnSOD and one as FeSOD. Concerning the Cu/ZnSOD family, two paralogs have also been detected, and thus annotated as EsCu/ZnSOD1 and EsCu/ZnSOD2. Both of these genes have a conserved Cu/ZnSOD dimerisation motive in the C-ter region. However, one of the two conserved His in the co-factor binding motive has been replaced by a PheA. Since this His residue is fundamental for enzyme activity, it is not sure that these enzymes are active. Both of these gene models are supported by ESTs, therefore they seem to be transcribed. On the other hand no copper chaperone for CuZnSOD (CCS) was identified, raising the question of how the copper cofactor is delivered into these proteins. No match was encountered in the *Ectocarpus* genome with the recently described Ni SOD found in marine cyanobacteria [28].

6.1.3.3.2 Catalase

Catalases (CAT) are plant haeme-dependent peroxidases that catalyse the destruction of hydrogen peroxide into oxygen. These enzymes are normally localized in the peroxisome and have important functions in the control of oxidative stress [1]. A total of 8 genes encoding potential catalases were found, the corresponding proteins exhibiting conserved heme domain, active sites, and substrate binding motive (Table 2). All CAT genes present high similarity (over 80-90%) to each other, suggesting that these proteins belong to a multigenic family. Most of these genes present a signal peptide which may targeted them to the peroxisome.

Table 2. Annotated *E. siliculosus* genes coding for antioxidant enzymes

Family	Name	Genome database accession code	Theoretical localisation	Signal peptide	Signal anchor	AA	TMD	EST	% Identity Blast	KOG	Description	Coments
SOD	EsFe/MnSOD1	Esi0201_0013	Mitochondria (Mn); Chloroplasts (Fe) and peroxisomes (Mn)	No	No	197	0	6	65%	KOG0876	Destroys Superoxide radical to produce hydrogen peroxyde	All blast matches with SOD from marine bacteria. Cofactor binding motif is present (DVWEHAYY). The exact co factor (Mn or Fe) is not clear
	EsFe/MnSOD2	Esi0219_0002	Mitochondria (Mn); Chloroplasts (Fe) and peroxisomes (Mn)	Yes	No	230	0	14	54%	KOG0876	Destroys Superoxide radical to produce hydrogen peroxyde	Cofactor binding motif is persent (DVWEHAYY). The exact co factor (Mn or Fe) is not clear
	EsFe/MnSOD5	Esi0342_0001	Mitochondria (Mn); Chloroplasts (Fe) and peroxisomes (Mn)	Yes	No	170	0	3	36%	KOG0876	Destroys Superoxide radical to produce hydrogen peroxyde	D is exchaged by F in the cofactor binding motif (DVWEHAYY). The exact co factor (Mn or Fe) is not clear
	EsMnSOD3 (putative)	Esi0002_0116	Peroxixome; Mitochondria	No	No	231	0	5	61%	KOG0876	Destroys Superoxide radical to produce hydrogen peroxyde	Cofactor binding motif is persent (DVWEHAYY). The exact co factor (Mn or Fe) is not clear
	EsMnSOD4 (putative)	Esi0091_0024	Peroxixome; Mitochondria	No	No	301	0	8	51%	KOG0876	Destroys Superoxide radical to produce hydrogen peroxyde	Cofactor binding motif is persent (DVWEHAYY). All blast are Mn SOD
	EsFeSOD5 (putative)	Esi0421_0005	Chloroplast	Yes	No	231	0	7	55%	KOG0876	Destroys Superoxide radical to produce hydrogen peroxyde	Cofactor binding motif is persent (DVWEHAYY). The exact co factor (Mn or Fe) is not clear
	EsCuZnSOD1 (putative)	Esi0003_0324	Chloroplast; Apoplasm; Cytosol	No	No	157	0	2	52%	KOG0441	Destroys Superoxide radical to produce hydrogen peroxyde	Cter motif (GNAGGRLACGV) is present, but in the cofactor bindin motif is one of the two important H has been replaced by R (GFHVHALGDTT); 70% identity with EsCuZnSOD2
	EsCuZnSOD2 (putative)	Esi1648_0001	Chloroplast; Apoplasm; Cytosol	No	No	117	0	4	63%	KOG0441	Destroys Superoxide radical to produce hydrogen peroxyde	Cter motif (GNAGGRLACGV) is present, but in the cofactor bindin motif is one of the two important H has been replaced by R (GFHVHALGDTT); 70% identity with EsCuZnSOD1
CAT	EsCAT1	Esi0043_0035	Peroxisome	No	No	631	0	0	46%		Destroys Hydogen peroxyde to produce Oxygen	Haem domain present. Paralog to Esi0083_0078
	EsCAT2	Esi0045_0115	Peroxisome	No	No	539	0	7	68%	KOG0047	Destroys Hydogen peroxyde to produce Oxygen	Haem domain present. Blast matches highly conserved metazoans catalases
	EsCAT3	Esi0079_0050	Peroxisome	Yes	No	509	0	2	44%		Destroys Hydogen peroxyde to produce Oxygen	Haem domain present
	EsCAT4	Esi0083_0078	Peroxisome	Yes	No	515	0	0	46%		Destroys Hydogen peroxyde to produce Oxygen	Haem domain present. Paralog to Esi0043_0035
	EsCAT5	Esi0262_0012	Peroxisome	Yes	No	517	0	0	37%		Destroys Hydogen peroxyde to produce Oxygen	heem domain present paralog to Esi0611_0008; ESi0612_0005, EsiEsi0079_0050 and Esi772_0002
	EsCAT6	Esi0611_0008	Peroxisome	Yes	No	1114	0	0	43%		Destroys Hydogen peroxyde to produce Oxygen	Haem domain present. The gene is not well annotated (two genes). This gene is paralog to Esi0262_0012; Esi0079_0050 and is duplicated in the locus Esi0612_0005 (98% identity)
	EsCAT7	Esi0612_0005	Peroxisome	Yes	No	504	0	1	43%		Destroys Hydogen peroxyde to produce Oxygen	Haem domain present parlog to Esi0612_0001; Esi0612_0004; Esi0612_0008; Esi0611_0008 (98% identity), Esi0262_0012 and Esi772_0002
	EsCAT8	Esi0772_0002	Peroxisome	Yes	No	505	0	1	43%		Destroys Hydogen peroxyde to produce Oxygen	Heem domain present This gene belong to a multigenic family with paralogy to Esi0611_0008; ESi0612_0005, Esi0079_0050 and Esi0262_0012

6.1.3.3.3 Glutathione peroxidase

Glutathione peroxidases (GPX) are enzymes that catalyse the reduction of hydroperoxides by glutathione (GSH) oxidation. They play an important antioxidant role in the plant GSH-ascorbate (AsA) and GPX cycles (see general introduction). A total of 7 members of this family were found in the *Ectocarpus* genome (Table 3). All proteins contain a thioredoxin fold, a dimerisation site, and Cys/Ura catalytic motives. EsGPX6 is encoded by the mitochondrial genome. Interestingly, this gene has high similarity with cyanobacterial GPX.

6.1.3.3.4 Glutathione redutase

Glutathione reductases (GR) are NADH oxidases that catalyze the reduction of oxydized gluthathione, using NAD(P)H as cofactor [1]. They are important members of the GSH-AsA cycle, and of the GPX cycle. The Blastp results showed two conserved GRs in the *E. siliculosus* genome (Table 3). Theses enzymes presented conserved GR features, with an NAD(P)H binding domain (Pyr_redox), and a dimerisation domain (Pyr_redox-dim). Eighteen EST are associated with EsGR1, while EsGR2 is represented by only one.

6.1.3.3.5 Dehydroascorbate reductase

One dehydroascorbate reductase (DHAR) was identified in *E. siliculosus* (Table 3). DHAR features were present, such as a thioredoxin-like and a DHAR-GST- C domain. DHARs are monomeric enzymes catalyzing the reduction of DHA into AsA using glutathione as the reductant. They allow plants to recycle oxidized AsA, therefore they are important in the GSH-AsA cycle [1]. This sequence has a signal peptide, but its specific subcellular location is unclear.

6.1.3.3.6 Monodehydroascorbate reductase

One sequence presented high similarity to a monodeshydroascorbate reductase (MDAR) gene in the *E. siliculosus* genome (Table 3). MDAR catalyses the reduction of monodehydroascorbate into AsA, therefore they are important for the AsA recycling in the GSH-AsA cycle [1]. Conserved MDAR features were found in this protein such as a NAD(P)H binding domain (Pyr_redox).

6.1.3.3.7 Ascorbate Peroxidase

One sequence coding for an ascorbate peroxidase (APX) was identified (Table 3). This heme metalloenzyme catalyses the peroxidation of AsA into MDA. Heme domain and iron co-factor His motive are conserved in the *E. siliculosus* sequence. This enzyme is encoded by the chloroplast genome.

Table 3. Annotated *E. siliculosus* genes coding for antioxidant enzymes

Family	Name	Genome database accession code	Theoretical localisation	Signal peptide	Signal anchor	AA	TMD	EST	% Identity Blast	KOG	Description	Coments
GPX	EsGPX1	Esi0152_0006	Mitochondrion	No	No	199	0	17	58%	KOG1651	Catalyses the reduction of hydroxyperoxides by glutathione oxydation	Thioredoxin fold, dimerisation site and Cys/Ura catalytic motifs presents
	EsGPX2	Esi0099_0085	Cytoplasm?	Yes	No	195	0	9	45%	KOG1652	Catalyses the reduction of hydroxyperoxides by glutathione oxydation	Thioredoxin fold, dimerisation site and Cys/Ura catalytic motifs presents
	EsGPX3	Esi0192_0041	Cytoplasm?	No	No	226	0	6	57%	KOG1653	Catalyses the reduction of hydroxyperoxides by glutathione oxydation	Thioredoxin fold, dimerisation site and Cys/Ura catalytic motifs presents
	EsGPX4	Esi0152_0008	Cytoplasm?	Yes	No	206	0	4	53%	KOG1654	Catalyses the reduction of hydroxyperoxides by glutathione oxydation	Thioredoxin fold, dimerisation site and Cys/Ura catalytic motifs presents
	EsGPX5	Esi0049_0025	Cytoplasm?	No	No	291	0	3	31%	KOG1655	Catalyses the reduction of hydroxyperoxides by glutathione oxydation	Thioredoxin fold, dimerisation site and Cys/Ura catalytic motifs presents
	EsGPX6	Esi0509_0009	mitochondrion	No	No	240	0	2	54%	KOG1656	Catalyses the reduction of hydroxyperoxides by glutathione oxydation	Thioredoxin fold, dimerisation site and Cys/Ura catalytic motifs presents. Matches to cyanobacterial peroxidases
	EsGPX7	Esi0007_0074	Cytoplasm?	No	No	141	0	0	52%	KOG1657	Catalyses the reduction of hydroxyperoxides by glutathione oxydation	Thioredoxin fold, dimerisation site and Cys/Ura catalytic motifs presents
GR	EsGR1	Esi0019_0176	?	No	No	483	0	18	54%	KOG0405	Converts oxidized glutathione to reduced glutathione using NADPH	Pyr_redox and Pyr_redox-dim domains are conserved
	EsGR2	Esi0888_0002	?	No	No	324	0	1	58%		Converts oxidized glutathione to reduced glutathione using NADPH	Pyr_redox and Pyr_redox-dim domains are conserved
DHAR	EsDHAR	Esi0041_0089	?	Yes	No	330	0	6	37%		Catalyze the reduction of dehydroascorbate into reduced ascrobate in prescence of reduced gluthatione	Thioredoxin-like and a DHAR-GST- C domains are conserved
MDAR	EsMDAR	Esi0039_0037	?	No	No	557	0	3	31%	KOG1336	Catalyse the reduction of Monodesydroascorbate into ascorbic acid	Pyr_redox NAD(P)H binding domain is conserved
APX	EsAPX1	Esi0438_0006	Chloroplast	No	No	379	0	5	55%		Catalyses the peroxydation of ascorbic acid into MDA	heme perxidase 4 daomain with conserved H Iron binding motif

6.1.4 CONCLUDING REMARKS

To summarize, I contributed to the expert annotation of more than 15 genes, encompassing proteins which are involved in copper transport and chelation. Most of them are supported by ESTs, accounting for their activity in cellular homeostasis. Some of them are represented by 1 or few ESTs, and other seems to be highly expressed, such as *EsMT2* with 40 ESTs. Copper-related transcription factors homologues such as the nutritional copper ion-sensing transcription factor, Mac1p, the yeast transcription factor Ace1 or metallothionein transcription factor Cup2 were not identified. Altogether, theses results indicate that copper homeostasis mechanisms in brown algae are for the most part conserved with other eukaryotic lineages, however their regulation by transcription factors seems to differ. Based on the annotated genes, theoretical models for copper homeostasis and detoxification in *E. siliculosus* are presented in figures 4-5. It is likely that these proteins play the same role as in other organisms. However, information only based on sequence analysis can not give a full picture of the actual mechanisms taking place in the cell. Therefore, experimental data are necessary to better characterize the mechanisms involved in copper homeostasis, and a preliminary account is provided in the next section. Furthermore, considering the bioavailability of copper in seawater, it is likely that additional mechanisms for copper concentration and uptake exist in algae. In this sense, it is possible that the mechanisms identified in other organisms and described through the annotation of the genes above interact with specific brown algal systems such as the charged polysaccharide cell wall that may play a pivotal role in metal transport and/or sequestration (see general introduction). Plant phytosiderophore systems such as nicotinamine were not found to be conserved in *Ectocarpus*, however, existing preliminary data account for the presence of bacterial siderophore-like Fe chelating mechanisms (Küpper, unpublished data). Therefore, it is not impossible that this latter system could also work for other divalent metals such as copper.

Concerning antioxidant systems, a total of 28 enzymes were annotated, corresponding to proteins involved in important ROS detoxification systems in plants and metazoans. Consequently, there is consistent evidence for the existence of conserved antioxidant enzymes and cycles in *Ectocarpus*. However, additional brown algal antioxidant systems have been described, involving iodide metabolism [29]. Although *E. siliculosus* has only one vBPO gene, further research must be carried out in order to fully elucidate the major antioxidant actors in this species.

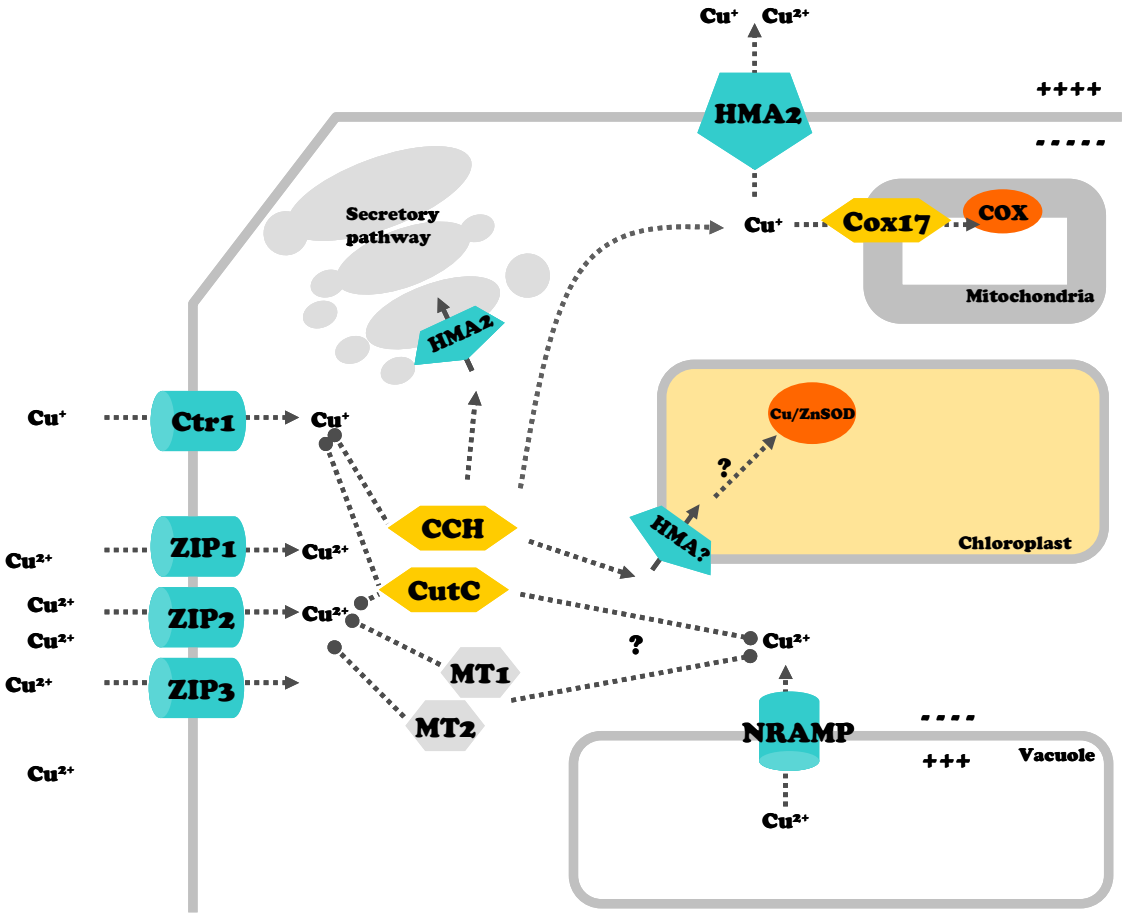

Figure 4. Putative subcellular distribution of copper in *E. siliculosus.* Cu transporters are represented in blue, Cu chaperones in orange, and copper metalloproteins in red. Dotted lines indicate putative Cu delivery pathways. Arrows at the end of lines mean copper delivery and balls mean copper binding. Question marks indicate unclear chaperones and/or unclear steps. Ctr1, copper transporter; COX, cytochrome *c* oxidase; CCH, copper chaperone; CutC, copper chaperone C of the Cut gene family; MT, metallothionein; SOD, superoxide dismutase; HMA, heavy metal P-type ATPase; NRAMP, natural resistance associated macrophage protein.

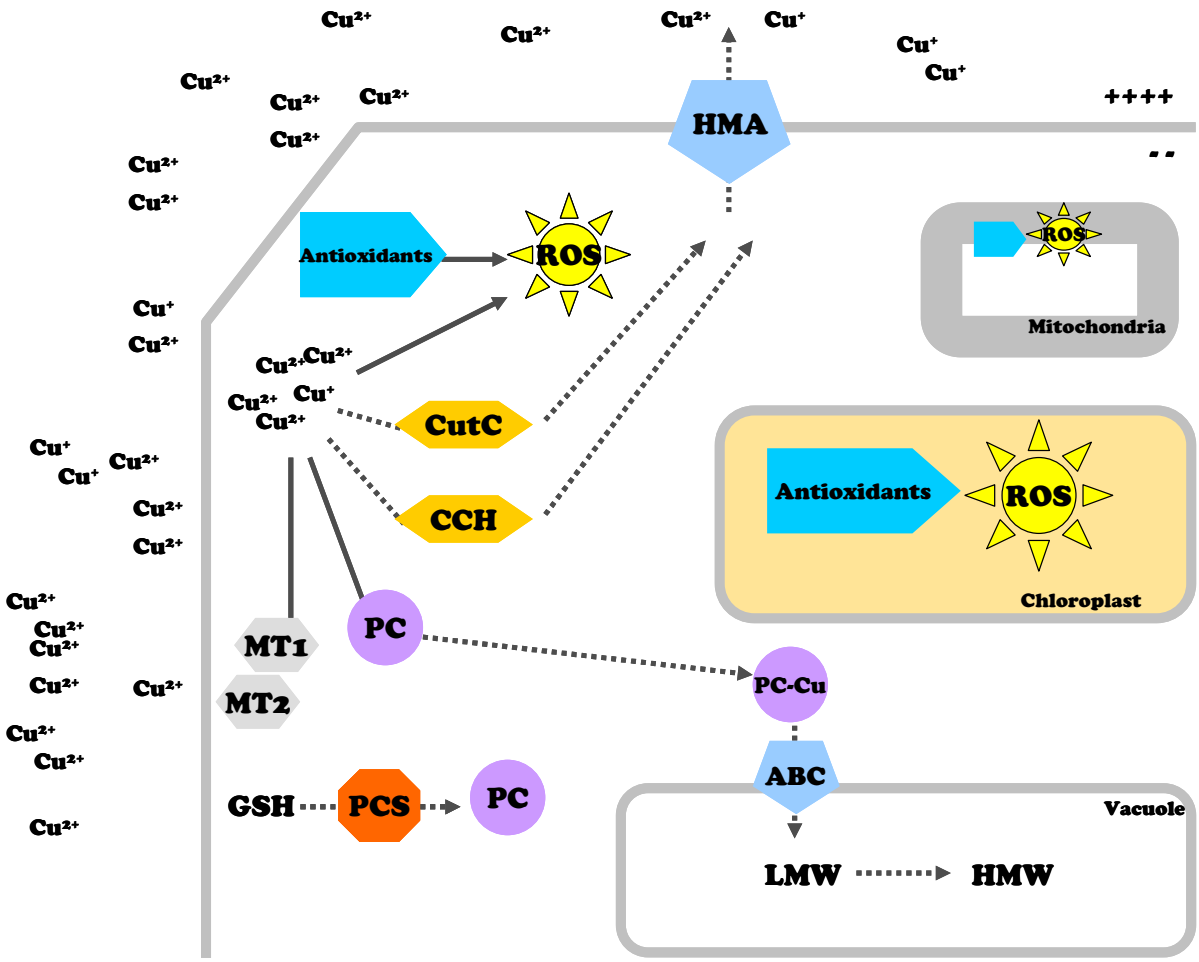

Figure 5. Speculative diagram of subcellular copper detoxification in *E. siliculosus*. Continuous lines represent demonstrated mechanisms in brown algae, and discontinuous lines are demonstrated mechanisms in other organisms. Balls at the end of lines mean copper binding. CCH, copper chaperone; CutC, copper chaperone C of the Cut gene family; MT, metallothionein; HMA, heavy metal P-type ATPase; PCS, phytochelatin synthase; GSH, glutathione; ABC, multidrug ABC transporter, LMW, phytochelatin low molecular weight complexes, HMW, phytochelatin high molecular weight complexes.

6.2 PRELIMINARY CHARACTERIZATION OF CANDIDATE GENES IDENTIFIED THROUGH E. siliculosus GENOME ANNOTATION

6.2.1 INTRODUCTION

Gene mining and annotation work was completed by preliminary functional characterization of a small subset of *Ectocarpus* genes, including analysis of gene expression by RT-PCR, and attempts of functional complementation of one yeast mutant by *EsMT1*. The candidate genes *EsMT1* and *EsPCS* were selected to be further characterized because of their important role in heavy metal detoxification in other organisms. We have also studied the expression of the copper-transporting chaperone gene *EsCCH* and the antioxidant copper metalloenzyme *EsCuZnSOD1*. The expression of all of these genes was monitored under chronic copper stress (and some also under acute stress) conditions, in order to observe whether metal stress affects their transcription pattern, thus indicating their probable involvement in metal homeostasis. For some enzymes such as the *EsMT1* and the *EsPCS,* the changes in gene expression were followed for two different strains presenting contrasting response to copper stress, the metal-tolerant strain Es524 and the copper sensitive Es32 (see chapter 5). Additional physiological tests such as the determination of lipoperoxide content were carried out for estimating potential oxidative stress damage under copper stress conditions.

6.2.2 MATERIALS AND METHODS

6.2.2.1 Plant material and treatments

E. siliculosus (Ectocarpales, Phaeophyceae) unialgal strains 32 (CCAP accession 1310/4, origin San Juan de Marcona, Peru 15°22'S, 75°10'W) and 524 (origin Caleta Palito, Chile 26°15'S, 70°40'W) were cultivated as described in Chapter 5. Two days before the set of the copper stress experiment, tissues were transferred into 1 L of organic matter-free seawater prepared with 0.22 µm filtered natural SW treated with 0.2 g/L of activated charcoal overnight. Then, the charcoal-treated seawater was re-filtered at 0.45 µm in order to remove charcoal. The culture flasks used during the experiments were washed with 1 % HCl overnight in order to limit copper absorption by glass. To initiate copper stress, the medium was changed with fresh organic matter-free seawater enriched with $CuCl_2$ (Merk, Germany) in order to obtain nominal copper final concentration of 25, 50, 250, and 500 µg/L. No nutrients were added during the experiment. For each kinetic point, three biological replicates were harvested. At the end of the experiment, thalli were frozen in liquid nitrogen and kept at -80 °C for analysis.

6.2.2.2 Lipoperoxide assay

E. siliculosus, strain 32 was submitted to 25 and 50 µg/L of nominal copper for 6, 8 and 10 days. Lipoperoxides were analysed after these periods of time. The TBAR test in *E. siliculosus* was operated as previously described in the materials and methods section of the chapter 2.

6.2.2.3 RNA extraction, cDNA synthesis, and RT-PCR

Total RNA from *E. siliculosus* was extracted as reported in chapter 5. The three RNA samples corresponding to the same condition were pooled at equal concentrations to help

minimizing variations between individual RNA extracts. After pooling, one µg of total RNA corresponding to each treatment was used to synthesize single strand cDNA using the SuperScript Double-Stranded cDNA Synthesis Kit (Invitrogen, USA), as recommended by the manufacturer. Semi-quantitative RT-PCR was carried out as previously described in chapter 2. Actin served as reference gene.

Quantitative PCR was run as previously described in chapter 2. Primers were designed as exposed in chapter 2, and are listed in Table 4.

Table 4. Specific characteristics of the primers utilized for gene expression analyses by reverse transcriptase quantitative polymerase chain reaction (RT-qPCR).

Gene	Primer name	Primer sequence (5'-3')	Tm	Amplified fragment size (bp)	*E. siliculosus* genome database matches and Accession Number	Comments
EsMT1	ESMT1F	CATGTTCTTCAACGCTAACACCA	55	154	Metallothionein; Esi0351_0016	semiQ RT-PCR
	ESMT1R	TGCGGATGCGGCAAGTAA	55			
	Esi0351_0016MTex2Qfw	TCGTGCTCTTGCGGTGAC	55	56	Metallothionein; Esi0351_0016	Q RT-PCR
	Esi0351_0016MTex2Qrv	GCGGACTTGGTCTGCTTC	55			
EsPCS	Esi0399_0022PCex1Qfw	TGCTGACACCATCTGCTGCTAC	60	82	Phytochelatin synthase; Esi0399_0022	Q RT-PCR
	Esi0399_0022PCex1Qrv	GGCGTTGCTACTCTTCCTCCTG	60			
EsACT	EsilACT1	CGGCATCGTGACCAACTGG	55	259	Actin; Esi0203_0038	semiQ RT-PCR
	3'Esactin	GACTCGGGTGACGGCGTG	55			
EsCCH	EsilCC1	ATGAGCGAGACGACCGTGTTC	55	231	Copper Chaperone; Esi0188_0038	semiQ RT-PCR
	EsilCC2	GTTATTCTAGCTGGCGAGCTC	55			
EsCuZnSOD1	EsSODCuZn1F	AAGGCAAGCTGCGTGATGAC	55	316	CuZn Superoxide dismutase; Esi0003_0324	semiQ RT-PCR
	EsSODCuZn1R	TAAGCCTCACCATTCGGTCTTC	55			

6.2.2.4 Complementation of the yeast mutant Δace1 by the EsMT1 gene

The entire *EsMT1* coding region was amplified from *E. siliculosus* strain 32 cDNA with primers GGGGAAGCTTACC**ATG***GCT*TCGAGCGGAGGATGCAAG -3′ (open reading frame (ORF) start codon is indicated by bold type; the underlined sequence is a *Hind*III site; the italic sequence is an added alanine codon, not present in the original sequence of *EsiMT1*) and CCCCCCGAATTC**CTA**CTTGCAGCCGCAGCC-3′ (ORF stop codon is indicated in bold type; underlined sequence is a *Eco*RI site). The amplified sequence was cloned into the pGEM-T vector and inserted into competent *E. coli* cells, strain JIM109,

following the manufacturer's instructions (Promega, USA). The *EsMT1* gene was then restricted by *Hind*III and *Eco*RI, gel-purified, and cloned into the corresponding sites behind the galactose-inducible GAL1 promoter of pYES2 (Invitrogen) to yield the plasmid pYEsMT1. This vector was transformed into *E. coli* strain JIM109 following the manufacturer's instructions (Promega, USA). The plasmid pYEsMT1 was then extracted from *E. coli*, and used to transform the *Saccharomyces cerevisiae* strain DTYG7 (Δace1, kindly provided by Jean Labarre) by the lithium acetate method; transformants were selected on minimal medium plates lacking uracil. As a control, empty pYES2 vector was also transformed into yeast. Presence of the gene within the recombinant yeast was checked by extraction of total DNA (STET buffer extraction) and PCR with primers specific of the *EsMT1* gene. For functional expression, cultures were grown at 22°C in the presence of 2% (w/v) raffinose and expression of the transgene was induced when OD_{600nm} reached 0.2–0.3 by supplementing galactose to 2% (w/v). After two days of culture, OD_{600nm} was adjusted to 1; 10^{-1}; 10^{-10}; 10^{-100}; 10^{-1000} by serial dilutions and 5 µl of each dilution were deposited on YPD media containing final concentrations of 150 µM, 300 µM, 600 µM, 800 µM, 1000µM 1200 µM and 1500 µM of $CuSO_4$, $ZnCl_2$ and $CdCl_2$. Plates were then incubated at 30°C for 5 days.

6.2.2.5 Statistical tests

Statistically significant differences among treatments were determined by the non-parametric Mann-Whitney U test run on Statistica version 5.1 software (StatSoft, USA). All conclusions are based on at least 5% level of significance ($P<0.05$).

6.2.3 RESULTS AND DISCUSSION

6.2.3.1 Influence of chronic copper stress on the expression of copper homeostasis and antioxidant-related genes in E. siliculosus strain 32

In order to asses the effect of chronic exposure to copper into the expression of the candidate genes *EsMT1*, *EsCCH* and *EsCu/ZnSOD1*, individuals of *E. siliculosus* strain 32 were submitted to chronic sublethal copper stress conditions of 25, 50 and 150 µg/L for 6, 8 and 10 days (see toxicity assays on Chapter 5). The lipoperoxide assay showed significantly increased levels in all of the stress conditions (Fig. 6A). Transcription patterns for all three candidate genes showed up-regulation of gene expression after 8 days of stress and for both copper stress conditions (Fig. 6B). As previously described in this chapter, EsCu/ZnSOD lacks a conserved His motif which is fundamental for the activity of this type of enzymes in other organisms. However, since the expression of this gene is induced under copper treatment, we can suggest its involvement in the heavy metal stress response. *EsMT1* and *EsCCH* are also induced after 8 days of stress. Both of these proteins are actively involved in the transport and chelation of intracellular copper [13,20]; therefore, they could be mobilized for acclimation processes. Although plants CCH expression is rather constitutive [30], preliminary studies in *E. siliculosus* strain 32 showed that this gene was up-regulated upon chronic copper stress (Fig. 6B).

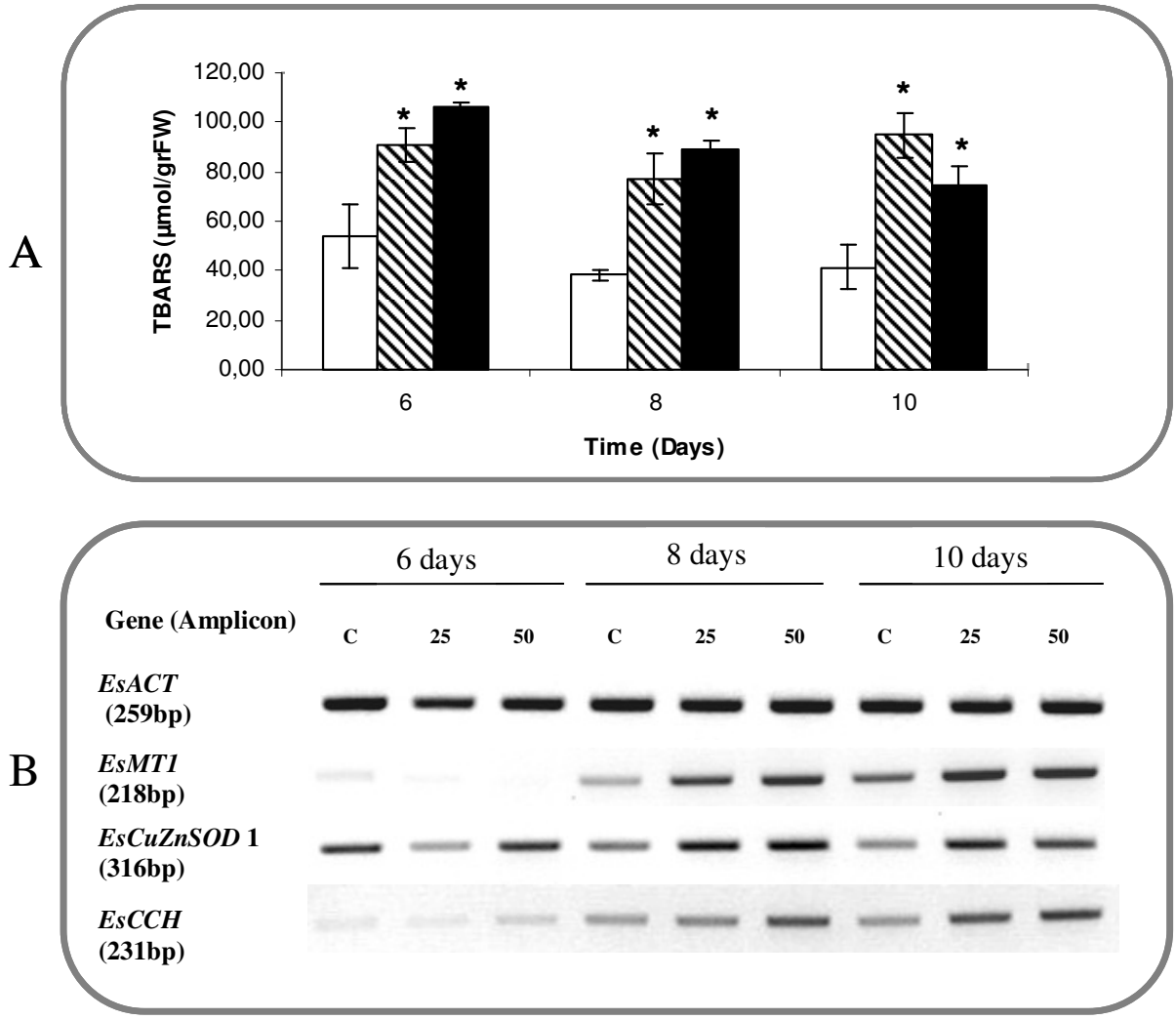

Figure 6. Evidence for chronic copper stress in *E. siliculosus*. (A) Lipid peroxidation measured by TBAR following 0, 6, 8 and 10 days of exposure to copper. White histograms represent the controls, striped histograms, 25 µg/L and black histograms 50 µg/L. Values represent means of three independent replicates and bars represents SE. * Significantly different from the control group ($P< 0.05$). (B) Simultaneous study of stress related gene expression by semi-quantitative RT-PCR analysis. Bands are organised from 6 to 10 days and on each gene conditions are displayed in the following order; controls, 25 µg/L and 50 µg/L.

6.2.3.2 Comparison of gene expression for EsPCS and EsMT under acute and chronic copper stress

In order to observe the possible differences between acute and chronic copper stress, the expression of *EsMT1* and *EsPCS* was followed in copper tolerant strain Es524 and the copper sensitive strains Es32 incubated both in the presence of 250 and 500 µg/L Cu for 4 and 8 hours, and treated with 50 and 150 µg/L for 8 and 10 days. Expression patterns showed

differences between strains and conditions. In Es32, *EsPCS* showed enhanced expression under acute stress, whereas *EsMT1* is induced slightly only after 10 days in presence of 50 µg/L (Fig. 7A). These observations confirm previous results obtained by semi-quantitative RT-PCR (Fig. 6B).

Only slight changes were monitored for *EsMT1* either under acute or under chronic stress in Es524 (Fig. 7B). Therefore, it is likely that EsMT1 do not play a major role in the copper stress response for both strains, at least in the conditions tested. On the other hand, amplification of *EsPCS* was not possible in Es524 because of interference in the PCR amplification. From the results of the annotation of the genome, Es32 possesses one copy of *EsPCS* gene, and a unique strong signal was obtained by PCR for this gene in the reference strain. In contrast, several weak bands were produced in Es524 under the same amplification conditions, preventing to draw any conclusion about changes in the expression of this gene in the tolerant strain (Fig. 8). Nevertheless, the presence of at least two PCS genes in Es524 can not be discarded.

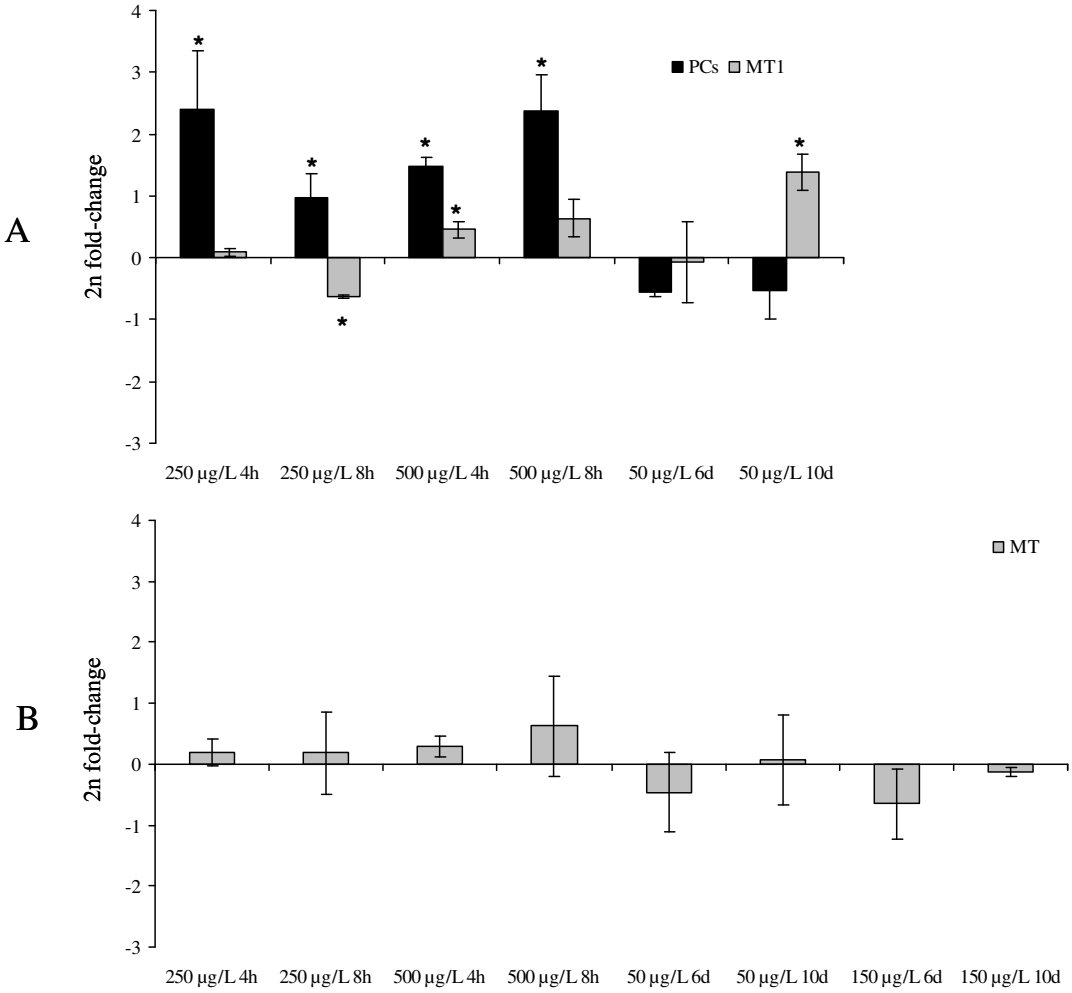

Figure 7. Changes in gene expression of *E. siliculosus* strains Es32 and Es524 submitted to acute and chronic stresses monitored by RT-qPCR. (A) Expression profile of *EsPCS* and *EsMT1* transcripts from Es32 submitted to acute Cu stresses (250 µg/L and 500 µg/L for 4 and 8 h) at the left and chronic Cu stresses (50 µg/L for 6 and 10 days) at the right. (B) Same condition applied to Es524 concerning *EsMT1* transcripts, with the additional condition of 150µg/L for 6 and 10 days. The relative gene expression ratios was calculate as 2n-fold variation as described in materials and methods. Results are means ± SE for two determinations from three independent biological samples. * Significantly different from the control group (P<0.05)

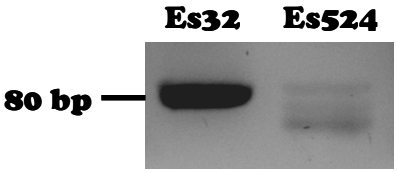

Figure 8. Agarose (4%) gel showing the RT-PCR amplification product of specific primers designed for the *EsPCS* gene in Es32 and Es524 respectively

6.2.3.3 Complementation of the yeast mutant Δace1 by EsMT1

In order to characterize the biochemical function of the *EsMT1* gene, complementation of the yeast mutant *ace*Δ, deficient for MT transcription factor, was conducted with the *EsMT1* gene. After induction of the expression of the transgene, recombinant yeast containing pYES2 and pYEsMT1 were plated on several copper-, zinc- and cadmium-enriched media, in order to observe if the presence of the algal gene contributes to improve the growth of the yeast mutant in presence of heavy metal. No clear difference was observed between the two types of transformed yeast, whatever the conditions tested (Fig. 9).

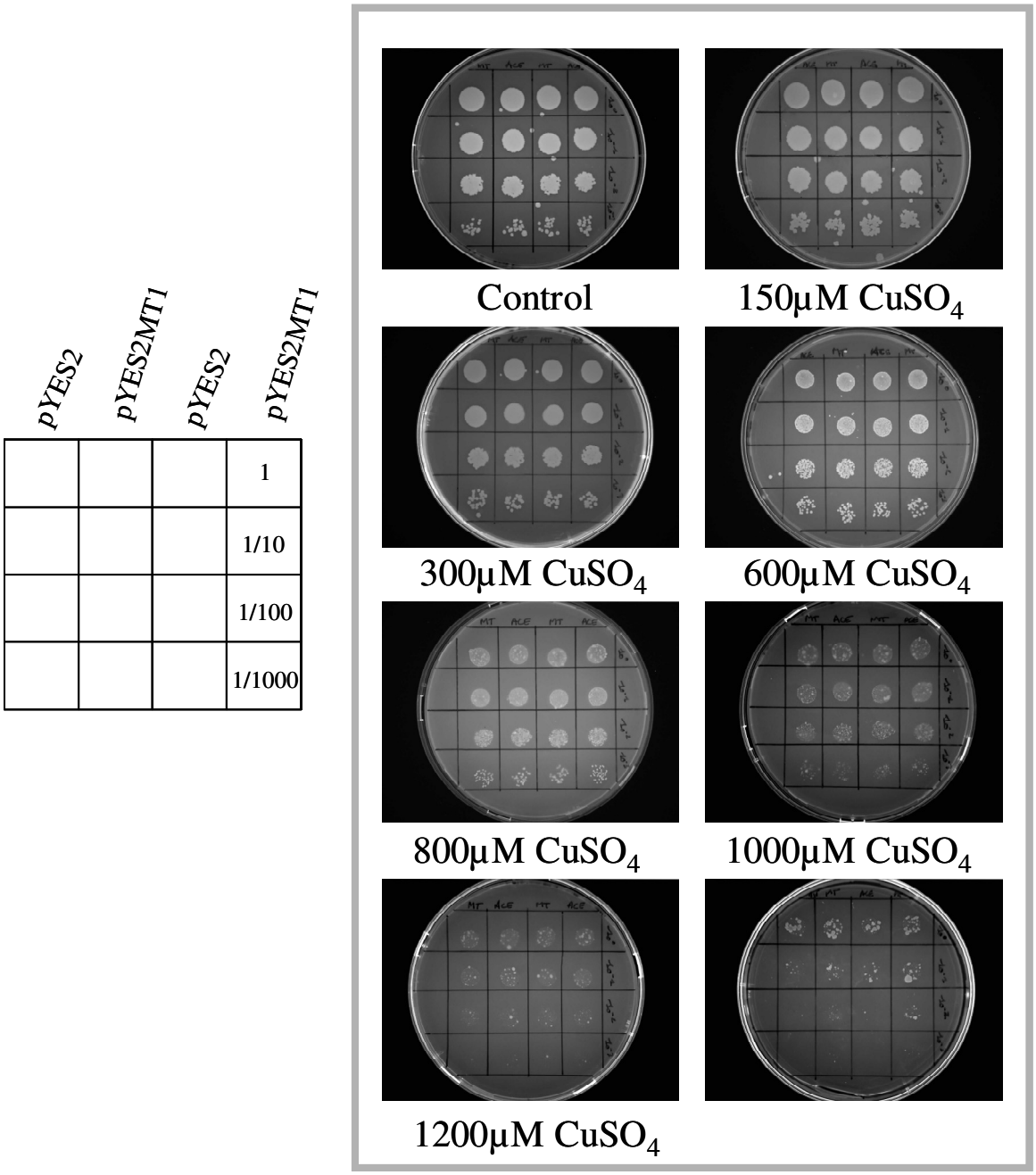

Figure 9. Platles of Δace1 mutants complemented with *EsMT1* exposed at varying copper concentrations. Diagram on the left shows the layout of the yeast colonies along the plates. The pYES2 means the control transformation; pYES2MT1 means transformed colonies. Colonies are disposed at 1/10 decreasing concentrations from the top to the bottom

Although results are still preliminary, different molecular mechanisms seem to operate under acute and chronic copper stress. *EsPCS* seem to be implicated in the differential response to acute copper stress, with a possible duplication in Es524. Finally *EsMT1* doesn't seem to play a key role in copper tolerance for *E. siliculosus*.

6.3 REFERENCES

[1] Mittler, R. (2002) Oxidative stress, antioxidants and stress tolerance. Trends in Plant Science 7, 405-410.

[2] Wu, C.H. et al. (2006) The Universal Protein Resource (UniProt): an expanding universe of protein information. Nucleic Acids Research 34, D187-D191.

[3] Krogh, A., Larsson, B., von Heijne, G. and Sonnhammer, E.L.L. (2001) Predicting transmembrane protein topology with a hidden Markov model: Application to complete genomes. Journal of Molecular Biology 305, 567-580.

[4] Ashburner, M. et al. (2000) Gene Ontology: tool for the unification of biology. Nature Genetics 25, 25-29.

[5] Gschloessl, B., Guermeur, Y. and Cock, J.M. (2008) HECTAR: A method to predict subcellular targeting in heterokonts. BMC Bioinformatics 9.

[6] Lu, G. and Moriyama, E.N. (2004) Vector NTI, a balanced all-in-one sequence analysis suite. Brief Bioinformatics 5, 378-388.

[7] Connolly, E.L., Fett, J.P. and Guerinot, M.L. (2002) Expression of the IRT1 metal transporter is controlled by metals at the levels of transcript and protein accumulation. Plant Cell 14, 1347-1357.

[8] Guerinot, M.L. (2000) The ZIP family of metal transporters. Biochimica et Biophysica Acta-Biomembranes 1465, 190-198.

[9] Maser, P. et al. (2001) Phylogenetic relationships within cation transporter families of *Arabidopsis*. Plant Physiology 126, 1646-1667.

[10] Korshunova, Y.O., Eide, D., Clark, W.G., Guerinot, M.L. and Pakrasi, H.B. (1999) The IRT1 protein from *Arabidopsis thaliana* is a metal transporter with a broad substrate range. Plant Molecular Biology 40, 37-44.

[11] Wintz, H., Fox, T., Wu, Y.-Y., Feng, V., Chen, W., Chang, H.-S., Zhu, T. and Vulpe, C. (2003) Expression Profiles of *Arabidopsis thaliana* in Mineral Deficiencies Reveal Novel Transporters Involved in Metal Homeostasis. Journal of Biological Chemistry 278, 47644-47653.

[12] Puig, S., Andres-Colas, N., Garcia-Molina, A. and Penarrubia, L. (2007) Copper and iron homeostasis in *Arabidopsis*: responses to metal deficiencies, interactions and biotechnological applications. Plant Cell and Environment 30, 271-290.

[13] Puig, S. and Thiele, D.J. (2002) Molecular mechanisms of copper uptake and distribution. Current Opinion in Chemical Biology 6, 171-180.

[14] Kim, B.E., Nevitt, T. and Thiele, D.J. (2008) Mechanisms for copper acquisition, distribution and regulation. Nature Chemical Biology 4, 176-185.

[15] Dancis, A., Yuan, D.S., Haile, D., Askwith, C., Eide, D., Moehle, C., Kaplan, J. and Klausner, R.D. (1994) Molecular characterization of a copper transport protein in *Saccharomyces cerevisiae* - an Unexpected Role for Copper in Iron Transport. Cell 76, 393-402.

[16] Baxter, I., Tchieu, J., Sussman, M.R., Boutry, M., Palmgren, M.G., Gribskov, M., Harper, J.F. and Axelsen, K.B. (2003) Genomic Comparison of P-Type ATPase Ion Pumps in *Arabidopsis* and Rice. Plant Physiology 132, 618-628.

[17] Nevo, Y. and Nelson, N. (2006) The NRAMP family of metal-ion transporters. Biochimica et Biophysica Acta-Molecular Cell Research 1763, 609-620.

[18] Pilon, M., Abdel-Ghany, S.E., Cohu, C.M., Gogolin, K.A. and Ye, H. (2006) Copper cofactor delivery in plant cells. Current Opinion in Plant Biology 9, 256-263.

[19] Cobine, P.A., Pieffel, F. and Winge, D.R. (2006) Copper trafficking to the mitochondrion and assembly of copper metalloenzymes. Biochimica et Biophysica Acta-Molecular Cell Research 1763, 759-772.

[20] Cobbett, C. and Goldsbrough, P. (2002) Phytochelatins and Metallothioneins: Roles in Heavy Metal Detoxification and Homeostasis. Annual Review of Plant Biology 53, 159-182.

[21] Morris, C.A., Nicolaus, B., Sampson, V., Harwood, J.L. and Kille, P. (1999) Identification and characterization of a recombinant metallothionein protein from a marine alga, *Fucus vesiculosus*. Biochem J 338 (Pt 2), 553-60.

[22] Murphy, A., Zhou, J., Goldsbrough, P.B. and Taiz, L. (1997) Purification and immunological identification of metallothioneins 1 and 2 from *Arabidopsis thaliana*. Plant Physiol 113, 1293-301.

[23] Hirata, K., Tsuji, N. and Miyamoto, K. (2005) Biosynthetic regulation of phytochelatins, heavy metal-binding peptides. Journal of Bioscience and Bioengineering 100, 593-599.

[24] Ha, S.B., Smith, A.P., Howden, R., Dietrich, W.M., Bugg, S., O'Connell, M.J., Goldsbrough, P.B. and Cobbett, C.S. (1999) Phytochelatin synthase genes from *arabidopsis* and the yeast *Schizosaccharomyces pombe*. Plant Cell 11, 1153-1163.

[25] Gekeler, W., Grill, E., Winnacker, E.L. and Zenk, M.H. (1988) Algae Sequester Heavy-Metals Via Synthesis of Phytochelatin Complexes. Archives of Microbiology 150, 197-202.

[26] Pawlik-Skowronska, B., Pirszel, J. and Brown, M.T. (2007) Concentrations of phytochelatins and glutathione found in natural assemblages of seaweeds depend on species and metal concentrations of the habitat. Aquatic Toxicology 83, 190-199.

[27] Ortiz, D.F., Ruscitti, T., McCue, K.F. and Ow, D.W. (1995) Transport of Metal-Binding Peptides by Hmt1, a Fission Yeast Abc-Type Vacuolar Membrane-Protein. Journal of Biological Chemistry 270, 4721-4728.

[28] Eitinger, T. (2004) In vivo production of active nickel superoxide dismutase from *Prochlorococcus marinus* MIT9313 is dependent on its cognate peptidase. Journal of Bacteriology 186, 7821-7825.

[29] Küpper, F.C. et al. (2008) Iodide accumulation provides kelp with an inorganic antioxidant impacting atmospheric chemistry. Proceedings of the National Academy of Sciences 105, 6954-6958.

[30] Himelblau, E., Mira, H., Lin, S.-J., Cizewski Culotta, V., Penarrubia, L. and Amasino, R.M. (1998) Identification of a Functional Homolog of the Yeast Copper Homeostasis Gene ATX1 from Arabidopsis. Plant Physiol. 117, 1227-1234.

6.4 SUPPLEMENTARY MATERIAL

EsZIP1 (Esi0016_0180)

A. Predicted TMD:

```
# Sequence Length: 353
# Sequence Number of predicted TMHs:  7
# Sequence Exp number of AAs in TMHs: 151.42853
# Sequence Exp number, first 60 AAs:  35.86409
# Sequence Total prob of N-in:        0.00407
# Sequence POSSIBLE N-term signal sequence
Sequence        TMHMM2.0        outside     1    14
Sequence        TMHMM2.0        TMhelix    15    34
Sequence        TMHMM2.0        inside     35    45
Sequence        TMHMM2.0        TMhelix    46    68
Sequence        TMHMM2.0        outside    69    82
Sequence        TMHMM2.0        TMhelix    83   105
Sequence        TMHMM2.0        inside    106   240
Sequence        TMHMM2.0        TMhelix   241   260
Sequence        TMHMM2.0        outside   261   269
Sequence        TMHMM2.0        TMhelix   270   292
Sequence        TMHMM2.0        inside    293   298
Sequence        TMHMM2.0        TMhelix   299   321
Sequence        TMHMM2.0        outside   322   330
Sequence        TMHMM2.0        TMhelix   331   352
Sequence        TMHMM2.0        inside    353   353
```

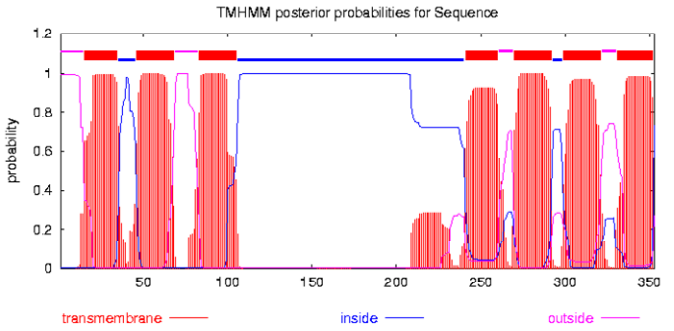

B. BlastP (Blosum 62):

Accession	Entry name	Status	Local alignment	Protein names	Organism	Length	Identity	Score	E-value
A8INX4	A8INX4_CHLRE	☆		**ZIP family transporter**	Chlamydomonas reinhardtii	413	29	145	4 e-33
B0S6Y6	B0S6Y6_DANRE	☆		**Solute carrier family 39** (Zinc transporter)	Danio rerio (Zebrafish) (Brachydanio rerio)	302	36	104	1 e-20
P59889	S39A1_DANRE	★		**Zinc transporter ZIP1** (Zrt- and Irt-like protein 1) (ZIP-1) (DrZIP1) (Solute carrier family 39 member 1)	Danio rerio (Zebrafish) (Brachydanio rerio)	302	36	104	1 e-20
Q55EA1	Q55EA1_DICDI	☆		**Putative uncharacterized protein**	Dictyostelium discoideum (Slime mold)	683	29	103	2 e-20
B5X4B9	B5X4B9_SALSA	☆		**Zinc transporter ZIP1**	Salmo salar (Atlantic salmon)	304	37	98	1 e-18
Q4R9D0	Q4R9D0_MACFA	☆		**Testis cDNA clone: QtsA-10276, similar to human solute carrier family 39** (zinc transporter)	Macaca fascicularis (Crab eating macaque) (Cynomolgus monkey)	309	38	98	1 e-18
Q4QQJ1	Q4QQJ1_HUMAN	☆		**Solute carrier family 39** (Zinc transporter)	Homo sapiens (Human)	309	37	98	1 e-18

Intensity 0% 25% 50% 75% 100% (Identity)

Figure S1. Sequence analysis of EsZIP1. (A) hydropathy test results run on TMHMM sever (http://www.cbs.dtu.dk/services/TMHMM/) . (B) BlastP results run on the uniprot server. Results displayed represent the best blast hits. For each protein accession, local alignment with our query is displayed, as well as the hit protein name, organism, hit protein length, protein identity, blast score and blast E-value.

EsZIP2 (Esi0016_0179)

A. Predicted TMD:

```
# Sequence Length: 353
# Sequence Number of predicted TMHs:  7
# Sequence Exp number of AAs in TMHs: 151.42853
# Sequence Exp number, first 60 AAs:  35.86409
# Sequence Total prob of N-in:        0.00407
# Sequence POSSIBLE N-term signal sequence
Sequence        TMHMM2.0        outside     1   14
Sequence        TMHMM2.0        TMhelix     15  34
Sequence        TMHMM2.0        inside      35  45
Sequence        TMHMM2.0        TMhelix     46  68
Sequence        TMHMM2.0        outside     69  82
Sequence        TMHMM2.0        TMhelix     83  105
Sequence        TMHMM2.0        inside      106 240
Sequence        TMHMM2.0        TMhelix     241 260
Sequence        TMHMM2.0        outside     261 269
Sequence        TMHMM2.0        TMhelix     270 292
Sequence        TMHMM2.0        inside      293 298
Sequence        TMHMM2.0        TMhelix     299 321
Sequence        TMHMM2.0        outside     322 330
Sequence        TMHMM2.0        TMhelix     331 352
Sequence        TMHMM2.0        inside      353 353
```

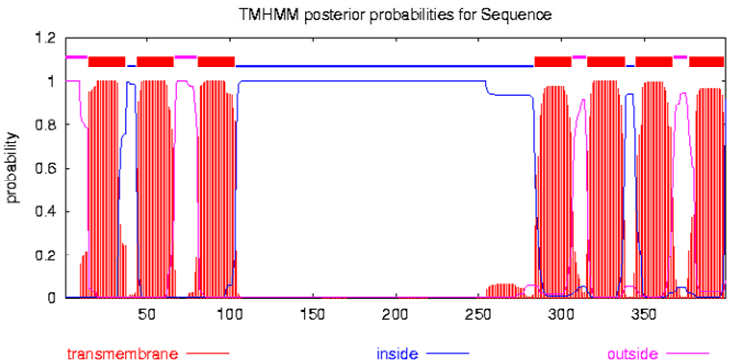

B. BlastP (Blosum 62):

Accession	Entry name	Status	Local alignment	Protein names	Organism	Length	Identity	Score	E-value
A8INX4	A8INX4_CHLRE	☆		**ZIP family transporter**	Chlamydomonas reinhardtii	413	30	132	4 e-29
B5X2K5	B5X2K5_SALSA	☆		**Zinc transporter ZIP1**	Salmo salar (Atlantic salmon)	339	28	119	3 e-25
B0S6Y6	B0S6Y6_DANRE	☆		**Solute carrier family 39** (Zinc transporter)	Danio rerio (Zebrafish) (Brachydanio rerio)	302	28	115	5 e-24
P59889	S39A1_DANRE	★		**Zinc transporter ZIP1** (Zrt- and Irt-like protein 1) (ZIP-1) (DrZIP1) (Solute carrier family 39 member 1)	Danio rerio (Zebrafish) (Brachydanio rerio)	302	28	115	5 e-24
A7SPR1	A7SPR1_NEMVE	☆		**Predicted protein**	Nematostella vectensis (Starlet sea anemone)	336	26	108	6 e-22
Q3UK48	Q3UK48_MOUSE	☆		**Putative uncharacterized protein**	Mus musculus (Mouse)	324	28	107	1 e-21
A2RTD4	A2RTD4_MOUSE	☆		**Slc39a1 proteinSolute carrier family 39** (Zinc transporter)	Mus musculus (Mouse)	324	27	105	5 e-21

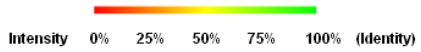

Figure S2. Sequence analysis of EsZIP2. (A) hydropathy test results run on TMHMM sever (http://www.cbs.dtu.dk/services/TMHMM/) . (B) BlastP results run on the uniprot server. Results displayed represent the best blast hits. For each protein accession, local alignment with our query is displayed, as well as the hit protein name, organism, hit protein length, protein identity, blast score and blast E-value.

EsZIP3 (Esi0444_0001)

A. Predicted TMD:

```
# Sequence Length: 276
# Sequence Number of predicted TMHs:  5
# Sequence Exp number of AAs in TMHs: 138.34855
# Sequence Exp number, first 60 AAs:  27.5547
# Sequence Total prob of N-in:        0.99603
# Sequence POSSIBLE N-term signal sequence
Sequence        TMHMM2.0        inside      1    20
Sequence        TMHMM2.0        TMhelix     21   43
Sequence        TMHMM2.0        outside     44   52
Sequence        TMHMM2.0        TMhelix     53   73
Sequence        TMHMM2.0        inside      74   187
Sequence        TMHMM2.0        TMhelix     188  210
Sequence        TMHMM2.0        outside     211  219
Sequence        TMHMM2.0        TMhelix     220  239
Sequence        TMHMM2.0        inside      240  251
Sequence        TMHMM2.0        TMhelix     252  269
Sequence        TMHMM2.0        outside     270  276
```

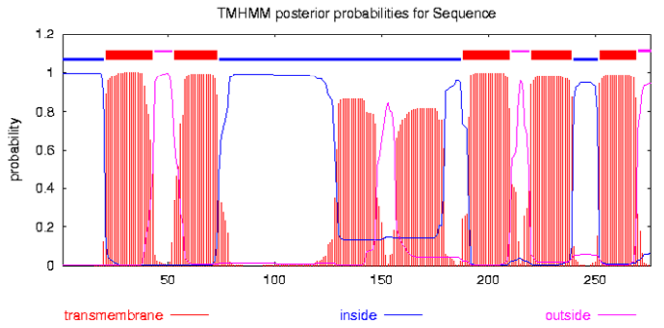

B. BlastP (Blosum 62):

Accession	Entry name	Status	Local alignment	Protein names	Organism	Length	Identity	Score	E-value
B5Y3R5	B5Y3R5_PHATR	☆		**Predicted protein**	Phaeodactylum tricornutum CCAP 1055/1	438	55	280	8 e-74
A4S8L4	A4S8L4_OSTLU	☆		**ZIP family transporter: zinc ion**	Ostreococcus lucimarinus (strain CCE9901)	468	30	124	6 e-27
Q00TZ7	Q00TZ7_OSTTA	☆		**Fe2+/Zn2+ regulated transporter** (ISS) (Fragment)	Ostreococcus tauri	442	30	118	5 e-25
A7SPR1	A7SPR1_NEMVE	☆		**Predicted protein**	Nematostella vectensis (Starlet sea anemone)	338	25	101	7 e-20
A0C7G5	A0C7G5_PARTE	☆		**Chromosome undetermined scaffold_155, whole genome shotgun sequence**	Paramecium tetraurelia	334	23	100	9 e-20
Q5T4K3	Q5T4K3_HUMAN	☆		**Solute carrier family 39** (Zinc transporter) (Fragment)	Homo sapiens (Human)	321	26	100	1 e-19
Q5T4K1	Q5T4K1_HUMAN	☆		**Solute carrier family 39** (Zinc transporter)	Homo sapiens (Human)	324	26	100	1 e-19

Figure S3. Sequence analysis of EsZIP3. (A) hydropathy test results run on TMHMM sever (http://www.cbs.dtu.dk/services/TMHMM/) . (B) BlastP results run on the uniprot server. Results displayed represent the best blast hits. For each protein accession, local alignment with our query is displayed, as well as the hit protein name, organism, hit protein length, protein identity, blast score and blast E-value.

EsZIP4 (Esi0111_0079)

A. Predicted TMD:

```
# Sequence Length: 429
# Sequence Number of predicted TMHs:  7
# Sequence Exp number of AAs in TMHs: 155.2823
# Sequence Exp number, first 60 AAs:  38.34767
# Sequence Total prob of N-in:        0.07893
# Sequence POSSIBLE N-term signal sequence
Sequence        TMHMM2.0        outside     1     9
Sequence        TMHMM2.0        TMhelix     10    32
Sequence        TMHMM2.0        inside      33    44
Sequence        TMHMM2.0        TMhelix     45    67
Sequence        TMHMM2.0        outside     68    84
Sequence        TMHMM2.0        TMhelix     85    107
Sequence        TMHMM2.0        inside      108   284
Sequence        TMHMM2.0        TMhelix     285   307
Sequence        TMHMM2.0        outside     308   344
Sequence        TMHMM2.0        TMhelix     345   367
Sequence        TMHMM2.0        inside      368   373
Sequence        TMHMM2.0        TMhelix     374   396
Sequence        TMHMM2.0        outside     397   410
Sequence        TMHMM2.0        TMhelix     411   428
Sequence        TMHMM2.0        inside      429   429
```

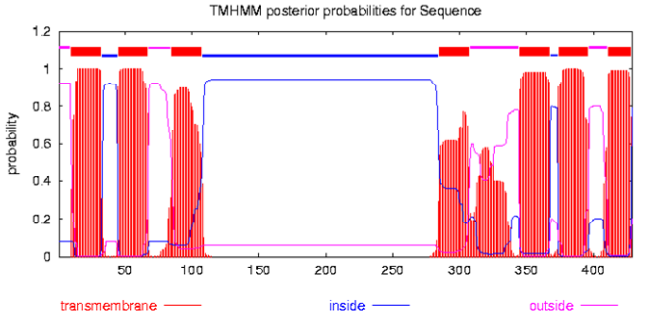

B. BlastP (Blosum 62):

Accession	Entry name	Status	Local alignment	Protein names	Organism	Length	Identity	Score	E-value
A8JCU2	A8JCU2_CHLRE	☆		**Zinc-nutrition responsive transporter**	Chlamydomonas reinhardtii	457	36	241	1 e-61
A4S1N2	A4S1N2_OSTLU	☆		**ZIP family transporter: zinc ion** (Fragment)	Ostreococcus lucimarinus (strain CCE9901)	269	63	198	8 e-49
Q013A1	Q013A1_OSTTA	☆		**Zinc transporter ZIP** (ISS)	Ostreococcus tauri	359	62	196	3 e-48
A8IW07	A8IW07_CHLRE	☆		**Iron-nutrition responsive ZIP family transporter**	Chlamydomonas reinhardtii	478	32	193	2 e-47
A8I452	A8I452_CHLRE	☆		**Putative iron-responsive transporter**	Chlamydomonas reinhardtii	391	32	180	2 e-43
Q30VE8	Q30VE8_DESDG	☆		**Zinc transporter** (Precursor)	Desulfovibrio desulfuricans (strain G20)	271	58	177	2 e-42
Q4UUW7	Q4UUW7_XANC8	☆		**Putative uncharacterized protein**	Xanthomonas campestris pv. campestris (strain 8004)	272	53	176	4 e-42

Figure S4. Sequence analysis of EsZIP4. (A) hydropathy test results run on TMHMM sever (http://www.cbs.dtu.dk/services/TMHMM/) . (B) BlastP results run on the uniprot server. Results displayed represent the best blast hits. For each protein accession, local alignment with our query is displayed, as well as the hit protein name, organism, hit protein length, protein identity, blast score and blast E-value.

EsCTR1 (Esi0021_0108)

A. Predicted TMD:

```
# Sequence Length: 151
# Sequence Number of predicted TMHs:  3
# Sequence Exp number of AAs in TMHs: 62.97406
# Sequence Exp number, first 60 AAs:  23.46995
# Sequence Total prob of N-in:        0.06221
# Sequence POSSIBLE N-term signal sequence
Sequence        TMHMM2.0        outside      1    23
Sequence        TMHMM2.0        TMhelix     24    46
Sequence        TMHMM2.0        inside      47    95
Sequence        TMHMM2.0        TMhelix     96   118
Sequence        TMHMM2.0        outside    119   121
Sequence        TMHMM2.0        TMhelix    122   144
Sequence        TMHMM2.0        inside     145   151
```

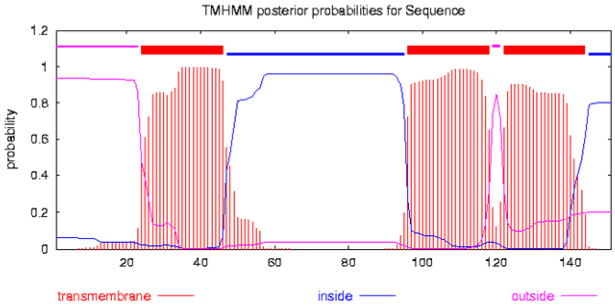

B. BlastP (Blosum 62):

Accession	Entry name	Status	Local alignment	Protein names	Organism	Length	Identity	Score	E-value
Q6FQY3	Q6FQY3_CANGA	☆		**Strain CBS138 chromosome I complete sequence**	Candida glabrata (Yeast) (Torulopsis glabrata)	175	34	65	2 e-9
Q6BI08	Q6BI08_DEBHA	☆		**DEHA2G14366p**	Debaryomyces hansenii (Yeast) (Torulaspora hansenii)	164	30	57	4 e-7
A2QEN7	A2QEN7_ASPNC	☆		**Contig An02c0360, complete genome**	Aspergillus niger (strain CBS 513.88 / FGSC A1513)	165	23	55	2 e-6
A5DMA3	A5DMA3_PICGU	☆		**Putative uncharacterized protein**	Pichia guilliermondii (Yeast) (Candida guilliermondii)	117	31	53	5 e-6
Q59JN8	Q59JN8_CANAL	☆		**Potential copper transport protein**	Candida albicans (Yeast)	162	28	52	1 e-5
B0WF61	B0WF61_CULQU	☆		**High affinity copper transporter**	Culex quinquefasciatus (Southern house mosquito)	200	32	51	2 e-5
A8N7M3	A8N7M3_COPC7	☆		**Predicted protein**	Coprinopsis cinerea (strain Okayama-7 / 130 / FGSC 9003) (Inky cap fungus)	205	28	51	2 e-5

Intensity 0% 25% 50% 75% 100% (Identity)

Figure S5. Sequence analysis of EsCTR1. (A) hydropathy test results run on TMHMM sever (http://www.cbs.dtu.dk/services/TMHMM/) . (B) BlastP results run on the uniprot server. Results displayed represent the best blast hits. For each protein accession, local alignment with our query is displayed, as well as the hit protein name, organism, hit protein length, protein identity, blast score and blast E-value.

EsHMA1 (Esi0125_0069)

A. Predicted TMD:

```
# Sequence Length: 762
# Sequence Number of predicted TMHs:  3
# Sequence Exp number of AAs in TMHs: 116.54161
# Sequence Exp number, first 60 AAs:  0.00012
# Sequence Total prob of N-in:        0.77853
Sequence        TMHMM2.0        outside     1   341
Sequence        TMHMM2.0        TMhelix   342   364
Sequence        TMHMM2.0        inside    365   689
Sequence        TMHMM2.0        TMhelix   690   712
Sequence        TMHMM2.0        outside   713   721
Sequence        TMHMM2.0        TMhelix   722   744
Sequence        TMHMM2.0        inside    745   762
```

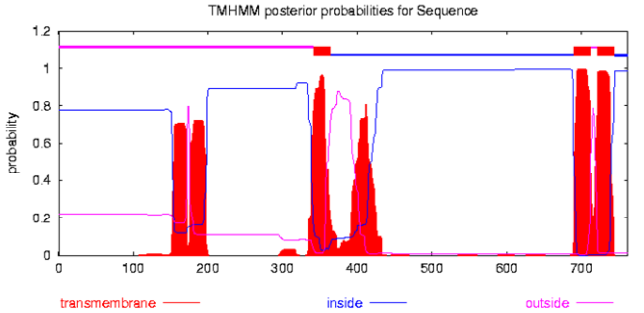

B. BlastP (Blosum 62):

Accession	Entry name	Status	Local alignment	Protein names	Organism	Length	Identity	Score	E-value
A0ZAE8	A0ZAE8_NODSP	☆		**Copper-translocating P-type ATPase**	Nodularia spumigena CCY 9414	812	42	492	1 e-137
Q2JR01	Q2JR01_SYNJA	☆		**Copper-translocating P-type ATPase**	Synechococcus sp. (strain JA-3-3Ab) (Cyanobacteria bacterium Yellowstone A-Prime)	835	43	491	1 e-137
Q3MCW5	Q3MCW5_ANAVT	☆		**Copper-translocating P-type ATPase**	Anabaena variabilis (strain ATCC 29413 / PCC 7937)	813	42	480	1 e-133
Q2JLG4	Q2JLG4_SYNJB	☆		**Copper-translocating P-type ATPase**	Synechococcus sp. (strain JA-2-3B'a(2-13)) (Cyanobacteria bacterium Yellowstone B-Prime)	864	42	480	1 e-133
Q8YQN8	Q8YQN8_ANASP	☆		**Cation-transporting P-type ATPase**	Anabaena sp. (strain PCC 7120)	815	42	480	1 e-133
B2J776	B2J776_NOSP7	☆		**Heavy metal translocating P-type ATPase**	Nostoc punctiforme (strain ATCC 29133 / PCC 73102)	808	43	477	1 e-132

Figure S6. Sequence analysis of EsHMA1. (A) hydropathy test results run on TMHMM sever (http://www.cbs.dtu.dk/services/TMHMM/) . (B) BlastP results run on the uniprot server. Results displayed represent the best blast hits. For each protein accession, local alignment with our query is displayed, as well as the hit protein name, organism, hit protein length, protein identity, blast score and blast E-value.

EsHMA2 (Esi0023_0054)

A. Predicted TMD:

```
# Sequence Length: 1052
# Sequence Number of predicted TMHs:  8
# Sequence Exp number of AAs in TMHs: 180.96573
# Sequence Exp number, first 60 AAs:  0.12464
# Sequence Total prob of N-in:        0.73094
Sequence        TMHMM2.0        inside      1   171
Sequence        TMHMM2.0        TMhelix   172   191
Sequence        TMHMM2.0        outside   192   210
Sequence        TMHMM2.0        TMhelix   211   233
Sequence        TMHMM2.0        inside    234   245
Sequence        TMHMM2.0        TMhelix   246   268
Sequence        TMHMM2.0        outside   269   277
Sequence        TMHMM2.0        TMhelix   278   300
Sequence        TMHMM2.0        inside    301   437
Sequence        TMHMM2.0        TMhelix   438   460
Sequence        TMHMM2.0        outside   461   479
Sequence        TMHMM2.0        TMhelix   480   502
Sequence        TMHMM2.0        inside    503   840
Sequence        TMHMM2.0        TMhelix   841   863
Sequence        TMHMM2.0        outside   864   872
Sequence        TMHMM2.0        TMhelix   873   895
Sequence        TMHMM2.0        inside    896  1052
```

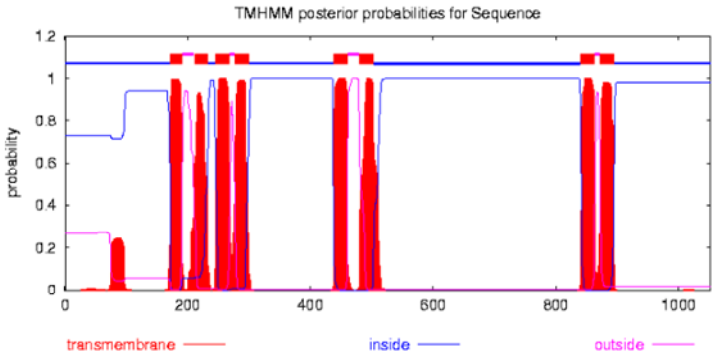

B. BlastP (Blosum 62):

Accession	Entry name	Status	Local alignment	Protein names	Organism	Length	Identity	Score	E-value
A9SME3	A9SME3_PHYPA	☆		**Predicted protein**	Physcomitrella patens subsp. patens	1009	42	564	1 e-158
Q6JAH7	Q6JAH7_MAIZE	☆		**Putative ATP dependent copper transporter**	Zea mays (Maize)	1001	41	563	1 e-158
A9T8Q3	A9T8Q3_PHYPA	☆		**Predicted protein**	Physcomitrella patens subsp. patens	1004	39	563	1 e-158
Q0E3J1	Q0E3J1_ORYSJ	☆		**Os02g0172600 protein**	Oryza sativa subsp. japonica (Rice)	1030	40	561	1 e-157
A3AWA4	A3AWA4_ORYSJ	☆		**Putative uncharacterized protein**	Oryza sativa subsp. japonica (Rice)	1002	40	559	1 e-157
A2XWB0	A2XWB0_ORYSI	☆		**Putative uncharacterized protein**	Oryza sativa subsp. indica (Rice)	1001	40	559	1 e-157
Q94KD6	Q94KD6_ARATH	☆		**AT5g44790/K23L20_14**	Arabidopsis thaliana (Mouse-ear cress)	1001	42	558	1 e-157

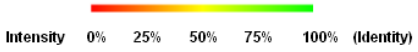

Figure S7. Sequence analysis of EsHMA2. (A) hydropathy test results run on TMHMM sever (http://www.cbs.dtu.dk/services/TMHMM/) . (B) BlastP results run on the uniprot server. Results displayed represent the best blast hits. For each protein accession, local alignment with our query is displayed, as well as the hit protein name, organism, hit protein length, protein identity, blast score and blast E-value.

EsHMA3 (Esi0009_0037)

A. Predicted TMD:

```
# Sequence Length: 1402
# Sequence Number of predicted TMHs:  7
# Sequence Exp number of AAs in TMHs: 164.28068
# Sequence Exp number, first 60 AAs:  0.02073
# Sequence Total prob of N-in:        0.10902
Sequence        TMHMM2.0        outside     1   575
Sequence        TMHMM2.0        TMhelix     576 598
Sequence        TMHMM2.0        inside      599 604
Sequence        TMHMM2.0        TMhelix     605 627
Sequence        TMHMM2.0        outside     628 646
Sequence        TMHMM2.0        TMhelix     647 666
Sequence        TMHMM2.0        inside      667 861
Sequence        TMHMM2.0        TMhelix     862 884
Sequence        TMHMM2.0        outside     885 908
Sequence        TMHMM2.0        TMhelix     909 931
Sequence        TMHMM2.0        inside      932 1249
Sequence        TMHMM2.0        TMhelix     1250 1269
Sequence        TMHMM2.0        outside     1270 1272
Sequence        TMHMM2.0        TMhelix     1273 1295
Sequence        TMHMM2.0        inside      1296 1402
```

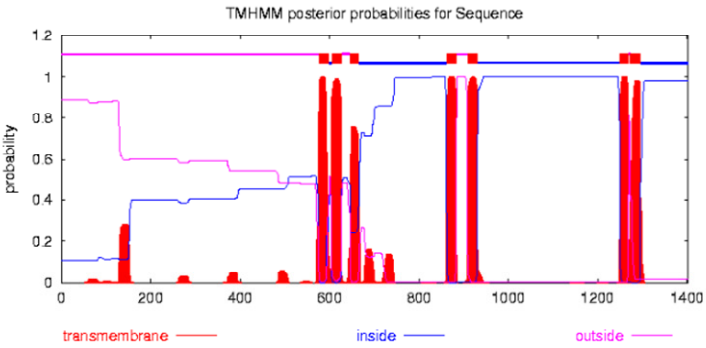

B. BlastP (Blosum 62):

Accession	Entry name	Status	Local alignment	Protein names	Organism	Length	Identity	Score	E-value
Q54Q77	Q54Q77_DICDI	☆		**P-type ATPase**	Dictyostelium discoideum (Slime mold)	985	40	642	0.0
Q9XT50-2	Q9XT50-2	★		**Copper-transporting ATPase 2** (EC 3.6.3.4) (Copper pump 2) (Wilson disease-associated protein homolog)	Ovis aries (Sheep)	1444	33	615	1 e-173
Q9XT50	ATP7B_SHEEP	★		**Copper-transporting ATPase 2** (EC 3.6.3.4) (Copper pump 2) (Wilson disease-associated protein homolog)	Ovis aries (Sheep)	1505	33	615	1 e-173
P35670-3	P35670-3	★		**Copper-transporting ATPase 2** (EC 3.6.3.4) (Copper pump 2) (Wilson disease-associated protein) [Cleaved into: WND/140 kDa]	Homo sapiens (Human)	1354	32	614	1 e-173
Q4U3G5	Q4U3G5_CANFA	☆		**Wilson's disease protein**	Canis familiaris (Dog)	1432	32	610	1 e-172

Intensity 0% 25% 50% 75% 100% (Identity)

Figure S8. Sequence analysis of EsHMA3. (A) hydropathy test results run on TMHMM sever (http://www.cbs.dtu.dk/services/TMHMM/) . (B) BlastP results run on the uniprot server. Results displayed represent the best blast hits. For each protein accession, local alignment with our query is displayed, as well as the hit protein name, organism, hit protein length, protein identity, blast score and blast E-value.

EsNRAMP1 (Esi0141_0009)

A. Predicted TMD:

```
# Sequence Length: 628
# Sequence Number of predicted TMHs:  12
# Sequence Exp number of AAs in TMHs: 247.72605
# Sequence Exp number, first 60 AAs:  0.03838
# Sequence Total prob of N-in:        0.66810
Sequence        TMHMM2.0        inside      1    86
Sequence        TMHMM2.0        TMhelix     87   109
Sequence        TMHMM2.0        outside     110  123
Sequence        TMHMM2.0        TMhelix     124  146
Sequence        TMHMM2.0        inside      147  166
Sequence        TMHMM2.0        TMhelix     167  186
Sequence        TMHMM2.0        outside     187  200
Sequence        TMHMM2.0        TMhelix     201  223
Sequence        TMHMM2.0        inside      224  229
Sequence        TMHMM2.0        TMhelix     230  249
Sequence        TMHMM2.0        outside     250  268
Sequence        TMHMM2.0        TMhelix     269  291
Sequence        TMHMM2.0        inside      292  311
Sequence        TMHMM2.0        TMhelix     312  334
Sequence        TMHMM2.0        outside     335  398
Sequence        TMHMM2.0        TMhelix     399  418
Sequence        TMHMM2.0        inside      419  437
Sequence        TMHMM2.0        TMhelix     438  457
Sequence        TMHMM2.0        outside     458  471
Sequence        TMHMM2.0        TMhelix     472  494
Sequence        TMHMM2.0        inside      495  505
Sequence        TMHMM2.0        TMhelix     506  528
Sequence        TMHMM2.0        outside     529  537
Sequence        TMHMM2.0        TMhelix     538  560
Sequence        TMHMM2.0        inside      561  628
```

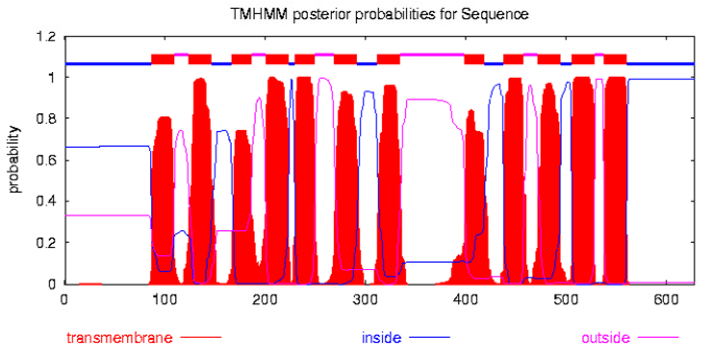

B. BlastP (Blosum 62):

Accession	Entry name	Status	Local alignment	Protein names	Organism	Length	Identity	Score	E-value
Q6EIC5	Q6EIC5_9ALVE	☆		**Divalent cation transporter**	Perkinsus marinus	558	49	454	1 e-125
Q869V1	NRAMP_DICDI	★		**Metal transporter nramp homolog**	Dictyostelium discoideum (Slime mold)	533	44	425	1 e-117
A9SZ07	A9SZ07_PHYPA	☆		**Predicted protein**	Physcomitrella patens subsp. patens	533	43	399	1 e-109
B1WBJ8	B1WBJ8_XENTR	☆		**Slc11a2 protein**	Xenopus tropicalis (Western clawed frog) (Silurana tropicalis)	553	44	395	1 e-108
A9RAW3	A9RAW3_PHYPA	☆		**Predicted protein**	Physcomitrella patens subsp. patens	534	41	395	1 e-108
Q1RLY4	Q1RLY4_DANRE	☆		**Solute carrier family 11** (Proton-coupled divalent metal ion transporters)	Danio rerio (Zebrafish) (Brachydanio rerio)	547	45	388	1 e-106
B3DGS9	B3DGS9_DANRE	☆		**Solute carrier family 11** (Proton-coupled divalent metal ion transporters)	Danio rerio (Zebrafish) (Brachydanio rerio)	547	45	388	1 e-106

Intensity 0% 25% 50% 75% 100% (Identity)

Figure S9. Sequence analysis of EsNRAMP1. (A) hydropathy test results run on TMHMM sever (http://www.cbs.dtu.dk/services/TMHMM/) . (B) BlastP results run on the uniprot server. Results displayed represent the best blast hits. For each protein accession, local alignment with our query is displayed, as well as the hit protein name, organism, hit protein length, protein identity, blast score and blast E-value.

Multidrug ABC transporter (Esi0060_0030)

A. Predicted TMD:

```
# Sequence Length: 904
# Sequence Number of predicted TMHs:  9
# Sequence Exp number of AAs in TMHs: 197.61999
# Sequence Exp number, first 60 AAs:  29.15628
# Sequence Total prob of N-in:        0.99921
# Sequence POSSIBLE N-term signal sequence
Sequence        TMHMM2.0        inside      1    11
Sequence        TMHMM2.0        TMhelix     12   31
Sequence        TMHMM2.0        outside     32   50
Sequence        TMHMM2.0        TMhelix     51   73
Sequence        TMHMM2.0        inside      74   93
Sequence        TMHMM2.0        TMhelix     94   116
Sequence        TMHMM2.0        outside     117  120
Sequence        TMHMM2.0        TMhelix     121  143
Sequence        TMHMM2.0        inside      144  218
Sequence        TMHMM2.0        TMhelix     219  241
Sequence        TMHMM2.0        outside     242  255
Sequence        TMHMM2.0        TMhelix     256  278
Sequence        TMHMM2.0        inside      279  325
Sequence        TMHMM2.0        TMhelix     326  348
Sequence        TMHMM2.0        outside     349  357
Sequence        TMHMM2.0        TMhelix     358  378
Sequence        TMHMM2.0        inside      379  483
Sequence        TMHMM2.0        TMhelix     484  503
Sequence        TMHMM2.0        outside     504  904
```

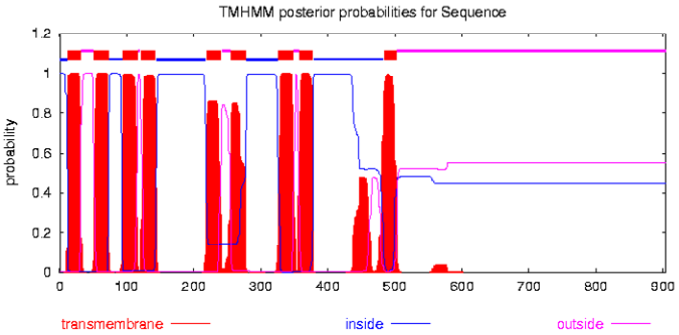

B. BlastP (Blosum 62):

Accession	Entry name	Status	Local alignment	Protein names	Organism	Length	Identity	Score	E-value
B3L9T8	B3L9T8_PLAKH	☆		**Multidrug resistance protein 2, putative**	Plasmodium knowlesi (strain H)	1395	44	540	1 e-151
A5K3T2	A5K3T2_PLAVI	☆		**Multidrug resistance protein 2, putative**	Plasmodium vivax	1605	44	536	1 e-150
Q8IKZ6	Q8IKZ6_PLAF7	☆		**Multidrug resistance protein 2**	Plasmodium falciparum (isolate 3D7)	1024	43	529	1 e-148
Q25693	Q25693_PLAFA	☆		**Pfmdr2 protein**	Plasmodium falciparum	1025	43	529	1 e-148
Q7Z1F1	Q7Z1F1_PLAFA	☆		**MDR2**	Plasmodium falciparum	1024	43	529	1 e-148
Q08667	Q08667_PLAFA	☆		**Transport protein**	Plasmodium falciparum	947	43	523	1 e-146
Q7RBT4	Q7RBT4_PLAYO	☆		**Transport protein**	Plasmodium yoelii yoelii	888	43	519	1 e-145
Q0BUJ2	Q0BUJ2_GRABC	☆		**Multidrug resistance ABC transporter ATP-binding and permease protein**	Granulibacter bethesdensis (strain ATCC BAA-1260 / CGDNIH1)	588	44	481	1 e-133

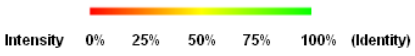

Figure S10. Sequence analysis of EsMultidrug ABC transporter. (A) hydropathy test results run on TMHMM sever (http://www.cbs.dtu.dk/services/TMHMM/) . (B) BlastP results run on the uniprot server. Results displayed represent the best blast hits. For each protein accession, local alignment with our query is displayed, as well as the hit protein name, organism, hit protein length, protein identity, blast score and blast E-value.

7 GENERAL CONCLUSIONS AND PERSPECTIVES

Taken together, the various contributions of my PhD work described in this manuscript have established an extended knowledge of biochemical and molecular bases of brown algal response to copper stress. Although oxylipins had previously been identified upon challenge with biotic elicitors in *Laminaria*, no link between abiotic stress and these compounds were shown in brown seaweeds prior to this study. On the other hand, we have conducted pioneering proteomic work in *E. siliculosus* that will benefit the whole scientific community. The set of proteins identified during this study will be included in a 2-DE proteome map of *Ectocarpus* soon available in the 2D-PAGE Expasy database (http://www.expasy.org/ch2d/). A 2-dimensional proteomic approach was employed because it allows carrying out global expression analyses with no *a priori,* and is complementary to the transcriptomic global approach developed recently for *Ectocarpus* by Dittami and collaborators to study short-term acclimation to abiotic stress (publication submitted). In this context, the proteomic analysis allowed to identify several proteins regulated upon copper stress and some potentially involved with copper tolerance in *Ectocarpus*; our results are in agreement with several previously reported observations gathered in different species of brown algae [1-4] and other organisms [5]. In addition to these experimental data, the annotation of the genome allowed to have an overview of the physiological processes potentially taking place upon copper stress in *Ectocarpus.* Finally, I have characterized two strains (Es32 and Es524) presenting contrasting copper tolerance. Their ability to resist to copper excess is correlated with the copper pollution history of their populations of origin. Consequently, these observations may highlight local adaptative traits, which represent an ideal model for establishing the genetic bases of copper tolerance adaptation in *Ectocarpus*.

7.1 Oxylipin metabolism in response to copper excess

Oxylipins play pivotal roles in the maintenance of cellular homeostasis, including under biotic or abiotic stress in plants and metazoans [6,7]. Our work has contributed to the understanding of oxylipin biosynthesis and provides multiple opportunities to test their biological significance in brown algae (chapter 2-3). Until recently, copper stress-induced fatty acid peroxidation was thought to result merely from the oxidative damage to membranes. Our study in *L. digitata* highlights that these oxidised FAs are produced both by non-enzymatic and enzymatic mechanisms. Interestingly, *L. digitata* seems to regulate oxylipin biosynthesis upon stress following two distinctive relaying mechanisms; one stands for early formation of volatile aldehydes, and a second latter system involves the synthesis of long aliphatic chain oxylipin structures such as cyclopentenones.

The first system was triggered during the first hour following copper exposure. The early release of aldehydes encompassed a bouquet of over 16 compounds, including enzyme-synthesised compounds such as the vascular plants C_6 and C_9 volatiles, but also C_8 and C_7 derivatives found also in diatoms. Although C_6 and C_9 such as hexanal and nonenal had previously been reported in the brown alga *L. angustata* after complete disruption of the tissues and incubation with exogenous fatty acids [8], no biological context was provided for this synthesis. In diatoms, polyunsaturated aldehyde synthesis is rapidly induced upon wounding [9] and under nutrient deprivation [10]; it was suggested that they are used by the cell as infochemicals to provide a surveillance system to evaluate stress conditions [11]. Therefore, it is tempting to speculate that in *L. digitata*, the synthesized aldehydes may trigger rapid detoxifying responses against copper excess.

On the other hand, 24 h of copper exposure triggered the liberation of C_{18} and C_{20} PUFAs in *L. digitata*. This liberation is concomitant with the activation of enzymatic

oxidative cascades leading to the production of “plant-like” octadecanoid and “mammal-like” eicosanoid oxylipins. Among these structures, complex cyclopentenones have been characterized for the first time in brown algae, such as the octadecanoid MeJa precursor 12-OPDA, or the mammalian eicosanoids, the prostaglandins. In addition, a new molecule was synthesized as a C20:5 derivative and was named 18-H-17-oxo-ETE. The synthesis of these compounds was correlated with the activation of several key enzymes involved in the copper stress detoxification, such as a GST and a HSP70. These results support the hypothesis that oxylipins activate copper stress resistance processes. This early and later oxylipin production could be related to two distinctive defensive mechanisms. The early release of aldehydes could mediate the rapid establishment of general stress mechanisms. Then a second downstream system could trigger transcriptional reprogramming, orchestrating stress acclimation. Supporting this theory, MeJa induced a variety of detoxification enzymes in the red alga *C. crispus* [12]. Furthermore, these compounds have recently been shown to induce genome-wide transcriptional reprogramming in *Arabidopsis*, inducing several protecting mechanisms that are involved in detoxification mechanisms [13]. Therefore, our observations raise several questions:

- What are the biosynthetic routes of oxylipins in brown algae?
- What are the signal transduction pathways involved in oxylipin signaling?
- Do oxylipins mediate transcriptional reprogramming upon stress?
- Do oxylipins confer copper tolerance?

Accession to the genome and genomic tools developed in *Ectocarpus* make this species an attractive organism for answering these questions. The genome exploration indicates that four loci present high similarity to LOX genes whose substrate specificity (C_{18} or C_{20} polyunsaturated fatty acids) can not be inferred from sequence homology. Based on our results, it is highly likely that 13- and 15-LOX are included among these candidates.

Concerning the biosynthetic pathway of C_{18} jasmonates, following the putative 13-LOX, one candidate of the CytP450 family presents similarity to an allene oxide synthase (AOS), which could catalyses the synthesis to an intermediate allene oxide structure. The next step is mediated by an allene oxide cyclase (AOC) that also seems to be present. This enzyme catalyse the synthesis of 12-OPDA, which was detected in *Laminaria*. The presence of enzymes potentially involved in the next step of jasmonate synthesis is less clear, except for the ones involved in beta-oxidation. In this context, since it has been demonstrated that 12-OPDA is a potent phytohormone itself [14,15], it is tempting to speculate that brown algae stop the synthesis at the level of 12-OPDA. Concerning prostaglandin biosynthesis, the genome includes one potential cyclooxygenase that could mediate the cyclisation of arachidonic and/or eicosapentaenoic acids. This enzyme could act in coordination with 3 microsomal GSTs that may be involved in the production of a wide range of prostaglandins. Concerning biosynthesis of aldehydes, two possibilities can be considered. The putative AOS also has similarity with plant hydroperoxide lyases, which could catalyse the synthesis of a variety of aldehydes depending on the hydroperoxy FA substrates. Another possibility for aldehyde biosynthesis could reside in the action of a bi-functional LOX, as previously described in the moss *Physcomitrella patens* [16]. Therefore, *E. siliculosus* contains several candidate genes that would be of interest to express in heterologous system, as it has been done in the green lineage [17] and in mammals [18], in order to characterise their activity and infer their importance in the synthesis of oxylipins by brown algae. In order to have a clear picture of these biosynthetic pathways, post-genomic approaches have to be integrated with profiling of oxygenated PUFA devivatives in *Ectocarpus*. Our preliminary studies have been unsuccessful to detect oxylipin signatures upon copper stress. However, based on the genomic information and previous work on the eicosanoid derivative ectocarpene (the *Ectocarpus*

sexual pheromone) [19], there is reasonable data accounting for oxylipin biosynthesis in this species.

The next question to be answered is the actual transcriptional reprogramming mediated by these compounds. *Ectocarpus* DNA microarrays representing almost the full extent of the genome has been already used for transcriptomic analysis of samples submitted to abiotic stresses (Dittami et al., submitted). This tool will allow to asses global gene regulation induced by some of the oxylipins/aldehydes mentioned above. The selection of relevant signal molecules should be driven by the acquisition of knowledge in relation to copper toxicity in *Ectocarpus* (see Chapter 5). Finally, a simple bioassay will allow evaluating the effect of differentially synthesized oxylipins upon the induced copper tolerance, and validate these candidates as potential signals involved in the regulation of post-transcriptional reprogramming leading to stress tolerance.

7.2 Proteomic developments and molecular actors of the E. siliculosus tolerance

The development of additional post-genomics tools, such as proteomics, is an important contribution of my PhD. Some prospects of using this technique will be described in the context of the following discussion. Combining proteomics with physiological and targeted transcriptional analyses allowed us to obtain the first overview of the molecular mechanisms that might be crucial for copper tolerance in *Ectocarpus.*

As in other organisms, gluthathione metabolism seems to be of pivotal importance [20,21]. Our proteomic work clearly pointed out that several enzymes involved in GSH biosynthesis were up-regulated by copper. This peptide has several important roles in detoxification processes, acting as antioxidant in the AsA-GSH cycle, preventing damages to

structures by GST conjugation, and as metal chelator through phytochelatin production [22-24]. All of these mechanisms should play important role in detoxification. Phytochelatin synthase and GST were up-regulated upon copper stress in *Ectocarpus* and *Laminaria* respectively (chapters 5-2). In agreement to our results, recent work on the *Ectocarpus* GST family clearly shows the regulation of these enzymes upon copper stress [25]. In addition Phytochelatins have also been found to be accumulated in brown algae from copper polluted areas [1]. Concerning this latter point, the copper resistant strain Es524 seems to posses several genes encoding for PCS. On the other hand Es32 has only PCS coding sequence (see chapter 4-5). This feature could be directly linked to its copper tolerance; however further characterization of these genes must be carried in order to clarify this function. In conclusion, we can reasonably believe that GSH metabolism is of primary importance for copper tolerance in brown algae.

Other general protective mechanisms such as protein folding and turn-over seem to be important. The proteins involved in these processes are important for the recycling of stress-damaged proteins, justifying their accumulation in response to stress. HSPs are known to be induced by a variety of stress conditions and play important roles in protecting cells against protein degradation [26,27]. Accounting for this, HSP70 was up-regulated by copper in *Laminaria* and *Ectocarpus* (chapters 2-5). Specific brown algal antioxidant systems seem also to play an important role in the copper antioxidant system. Previous reports have described the importance, of plant antioxidant systems such as the GSH-AsA cycle upon copper stress in brown algae [3]. However, the involvement of specific phaeophycean systems such as halide metabolism or the polyphenols was less clear. In relation to this, copper stress proteomic results demonstrate the up-regulation of enzymes implicated in halide and phenolics metabolism. These results underline their implication in cellular detoxification mechanisms (chapter 5). In addition, brown algal phenolics have been suggested to act as

metal chelating compounds because of their high affinity to metals [28]. Phenolic compounds are concentrated in the physodes, where high concentrations of heavy metals have also been observed [29,30]. On the other side, early studies have demonstrated that brown algae excrete polyphenols which are able to chelate divalent cations [31]. In relation to these observations, copper stress up-regulates the expression of an aryl-sulfotransferase in *Ectocarpus*, which is thought to be involved in phenolics biosynthesis.

Another important feature of brown algae resides in their high capability to bind divalent metals through their cell wall polysaccharides. For this reason, these organisms are effective heavy metal biosorption systems [32]. Based on this, brown seaweed should play a key role in the control of coastal seawater heavy metal concentrations, even if no study has investigated this topic so far. This mechanism is believed to be important for metal nutrition [33]. Alginates, especially α-L-guluronic acid, and fucoidan have a very high affinity to bind Cu^{2+} by their carboxylic and sulfonate groups respectively. The metal uptake mechanism is thought to be directed by the ionic exchange between Na^{+} bound in cell wall polysaccharides and Cu^{2+}. However, the precise mechanism is still unclear. Much less is known about polysaccharides behaviour upon copper excess. Several studies report the release of organic chelating substances upon copper stress in *E. siliculosus*, however the precise composition of these exudates is unknown [34,35]. Taking into account the chelation properties of brown algal polysaccharides and their high abundance in these organisms (up to 60% of the dry weight), it is tempting to speculate that some can be released as extracellular chelating substances. In relation to this, copper stress up-regulates the expression of a mannose-6-phosphate isomerase in *E. siliculosus,* which is thought to be one the enzyme involved in the biosynthesis of alginate (chapter 5).

The enhanced synthesis of proteins affected by copper should also be related to stress tolerance. Copper is a major inhibitor of photosynthesis, altering the composition and

functioning of photosystem proteins. Therefore, a marked increased turnover of photosystem proteins in the copper tolerant *Ectocarpus* strain Es524 seems to be related to its metal tolerance. Other mechanisms such as copper transport mechanisms could not be studied by 2-DE gel approach. Effectively, this method is not adapted for the isolation of membrane proteins such as copper transporters and low molecular weight proteins like copper chaperones. Consequently, alternative studies must be carried out in the future in order to elucidate this aspect. One complementary approach would be gel-free differential protein analysis employing recently developed shotgun proteomics techniques [36-38]. Another option could be to focus on specific proteins of subcellular fractions. Several putative copper transporters such as HMA could be actively involved in metal resistance. Therefore, the comparison of cytoplasmic membrane proteomes between the copper-resistant and sensitive strains could reveal important features. For analyzing the membrane proteome, alternative techniques such as blue-native electrophoresis appeared to be more adapted than 2-D PAGE [39]. Another way of studying specific candidates, such as P-type ATPases, would be to use deficient yeast mutant for functional complementation. Transcriptomic analysis of copper-stressed *Ectocarpus*, using the available array for this alga can also bring complementary answers. This approach will allow obtain a global view of transcriptomic reprogramming under this stress condition. Moreover, it would be instructing to compare global gene expression profiles between the sensitive strain Es32 and the copper-tolerant strain Es524 submitted to copper excess. Comparative genetic approaches such as association or QTL (Quantitative Trait Loci) mapping may also contribute to the elucidation of new mechanisms of copper tolerance in brown algae (see below).

7.3 Population genomics of E. siliculosus strains from copper polluted areas

Heavy metal tolerance constitutes a classic example of genetic tolerance evolution in land plants [40]. Consequently, it represents an excellent model for the study of genetic adaptative traits [30]. Markers exhibiting highest levels of population divergence are supposed to reveal selection on loci involved in adaptive divergence among populations. Our study has characterized two contrasting strains presenting tolerance and sensitivity to copper. Their differential tolerance is linked to their historical copper pollution context, accounting for an adaptative trait. This result raises several questions concerning the genetic bases of copper tolerance in *E. siliculosus*:

- Are populations inhabiting in copper polluted sites genetically structured?

- Does copper tolerance correspond to a local adaptative trait in copper polluted areas?

- What are the genomic features leading to this tolerance?

Answering the first question will require to scan genetic diversity in natural populations with molecular markers, such as micro-satellites and Amplified Fragment Length Polymorphisms (AFLPs). These techniques would allow to determine in *Ectocarpus* the genotypes of the individuals growing in divergent copper-polluted around the Chañaral bay [41,42]. Results will reveal population differentiation, gene flow, and genetic variations between metallicolous and non-metallicolous populations. On the other side, the *Ectocarpus* genome has allowed to identify and validate polymorphic micro-satellite loci together with AFLP markers, that will allow soon to establish a genetic map (Heesch, Coelho, Bothwell, Peters & Cock, unpublished data). This offers the opportunity to address the second and third questions by detecting association(s) among molecular marker(s) and phenotype(s), and thus to develop quantitative genetics. This will consist in association mapping for isolates from natural populations and from individuals obtained within experimental segregating populations with known pedigree (QTL mapping). The characterisation of strains presenting opposite behaviour, such as Es32

and Es524, will allow to select accessions to map the genome regions presenting genetic variations between the two ecotypes. These regions, when associated to adaptive phenotypes in QTL analyses, are very likely to be in the vicinity of gene(s) that provide local adaptative traits, which in our case could reveal copper tolerance mechanisms.

Finally, as previously discussed in this chapter, global transcriptomic and metabolomic approaches could also refine phenotypic features to compare the differential copper response between two contrasting strains, and merge population genomics with quantitative genetic approaches.

7.4 New functional approaches in brown algae to identify copper tolerance mechanisms

Validating the biological function of genes identified by global or quantitative genetic approaches will also require the use of forward and/or reverse genetics tools. The mutagenesis approach is able to create organisms with a total disruption of gene function (null mutant), as well as its fine-tuned modification, in a very stable way throughout several generations, allowing the possibility to study the combination of several phenotypic alterations by crosses. In addition, it does not require transformation, which is not yet operational in brown algae, acts randomly, and allows characterising new gene functions (strategy without *a priori*). Several developmental mutants have been isolated using UV-mutagenesis in *E. siliculosus* and positional cloning of some of the affected genes should be completed in the near future ([43]; Coelho *et al.*, unpublished data; Charrier *et al.*, unpublished data). Simple visual mutagenesis screens could be established to select mutants exhibiting improved tolerance to copper stress using mutagenized gametes which can survive a lethal dose of copper. Sensitive mutants can be isolated as well from individuals showing lethal phenotypes to moderate copper concentrations. Several tools and expertise have been developed within the *Ectocarpus*

genome consortium that should facilitate such approaches. The UV-mutagenesis approach is also currently applied to develop Targeting Local Lesions IN Genomes (TILLING) in *Ectocarpus* [44]. TILLING could allow to search the genome of mutagenized gametes for single base-pair substitutions or other mutations in a gene identified to be important for adaptation to copper stress. Such an approach is envisioned in our research team in the near future to identify a phenotype associated with the mutation of the single vBPO gene of *E. siliculosus*.

In conclusion, in spite of extensive progress which have been made during the course of my PhD project to better understand copper tolerance mechanisms in brown algae, a lot still needs to be done and new approaches remain to be developed in order to integrate what is learned on the cellular processes involved in copper tolerance with the ecological context and adaptation strategies of metallicolous strains; some exciting discoveries can be expected in this domain in the coming years.

7.5 REFERENCES

[1] Pawlik-Skowronska, B., Pirszel, J. and Brown, M.T. (2007) Concentrations of phytochelatins and glutathione found in natural assemblages of seaweeds depend on species and metal concentrations of the habitat. Aquatic Toxicology 83, 190-199.

[2] Küpper, H., Setlik, I., Spiller, M., Küpper, F.C. and Prasil, O. (2002) Heavy metal-induced inhibition of photosynthesis: targets of in vivo heavy metal chlorophyll formation. Journal of Phycology 38, 429-441.

[3] Contreras, L., Moenne, A. and Correa, J.A. (2005) Antioxidant responses in *Scytosiphon lomentaria* (Phaeophyceae) inhabiting copper-enriched coastal environments. Journal of Phycology 41, 1184-1195.

[4] Nielsen, H.D., Brownlee, C., Coelho, S.M. and Brown, M.T. (2003) Inter-population differences in inherited copper tolerance involve photosynthetic adaptation and exclusion mechanisms in *Fucus serratus*. New Phytologist 160, 157-165.

[5] Hall, J.L. (2002) Cellular mechanisms for heavy metal detoxification and tolerance. Journal of Expperimental Botany 53, 1-11.

[6] Funk, C.D. (2001) Prostaglandins and Leukotrienes: Advances in Eicosanoid Biology. Science 294, 1871-1875.

[7] Blee, E. (2002) Impact of phyto-oxylipins in plant defense. Trends in Plant Science 7, 315-322.

[8] Boonprab, K., Matsui, K., Akakabe, Y., Yotsukura, N. and Kajiwara, T. (2003) Hydroperoxy-arachidonic acid mediated n-hexanal and (Z)-3- and (E)-2-nonenal formation in *Laminaria angustata*. Phytochemistry 63, 669-678.

[9] Pohnert, G. (2005) Diatom/copepod interactions in plankton: The indirect chemical defense of unicellular algae. Chembiochem 6, 946-959.

[10] Vidoudez, C. and Pohnert, G. (2008) Growth phase-specific release of polyunsaturated aldehydes by the diatom *Skeletonema marinoi*. Journal of Plankton Research 30, 1305-1313.

[11] Vardi, A., Formiggini, F., Casotti, R., De Martino, A., Ribalet, F., Miralto, A. and Bowler, C. (2006) A stress surveillance system based on calcium and nitric oxide in marine diatoms. PLOS Biology 4, 411-419.

[12] Collén, J., Hervé, C., Guisle-Marsollier, I., Léger, J.J. and Boyen, C. (2006) Expression profiling of *Chondrus crispus* (Rhodophyta) after exposure to methyl jasmonate. J. Exp. Bot. 57, 3869-3881.

[13] Pauwels, L., Morreel, K., De Witte, E., Lammertyn, F., Van Montagu, M., Boerjan, W., Inze, D. and Goossens, A. (2008) Mapping methyl jasmonate-mediated transcriptional reprogramming of metabolism and cell cycle progression in cultured *Arabidopsis* cells. Proceedings of the National Academy of Sciences 105, 1380-1385.

[14] Farmer, E.E., Almeras, E. and Krishnamurthy, V. (2003) Jasmonates and related oxylipins in plant responses to pathogenesis and herbivory. Current Opinion in Plant Biology 6, 372-378.

[15] Farmer, E. and Schulze-Lefert, P. (2005) Biotic interactions: From molecular networks to inter-organismal communities. Current Opinion in Plant Biology Biotic interactions 8, 343-345.

[16] Wichard, T., Gobel, C., Feussner, I. and Pohnert, G. (2004) Unprecedented lipoxygenase/hydroperoxide lyase pathways in the moss *Physcomitrella patens*. Angewandte Chemie International Edition 44.

[17] Howe, G.A., Lee, G.I., Itoh, A., Li, L. and DeRocher, A.E. (2000) Cytochrome P450-dependent metabolism of oxylipins in tomato. Cloning and expression of allene oxide synthase and fatty acid hydroperoxide lyase. Plant Physiology 123, 711-724.

[18] Moriuchi, H. et al. (2008) Molecular characterization of a novel type of prostamide/prostaglandin F synthase, belonging to the thioredoxin-like superfamily. Journal of Biological Chemistry 283, 792-801.

[19] Stratmann, K., Boland, W. and Muller, D.G. (1993) Biosynthesis of pheromones in female gametes of marine brown-algae (Phaeophyceae). Tetrahedron 49, 3755-3766.

[20] Meister, A. and Anderson, M.E. (1983) Glutathione. Annual Review of Biochemistry 52, 711-760.

[21] Xiang, C. and Oliver, D.J. (1998) Glutathione Metabolic Genes Coordinately Respond to Heavy Metals and Jasmonic Acid in Arabidopsis. Plant Cell 10, 1539-1550.

[22] Halliwell, B. and Gutteridge, J. (1989) Free Radicals in Biology and Medicine.

[23] Dixon, D., Lapthorn, A. and Edwards, R. (2002) Plant glutathione transferases. Genome Biology 3, reviews3004.1 -10.

[24] Cobbett, C. and Goldsbrough, P. (2002) Phytochelatins and Metallothioneins: Roles in Heavy Metal Detoxification and Homeostasis. Annual Review of Plant Biology 53, 159-182.

[25] de Franco, P.-O., Rousvoal, S., Tonon, T. and Boyen, C. (*In press*) Whole genome survey of the glutathione transferase family in the brown algal model *Ectocarpus siliculosus*. Marine Genomics.

[26] Vierling, E. (1991) The Roles of Heat Shock Proteins in Plants. Annual Review of Plant Physiology and Plant Molecular Biology 42, 579-620.

[27] Lindquist, S. and Craig, E.A. (1988) The Heat-Shock Proteins. Annual Review of Genetics 22, 631-677.

[28] Karez, C.S. and Pereira, R.C. (1995) Metal contents in polyphenolic fractions extracted from brown alga *Padina gymnospora*. Botanica Marina 38, 151-155.

[29] Andrade, L.R., Farina, M. and Amado Filho, G. (2002) Role of *Padina gymnospora* (Dictyotales, Phaeophyceae) cell walls in cadmium accumulation. Phycologia 41, 39-48.

[30] Salgado, L.T., Andrade, L.R. and Filho, G.M.A. (2005) Localization of specific monosaccharides in cells of the brown alga *Padina* gymnospora and the relation to heavy-metal accumulation. Protoplasma 225, 123-128.

[31] Ragan, M.A., Ragan, C.M. and Jensen, A. (1980) Natural Chelators in Sea-Water - Detoxification of Zn^{2+} by Brown Algal Polyphenols. Journal of Experimental Marine Biology and Ecology 44, 261-267.

[32] Davis, T.A., Volesky, B. and Mucci, A. (2003) A review of the biochemistry of heavy metal biosorption by brown algae. Water Research 37, 4311-4330.

[33] Kloareg, B., Demarty, M. and Mabeau, S. (1987) Ion-Exchange Properties of Isolated Cell Walls of Brown Algae: The Interstitial Solution. Journal of Experimental Botany 38, 1652-1662.

[34] Sueur, S., van den Berg, C.M.G. and Riley, J.P. (1982) Measurement of the metal complexing ability of exudates of marine macroalgae. Limnology and Oceanography 27, 536-543.

[35] Gledhill, M., Nimmo, M., Hill, S.J. and Brown, M.T. (1997) The toxicity of copper (II) species to marine algae, with particular reference to macroalgae. Journal of Phycology 33, 2-11.

[36] Chitteti, B.R., Tan, F., Mujahid, H., Magee, B.G., Bridges, S.M. and Peng, Z.H. (2008) Comparative analysis of proteome differential regulation during cell dedifferentiation in *Arabidopsis*. Proteomics 8, 4303-4316.

[37] Wolters, D.A., Washburn, M.P. and Yates, J.R. (2001) An automated multidimensional protein identification technology for shotgun proteomics. Analytical Chemistry 73, 5683-5690.

[38] Liu, H.B., Sadygov, R.G. and Yates, J.R. (2004) A model for random sampling and estimation of relative protein abundance in shotgun proteomics. Analytical Chemistry 76, 4193-4201.

[39] Wittig, I. and Schagger, H. (2008) Features and applications of blue-native and clear-native electrophoresis. Proteomics 8, 3974-3990.

[40] Macnair, M.R. (1993) The Genetics of Metal Tolerance in Vascular Plants. New Phytologist 124, 541-559.

[41] Medina, M., Andrade, S., Faugeron, S., Lagos, N., Mella, D. and Correa, J.A. (2005) Biodiversity of rocky intertidal benthic communities associated with copper mine tailing discharges in northern Chile. Marine Pollution Bulletin 50, 396-409.

[42] Correa, J.A. et al. (1999) Copper, copper mine tailings and their effect on the marine algae in Northern Chile. Journal of Applied Phycology 11, 57-67.

[43] Peters, A.F. et al. (2008) Life-cycle-generation-specific developmental processes are modified in the immediate upright mutant of the brown alga *Ectocarpus siliculosus*. Development 135, 1503-1512.

[44] Comai, L. and Henikoff, S. (2006) TILLING: practical single-nucleotide mutation discovery. Plant Journal 45, 684-694.

8 SUPPLEMENTARY MATERIAL

8.1 CURRICULUM VITAE

Andrés S. Ritter

6, rue basse, 29600 Morlaix - France
Phone: 33-628046787
Email: ritter@sb-roscoff.fr

CIVIL STATUS

Nationality: Chilean and German
Date of birth: 12th August 1980

EDUCATION

Since 2005 PhD student in the Biochemistry of algal defenses team at the Station Biologique de Roscoff, France. Co-supervised by Pr. Dr. Juan Correa at the Pontificia Universidad Católica de Chile and Dr. Philippe Potin at the University of Paris VI - France Subject: *Mechanisms involved in the establishment of copper tolerance in brown algae.*

2004-2005 Master degree in integrative biology and physiology with specialty in Plant Sciences at the University of Paris VI – France.

2003-2004 Graduate (Maîtrise) in Population biology with specialty in Marine Sciences at the University of Bretagne Occidentale Brest – France.

PROFESSIONAL EXPERIENCE AND TRAINING

Dec 2007 Instructorship during the ESTeam (EU-funded Marie Curie Actions) teaching course: *Abiotic and biotic stresses in algae and cyanobacteria* in Roscoff, France.

Sept 2007 Instructorship during the Paris VI (Master) training course: *Measurement of the stress caused by copper in the brown algae E. siliculosus* in Roscoff, France.

Jul 2006 Instructorship during a 2-week field course of Phycology at the University of Paris VI in Roscoff, France.

Jan 2006 Attendance to the Marine Genomics Europe **Proteomic training workshop** (Jan 23-27, 2006) at the proteomic platform (Innova proteomics) in Rennes France.

Feb – Jul 2005 Master research project (Stage de Master II) at the Station Biologique de Roscoff under the supervision of Dr. Philippe Potin. Subject: *Study of the rapid responses and gene expression of the brown algae Laminaria digitata in response to copper stress.*

Feb - Mar 2004 Graduate research project (Stage de Maitrise) at the Pontificia Universidad Católica de Chile, under supervision of Pr. Dr. Juan Correa. Subject: *Effects of copper stress on photosynthetic parameters in the brown algal kelp* Lessonia nigrescens *(Laminariales).*

Aug – Sept 2003 Undergraduate research trainership (Stage de licence) at the Station Biologique de Roscoff under supervision of Pr. Dr. François Lallier. Subject: *Original adaptations to hypercapnia of the thermal vent crab Bythograea thermydron.*

May - Jul 2003 Scientific SCUBA diving trainership at the Station Biologique de Concarneau, France. Subject: *Evaluation of the impact of the ERIKA's wreck on the underwater flora and fauna.*

Mar – Aug 2002 Teaching assistant at the Limnological Institute of the Konstanz University – Germany under the supervision of Pr. Dr. Elisabeth Gross. Subject: *Interactions between the macrophytes* Elodea nuttallii, Myriophyllum spicatum *and* Najas marin *and the insect herbivore* Acentria ephemerella *(lepidoptera:pyralidae)*

PUBLICATIONS

- Ritter A.*, Goulitquer S*., Salaün J.P., Tonon T.,. Correa J. A and Potin P. **Copper stress induces biosynthesis of octadecanoid and eicosanoid oxygenated derivatives in the brown algal kelp *Laminaria digitata*.** New Phytologist 180(4), 809-21 (2008). *These two authors contributed equally to this work

- Goulitquer S., Ritter A., Thomas F., Salaün J.P. and Potin P. **Natural emissions of volatile fatty acid aldehydes in the brown algal kelp *Laminaria digitata* in response to both biotic and abiotic stresses.** ChemBioChem, *In Press* (2009).

- Contreras L. *, Ritter A.*, Boehmwald F., Guitton N., Moenne A, Potin P. and Correa J. **Brown algae (Phaeophyceae) protein extraction methods for two-dimensional protein electrophoresis analysis**. Journal of Phycology 44, 1315-1321 (2008). *These two authors contributed equally to this work

- Ritter A., Ubertini M., Romac S., Gaillard F., Delage L., Beltran J., Mann A., Tonon T.,. Correa J. A and Potin P. **Copper stress proteomics highlights local adaptation of two strains of the model brown alga *Ectocarpus siliculosus*.** In preparation. To be submitted to Proteomics.

CONGRESS & COMMUNICATIONS

- **Ritter A**, Contreras L, Tonon T, Correa J and Potin P. "Proteomic tool development and differential copper stress proteome analysis in *E. siliculosus*". May 2008, Oban England. **(Oral presentation).**

- Tonon T, Goulitquer S, **Ritter A**, Dittami S, Cock JM, Salaün JP, Correa J, Boyen C and Potin P. From the shore: "molecular changes in the fatty acid metabolism of brown algae under abiotic stress conditions". July 2008. 17th International Symposium on plant Lipids, Bordeaux. **(Poster).**

- Goulitquer S, **Ritter A**, Thomas F, Lucas D, Salaün JP and Potin P. "Aldehyde biosynthesis during oligoguluronate elicitation in the brown algal kelp *Laminaria digitata*" July 2008. 17th International Symposium on plant Lipids, Bordeaux, France **(Poster).**

- Goulitquer S, **Ritter A**, Thomas F, Lucas D, Salaün JP and Potin P. "Biosynthèse précoce d'aldéhydes en réponse qu stress chez l'algue brune marine *Laminaria digitata*". April 2008. Journée des jeunes chercheurs de la Faculté de medicine de Brest. **(Oral presentation).**

- Goulitquer S, **Ritter A**, Thomas F, Lucas D, Salaün JP and Potin P. "Biosynthèse précoce d'aldéhydes en réponse qu stress chez l'algue brune marine *Laminaria digitata*". April 2008. Journée Stress Oxydant ouest Genopôle. **(Oral presentation).**

- **Ritter A**., Goulitquer S, Salaün JP, Tonon T, Correa J and Potin P. "Mechanisms implicated in the establishment of copper tolerance of brown algae". October 2007. Workshop Marine Genomics Europe: "an ocean of techniques". Kolombari Greece **(Poster)**.

- Tonon T, **Ritter A**, Defranco PO, Rousvoal S, Grosillier A, Hérvé C, LeBail A, Scornet D, Charrier B, Corre E, Michel G, Potin P, CockM and Boyen C. "Contribution to the molecular characterisation of genes involved in abiotic stress response in brown algae". October 2006. Marine Genomics International conference, Sorrento - Italy. **(Poster).**

- **Ritter A**, Henriquez C, Goulitquer S, Salaün JP, Tonon T, Correa J and Potin P. "Physiological and molecular response of the brown alga *Laminaria digitata* in reaction to copper stress". July 2006. Congress of Federation of the European Society in Plant Biology, Lyon – France. **(Poster)**.

- Goulitquer S., Gaquerel E, **Ritter A.**, Lucas D. and Potin P. "Mapping Oxylipids in Biological Samples" May 2006. 3rd Lipidomics Meeting "From Lipid Analysis to Genetic Disorders" Marseille France. **(Poster).**

LANGUAGES

Spanish, English, French and German

REFERENCES

Dr. Philippe POTIN
Team Biochemistry of algal defenses UMR 7139 CNRS-UPMC & LIA-DIAMS
Station Biologique, Place Georges Teissier B.P. 74, F29682 Roscoff Cedex, France
Phone : 33 (0)2 98 29 23 75; Fax : 33 (0)2 98 29 23 85

Pr. Dr. Juan CORREA
Pontificia Universidad Católica de Chile
Av. Libertador Bernardo O'Higgins 340, CP 6513677, Chile
Phone : (56-2) 354 2642 Fax:(56-2) 354 2621

8.2 POSTERS

Physiological and molecular response of the brown alga *Laminaria digitata* in reaction to copper stress

Andrés Ritter[1-3], Sophie Goulitquer[2], Carolina Henriquez[1], Jean Pierre Salaün[2], Thierry Tonon[1], Juan Correa[3] and Philippe Potin[1]

UMR 7139 (CNRS-UPMC-Paris 6), LIA DIAMS, [1]Station Biologique, F-29682 Roscoff cedex, France, [2]Laboratoire de Biochimie-EA-948, Université de Bretagne Occidentale, Faculté de Médicine, F-29285 Brest, France [3]Pontificia Universidad Católica de Chile, Facultad de ciencias biologicas, departamento de Ecología, Santiago de Chile.

As a consequence of human activities, heavy metals have become a common pollution source in marine systems. Brown algae (Phaeophyceae) are sedentary benthic macroscopic organisms that must deal with this stress. In this study, we have monitored the physiological and molecular responses of the brown algal kelp *Laminaria digitata* to high copper concentration. Our preliminary results suggest that the effects of copper in brown algae are buffered by protective mechanisms, which may be specific to this phylum or to their aquatic environment.

I. Induction of an oxidative stress in response to copper challenge

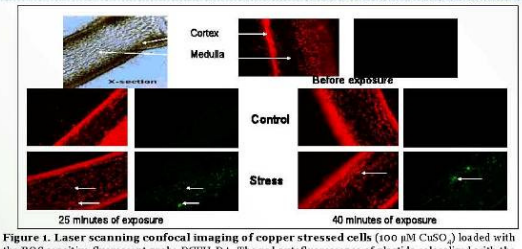

Figure 1. Laser scanning confocal imaging of copper stressed cells (100 µM $CuSO_4$) loaded with the ROS sensitive fluorescent probe DCFH-DA. The red autofluorescence of plastids colocalized with the green fluorescence generated by the ROS production. Three sets of images are presented, representative of the time course following the stress.
The results indicate a ROS productions within the chloroplasts of medullar cells.

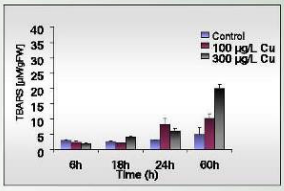

Figure 2. Peroxidation of lipids monitored by formation of thiobarbituric acid reactive compounds (TBARs).
Lipoperoxides (LPO) underline the cellular damage caused by ROS. The levels increase in function of the time and the metal concentration.

II. Copper-induced stress activates the synthesis of oxylipins derivated from C-18 and C-20 fatty acids

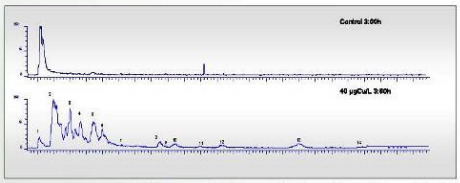

Figure 3. LC-MS profiling of oxygenated free fatty acids released by *L. digitata* following challenge with copper. Among peroxidated lipids, some of the oxidized free fatty acids are known to be involved in signaling stress responses. The compounds identified by characteristic ions in LC-MS chromatograms are numbered and correspond to oxygenated free fatty acid products induced by copper stress in *L. digitata* plantlets, which are detailed in the Table 1.

Number	Tr (min)	Ions	Identification
1	4.013 à 4.333	295, 307, 269	PGD2, PGE2
2	5.402	309, 291	13-hydroxy-12-oxoODE
3	6.224	307, 291, 221	Isoprostane I2
4	7.385	309, 333	?
5	8.333	307, 291, 237	Isoprostane
6	9.472	479, 309	?
7	11.424	321	13 hydroxy-12-oxoOME
8	13.498	291	12-oxo-PDA
9	14.219	333, 315 (-H2O)	C20:4-COOH, EpH-LETrE, PGA1 ou PGE1 ou LTE4
10	14.813	289	oxo-octatetraenoic acid
11	16.6	293	13-HOTrE
12	19.038	485, 413, 401	?
13	25.131	319	12-HETE
14	30.237	343	oxo-EPE

Table 1 . Tentative identification of many oxylipins produced in response to copper treatment.. The analysis indicate the production of potentials oxylipins derivates from animal-like Eicosanoid (in black) and plant-like Octadecanoid (in green) pathways. These responses may lead to the regulation of various pathways including anti-oxidant genes activation.

III. Regulation of the expression of stress genes in response to copper challenge

Gene	Annotation	Function and catalyzed reaction
Superoxide dismutase (cofactor: Mn^{2+})	MnSOD	Protect against oxidative stress $2O_2^- + 2H^+ \rightarrow H_2O_2 + O_2$
Glutation S-transferase	GST78	Protect against oxidative and Heavy metal Stress $RX + GSH \rightarrow R-SG + XH$
2 Peptide Methionine Sulfoxide Reductases	MSR1, MSR3	Protect against oxidative stress $Met(O) \rightarrow Met + H_2O$
Heat shock protein 70 kds	HSP70	Protection and repair of proteins under stress conditions. Most present in EST library
4 Thioredoxines	TRX1, TRX2, TRX3, TRX4	DNA synthesis, hydrogen donor for ribonucleotide reductase and Protein disulfide reduction. In plant, photosynthesis regulation by light via ferredoxin. Protection against ROS and Heavy Metals $Prot-S_2 + Prot'(SH)_2 \rightarrow Prot(SH)_2 + Prot'-S_2$
Peroxiredoxine	PRX	Cellular protection against oxidative stress, modulation of intracellular signaling cascades that apply hydrogen peroxide as a second messenger molecule, and regulation of cell proliferation $ROOH + R'(SH)_2 \rightarrow ROH + R'S_2 + H_2O$

Table 2. Stress genes identified from *L. digitata* EST database obtained after sequencing of cDNA libraries. In order to analyze the expression pattern of these genes, we have designed specific primer pairs for each gene.

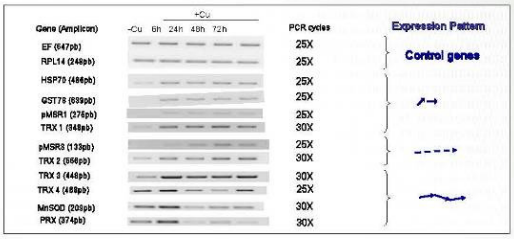

Figure 4. Semi-quantitative RT-PCR analysis of stress genes. Gene expression analyze was conducted on algae sampled 6, 24, 48 and 72 hours after the beginning of the copper stress (300 µg Cu/L). The synthesis of cDNA was carried out on RNA pool representing 3 individuals. Changes in accumulation of transcripts were observed for all the selected genes. Three different expression patterns can be identified.

Conclusion and Perspectives

➢ These results suggest that brown alga exhibit original features such as production of C18 and C20 oxylipins derivates signaling molecules during heavy metal response. Further studies will allow us to determinate whether these secondary metabolisms are synthesized by enzymatic or non enzymatic pathways and their probable subsequent target genes.

➢ Following the downstream response pathway, stress responsive genes are differentially regulated. Additional studies will establish probable coordinated expression of these genes.

➢The ongoing genome sequencing project of the brown algal model *Ectocarpus siliculosus* will give us strong tools to improve our understanding of stress metabolism of brown alge in response to heavy metal through transcriptomics and proteomics approaches.


L. digitata on rocky shores


L. digitata culture


Brown alga 2D PAGE

Natural Emissions of Volatile Aldehydes in the Brown Algal Kelp *Laminaria digitata* in Response to Both Biotic and Abiotic Stresses.

Sophie Goulitquer[1-2], **Andrés Ritter**[3], **François Thomas**[3], **Danièle Lucas**[1-2], **Jean-Pierre Salaün**[1-3], **Laurent Corcos**[1-2] **and Philippe Potin**[3]

[1]EA-948, « Oxylipides », Université de Bretagne Occidentale, Faculté de Médecine, CS 93837, 29238 Brest-Cedex 3, France
[2]U-613 INSERM, Laboratoire de Génétique Moléculaire et Epidémiologique,
[3]UMR 7139 (CNRS-UPMC-Paris 6), LIA DIAMS, Station Biologique, F-29682 Roscoff Cedex, France,

Introduction

In higher plants, numerous studies have established that short chain aldehydes, odorant and volatile compounds, play a major role in stress response. These compounds are synthesized from polyunsaturated fatty acids (PUFAs) via lipases, lipoxygenases (LOXs) and hydroperoxidelyases (HPLs) pathways. Some of these aldehydes have also been detected in diatoms (micro-algae) and in *Laminariales* (macro-algae), after mechanical wounding or PUFA incubations. The present work aims at defining if aldehydes are also produced in *Laminaria digitata* in physiological conditions in response to oligoguluronate (GG) elicitation, cell wall polysaccharides released from the alga during herbivore or bacterial attack, or during environmental stress such as emersion at very low tide.

Aldehyde biosynthesis pathways [Bonnprab et al. (2006) J. of Applied Phycol.]

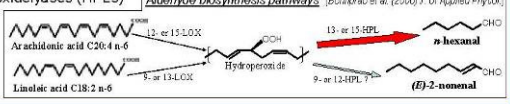

Method

The development of a method based on gas chromatography coupled to mass spectrometry in the negative ion chemical ionization mode (GC/MS/NICI) allowed the identification and quantification of aldehydes contained in both the surrounding seawater and in the air phase of the incubation flask after oximation as pentafluorobenzyl-oximes. The scheme below describes the experimental set-up to elicit *L. digitata* with oligoguluronates and the collection and detection of aldehydes in the surrounding seawater and the air phase.

Aldehydes from the air volatile fraction were eluted from the adsorbent (Super Q, Supelco) with 0.05 M PFBHA-HCl in MeOH then TMS esters were formed. The surrounding seawater was extracted by ethyl acetate and after gentle evaporation, aldehydes were converted to their PFB-oximes/TMS analogs. In environmental conditions, seawater samples were collected along low tide in a rockpool containing *L. digitata* as the dominant specie.

Results

Oligoguluronate Elicitation

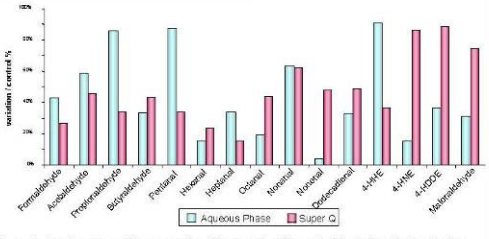

Our study shows an increase in the production of aldehydes in both the aqueous phase and the air phase in response to oligoguluronates.

↳ Then, further studies have focused on the aqueous phase

GG elicitation scheme

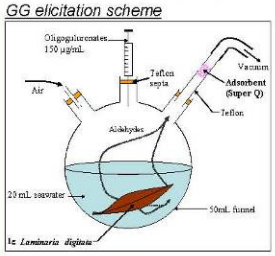

4-hydroxy-(*E*)-2-nonenal-d3 (4-HNE-d3) was used as internal standard.

Compounds were analyzed in GC/MS/NICI monitoring their [M-HF]⁻ ion ([M- 20 *m/z*]⁻).

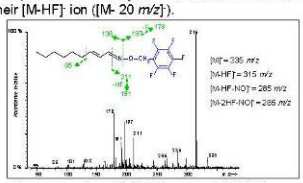

Mass spectra of 2E-Nonenal-O-PFB

A piece of evidence for an enzymatic pathway

Oligoguluronates

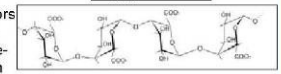

A pharmacological approach, using inhibitors of LOXs (SHAM), of flavoprotein oxidases (Quinacrin) and of lipases (Chlorpromazine-HCl), was adopted to study the mechanism of aldehyde production.

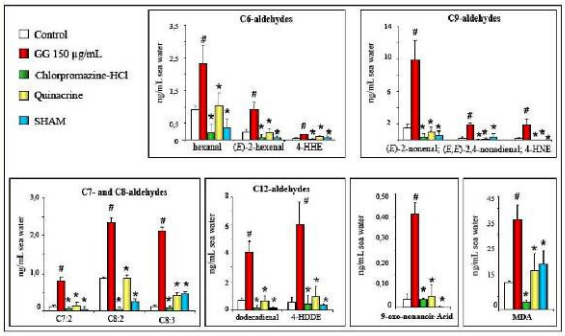

GG elicitation dramatically induce aldehyde production, in the surrounding seawater, by *L. digitata*. Pre-incubation of inhibitors blocks aldehyde production. Thus, our results suggests that these compounds are enzymatically synthesized.

(# $p < 0.05$ vs Control ; ✱ $p < 0.05$ vs. GG elicitation)

Emersion in environmental conditions

As we proved that *L. digitata* can produce aldehyde in laboratory conditions, we focused on stress generated by emersion at low tide. A tide pool, where algae are emerged only during low Spring tides (Coeff > 92) was selected. Aldehyde production and environmental conditions were monitored all along the tide.

Time to low tide	- 1hour	0	+30 min	+1 hour	+1 hour 30
T °C	15,9	15,8	16,0	16,8	15,7
Brightness (µmol photons/m²/s)	450	254	353	422	316
pH	8,35	8,44	8,25	8,30	8,29
Salinity	35,10	35,20	35,20	35,20	35,20
O_2 (mg/L)	11,8	9,0	8,0	8,3	7,9

Results

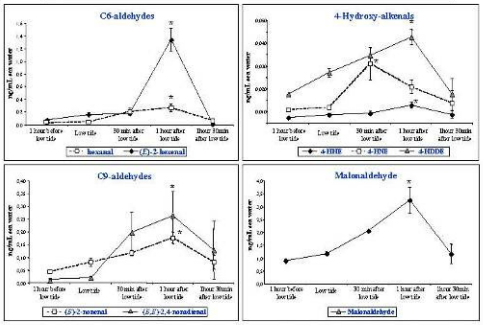

In environmental conditions, in response to emersion, C6 and C9, polyunsaturated or not, aldehyde production is induced. (*E*)-2-hexenal was the most induced compound (13 times). The climax was reached 1 hour after low tide. Aldehyde levels dramatically decreased after 1h30 due to the flooding of the tide pool by the rising tide. $p < 0.05$ vs. 1 hour before low tide.

Conclusion & Perspectives

Our results clearly show that the brown marine kelp *Laminaria digitata* produce a large panel of aldehydes in response to oligoguluronate elicitation (150 µg/mL) or to the simple emersion at very low tide. The synthesis of these compounds, polyunsaturated or not, in C6 and in C9, including 4-hydroxy-alkenals and 9-oxo-nonanoic acid was demonstrated using mass spectrometry. Volatile aldehyde emission was detected during the hour after elicitation, which implies early stress-related mechanisms. A pharmacological approach using various inhibitors strongly suggests that these compounds are enzymatically synthesized. These aldehydes are good candidates to test as intra- and/or inter-algae messengers of communication and act as repulsive or attractant signals for marine invertebrates. Stir bar sorptive extraction (SBSE) experiments are envisaged to avoid samples evaporation and the subsequent loss of volatiles.

From the shore: Molecular changes in the fatty acid metabolism of brown algae under abiotic stress conditions

Tonon T.[1,2], Goulitquer S.[3], Ritter A.[1,2,4], Dittami S.[1,2], Cock J.M.[1,2], Salaün J.-P.[3], Correa J.A.[4], Potin P. [1,2], and Boyen C.[1,2]

[1]UPMC Univ Paris 6, UMR 7139 Végétaux marins et Biomolécules, Station Biologique, F-29682, Roscoff, France.
[2]CNRS, UMR 7139 Végétaux marins et Biomolécules, Station Biologique, F-29682, Roscoff, France.
[3]Laboratoire de Biochimie-EA-948, Université de Bretagne Occidentale, Faculté de Médecine, F-29285 Brest, France.
[4]Center for Advanced Studies in Ecology & Biodiversity, Departamento de Ecología, Facultad de Ciencias Biológicas, Pontificia Universidad Católica de Chile, Santiago, Chile.

Introduction

Intertidal seaweeds are subject to a number of physical changes related to their habitat and as a result frequently exhibit remarkable levels of tolerance to abiotic stresses. Little, however, is known about the mechanisms underlying this tolerance, making intertidal seaweeds interesting models with large potentials for new discoveries. Among these organisms, brown algae have diverged independently from green plants [1, see eukaryotes tree of life on the right side].

Over the last five years, the filamentous, the cosmopolitan filamentous alga *Ectocarpus siliculosus* has been established as a genetic and genomic model for brown algae [2,3]. In addition, the kelp *Laminaria digitata* forms dense populations on rocky shores, with a major role in the marine coastal biodiversity and commercial applications [4].

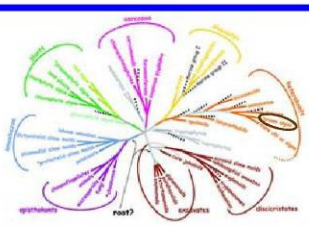

Integrative approach in *Ectocarpus siliculosus*

We have developed an EST-based pilot microarray, based on the NimbleGen technology, to study the transcriptomic response of *E. siliculosus* to three abiotic stresses (hypersaline, hyposaline, oxidative) after 6h00 of incubation (tidal cycle). We have also measured the total fatty acids content in these samples.

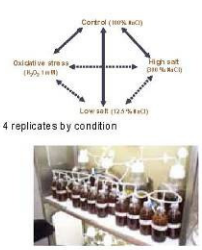

Samples

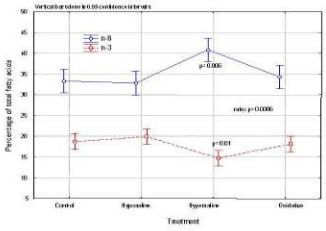

Total fatty acids content

5 cDNA libraries
↓
91,396 ESTs
↓
17,039 unigenes
+
231 EsV-1 sequences
↓
4 probes (60mères) by sequence
↓
Chips

samples
↓
mRNA
↓
Reverse transcription
↓
Amplification by PCR
↓
Double strand cDNA
↓
Single dye labeling

NimbleGen Iceland
↓
Roscoff

Transcriptomic approach

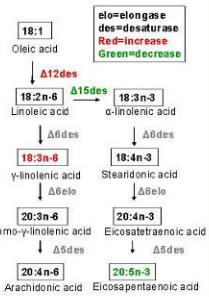

model

Most changes in FA metabolism occur under high salt conditions. We observed a correlation between the changes in fatty acids content and the variations of the level of expression of the putative Δ12- and Δ15-desaturase genes annotated in the genome. These changes may affect membrane stability/fluidity and be related to the synthesis of signaling compounds (oxylipins ?) under the hypersaline stress.

Oxylipins synthesis in *Laminaria digitata* under copper stress

LC-MS and GC-MS analysis of copper treated *L. digitata* shows that late stress (24h00) induces the liberation of free fatty acids, concomitant with the biosynthesis of octadecanoid (plant-like) and eicosanoid (mammal-like) oxygenated derivatives. To our knowledge, this is the first time that production of prostaglandins is reported in brown algae. In addition, a new compound, the 17-oxo,18-hydroxy-eicosatetraenoic acid, was identified.

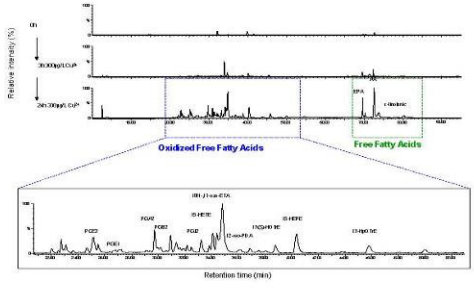

LC-MS profiling

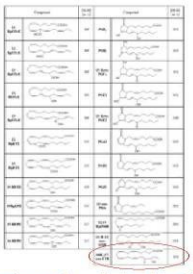

structure of oxylipins identified in copper stressed *L. digitata*

LC-MS chromatogram of 17-oxo,18-hydroxy-eicosatetraenoic acid (17oxo,18H-ETA, *m/z* 333 [M-H](-)). Spectrum are presented in negative APCI mode (**A**) and EI mode as a TMS derivative (**B**).

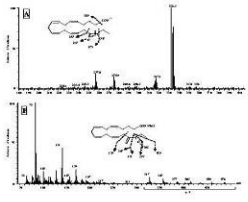

A new molecule: 17oxo,18H-ETA

Conclusion

The production of C18 and C20 oxygenated fatty acid derivatives in stressed *L. digitata*, including the identification of new oxylipins, raise interesting questions on the role(s) of these molecules in these organisms, and the enzymes involved in their biosynthesis. It is tempting to suggest that these oxylipins are acting as signaling molecules under stress condition in brown algae.

The emergence of the model *E. siliculosus*, with the development of several genetic and genomic tools, should allow to understand the physiological functions of the fatty acids and their derivatives, and also to decipher the pathways leading to the production of these molecules.

[1] Baldauf S., 2003. The deep root of eukaryotes. Science 300, 1703-1706.
[2] Peters et al., 2004. Proposal of *Ectocarpus siliculosus* (Ectocarpales, Phaeophyceae) as a model organism from brown algal genetics and genomics. J. Phycol. 40, 1079-1088.
[3] Charrier et al., 2008. Development and physiology of the brown alga *Ectocarpus siliculosus*: two centuries of research. New Phytol. 177, 319-322.
[4] Bartsch et al., 2008. The genus Laminaria sensu lato: recent insights and developments. Eur. J. Phycol. 43, 1-86.

Mapping Oxylipids in Biological Samples

S. Goulitquer[1], E. Gaquerel[1], A. Ritter[2], D. Lucas[1] & P. Potin[2]

[1]EA-948 "Oxylipids" Faculté de Médecine, CS 93837, 29238 Brest-Cedex 3, France
[2]UMR 7139, Station Biologique, F-29682 Roscoff cedex, France
sophie.goulitquer@univ-brest.fr

Introduction: Similarities in the production of oxygenated derivatives of polyunsaturated acids (PUFAs) known as **oxylipids**, have been observed in humans and marine red algae when subjected to biotic and abiotic stresses. Oxylipids play an essential role in many biological processes (regulation of vascular tone, inflammatory response, homeostasis…) To date epoxide and hydroxyle derivatives of arachidonic acid profiles have not been established in humans while in the red alga *Chondrus crispus*, eicosanoids and octadecanoids derivatives naturally act as defense mediators[1].

Mapping the variety of oxylipids generated in both humans and algae should document on the lipidomic profile associated with selective stresses

Human Red Blood Cells (RBCs) from subjects with inflammatory disease

Methods: Extraction by [$CHCl_3$/CH_3OH (2/1)];
SPE purification of **phospholipids**; hydrolysis by Phospholipase A2 and derivatization of oxylipids as pentafluorobenzyl (PFB) esters and (*bis*)-*t*-butyldimethylsilyl (TMS) ethers.
Oxylipids from RBCs are analyzed by **GC/MS** in the **NCI** mode using methane as reagent gas.
Internal standard :14,15-EET-d8 (epoxyeicosatrienoic acid)

EETs quantification in RBCs (epoxyeicosatrienoic acids)

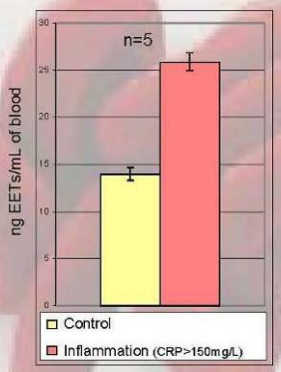

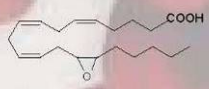

14,15-EET regioisomer
EET ⇦ epoxyeicosatrienoic acid

An increase of EETs level, from 14±4,8ng/mL to 25,9±3,5ng/mL of blood has been observed in red bloods cells from subjects with inflammatory disease.

Our results confirm the involvement of oxylipids in the inflamatory process

Algae

Chondrus crispus was elicitated with pathogen extract from another alga or methyl jasmonate.

Laminaria Digitata was stressed with $CuSO_4$ increasing concentrations during different times.

After ethyle acetate extraction, oxylipids from algae are either analysed by **LC/MS/APCI** or/and **GC/MS/NCI.**

The red alga ***Chondrus Crispus***

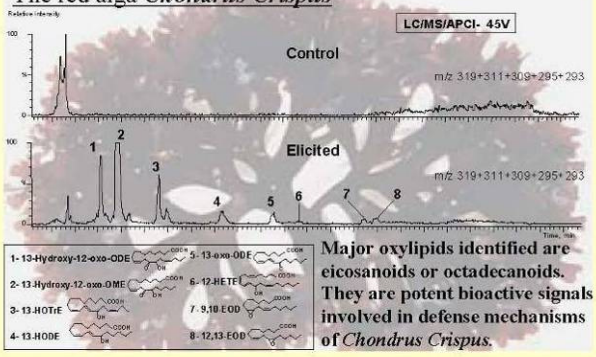

Major oxylipids identified are eicosanoids or octadecanoids. They are potent bioactive signals involved in defense mechanisms of *Chondrus Crispus*.

The brown alga ***Laminaria Digitata***

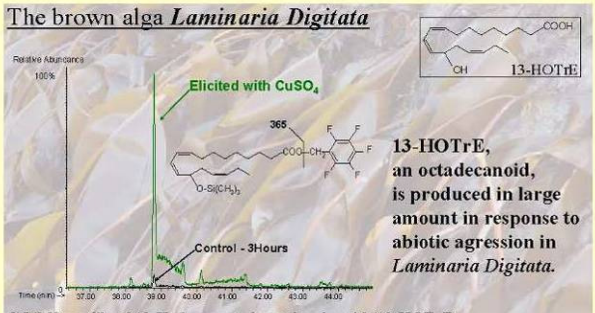

13-HOTrE, an octadecanoid, is produced in large amount in response to abiotic agression in *Laminaria Digitata*.

GC/MS profile of 13-Hydroxyoctadecatrienoic acid (13-HOTrE)
The m/z 365 [M-$C_6F_5CH_2$] was monitored in the negative- ion chemical ionization.

Conclusion: This study provides evidence that the oxylipid profiles, which are representative of the oxidative enzyme cascades of PUFAs, are modified according to the stress in both plants and humans.

1. Bouarab K, Adas F, Gaquerel E, Kloareg B, Salaun JP, Potin P. Plant Physiol. 2004 Jul;135(3):1838-48.

Physiological and molecular responses of brown algae under copper stress

Andrés Ritter[1-3], Sophie Goulitquer[2], Nathalie Guitton[3], Francis Le madec[1], Charles Pineau[4], Jean Pierre Salaün[2], Thierry Tonon[1], Juan Correa[3] and Philippe Potin[1]

UMR 7139 (CNRS-UPMC-Paris 6), LIA DIAMS, [1]Station Biologique, F-29682 Roscoff cedex, France; [2]Laboratoire de Biochimie-EA-948, Université de Bretagne Occidentale, Faculté de Médicine, F-29285 Brest, France; [3]Pontificia Universidad Católica de Chile, Facultad de ciencias biologicas, departamento de Ecología, Santiago de Chile; [4]High-Throughput Proteomics Platform OUEST-genopole®; UPRES JE 2459; INSERM, U625, Campus de Beaulieu F-35042, France

As a consequence of human activities, heavy metals have become a common pollution source in marine systems. Brown algae (Phaeophyceae) are benthic macroscopic organisms that must deal with this stress. In this study, we have monitored the physiological and molecular responses of the brown algae to high copper concentration. Our results suggest that these organisms may respond to stress utilising original physiological pathways.

I. Mammal and plant like oxylipin hormones are biosynthesized following copper stress in the kelp *Laminaria digitata*

Oxylipins constitute a diverse group of oxidized fatty acid metabolites. These metabolites are known as defense signal cues in plants and animals

Free Fatty Acid (FFA) liberation is induced by copper stress

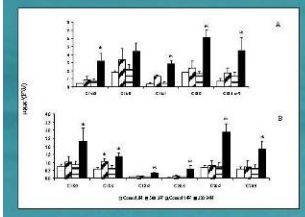

Late stress conditions (24h) induces FFA liberation (A,B), in particular the Poly unsaturated FFA (B) which constitute the oxylipin precursors

Mammal and plant like oxylipins synthesis is triggered by copper

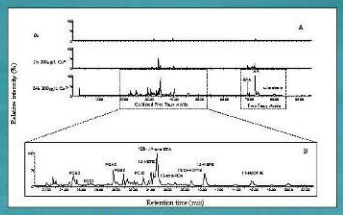

(A) Late stress (24h) LC/MS profiles show the liberation of FFA, correlated with oxylipins biosynthesis. (B) Oxylipin identification indicates the presence of C:18 (plant like) and C:20 (animal like) oxylipins, in particular the mammal prostaglandins

Oxylipins are synthesized by enzymatic processes

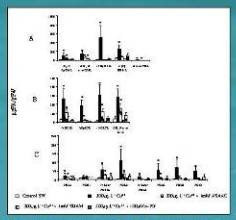

Inhibition is observed for C:18 (A) or C:20 derivatives (B,D). This results point out the enzymatic process taken place by pathways that may be original to brown algae

Copper stress induces cellular detoxification mechanisms

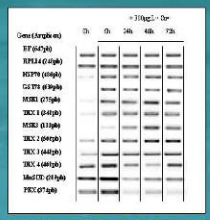

Expression levels obtained by semi-quantitative RT-PCR show the induction of cellular defensive mechanisms within rapid and late kinetics.

II. Comparative responses of copper stressed in *Ectocarpus siliculosus*: sensitive *vs.* tolerant strains

Physiological and molecular analyzes have been carried between copper tolerant strain from mine waste polluted areas of northern Chile and sensitive strain from Peru

Strains from copper polluted areas do not exhibit chlorophyll inactivation thus its photosynthesis is not affected

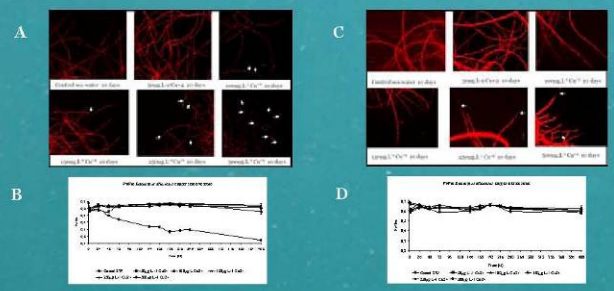

Epifluorescence microscopy images show that sensitive strains exhibit high autofluorescence extinction under copper stress. These results indicate chlorophyll degradation by copper. In consequence a decline of photosynthetic yield is observed (B). On the other hand, resistant strains show reduced amounts of autofluorescence extinction (C) thus no photosynthetic yield decline (D)

Molecular analysis show the induction of cellular detoxification systems for the sensitive strain

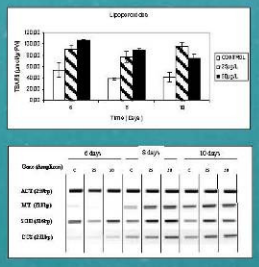

As a consequence of copper stress, lipid peroxidation is observed (A). In order to avoid the oxidative stress conditions created by copper, antioxidant enzymes such as Super Oxide Dismutase (SOD) and heavy metal detoxification proteins such as metallothioneins (MT) and Copper chaperones (CCS) are up-regulated (B)

III. Post-genomic approaches in the brown algal model *E. siliculosus* to study the copper stress response

New 2D protein extraction method for Brown algae

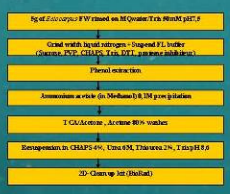

Resolved 2-D PAGE Gels

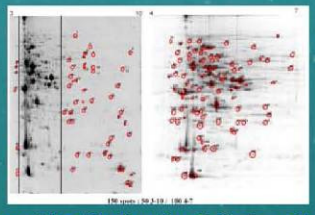

Representative 2-DE patterns from *E. siliculosus*. 2D gels allowed to excise 150 spots for MALDI-TOF analysis

Spot Identification

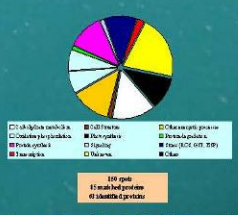

60% peptides fragments matched with ESTs from library of *E. siliculosus* sporophyte. Proteins are sorted by biological function

Name: Andrés Ritter
Nationality: Chilean / German
Date of Birth: 12.08.1980
Start of PhD Thesis: 15.11.2005
Funding: CNRS - CONICYT
Supervisors: Dr. Philippe Potin, Pr.Dr. Juan Correa

Red and brown algae as a source of fatty acid derived bioactive molecules with potential applications for skin care.

Sophie Goulitquer[1], Andrés Ritter[2], Emmanuel Gaquerel[1-2], Thierry Tonon[2], Danièle Lucas[1], Jean-Pierre Salaün[1-2] and Philippe Potin[2]

[1]EA-948, « Oxylipids », Université de Bretagne Occidentale, Faculté de Médecine, CS 93837, 29238 Brest-Cedex 3, France
[2]UMR 7139 (CNRS-UPMC-Paris 6), LIA DIAMS, Station Biologique, F-29682 Roscoff Cedex, France,

Introduction

Prostaglandins (PGs), such as PGE_1, contribute to the maintenance of a healthy skin by the regularization of keratinisation thus reducing the synthesis of sterols. [1]
Our results indicate that seaweeds such as the red alga *Chondrus crispus* (rhodophyta) and the brown alga *Laminaria digitata* (phaeophyceae), employ both C18 and C20 polyunsaturated fatty acid oxygenated derivatives (oxilipins) as defence responsive hormones.
Studies of the molecular mechanisms by which some of these marine oxilipins are formed have revealed that novel oxidative reactions are utilized and that some metabolization products resemble the eicosanoid derivatives from mammals.
We have extended these studies to members of the brown alga *Laminaria digitata* and find they also possess similar biosynthetic pathways.

Methods

The marine brown algae *Laminaria digitata* was collected on intertidal zone close to Roscoff, France, during low tide and elicited with 300µg of Cu^{2+} per litter . Unialgal cultures of gametophytes from Chondrus crispus were used for *Acrochaete Operculata* infection trials. Frozen algae were crushed and grounded in the presence of liquid nitrogen. Extraction of lipids was carried out with 2 mL ethyl acetate on a rotary shaker for 1 hour. Ethyl acetate was evaporated under a gentle stream of nitrogen and dissolved in MeOH.

Oxilipins were resolved and characterized by RP-HPLC coupled to a Navigator LC/MS mass spectrometer (Finnigan), equipped with an ionization source at atmospheric pressure (APCI) running on the negative ion mode. Separation was carried out on a 5 µm Ultrasphere C18 column 250 x 4,6 mm (Beckman). The mobile phase (0,2 % acetic acid in water/acetonitrile) program began by a 30 min-linear gradient to separate prostaglandins, mixture was then set at 40/60 (v/v), to resolve oxilipins.

Results

Elicitors inducing fatty acids oxidative metabolism in red and brown algae

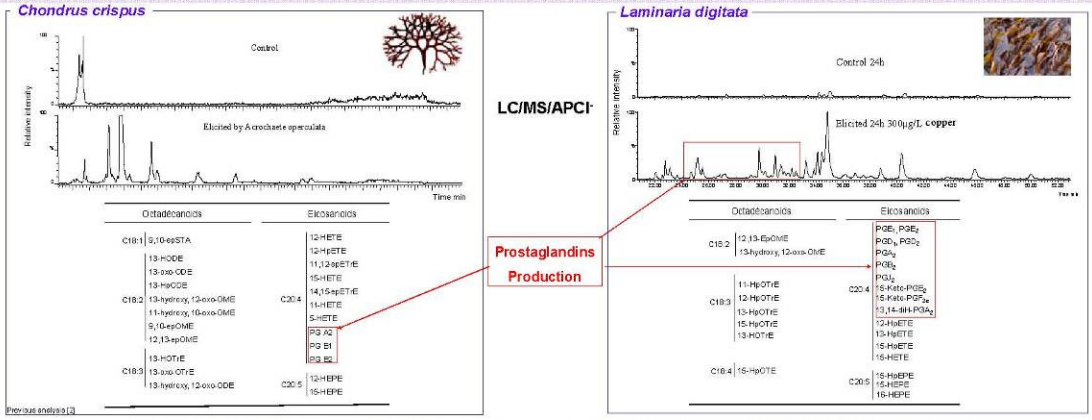

Both animal-like (C:20) and plant-like (C:18) oxylipins are produced *in C. crispus* and in *L. digitata* following stress.
Both lipoxygenase-like (LOX) and cyclooxygenase-like (COX) reactions are involved in fatty acids metabolism.
Treatment with copper salt induces prostaglandins synthesis in brown algae

Evidence for oxilipins' enzymatic biosynthesis.

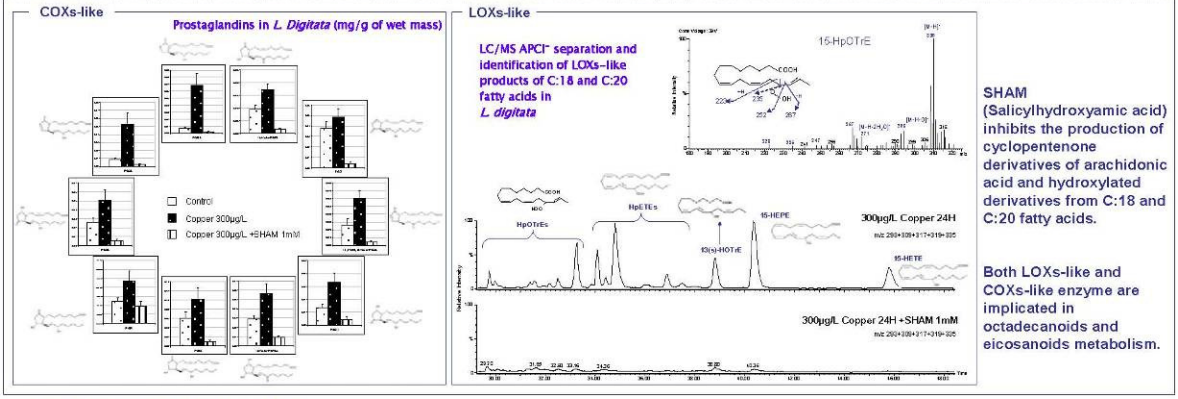

SHAM (Salicylhydroxyamic acid) inhibits the production of cyclopentenone derivatives of arachidonic acid and hydroxylated derivatives from C:18 and C:20 fatty acids.

Both LOXs-like and COXs-like enzyme are implicated in octadecanoids and eicosanoids metabolism.

Conclusion and Perspectives

Our results demonstrate that biotic and abiotic stress of red and brown algae triggers a cascade of oxidation of PUFAs leading to the synthesis of prostaglandins and other oxygenated fatty acids. Among a large variety of octadecanoids and eicosanoids, a series of cyclopentenones with chemical structures similar to animals prostaglandins have been characterised. Prostaglandins are autocrine and paracrine lipid mediators and have a variety of strong physiological effects in animals. The physiological role of prostaglandins in marine algae is still unclear.
These oxilipin biosynthetic pathways are integral part of the defense reactions triggerring signal activation of oxidative enzymes.
Here we demonstrate that marine algae are a potent source of lipid mediators (oxylipins) with hormonal properties and medical interest.

[1] Boelsma *et al.* Am. J. Clin. Nutr. 2001; 73 (5) : 853-64. ; [2] Bouarab et al. Plant Physiol. 2004 (135) : 1838-1848.

Mécanismes moléculaires impliqués dans l'établissement de la tolérance au cuivre chez les algues brunes

Martin Ubertini, Andrés Ritter, Philippe Potin, UMR 7139 CNRS-UPMC, Station biologique, 29682 Roscoff, France

Introduction

Le cuivre (Cu), micronutriment essentiel pour les producteurs primaires aquatiques, peut être toxique à haute concentration (1). Afin de lutter contre ce stress, les algues brunes, organismes benthiques sédentaires, expriment des protéines spécifiques impliquées dans la tolérance aux métaux lourds et l'adaptation à long terme (2). La pollution au Cu dans le nord du Chili a généré des déserts biologiques (3) où seulement espèces d'algues dont ***Ectocarpus siliculosus*** (5), une Phaeophycée tolérante aux métaux, ont résisté.

Notre projet vise à identifier les différentes réactions d'***E. siliculosus*** face à un stress au cuivre en étudiant ses réponses physiologiques et moléculaires, ainsi que la régulation de gènes potentiellement impliqués dans la tolérance au Cu.

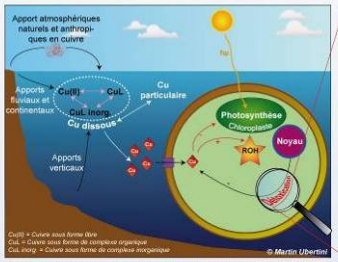

1) **La spéciation du cuivre dans l'océan et ses effets à haute concentration sur une cellule d'algue brune.**

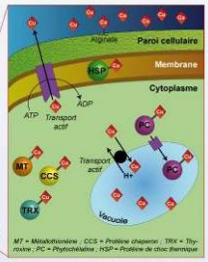

2) **Mécanismes de tolérance au cuivre ches les algues brunes.**

E. siliculosus : Algue brune filamenteuse, ordre des Ectocarpales, cosmopolite. Se développe sur des substrats abiotiques, en épiphyte sur des macroalgues, ou encore sous forme libre.

3) milieu sain ; 4) milieu contaminé.
5) *E. siliculosus* vue en microscopie optique

Résultats

Approche physiologique

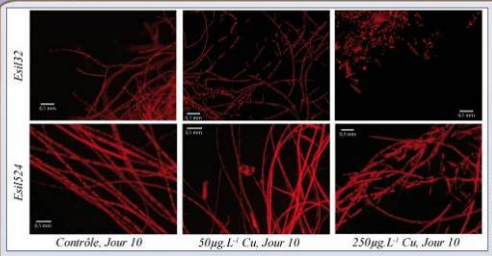

Expérience 1 : Stress chronique, durée 10 jours

► La souche Esil524 est résistante au Cu, tandis que la souche Esil32 tolère ce dernier (6-7).

6) **Autofluorescence des chloroplastes vue par microscopie en épifluorescence.** Les souches Esil32 et Esil524 proviennent respectivement d'une source non contaminée et d'une source contaminée au Cu.

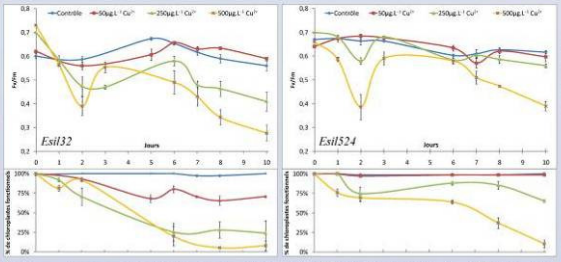

7) **Mesure du rapport Fv/Fm des souches Esil32 et Esil524 à l'aide du Pulse Amplified Modulator (PAM) durant un stress chronique en présence de Cu^{2+} pendant 10 jours et pourcentage de chloroplastes fonctionnels évalué par comptage.** Fv/Fm : Efficacité photosynthétique, la norme étant fixée entre 0,6 et 0,7. Chaque donnée correspond à la moyenne des triplicats +/- SE.

► Esil524 n'est pas affectée par une concentration de 50 µg.L^{-1} de Cu^{2+} (6-7).

Expérience 2 : Stress précoce, durée 8h

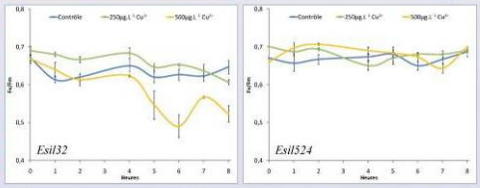

8) **Stress précoce des souches Esil32 et Esil524 en présence de Cu(II) pendant 8h.** Chaque donnée correspond à la moyenne des triplicats +/- SE.

► Diminution de l'activité photosynthétique à partir d'une durée de 4h à 500µg.L^{-1} de Cu^{2+} pour la souche Esil32 (8).

► La souche Esil 524 n'est pas affectée par ce type de stress précoce (8).

Matériels & Méthodes

1. Approche physiologique : Culture d'algues en condition de stress au cuivre

→ Mesure de l'efficacité photosynthétique à l'aide du PAM

→ Suivi d'autofluorescence des chloroplastes par microscopie en épifluorescence.

2. Aproche transcriptomique : Etude de la régulation des gènes impliqués dans le stress au Cu chez la souche Esil32 par RT-qPCR

3. Aproche fonctionnelle : Complémentation fonctionnelle de levures transformées avec le gène de la MT d'*E. siliculosus*.

Approche transcriptomique

► Induction précoce des gènes codant pour les enzymes PCs et BPO (9).

► La MT serait impliquée dans les mécanismes de la régulation du stress chronique au Cu (9).

9) **Profils d'accumulations des transcrits après traitement de la souche *Esil32* par du $CuCl_2$, normalisés par la dynéine et les conditions témoins.** Chaque donnée correspond à la moyenne des duplicats +/- SE (* significativement différentes du témoin).

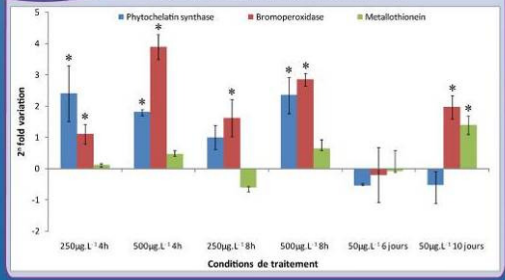

Approche Fonctionnelle

Complémentation fonctionnelle de levures déficientes aux gènes de la métallothionéine par le gène de la métallothionéine d'*Ectocarpus siliculosus* (EsilMT) :

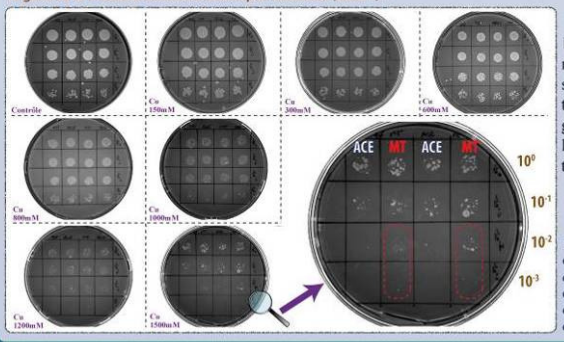

► A 1500 mM de $CuSO_4$ seules les levures transformées avec le gène EsilMT se développent pour les dilutions 10^{-2} et 10^{-3} (10).

10) **Photographies de cultures de levures *Saccharomices cerevisiae* dans des milieux de concentration croissante en $CuSO_4$.**

Discussion - Conclusion

► La pollution chimique de la côte Nord du Chili a conduit à la séléction d'individus résistants au Cu.

► L'approche transcriptomique nous permet de faire l'hypothèse de l'existence de mécanismes de tolérance à court terme (PCs et BPO) et à long terme (MT).

► Grâce à la complémentation des levures nous avons pu mettre en évidence la fonction de la MT dans la résistance au Cu chez *E. siliculosus*.

Perspectives :

►Analyse comparée de la souche Esil524 par RT-qPCR, étude transcriptomique à haut débit par hybridation d'une puce à ADN.

►Caractérisation des activités enzymatiques des gènes candidats étudiés par RT-qPCR.

Abstract Copper is an essential cofactor for metalloproteins involved in many physiological processes including photosynthesis, respiration. However, this metal is extremely toxic at high concentrations. Over 60 years of mine activities in northern Chile have led to a major decrease in biodiversity along coastal areas polluted by mine wastes allowing few brown algal species to establish such as *Ectocarpus sp*. Therefore our aim was to investigate the molecular mechanisms leading to copper tolerance in brown algae.

Copper excess in *Laminaria digitata*, triggered, rapid responses involved in the formation of C_6 and C_9 aldehydes. These compounds are thought to activate rapid general stress responses. Later, long chain oxylipins are produced including C_{18} and C_{20} cyclopentenones such as 12-OPDA and prostaglandins as well as unique compounds such as the 18-hydroxy-17-oxo-eicosatetraenoic acid. These mechanisms were correlated with the up-regulation of stress-responsive genes. Our results suggest that copper-induced lipid peroxidation may regulate protective mechanisms employing plant-like octadecanoid signals but also eicosanoid oxylipins which are absent in vascular plants.

Furthermore, we have characterized through physiological approaches two strains of *E. siliculosus* isolated from an uncontaminated coast in southern Peru (strain Es32) and from a copper-polluted coast in northern Chile (strain Es524). Analysis of copper toxicity in both strains revealed high-tolerance in Es524, contrasting to Es32. In order to analyze global soluble proteomes from these strains by 2-DE analysis, a reliable protein extraction method was developed. Differential soluble proteome profiling between control and copper stress conditions for each strain allowed to identify the induction of proteins involved in stress responses related to processes such as energy production, glutathione metabolism, phenolics biosynthesis or Heat Shock Protein accumulation. In addition, the comparison of stress-related proteomes between strains led to features related to copper tolerance in Es524. This strain presented marked expression of the copper stress targeted proteins OEC33 and fucoxanthine chlorophyll a-c binding protein, which are important components of the photosynthetic apparatus. In addition, Es524 expressed specific stress-related enzymes such as RNA helicases from the DEAD box families involved in RNA folding and maturation and a vanadium-dependent bromoperoxidase. Therefore, two different phenotypes at the proteomic level strongly suggest that persistent copper stress may have driven selective forces leading to the development of ecotypes genetically adapted to copper-contaminated sites. In addition the exploration of the recently sequenced *Ectocarpus* genomes allowed the identification of conserved features of copper homeostasis and detoxification and to initiate preliminary characterization of some important metal-chelating mechanisms using functional approaches.

Resumen El cobre es un cofactor esencial para metaloproteínas, por lo que es fundamental para procesos biológicos tales como la fotosíntesis o la respiración celular. Sin embargo, una acumulación incontrolada de este metal puede acarrear efectos nefastos a nivel celular. Más de 60 años de actividad minera en el norte de Chile ha causado un gran impacto en la biodiversidad de las zonas costeras contaminadas por cobre. En aquellas zonas, solamente algunas especies de algas pardas (Phaeophyceae) han logrado establecerse tales como *Ectocarpus sp*. Tomando en cuenta la poca información bioquímica y molecular acerca de estos organismos, mi trabajo de tesis consistió en estudiar estos mecanismos.

El estrés por cobre en *Laminaria digitata* acarrea respuestas rápidas asociadas a la aparición de oxilipinas volátiles de tipo aldeídos en C_6 y C_9. Estos derivados de ácidos grasos podrían activar mecanismos generales de respuesta al estrés. En un mayor lapso de tiempo (24h) un segundo tipo de oxilipinas en C_{18} y C_{20} fueron detectadas. Estos compuestos incluyen la presencia de ciclopentenonas de carácter enzimatico como el ácido 12-oxo-fitodienoico, característico de plantas o prostaglandinas, característico de animales. Además se descubrieron compuestos únicos en algas pardas como el ácido 18-hidroxi-17-oxo–eicosatetraenoico. La biosíntesis de estos compuestos se relaciona con la regulación de genes implicados en mecanismos de desintoxicación celular. En conclusión, pese a que la peroxidación lipídica constituye uno de los efectos nocivos del exceso de cobre, algunos de estos compuestos octadecanoicos y eicosanoicos son producidos de forma enzimática los que podrían relacionarse con la activación de mecanismos de tolerancia al cobre.

Por otro lado las respuestas fisiológicas al estrés por cobre fueron evaluadas en aislados de *E. siliculosus* provenientes de una zona sin registros de contaminacion por cobre (Es32) en comparación con otro aislado (Es524) proveniente de áreas contaminadas por cobre en la bahía de Chañaral, Chile. Los resultados muestran la clara tolerancia al cobre en el aislado Es524 comparado a Es32. Para llevar a cabo un análisis global de la expresión protéica por electroforesis bidimensional, fue previamente necesario crear un protocolo adaptado a esta especie. Los patrones de expresión protéicos en ambos aislados estresados por cobre, mostraron rasgos comunes tales como la aumentación de procesos energéticos, la activación del metabolismo del glutatión y de compuestos fenólicos o la accumulación de HSP (Heat Shock Proteins). Por otro lado la comparación de patrones entre ambos aislados mostró la aumentación marcada en Es524 de proteínas preferencialmente degradadas por cobre tales como componentes estructurales fotosintéticos. Además, este aislado expresa proteínas importantes para la desintoxicación como por ejemplo DEADbox helicasas o Bromoperoxidasas a vanadio. Estas observaciones nos han llevado a proponer la hipótesis que la tolerancia al cobre en Es524 es la resultante de un proceso adaptativo. Por otro lado la participación al proceso de anotación del genoma de *E. siliculosus* permitió identificar por homología a otros organismos componentes moleculares adicionales que participarían en la homeostasis y desintoxicación de cobre.